CRWMS/M&O

Calculation Cover Sheet

Complete only applicable items.

1. QA: L

Page: 1 Of: 110

2. Calculation Title	MOL.19990329.0394
LCE for Research Reactor Benchmark Calculations	

3. Document Identifier (including Revision Number)	4. Total Pages
B00000000-01717-0210-00034 REV 00	110

5. Total Attachments	6. Attachment Numbers - Number of pages in each
8	I-5, II-5, III-5, IV-5, V-4, VI-4, VII-22, VIII-17 (See Box 10)

	Print Name	Signature	Date
7. Originator	John M. Scaglione Laetitia Angers	John M. Scaglione Laetitia G. Angers	3/5/99 3/5/99
8. Checker	Abdelhalim A. Alsaed	aaalsaed	3/15/99
9. Lead Design Engineer	Daniel A. Thomas	D A Thomas	3/16/99

10. Remarks

Attachments I through VI are contained on an attachment compact disc of this calculation file (the attachment compact disc has been moved to Reference 7.28). The numbers shown in box 6 for Attachments I through VI refer to the number of pages in the hard-copy listing of each files' content on the compact disc.

Revision History

11. Revision No.	12. Date Approved	13. Description of Revision
00		Initial Issuance

Table of Contents

1. Purpose

The purpose of this calculation is to document the MCNP4B2LV evaluations of Laboratory Critical Experiments (LCEs) performed as part of the Disposal Criticality Analysis Methodology program. LCE evaluations documented in this report were performed for 182 different cases with varied design parameters. The objective of this analysis is to quantify the MCNP4B2LV code system's ability to accurately calculate the effective neutron multiplication factor (k_{eff}) for various critical configurations. The LCE evaluations support the development and validation of the neutronics models used for criticality analyses involving research reactor spent nuclear fuel in a geologic repository.

2. Method

The calculational method used to perform the research reactor reactivity calculations consisted of using the MCNP Version 4B2LV code (Ref. 7.1) to calculate the effective neutron multiplication factor (k_{eff}) for the various experimentally determined critical core configurations. The calculations were performed using continuous energy cross section libraries from Evaluated Nuclear Data File (ENDF/B-V, ENDF/B-VI, and a combination of the two as selected in the *Selection of MCNP Cross Section Libraries* report (pp. 61-68, Ref. 7.2)). Each of the critical core configurations was simulated, and the results reported from the MCNP calculations were the combined average values of k_{eff} from the three estimates (collision, absorption, and track length) listed in the final generation summary in the MCNP output. The LCEs documented in this report may be used to determine appropriate bias values for use in subsequent criticality evaluations performed with MCNP Version 4B2LV.

2.1 Statistical Treatment

Statistical tests were performed on the results generated by MCNP to determine the statistical validity of the results. According to page 247 of Reference 7.9, the first step is to see if there is a clear trend in the calculated results. Such a trend would indicate a tendency of the code to bias the results on an independent parameter. Standard regression techniques contained in Microsoft® Excel 97 software were used to determine the presence of a trend of MCNP results against the independent variables average energy of a neutron causing fission (AENCF) and hydrogen to fissile nuclide ratio (H/X). Formulas for calculations of AENCF and H/X are discussed in Section 5.

3. Assumptions

3.1 The experimentally determined eigenvalues and uncertainty for 2 of the FFTF Fuel Pin Array experiments (experiment 03R and 029) were not available and were assumed to be unity. The uncertainty associated with these two experiments was assumed to be an average of the uncertainties reported in Reference 7.3 MIX-COMP-THERM-001 for 4 other similar experiments and was thus assumed to be ± 0.00305. The basis for this assumption is that the experiments were performed in the same environment so that the factors involved in the uncertainty for the other experiments would be present for these 2 experiments. This assumption was used in Sections 5 and 6.

3.2 The experimentally determined eigenvalues and uncertainty for the multi-region Saxton experiments were not available and were assumed to be unity. The basis of this assumption is that page 231 of Reference 7.16 states that criticality was achieved entirely by adjusting the water level in the tank. Thus, it is assumed that when the water height is sufficient to cause the system to be critical, means that the eigenvalue is unity. The uncertainty for this value was assumed to be an average of the values reported in Section 5.1.4.2 for the single-region experiments, which equals ± 0.0042. This assumption was used in Sections 5 and 6.

3.3 The cross section libraries for zinc are not available on the Waste Package Organization (WPO) computer systems. Certain aluminum alloys used throughout this analysis contained the element zinc in trace quantities. Whenever this element was part of the material composition, its mass fraction was added to that of copper. It was assumed that this small addition of copper would have a negligible effect on the system reactivity. The basis of this assumption is that the evaluator sample MCNP deck does this, and is listed on page 36 of Reference 7.3, LEU-COMP-THERM-001. This assumption was used in Section 5.

3.4 The top grid plate in the TRIGA experiments was not modeled in the MCNP representations. This is assumed to have a negligible effect on system reactivity. The basis of this assumption is that the material that the grid was made of was aluminum, which is virtually transparent to neutrons, the grid contained holes above each fuel element as stated on page 38 of Reference 7.14, and that there was no moderator displacement by the grid. This assumption was used in Section 5.

3.5 It was assumed that omission of the steel diaphragm would have a negligible effect on system reactivity in the Pu-Metal-Fast set of experiments. The basis of this assumption is from Table 2, on page 4 of Reference 7.3, PU-MET-FAST-023. This assumption was used in Section 5.

4. Use of Computer Software

4.1 Software Approved for QA Work

4.1.1 MCNP

The MCNP code was used to calculate the k_{eff} of the research reactor critical configurations. The software specifications are as follow:

- Program Name: MCNP
- Version/Revision Number: Version 4B2
- CSCI Number: 30033 V4B2LV
- Computer Type: Hewlett Packard (HP) 9000 Series Workstations

The input and output files for the various MCNP calculations are documented in the attachments to this calculation file as described in Sections 5 and 8 (the attachment compact disc (CD) has been moved to Reference 7.28), such that an independent repetition of the software use may be performed. The MCNP software used was: (a) appropriate for the application of research reactor k_{eff} calculations, (b) used only

within the range of validation as documented throughout References 7.1 and 7.4, and (c) obtained from the Software Configuration Manager in accordance with appropriate procedures.

4.2 Software Routines

4.2.1 Excel

- Title: Excel
- Version/Revision Number: Microsoft® Excel 97

The Excel spreadsheet program was used for performing regression analysis as documented in Section 5 of this calculation file. The user-defined formulas, inputs, and results were documented in sufficient detail in Sections 5 and 6 to allow an independent repetition of the various computations. The plots of the regression analysis were presented in Attachment VII.

4.2.2 NCSS

- Title: NCSS 97 for Statistical System for Windows
- Version/Revision Number: Dr. Jerry L. Hintze® Number Cruncher Statistical Systems 97

The NCSS spreadsheet program was used for performing normality tests of the results listed in Section 6 of this calculation file. The output contained all necessary information to verify that the entire input was provided correctly. The output from the NCSS 97 usage was presented in Attachment VIII. The k_{eff} values provided in Section 6 and the corresponding description of the NCSS 97 software routine, are sufficient such that an independent repetition of the software routine use could be performed. The description of the NCSS 97 software routine was provided on pages 80 through 85 of Reference 7.27.

5. Calculation

The research reactor reactivity calculations are detailed calculations of the neutron multiplication factor for actual experimental critical configurations. This report provides a comparison of the calculations performed with MCNP--utilizing cross section libraries from ENDF/B-V, ENDF/B-VI, or a combination of both--operating on the Waste Package Organization (WPO) HP computer platform against each LCE reactivity benchmark calculation. The MCNP input decks are presented in Attachments I, III, and V. The MCNP output files are presented in Attachments II, IV, and VI. The k_{eff} results for each reactivity calculation are presented in Section 6. All of the critical configurations can be divided into six main groups as follows:

1) Highly enriched uranium (HEU) systems where the fuel is enriched to 80 weight percent (wt%) U^{235} or greater
2) Intermediate enriched uranium (IEU) systems where the enrichment is greater than 10 wt% U^{235} but less than 80 wt% U^{235}
3) Low enriched uranium (LEU) systems where the enrichment varies from natural uranium enriched up to 10 wt% U^{235}

4) Plutonium fuel thermal systems
5) Fast metal fuel systems
6) Homogenous critical solutions

Attachment VII illustrates the results where k_{eff} is trended against AENCF and H/X using regression analysis. Tests for normality in the 95% confidence interval were also performed and are shown in Attachment VIII. A "goodness-of-fit" test was used to determine whether the linear relationship between the independent and dependent variables is statistically valid or not in the regression analysis. The "goodness-of-fit" test was performed by visual inspection of the data plot and the associated fit, and through the use of the linear correlation coefficient. The linear correlation coefficient is a quantitative measure of the degree to which a linear relationship exists between two variables. The linear correlation coefficient is often expressed as a squared term, r^2. This value is calculated with the Excel 97 regression analysis tool. The closer r^2 approaches the value of 1, the better the fit of the data to the linear equation.

Regression analysis was performed using the *Regression Analysis Tool* provided by Excel 97. This analysis tool performs linear regression analysis by using the "least squares" method to fit a line through a set of observations. A simple linear equation is obtained in each case, which relates the multiplication factor (k_{eff}) to the corresponding independent variable, obtaining an equation of the form:

Equation 5.1 $k(x) = a + bx$

where k is the multiplication factor, a is the intercept coefficient, b is the slope, and x is the data that is trended against. The plots of the regression analysis are illustrated for each grouping of experiments in Attachment VII. The variables that the k_{eff} values were trended against were the AENCF and the H/X ratio. The AENCF was calculated directly from values that are provided in the MCNP outputs. The values from the output files for calculating AENCF are the weight per source particle of a neutron lost to fission and the energy per source particle of a neutron lost to fission. The AENCF is then calculated using equation 5.2.

Equation 5.2 AENCF (MeV) = energy per source particle/ weight per source particle

The calculation of the H/X ratio was performed by two methods based upon whether the critical configuration was symmetrical or not. For symmetric cases, the number of hydrogen atoms per unit cell was calculated and divided by the number of fissile atoms per unit cell. In the non-symmetric cases the moderator volume was determined by taking the volume of moderator from each unit cell plus additional moderator that neutrons would "see" in a path to another fuel rod as illustrated in Figure 5.1. This volume was used to determine the total number of hydrogen atoms present in that volume then dividing it by the total number of fissile atoms present in that volume. The calculated values for AENCF are provided in Section 6, and the H/X values for each of the cases are provided in Section 5.

The normality tests were performed by generating a "normal region" where the sample data must fall in, to ascertain its normality. This normality test was performed with the NCSS 97 software routine using a 95% confidence band. Plots of the normality tests are illustrated for each grouping of experiments in Attachment VIII.

The sources of data used in this calculation come from published reports and a handbook on benchmark experiments. Due to the nature of these sources, the data in it are established fact, and should therefore be considered accepted.

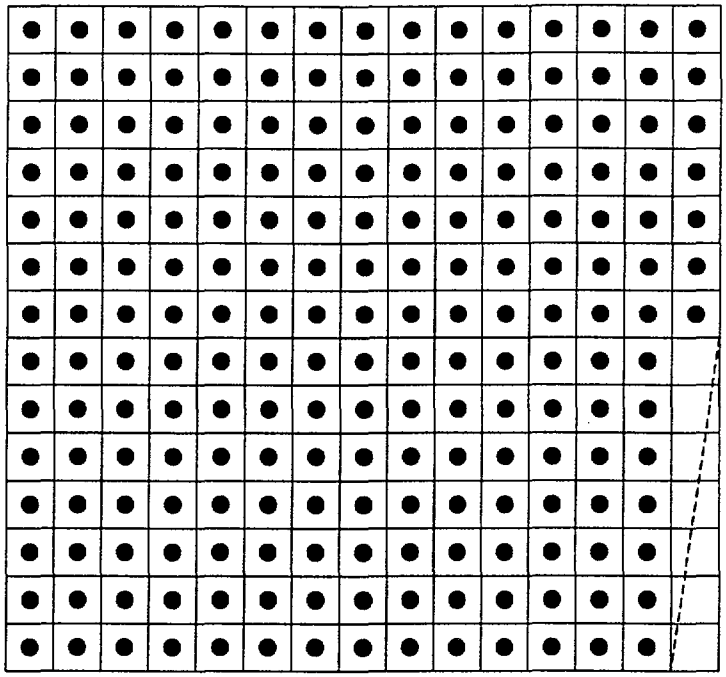

Figure 5.1. Example Figure for Non-Symmetric Geometry Moderator Addition

5.1 Research Reactor LCE Reactivity Calculations

The research reactor LCE reactivity calculations represent 182 critical core configurations. The different configurations are discussed in Sections 5.1.1 through 5.1.16 with the results of the experiments listed in Section 6.

5.1.1 LEU Systems

5.1.1.1 Water-Reflected Fuel Rod Clusters in Square Pitched Arrays

A series of critical experiments with clusters of aluminum clad UO_2 fuel rods in a large water-filled tank was performed over a period of several years at the Critical Mass Laboratory at Pacific Northwest Laboratories (PNL). Eight cases were analyzed under this category in this report that correspond to water-reflected clusters at 2.032 cm square pitch with no absorber plates, reflecting walls, dissolved poison, or gadolinium impurity. A detailed description of the experimental configuration is provided on pages 9 and 11 of Reference 7.3, LEU-COMP-THERM-001 (LCT-001). The benchmark $k_{eff} \pm$ standard deviation (σ) for this set of experiments is 0.9998 ± 0.0031 (p. 25, Ref. 7.3, LCT-001). Table 5.1.1.1-1 provides a brief description of the experiments and the MCNP case names. Each of the experiments

used 2.35 wt% U^{235} enriched UO_2 fuel with an average loading of 17.08 g of U^{235} per rod (p. 7, Ref. 7.3, LCT-001).

Table 5.1.1.1-1. Water-Reflected Fuel Rod Cluster Critical Experiments

Handbook case name	Description (p. 10, Ref. 7.3, LCT-001) Number of rods[1] (X x Y), number of clusters, cluster separation	H/X ratio	MCNP case name
Case 1	20 x 18.08, 1 cluster	459.0644	Case1
Case 2	20 x 17, 3 clusters, 11.92 ± 0.04 cm separation	486.8467	Case2
Case 3[2]	20 x 16, 3 clusters, 8.41 ± 0.05 cm separation	469.1267	Case3
Case 4	20 x 16 (center), 22 x 16 (two outer), 3 clusters, 10.05 ± 0.05 cm separation	474.2351	Case4
Case 5	20 x 15, 3 clusters, 6.39 ± 0.05 cm separation	458.9289	Case5
Case 6	20 x 15 (center), 24 x 15 (two outer), 3 clusters, 8.01 ± 0.06 cm separation	462.3500	Case6
Case 7	20 x 14, 3 clusters, 4.46 ± 0.10 cm separation	449.1855	Case7
Case 8[3]	19 x 6, 3 clusters, 7.57 ± 0.04 cm separation	466.8974	Case8

[1] For three-cluster configurations, the first dimension is along the direction of the cluster placement. The second dimension is the width of facing sides, as shown in Figure 5 on p. 11 of Reference 7.3, LCT-001.

[2] The cluster separation referenced was 8.41 cm, but footnote (d) on page 10 of Reference 7.3, LCT-001 states that the cluster separation should be 0.762 cm less. Thus, 7.648 cm was represented in the MCNP case for the cluster separation.

[3] The cluster separation referenced was 7.57 cm, but footnote (d) on page 10 of Reference 7.3, LCT-001 states that the cluster separation should be 0.762 cm less. Thus, 6.808 cm was represented in the MCNP case for the cluster separation.

Table 5.1.1.1-2. Material Atom Densities for LCT-001 Experiments (pp. 21, 23, Ref. 7.3, LCT-001)

Material	Element/Isotope	Atom density (atoms/b-cm)
$U(2.35)O_2$ Fuel	U^{234}	2.8563E-06
	U^{235}	4.8785E-04
	U^{236}	3.5348E-06
	U^{238}	2.0009E-02
	O	4.1202E-02
1100 Aluminum (top end plug: 2.70 g/cm^3)	Al	5.9660E-02
	Cu	3.0705E-05
	Mn	7.3991E-06
	Zn (added as copper)	1.2433E-05
	Si	2.3302E-04
	Fe	1.1719E-04

Table 5.1.1.1-2. Material Atom Densities for LCT-001 Experiments (pp. 21, 23, Ref. 7.3, LCT-001)

Material	Element/Isotope	Atom density (atoms/b-cm)
5052 Aluminum (lower end plug: 2.69 g/cm^3)	Al	5.8028E-02
	Cr	7.7888E-05
	Cu	1.2746E-05
	Mg	1.6663E-03
	Mn	1.4743E-05
	Zn (added as copper)	1.2387E-05
	Si	1.2978E-04
	Fe	6.5265E-05
6061 Aluminum (clad: 2.69 g/cm^3)	Al	5.8433E-02
	Cr	6.2310E-05
	Cu	6.3731E-05
	Mg	6.6651E-04
	Mn	2.2115E-05
	Ti	2.5375E-05
	Zn (added as copper)	3.0967E-05
	Si	3.4607E-04
	Fe	1.0152E-04
Water	H	6.6706E-02
	O	3.3353E-02
Acrylic	H	5.6642E-02
	C	3.5648E-02
	O	1.4273E-02

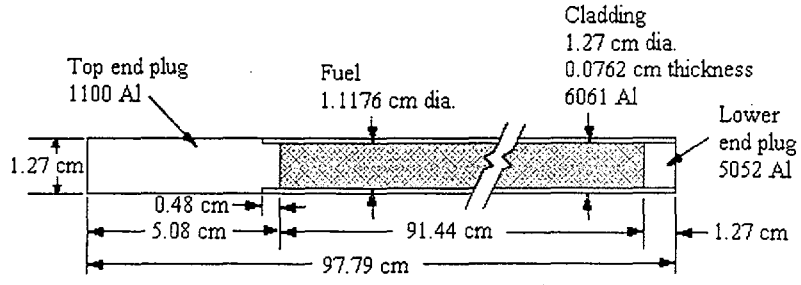

Figure 5.1.1.1-1. Fuel Rod for LCT-001

5.1.1.2 LEU Systems Typical of N Reactor Fuel in the K Basin

Three cases which analyze a lattice of actual N Reactor MKIA fuel elements were evaluated in this report. The MKIA cases analyzed 101.2 fuel elements, 67.4 fuel elements, and 90.3 fuel elements with corresponding pitches of 7.112 cm, 7.874 cm, and 8.636 cm, respectively (p. 5, Ref. 7.18). The MKIA experiments were performed for three different lattice pitches resulting in three experimental values to

achieve a k_{eff} of unity. The lattice pitches and corresponding critical number of fuel elements are listed in Table 5.1.1.2-1, and Table 5.1.1.2-2 provides the physical dimensions for the MKIA fuel rods. It should be noted that the MKIA experiments used 26.2 in. (66.548 cm) long fuel elements stacked two high for a 52.4 in. (133.096 cm) fuel column per lattice (p. 5, Ref. 7.19) with 121 filled fuel lattices (p. 52, Ref. 7.17). In this set of experiments the number of fuel elements was extrapolated to critical.

Table 5.1.1.2-1. MKIA Fuel Assembly Experiments (p. 5, Ref. 7.18)

Lattice pitch	Critical number of fuel elements experimentally determined	Benchmark $k_{eff} \pm \sigma$[a]	H/X ratio	MCNP case name
7.112 cm	101.2	1.000 ± 0.005	993.7259	SUBC2P8H
7.874 cm	67.4	1.000 ± 0.005	1413.6232	SUBC3P1H
8.636 cm	90.3	1.000 ± 0.005	1876.2220	SUBC3P4H

[a] σ is from page 7 of Reference 7.18.

Table 5.1.1.2-2. MKIA Fuel Element Parameters (p. 5, Ref. 7.17)

Parameter	Outer tube	Inner tube
zirconium clad OD[1] cm (in.)	6.106 (2.404)	3.165 (1.246)
uranium OD cm (in.)	5.979 (2.354)	2.962 (1.166)
uranium ID[2] cm (in.)	4.592 (1.808)	1.245 (0.490)
zirconium clad ID cm (in.)	4.481 (1.764)	1.118 (0.440)
wt% U^{235}	1.25	0.947
wt% U^{236}	0.0392	0.0392
wt% U^{238}	98.7108	99.0138
end cap thickness cm (in.)	0.483 (0.190)	0.483 (0.190)
fuel density (g/cm^3)	18.82	18.82
clad density (g/cm^3)	6.55	6.55
moderator density (g/cm^3)	1.00	1.00

[1] OD = Outer diameter

[2] ID = Inner diameter

5.1.1.3 LEU Solution Experiments

This set of experiments is comprised of twelve cases that look at UO_3-H_2O critical solutions. The UO_3-H_2O experiments differed by varying enrichment and the (hydrogen to uranium) H/U ratio. The UO_3-H_2O sets of experiments were simulated as homogeneous spheres and k_∞ was calculated with MCNP. Table 5.1.1.3-1 contains a description of the UO_3-H_2O experiments.

Table 5.1.1.3-1. UO_3-H_2O Solution Experiments (p. 43, Ref. 7.17)

Enrichment (wt% U^{235})	H/U	$k_\infty \pm$ experimental uncertainty	H/X ratio	MCNP case name
1.0059	3.772	0.9920 ± 0.0060	370.2986	SPHU9A
1.0059	4.999	0.9925 ± 0.0050	490.7555	SPHU9B
1.0059	6.164	0.9875 ± 0.0058	605.1229	SPHU9C
1.0059	6.881	0.9821 ± 0.0054	675.5099	SPHU9D
1.0059	7.449	0.9702 ± 0.0070	731.2706	SPHU9E
1.0704	3.728	1.0063 ± 0.0073	343.9305	SPHU9F
1.0704	5.778	1.0064 ± 0.0078	533.0517	SPHU9G
1.0704	7.075	0.9957 ± 0.0061	652.7077	SPHU9H
1.1586	3.728	1.0298 ± 0.0056	317.7489	SPHU9I
1.1586	5.926	1.0330 ± 0.0051	475.6274	SPHU9J
1.1586	6.838	1.0313 ± 0.0032	582.8262	SPHU9K
1.1586	7.449	1.0209 ± 0.0051	634.9047	SPHU9L

5.1.2 IEU Systems

5.1.2.1 TRIGA (Training, Research, Isotopes, General Atomics) Fuel Rod Experiments

The benchmark experiments used fresh stainless steel clad TRIGA fuel rods in a TRIGA Mark II reactor. The configuration was a water filled reactor with graphite reflector. The fuel rods were made up of 20 wt% U^{235} mixed with zirconium hydride. The fuel had a 1.65 hydrogen-zirconium atom ratio. Table 5.1.2.1-1 provides a brief listing of the reference identifier name, some information about the experiment, the benchmark k_{eff} value, and the MCNP case name. A more detailed description of the critical configurations is available on pages 38 through 44 of Reference 7.14.

Table 5.1.2.1-1. TRIGA Fuel Rod Experiments

Case name	Description	Benchmark $k_{eff} \pm \sigma$[a] (p. 45, Ref. 7.14)	MCNP case name
TRI17	Core 132 with explicit fuel	-135 ± 15[b] pcm (0.99865 ± 0.00015)	tri17
TRI18	Core 133 with explicit fuel	280[c] ± 15 pcm (1.00280 ± 0.00015)	tri18

[a] The reactivity measurement results were listed in units of pcm (percent mil) in the reference.

[b] Uncertainty value is from page 42 of Reference 7.14.

[c] Average of four different experimental k_{eff} values that varied with source position (p. 45, Ref. 7.14).

5.1.3 HEU Thermal Systems

5.1.3.1 SPERT-D Fuel Experiments

Twenty-three critical experiments involving lattices of SPERT-D fuel elements were performed at Oak Ridge National Laboratories (ORNL). The fuel elements consisted of plates of uranium-aluminum alloy. Each fuel element contained approximately 300 grams (p. 1, Ref. 7.3, HEU-MET-THERM-006 (HMT-006)) of U^{235} in 22 aluminum clad fuel plates. All 23 experiments were considered acceptable for use as benchmark experiments by the evaluator and detailed descriptions of each critical configuration is reported on pages 18 through 22 of Reference 7.3, HMT-006. Table 5.1.3.1-1 provides a listing of the various SPERT-D cases, the benchmark k_{eff} values, and the MCNP filenames. Figures 5.1.3.1-1 and 5.1.3.1-2 illustrate the physical dimensions of the SPERT-D fuel element as represented in the MCNP input decks. The critical experiments were represented on a 12-inch thick Plexiglas table (p. 11, Ref. 7.3, HMT-006). The reflector and moderator for cases 1 through 18 was demineralized water, and an aqueous solution of uranyl nitrate $U(92.6)O_2(NO_3)_2$ in cases 19 through 23 (p. 10, Ref. 7.3, HMT-006). Tables 5.1.3.1-2 through 5.1.3.1-7 provide the atom densities used for each of the material compositions used.

Table 5.1.3.1-1. SPERT-D Fuel Element Critical Experiments (Ref. 7.3, HMT-006)

Handbook case name	Global description	Reflector above fuel (cm) (p. 23, HMT-006)	Benchmark $k_{eff} \pm \sigma$ (p. 28, HMT-006)	H/X ratio	MCNP case name
CASE1	4 x 3.77 lattice, 4.63 kg U^{235}, 0.0" spacing	9.825	1.000 ± 0.004	193.3124	spert1
CASE 2	4 x 3.16 lattice, 3.87 kg U^{235}, 0.25" spacing	12.8982	1.000 ± 0.004	255.0128	spert2
CASE 3	4 x 3.09 lattice, 3.79 kg U^{235}, 0.50" spacing	9.8401	1.000 ± 0.004	264.1613	spert3
CASE 4	circular, 3.48 kg U^{235}, 0.50" spacing	7.3136	1.000 ± 0.004	297.9842	spert4
CASE 5	4 x 3.16 lattice, 3.87 kg U^{235}, 0.75" spacing	17.21	1.000 ± 0.004	256.7681	spert5
CASE 6	4 x 3.70 lattice, 4.54 kg U^{235}, 1.00" spacing	13.853	1.000 ± 0.004	202.076	spert6
CASE 7	5 x 4.03 lattice, 6.16 kg U^{235}, 1.25" spacing	13.0186	1.000 ± 0.004	252.5202	spert7
CASE 8	6 x 5.34 lattice, 9.82 kg U^{235}, 1.50" spacing	11.3984	1.000 ± 0.004	217.5652	spert8
CASE 9	7 x 6.68 lattice, 6.16 kg U^{235}, 1.60" spacing	12.0359	1.000 ± 0.004	195.381	spert9
CASE 10	4 x 3.2 x 3 lattice, 11.78 kg U^{235}, 0.0" spacing	9.4309	1.000 ± 0.004	248.8977	spert10
CASE 11	3 x 3.36 x 3 lattice, 9.28 kg U^{235}, 0.50" spacing	12.0994	1.000 ± 0.004	232.9062	spert11

Table 5.1.3.1-1. SPERT-D Fuel Element Critical Experiments (Ref. 7.3, HMT-006)

Handbook case name	Global description	Reflector above fuel (cm) (p. 23, HMT-006)	Benchmark $k_{eff} \pm \sigma$ (p. 28, HMT-006)	H/X ratio	MCNP case name
CASE 12	4 x 4 x 3 lattice, 14.71 kg U^{235}, 1.25" spacing	8.0	1.000 ± 0.004	179.0618	spert12
CASE 13	slab 16 x 2.32, 11.37 kg U^{235}, 1.25" spacing	11.6162	1.000 ± 0.004	262.4671	spert13
CASE 14	slab 16 x 3, 14.71 kg U^{235}, 0.50"/2.19" spacing	7.5728	1.000 ± 0.004	179.0435	spert14
CASE 15	slab 16 x 4, 19.62 kg U^{235}, 0.50"/2.56" spacing	10.75	1.000 ± 0.004	179.9174	spert15
CASE 16	2 slabs 16 x 2, 19.62 kg U^{235}, 0.50"/0.50"/6.37" spacing	12.7351	1.000 ± 0.004	179.7702	spert16
CASE 17	slab 4 x 5.0 w/ Cd, 6.19 kg U^{235}, 0.0"/0.75" spacing	10.7471	1.000 ± 0.004	234.3386	spert17
CASE 18	slab 4 x 7.04 w/ Cd, 8.64 kg U^{235}, 0.0"/0.75" spacing	13.8573	1.000 ± 0.004	217.6127	spert18
CASE 19	U Nitrate (3.99 g U^{235}/liter) & 3 x 3.09, 2.86 kg U^{235}, 0.5" spacing, 0.0 g B/liter	6.8208	1.000 ± 0.004	500.2345	spert19
CASE 20	U Nitrate (3.99 g U^{235}/liter) & 4 x 4.20, 5.15 kg U^{235}, 0.5" spacing, 0.389 g B/liter	8.3311	1.000 ± 0.004	376.0098	spert20
CASE 21	U Nitrate (3.99 g U^{235}/liter) & 5 x 4.41, 6.76 kg U^{235}, 0.5" spacing, 0.579 g B/liter	4.6946	1.000 ± 0.004	213.2793	spert21
CASE 22	U Nitrate (3.99 g U^{235}/liter) & 6 x 4.96, 8.90 kg U^{235}, 0.5" spacing, 0.773 g B/liter	5.5725	1.000 ± 0.004	157.7264	spert22
CASE 23	U Nitrate (3.99 g U^{235}/liter) & 6 x 5.55, 10.15 kg U^{235}, 0.5" spacing, 0.871 g B/liter	7.7118	1.000 ± 0.004	134.4288	spert23

Table 5.1.3.1-2. Material Atom Densities for SPERT-D Fuel Plate (p. 24, Ref. 7.3, HMT-006)

Case Number	U^{235} (atoms/b-cm)	U^{238} (atoms/b-cm)	Aluminum (atoms/b-cm)
1-23	1.8490E-03	1.3383E-04	5.5350E-02

Table 5.1.3.1-3. Structural Atom Densities for SPERT-D Fuel (p. 25, Ref. 7.3, HMT-006)

Element	Number density (atoms/b-cm)
Aluminum	6.0238E-02

Table 5.1.3.1-4. Material Atom Densities for Plexiglas Table (p. 25, Ref. 7.3, HMT-006)

Element	Element wt%	Number density (atoms/b-cm)
Carbon	60.024	3.5512E-02
Hydrogen	8.071	5.6902E-02
Oxygen	32.302	1.4347E-02

Table 5.1.3.1-5. Material Atom Densities for Cadmium Sheets (p. 25, Ref. 7.3, HMT-006)

Element	Number density (atoms/b-cm)
Cadmium	4.6340E-02

Table 5.1.3.1-6. Atom Densities for Water (p. 26, Ref. 7.3, HMT-006)

Element	Number density (atoms/b-cm)
Hydrogen	6.6735E-02
Oxygen	3.3368E-02

Table 5.1.3.1-7. Atom Densities for Uranyl Nitrate in Solution (p. 28, Ref. 7.3, HMT-006)

Case number	U^{235}	U^{238}	B^{10}	B^{11}	O	N	H
19	1.0223E-05	8.0663E-07	0.0	0.0	3.3276E-02	2.2059E-05	6.6377E-02
20	1.0223E-05	8.0663E-07	4.2732E-06	1.7392E-05	3.3267E-02	2.2059E-05	6.6293E-02
21	1.0223E-05	8.0663E-07	6.3604E-06	2.5887E-05	3.3263E-02	2.2059E-05	6.6252E-02
22	1.0223E-05	8.0663E-07	8.4915E-06	3.4560E-05	3.3258E-02	2.2059E-05	6.6210E-02
23	1.0223E-05	8.0663E-07	9.5680E-06	3.8942E-05	3.3256E-02	2.2059E-05	6.6189E-02

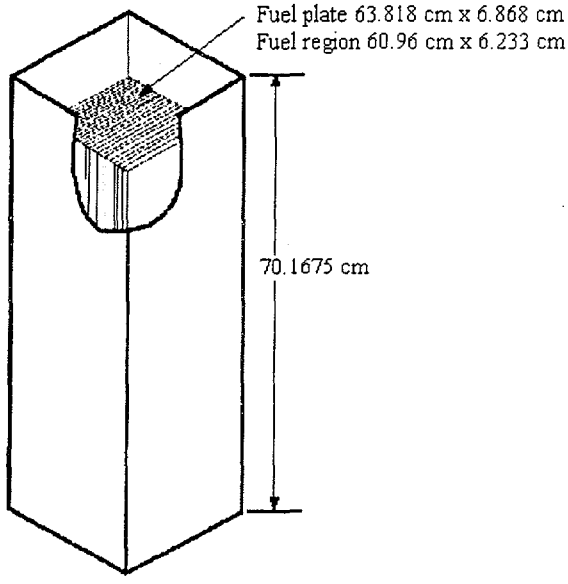

Figure 5.1.3.1-1. Side View of SPERT-D Fuel Element

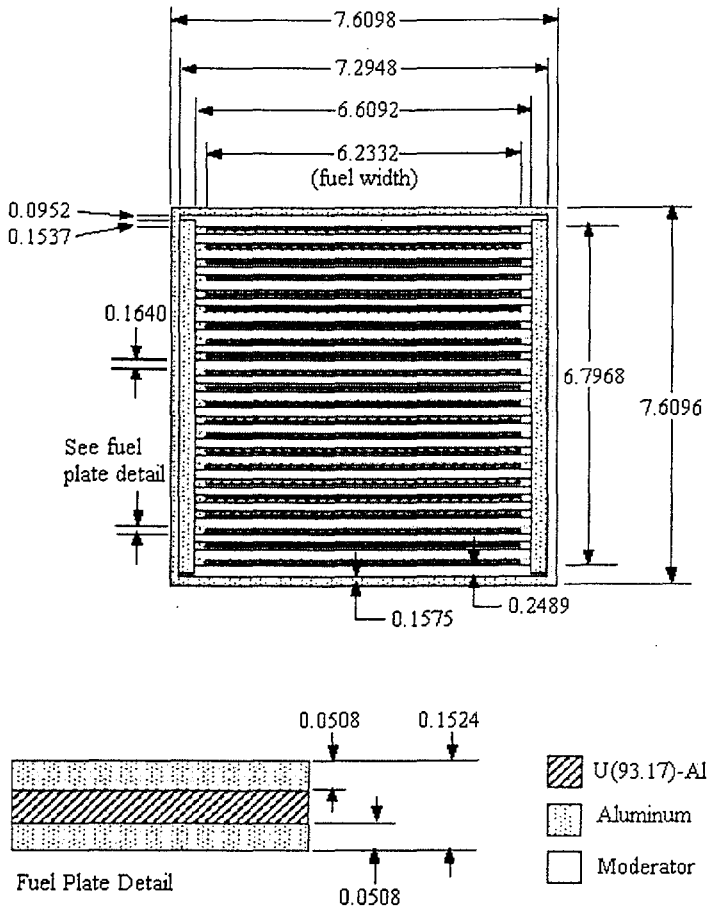

Figure 5.1.3.1-2. Top View of SPERT-D Fuel Element (dimensions in cm)

5.1.3.2 Water-Moderated Hexagonally Pitched Lattices of Highly Enriched Fuel Rods of Cross-Shaped Cross Section

A series of critical experiments with water moderated hexagonally pitched lattices of highly enriched fuel rods of cross-shaped cross section was performed over several years in the Russian Research Center (RRC) "Kurchatov Institute". The 28 experiments analyzed under this category in this report consist of the following:

1) Fifteen critical two-zone lattice experiments corresponding to different combinations of inner and peripheral zones of cross-shaped fuel rods at two pitches. For detailed descriptions of these experimental configurations see pages 2, and 7 through 14 of Reference 7.3, HEU-COMP-THERM-003 (HCT-003). Material compositions used in the cases for this set of experiments are shown in Table 5.1.3.2-2.

2) Four critical configurations of hexagonal lattices of fuel rods with gadolinium (Gd) or Samarium (Sm) rods. These experiments consisted of double lattices of fuel rods and absorber rods containing Gd or Sm. Detailed experimental configuration descriptions are available on pages 2, 7, and 8 of

Reference 7.3, HEU-COMP-THERM-004 (HCT-004). Material compositions used in the cases for this set of experiments are shown in Table 5.1.3.2-3.

3) One critical configuration of hexagonal pitched clusters of lattices of fuel rods with copper (Cu) rods. Detailed experimental configuration descriptions are available on pages 2 through 8 of Reference 7.3, HEU-COMP-THERM-005 (HCT-005). Material compositions used in the cases for this set of experiments are shown in Table 5.1.3.2-4. Two cases were used: one considers the fuel rod as cylinder and the other represents the fuel rod as it is in reality.

4) Three critical configurations with uniform hexagonal lattices with pitch values of 5.6, 10.0, and 21.13 mm. Detailed experimental configuration descriptions are available on pages 2, 5, and 6 of Reference 7.3, HEU-COMP-THERM-006 (HCT-006). Material compositions used in the cases for this set of experiments are shown in Table 5.1.3.2-5.

5) Three critical configurations with double hexagonal lattices of fuel rods and zirconium hydride rods. Detailed experimental configuration descriptions are available on pages 2 through 8 of Reference 7.3, HEU-COMP-THERM-007 (HCT-007). Material compositions used in the cases for this set of experiments are shown in Table 5.1.3.2-6. Two cases were used: one considers the fuel rod as a cylinder and the other represents the fuel rod as it is in reality.

6) Two critical configurations with double hexagonal lattices of fuel rods and boron carbide rods. Detailed experimental configuration descriptions are available on pages 2, 7, and 8 of Reference 7.3, HEU-COMP-THERM-008 (HCT-008). Material compositions used in the cases for this set of experiments are shown in Table 5.1.3.2-7.

Table 5.1.3.2-1 provides a listing of these various cases, the benchmark k_{eff} values, and the MCNP filenames. Figures 5.1.3.2-1 and 5.1.3.2-2 illustrate the fuel rod dimensions employed in the HCT-003 and HCT-007 sets of experiments. Figures 5.1.3.2-3, 5.1.3.2-4, and 5.1.3.2-5 provide the fuel rod and absorber rod dimensions used in the HCT-004 set of experiments. Figures 5.1.3.2-6 and 5.1.3.2-7 provide the fuel rod dimensions used for the HCT-005, HCT-006, and HCT-008 sets of experiments.

Table 5.1.3.2-1. Cross-Shaped Fuel Rods Critical Experiments

Handbook case name	Description	Benchmark $k_{eff} \pm \sigma$	H/X ratio	MCNP case name
HCT-003 2-Zone Critical Arrays with $U(80\ wt\%)O_2$+Cu Fuel and Lightweight Moderator				
Array Number 1	Center zone: 12.2 mm pitch, 19 rods Outer zone: 6.1 mm pitch, 1390 rods	1.000 ± 0.0044[a]	50.9897	hct3-1
Array Number 2	Center zone: 12.2 mm pitch, 61 rods Outer zone: 6.1 mm pitch, 1182 rods	1.000 ± 0.0044	59.18833	hct3-2
Array Number 3	Center zone: 12.2 mm pitch, 121 rods Outer zone: 6.1 mm pitch, 897 rods	1.000 ± 0.0044	75.26434	hct3-3
Array Number 4	Center zone: 12.2 mm pitch, 199 rods Outer zone: 6.1 mm pitch, 577 rods	1.000 ± 0.0044	106.9583	hct3-4
Array Number 5	Center zone: 12.2 mm pitch, 271 rods Outer zone: 6.1 mm pitch, 325 rods	1.000 ± 0.0044	152.6288	hct3-5

Table 5.1.3.2-1. Cross-Shaped Fuel Rods Critical Experiments

Handbook case name	Description	Benchmark $k_{eff} \pm \sigma$	H/X ratio	MCNP case name
Array Number 6	Center zone: 6.1 mm pitch, 1099 rods Outer zone: 12.2 mm pitch, 167 rods	1.000 ± 0.0044	73.41705	hct3-6
Array Number 7	Center zone: 6.1 mm pitch, 793 rods Outer zone: 12.2 mm pitch, 250 rods	1.000 ± 0.0044	103.0997	hct3-7
Array Number 8	Center zone: 6.1 mm pitch, 757 rods Outer zone: 12.2 mm pitch, 249 rods	1.000 ± 0.0044	104.9015	hct3-8
Array Number 9	Center zone: 6.1 mm pitch, 445 rods Outer zone: 12.2 mm pitch, 319 rods	1.000 ± 0.0044	144.0688	hct3-9
Array Number 10	Center zone: 6.1 mm pitch, 217 rods Outer zone: 12.2 mm pitch, 372 rods	1.000 ± 0.0044	193.3755	hct310
Array Number 11	Center zone: 6.1 mm pitch, 85 rods Outer zone: 12.2 mm pitch, 415 rods	1.000 ± 0.0044	239.0843	hct311
Array Number 12	Center zone: 18.3 mm pitch, 121 rods Outer zone: 6.1 mm pitch, 985 rods	1.000 ± 0.0044	115.0898	hct312
Array Number 13	Center zone: 18.3 mm pitch, 301 rods Outer zone: 6.1 mm pitch, 426 rods	1.000 ± 0.0044	302.2223	hct313
Array Number 14	Center zone: 6.1 mm pitch, 763 rods Outer zone: 18.3 mm pitch, 186 rods	1.000 ± 0.0044	168.2836	hct314
Array Number 15	Center zone: 6.1 mm pitch, 337 rods Outer zone: 18.3mm pitch, 325 rods	1.000 ± 0.0044	349.4658	hct315
HCT-004 Water Moderator Hexagonally Pitched (5.3 mm) Lattices of $U(90 wt\%)O_2$+Cu Fuel With Gd or Sm Rods				
Case1	106 Gd rods on 27.54 mm pitch, 2760 fuel rods	1.0000 ± 0.0038[b]	34.84568	hct4-1
Case2	55 Gd rods on 36.72 mm pitch, 2520 fuel rods	1.0000 ± 0.0039	34.61446	hct4-2
Case3	121 Sm rods on 27.54 mm pitch, 3198 fuel rods	1.0000 ± 0.0037	34.83774	hct4-3
Case4	58 Gd rods on 36.72 mm pitch, 2727 fuel rods	1.0000 ± 0.0038	34.6067	hct4-4
HCT-005 Water Moderator Hexagonally Pitched (5.2 mm) Lattices of $U(80 wt\%)O_2$+Cu Fuel Rods				
Case 1	Fuel rod hexagonal-lattice pitch 5.2 mm, 2257 rods	1.0000 ± 0.0094[c]	23.201	hct5-2
HCT-006 Water Moderator Hexagonally Pitched Lattices of $U(80 wt\%)O_2$+Cu Fuel Rods				
Case1	1819 fuel rods on a 5.6 mm pitch	1.0000 ± 0.0058[d]	30.02072	hct6-t1
Case2	457 fuel rods on a 10.0 mm pitch	1.0000 ± 0.0020	143.5223	hct6-t2

Table 5.1.3.2-1. Cross-Shaped Fuel Rods Critical Experiments

Handbook case name	Description	Benchmark $k_{eff} \pm \sigma$	H/X ratio	MCNP case name
Case3	554 fuel rods on a 21.13 mm pitch	1.0000 ± 0.0048	716.4491	hct6-t3
HCT-007 Water Moderator Hexagonally Pitched Lattices of U(80 wt%)O_2+Cu Fuel Rods and Zirconium Hydride Rods				
Case 1	523 Zr rods on 10.5655 mm pitch, 1064 fuel rods	1.0000± 0.0035[c]	90.96	hct7-4
Case 2	121 Zr rods on 21.1310 mm pitch, 1400 fuel rods	1.0000± 0.0041	64.7245	hct7-5
Case 3	31 Zr rods on 42.2620 mm pitch, 1484 fuel rods	1.0000± 0.0043	60.02	hct7-6
HCT-008 Water Moderator Haxagonally Pitched (5.3 mm) Double Lattices of U(80 wt%)O_2+Cu Fuel and Boron Carbide Rods				
Case1	217 B_4C rods (1.0 g B/rod) on 21.2 mm pitch, 3460 fuel rods	1.0000 ± 0.0055[f]	25.28405	hct8-1
Case2	169 B_4C rods (3.5 g B/rod) on 26.5 mm pitch, 4130 fuel rods	1.0000 ± 0.0056	25.05101	hct8-2

[a] Benchmark k_{eff} values are from page 23 of Reference 7.3, HCT-003.

[b] Benchmark k_{eff} values are from page 19 of Reference 7.3, HCT-004.

[c] Benchmark k_{eff} values are from page 15 of Reference 7.3, HCT-005.

[d] Benchmark k_{eff} values are from page 17 of Reference 7.3, HCT-006.

[e] Benchmark k_{eff} values are from page 17 of Reference 7.3, HCT-007.

[f] Benchmark k_{eff} values are from page 19 of Reference 7.3, HCT-008.

Table 5.1.3.2-2. Material Atom Densities for HCT-003 Experiments (p. 24, Ref. 7.3, HCT-003)

Material	Element/Isotope	Atom density (atoms/b-cm)
Fuel	U^{234}	4.4189E-05
	U^{235}	3.6290E-03
	U^{236}	1.0022E-05
	U^{238}	8.7239E-04
	Cu	5.4675E-02
	O	9.4096E-03
Stainless Steel Clad	Fe	5.4226E-02
	Cr	1.4639E-02
	Ni	1.2159E-02
	Mo	1.3637E-03
	Si	1.3551E-03

Table 5.1.3.2-2. Material Atom Densities for HCT-003 Experiments (p. 24, Ref. 7.3, HCT-003)

Material	Element/Isotope	Atom density (atoms/b-cm)
	Mn	5.1958E-04
	Nb	3.8405E-04
	C	3.5643E-04
	Cu	2.2460E-04
	P	5.3759E-05
	S	2.9669E-05
Duralumin Alloy AD1	Fe	8.7667E-05
	Si	2.0338E-04
	Cu	1.2841E-05
	Al	6.0062E-02
Plexiglas	H	5.6782E-02
	O	1.4196E-02
	C	3.5489E-02
Water	H	6.6736E-02
	O	3.3368E-02

Table 5.1.3.2-3. Material Atom Densities for HCT-004 Experiments (pp. 18, 19, Ref. 7.3, HCT-004)

Material	Density (g/cm^3)	Element/Isotope	wt%	Atom density (atoms/b-cm)
Water	0.9982	H	11.19	6.6736E-02
		O	88.81	3.3368E-02
Alloy AD1	2.71	Al	99.3	6.0062E-02
		Si	0.35	2.0337E-04
		Fe	0.3	8.7667E-05
		Cu	0.05	1.2841E-05
		C	0.09	3.5648E-04
		Si	0.8	1.3551E-03
Stainless Steel (cladding and end caps)	7.90	Cr	16.0	1.4639E-02
		Fe	64.21	5.4698E-02
		Ni	15.0	1.2159E-02
		Nb	0.9	4.6086E-04
		Mo	3.0	1.4876E-03
Plexiglas	1.18	H	8.06	5.6826E-02
		O	31.96	1.4194E-02
		C	59.98	3.5486E-02
Fuel	8.3922	U^{234}	0.227109	4.9042E-05
		U^{235}	23.84669	5.1275E-03
		U^{236}	0.075453	1.6155E-05
		U^{238}	2.71765	5.7696E-04
		O	3.777326	1.1932E-02
		Cu	69.35577	5.5159E-02

Table 5.1.3.2-3. Material Atom Densities for HCT-004 Experiments (pp. 18, 19, Ref. 7.3, HCT-004)

Material	Density (g/cm^3)	Element/Isotope	wt%	Atom density (atoms/b-cm)
Bronze	8.30	Ni	0.5	4.2582E-04
		Be	2.2	1.2201E-02
		Cu	97.3	7.6533E-02
Absorber (Case 1 and 2)	1.31	Gd^{152}	0.011999	6.2309E-07
		Gd^{154}	0.13251	6.7917E-06
		Gd^{155}	0.905465	4.6109E-05
		Gd^{156}	1.260435	6.3773E-05
		Gd^{157}	0.969837	4.8757E-05
		Gd^{158}	1.549156	7.7388E-05
		Gd^{160}	1.380598	6.8104E-05
		Al	49.14	1.4368E-02
		O	44.65	2.2016E-02
Absorber (Case 3 and 4)	1.59	Sm	34.64	2.2059E-03
		Al	31.67	1.1239E-02
		O	33.690	2.0162E-02
Stainless Steel (absorber rod plug)	7.90	C	0.12	4.7531E-04
		Si	0.18	3.0490E-04
		Mn	2.0	1.7319E-03
		Cr	18.0	1.6469E-02
		Fe	69.7	5.9375E-02
		Ni	10.0	8.1060E-03
Rubber	1.07	C	84.0	4.5064E-02
		H	11.0	7.0324E-02
		S	5.0	1.0047E-03

Table 5.1.3.2-4. Material Atom Densities for HCT-005 Experiments (p. 14, Ref. 7.3, HCT-005)

Material	Density (g/cm^3)	Element/Isotope	wt%	Atom density (atoms/b-cm)
Water	0.9982	H	11.19	6.6736×10^{-2}
		O	88.81	3.3368×10^{-4}
Aluminum alloy AD1	2.71	Al	99.30	6.0062×10^{-2}
		Si	0.35	2.0337×10^{-4}
		Fe	0.30	8.7667×10^{-5}
		Cu	0.05	1.2841×10^{-5}
Stainless Steel	7.90	C	0.09	3.5648×10^{-4}
		Si	0.80	1.3551×10^{-3}
		Cr	16.00	1.4639×10^{-2}
		Fe	64.21	5.4698×10^{-2}
		Ni	15.00	1.2159×10^{-2}
		Nb	0.90	4.6086×10^{-4}

Table 5.1.3.2-4. Material Atom Densities for HCT-005 Experiments (p. 14, Ref. 7.3, HCT-005)

Material	Density (g/cm^3)	Element/Isotope	wt%	Atom density (atoms/b-cm)
		Mo	3.00	1.4876×10^{-3}
Plexiglas	1.18	H	8.06	5.6826×10^{-2}
		O	31.96	1.4194×10^{-2}
		C	59.98	3.5486×10^{-2}
Fuel	8.1118	U^{234}	0.2579	5.3830×10^{-5}
		U^{235}	21.2707	4.4208×10^{-3}
		U^{236}	0.0590	1.2208×10^{-5}
		U^{238}	5.1788	1.0627×10^{-3}
		O	3.7206	1.1360×10^{-2}
		Cu	69.5130	5.3437×10^{-2}

Table 5.1.3.2-5. Material Atom Densities for HCT-006 Experiments (p. 16, Ref. 7.3, HCT-006)

Material	Density (g/cm^3)	Element/Isotope	wt%	Atom density (atoms/b-cm)
Water	0.9982	H	11.19	6.6736E-02
		O	88.81	3.3368E-02
Alloy AD1	2.71	Al	99.3	6.0062E-02
		Si	0.35	2.0337E-04
		Fe	0.3	8.7667E-05
		Cu	0.05	1.2841E-05
Stainless Steel	7.90	C	0.09	3.5648E-04
		Si	0.8	1.3551E-03
		Cr	16.0	1.4639E-02
		Fe	64.21	5.4698E-02
		Ni	15.0	1.2159E-02
		Nb	0.9	4.6086E-04
		Mo	3.0	1.4876E-03
Plexiglas	1.18	H	8.06	5.6826E-02
		O	31.96	1.4194E-02
		C	59.98	3.5486E-02
Fuel	8.1118	U^{234}	0.2579	5.3830E-05
		U^{235}	21.2707	4.4208E-03
		U^{236}	0.05899	1.2208E-05
		U^{238}	5.1788	1.0627E-03
		O	3.7206	1.1360E-02
		Cu	69.513	5.3437E-02

Table 5.1.3.2-6. Materials Atom Densities for HCT-007 Experiments (p. 18, Ref. 7.3, HCT-007)

Material	Element/Isotope	Atom density (atoms/b-cm)
Water	H	6.6736×10^{-2}
	O	3.3368×10^{-4}
Aluminum alloy AD1	Al	6.0062×10^{-2}
	Si	2.0337×10^{-4}
	Fe	8.7667×10^{-5}
	Cu	1.2841×10^{-5}
Stainless Steel	C	3.5648×10^{-4}
	Si	1.3551×10^{-3}
	Cr	1.4639×10^{-2}
	Fe	5.4698×10^{-2}
	Ni	1.2159×10^{-2}
	Nb	4.6086×10^{-4}
	Mo	1.4876×10^{-3}
Plexiglas	H	5.6826×10^{-2}
	O	1.4194×10^{-2}
	C	3.5486×10^{-2}
Fuel	U^{234}	5.3830×10^{-5}
	U^{235}	4.4208×10^{-3}
	U^{236}	1.2208×10^{-5}
	U^{238}	1.0627×10^{-3}
	O	1.1360×10^{-2}
	Cu	5.3437×10^{-2}
Zirconium Hydride	Zr	2.8722×10^{-2}
	H	5.3423×10^{-2}
	Fe	2.4018×10^{-5}
	Ni	1.1427×10^{-5}
	Mn	9.7660×10^{-6}
	C	6.7005×10^{-5}
	Si	4.7758×10^{-5}
	Hf	1.5029×10^{-6}
	O	8.3836×10^{-5}
	Be	8.9300×10^{-5}
	Ca	2.0081×10^{-5}

Table 5.1.3.2-7. Material Atom Densities for HCT-008 Experiments (p. 17, Ref. 7.3, HCT-008)

Material	Density (g/cm^3)	Element/Isotope	wt%	Atom density (atoms/b-cm)
Water	0.9982	H	11.19	6.6736E-02
		O	88.81	3.3368E-02

Table 5.1.3.2-7. Material Atom Densities for HCT-008 Experiments (p. 17, Ref. 7.3, HCT-008)

Material	Density (g/cm^3)	Element/Isotope	wt%	Atom density (atoms/b-cm)
Alloy AD1	2.71	Al	99.3	6.0062E-02
		Si	0.35	2.0337E-04
		Fe	0.3	8.7667E-05
		Cu	0.05	1.2841E-05
Stainless Steel	7.90	C	0.09	3.5648E-04
		Si	0.8	1.3551E-03
		Cr	16.0	1.4639E-02
		Fe	64.21	5.4698E-02
		Ni	15.0	1.2159E-02
		Nb	0.9	4.6086E-04
		Mo	3.0	1.4876E-03
Plexiglas	1.18	H	8.06	5.6826E-02
		O	31.96	1.4194E-02
		C	59.98	3.5486E-02
Fuel	8.11181	U^{234}	0.2579	5.3830E-05
		U^{235}	21.2707	4.4208E-03
		U^{236}	0.05899	1.2208E-05
		U^{238}	5.1788	1.0627E-03
		O	3.7206	1.1360E-02
		Cu	69.513	5.3437E-02
Absorber (Case 1)	1.13505	B^{10}	1.6418	1.1208E-03
		B^{11}	7.2662	4.5114E-03
		C	2.4742	1.4081E-03
		Al	46.9010	1.1882E-02
		O	41.7168	1.7823E-02
Absorber (Case 2)	1.17771	B^{10}	5.5370	3.9220E-03
		B^{11}	24.5051	1.5786E-02
		C	8.3442	4.9271E-03
		Al	32.6091	8.5716E-03
		O	29.0046	1.2857E-02

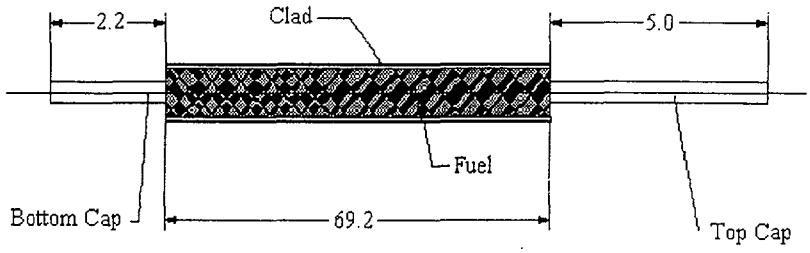

Figure 5.1.3.2-1. Fuel Rod Representation for HCT-003 and HCT-007 (dimensions in cm)

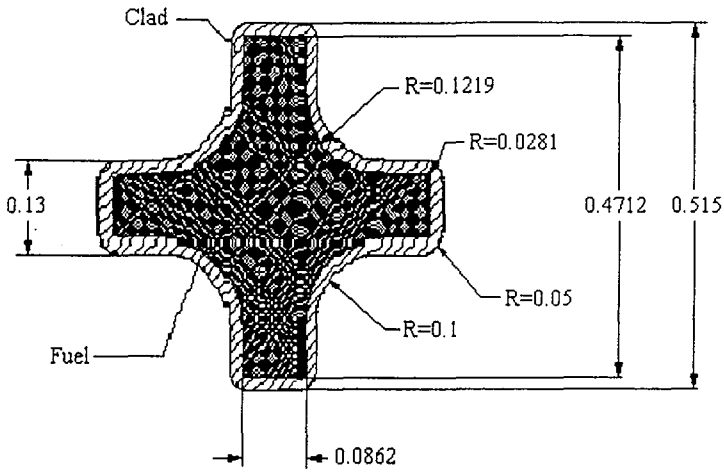

Figure 5.1.3.2-2. Cross Section of Cross-Shaped Fuel Rod for HCT-003 and HCT-007 (dimensions in cm)

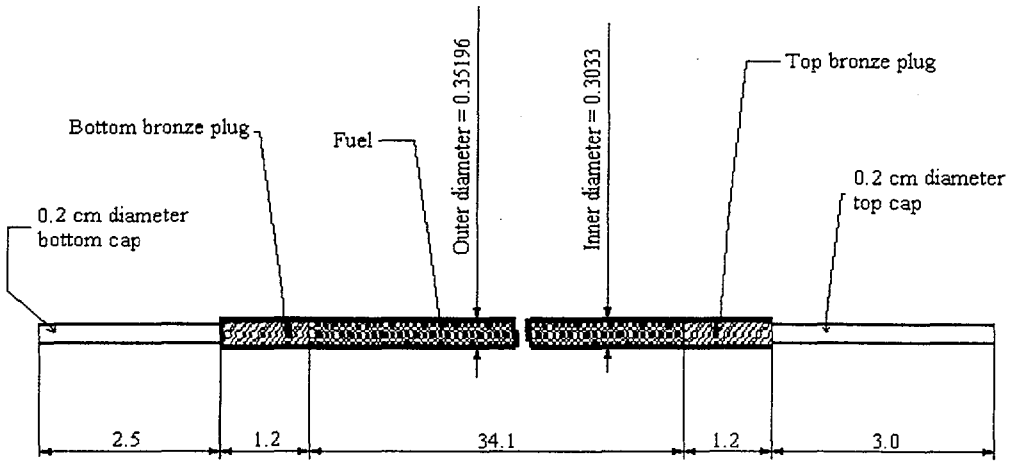

Figure 5.1.3.2-3. Cylindrical Representation of Fuel Rod for HCT-004 (dimensions in cm)

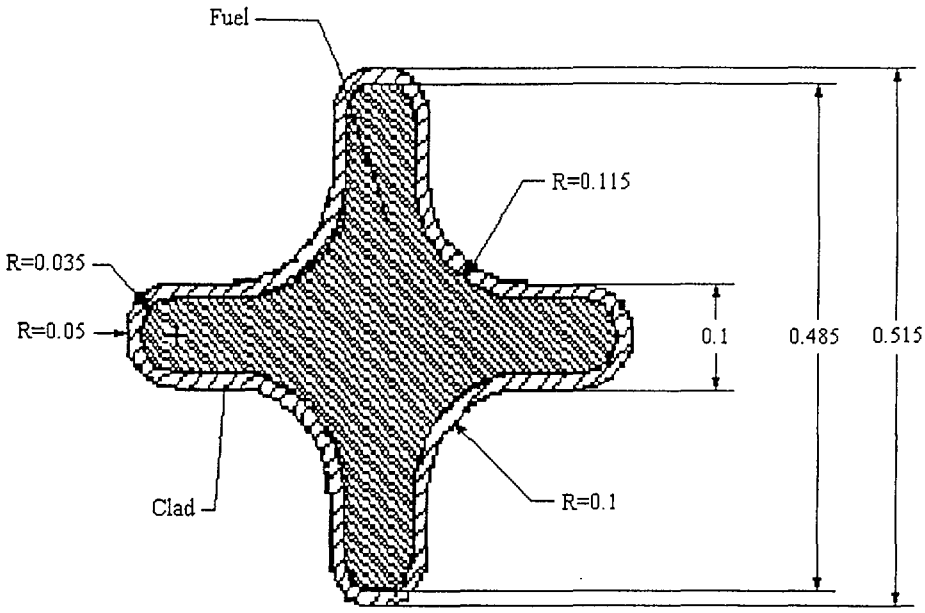

Figure 5.1.3.2-4. Cross Section of Cross-Shaped Fuel Rod for HCT-004 (dimensions in cm)

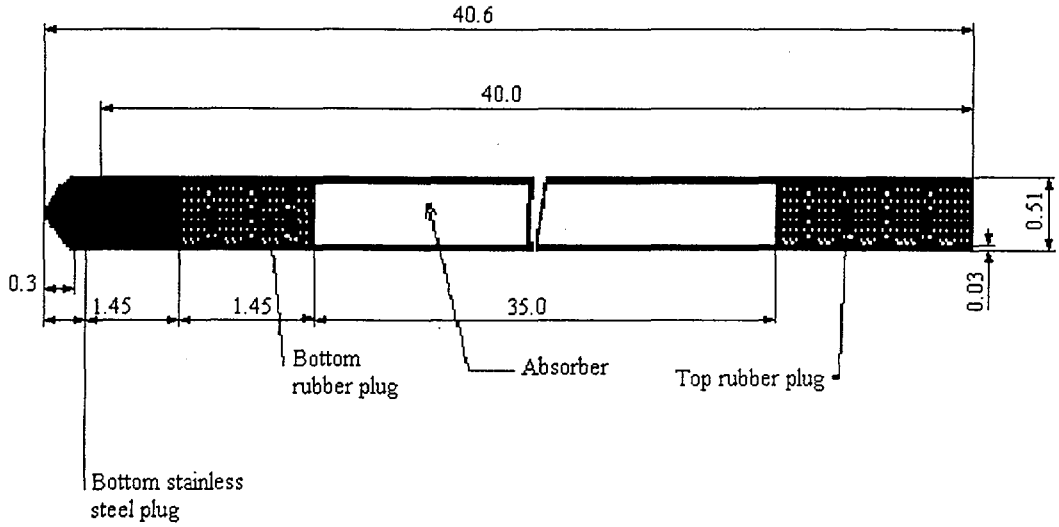

Figure 5.1.3.2-5. Absorber Rod for HCT-004 (dimensions in cm)

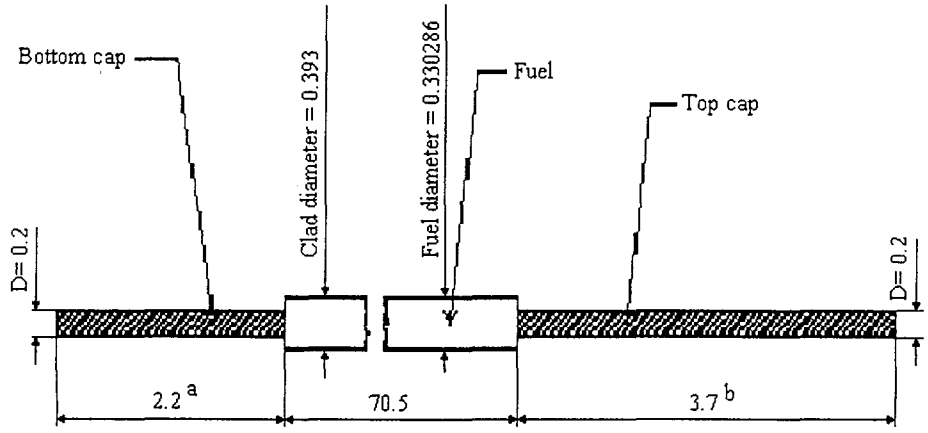

a 2.5 is actually used in model
b 3.4 is actually used in model

Figure 5.1.3.2-6. Cylindrical Representation of Fuel Rod for HCT-005, 006, & 008 (dimensions in cm)

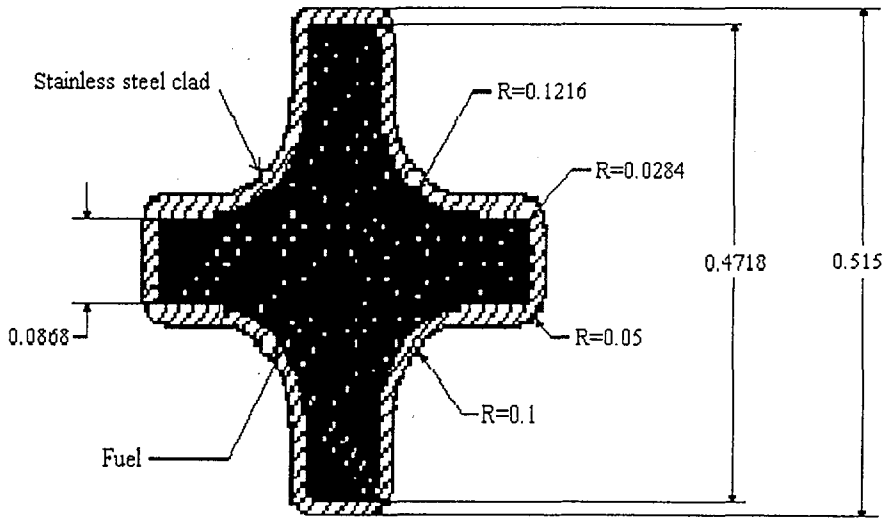

Figure 5.1.3.2-7. Cross Section of Cross-Shaped Fuel Rod in HCT-005, 006, & 008 (dimensions in cm)

Note: Length of the fuel region and dimensions of fuel rod caps in the cross-shaped representation of the fuel rods are the same as in the cylindrical representation for cases from HCT-003 through HCT-008.

5.1.3.3 Critical Experiments of EBOR Fuel Pins in Water

Twenty-one critical experiments involving lattices of EBOR (Experimental Beryllium Oxide Reactor) fuel pins were performed in 1967 at Oak Ridge National Laboratory. The fuel pins consisted of compressed ceramic pellets contained in Hastelloy X-280 tubes. The pellets were a homogeneous mixture of $U(62.4)O_2$ and BeO. Two sets of experiments were conducted. The first set of experiments (total of 15 experiments) consisted of EBOR fuel pins arranged in various lattice configurations moderated and reflected by water (p. 8, Ref 7.3, HEU-COMP-THERM-010 (HCT-010)). The second set (6 experiments) consisted of EBOR fuel pins arranged in various lattice configurations with boron and/or with uranyl nitrate in the water (p. 14, Ref. 7.3, HCT-010). All 21 fuel-pin experiments are considered acceptable for use as benchmark experiments by the evaluators. Detailed experimental configuration descriptions are available on pages 21 through 28 of Reference 7.3, HCT-010. Figure 5.1.3.3-1 shows the MCNP case EBOR fuel pin. Table 5.1.3.3-1 provides a listing of the 21 cases and the k_{eff} values in the experimental configurations. Descriptions of the experimental case materials are given in Tables 5.1.3.3-2 through 5.1.3.3-5. The plexiglas spacers and grid plates were omitted from the MCNP representation because they were considered to have a negligible effect on system reactivity by the evaluator (< 0.0005 (p. 21, Ref. 7.3, HCT-010)).

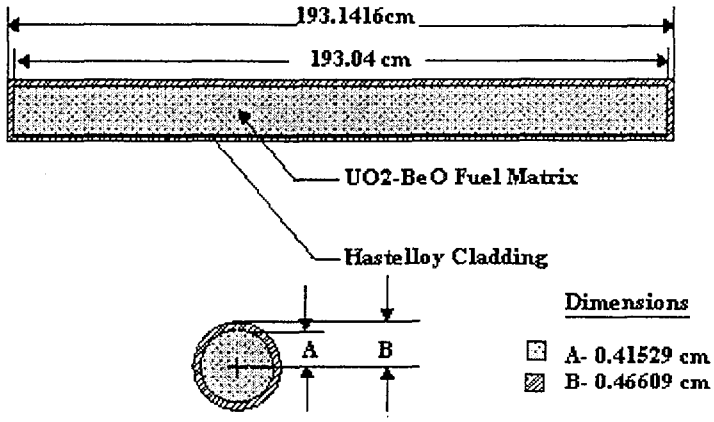

Figure 5.1.3.3-1. EBOR Fuel Pin (p. 22, Ref. 7.3, HCT-010)

Table 5.1.3.3-1. Configurations of HCT-010 Experiments

Handbook case name	Surface separation (cm)	Critical number of pins	Critical height of solution above the fuel in the fuel tank (cm)[a]	Solution inside the core	Benchmark $k_{eff} \pm \sigma$ (p. 27, Ref. 7.3, HCT-010)	H/X ratio	MCNP case name
1	0.290	222	15.2000	Water	1.0000 ± 0.0050	48.54482	hct101
2	0.290	223	-50.3000	Water	1.0000 ± 0.0050	35.82476	hct102
3	0.536	138	30.8000	Water	1.0000 ± 0.0050	72.18697	hct103
4	0.790	102	-21.3000	Water	1.0000 ± 0.0050	100.5069	hct104
5	1.046	85	15.2000	Water	1.0000 ± 0.0050	147.8713	hct105

Table 5.1.3.3-1. Configurations of HCT-010 Experiments

Handbook case name	Surface separation (cm)	Critical number of pins	Critical height of solution above the fuel in the fuel tank (cm)[a]	Solution inside the core	Benchmark $k_{eff} \pm \sigma$ (p. 27, Ref. 7.3, HCT-010)	H/X ratio	MCNP case name
6	1.046	86	-60.8000	Water	1.0000 ± 0.0050	100.1198	hct106
7	1.323	78	15.2000	Water	1.0000 ± 0.0050	169.6527	hct107
8	1.323	79	-39.0000	Water	1.0000 ± 0.0050	133.664	hct108
9	1.300	77	-3.90000	Water	1.0000 ± 0.0050	203.7219	hct109
10	1.554	75	15.2000	Water	1.0000 ± 0.0050	264.8866	hct110
11	1.554	76	-61.3000	Water	1.0000 ± 0.0050	178.3931	hct111
12	1.826	77	-43.2000	Water	1.0000 ± 0.0050	246.5002	hct112
13	2.042	83	-34.1000	Water	1.0000 ± 0.0050	282.1252	hct113
14	1.544 1.585 [b]	96	-10.4000	Water	1.0000 ± 0.0050	189.3971	hct114
15	1.6477	75	-12.2000	Water	1.0000 ± 0.0050	218.6614	hct115
16	1.5478	99	19.3675	Water	1.0001 ± 0.0044	203.6688	hct116
17	1.5478	114	19.3675	Aqueous solution of boron	1.0010 ± 0.0074	197.7812	hct117
18	1.5478	113	19.3675	Aqueous solution of boron	1.0000 ± 0.0074	199.5315	hct118
19	1.5478	133	19.3675	Aqueous solution of boron	1.0000 ± 0.0074	197.711	hct119
20	1.5478	83	19.3675	Aqueous solution of uranyl nitrate	1.0001 ± 0.0047	302.2943	hct120
21	1.5478	133	19.3675	Aqueous solution of uranyl nitrate and boron	1.0007 ± 0.0076	191.7556	hct121

[a] Negative water heights refer to distance below top of fuel.

[b] The average surface separation was 1.544 cm between pins in the 16-pin direction and 1.585 cm in the 6-pin direction.

Table 5.1.3.3-2. Fuel Matrix Atom Density in atoms/b-cm for HCT-010 Experiments (p. 25, Ref. 7.3, HCT-010)

Cases	U^{235}	U^{234}	U^{236}	U^{238}	Be	O
1-21	3.8280×10^{-3}	2.5881×10^{-5}	1.7715×10^{-5}	2.2351×10^{-3}	4.9386×10^{-2}	6.1599×10^{-2}

Table 5.1.3.3-3. Structural Materials for HCT-010 Experiments (pp. 25, 26, Ref. 7.3, HCT-010)

Material	Element/Isotope	wt%	Atom Density (atoms/b-cm)
Hastelloy X-280 (8.23 g/cm^3)	Co	1.50[a]	1.2615×10^{-3}
	Fe	18.50	1.6418×10^{-2}
	Cr	22.00	2.0970×10^{-2}
	Mo	9.00	4.6493×10^{-3}
	W	0.60	1.6175×10^{-4}
	C	0.15[a]	6.1896×10^{-4}
	Ni	48.28[b]	4.0746×10^{-2}
Stainless Steel 304 (7.92 g/cm^3)	Fe	69.50	5.9355×10^{-2}
	Cr	19.00	1.7428×10^{-2}
	Ni	9.50	7.7203×10^{-3}
	Mn	2.00	1.7363×10^{-3}
Water	H	N/A	6.6735×10^{-2}
	O	N/A	3.3368×10^{-2}

[a] maximum value

[b] balance

Table 5.1.3.3-4. Solution in the Tank Atom Density (p. 26, Ref. 7.3, HCT-010)

Cases	U^{235}	U^{238}	B^{10}	B^{11}	O ($\times10^{-2}$)	N ($\times10^{-5}$)	H ($\times10^{-2}$)
1-16	0.0	0.0	0.0	0.0	3.3368	0.0	6.6735
17	0.0	0.0	4.3231×10^{-7}	1.7401×10^{-6}	3.3381	0.0	6.6762
18	0.0	0.0	4.3231×10^{-7}	1.7401×10^{-6}	3.3381	0.0	6.6762
19	0.0	0.0	2.1061×10^{-6}	2.1061×10^{-6}	3.3365	0.0	6.6729
20	9.4286×10^{-6}	7.4396×10^{-7}	0.0	0.0	3.3342	2.0345	6.6521
21	9.4286×10^{-6}	7.4396×10^{-7}	3.4918×10^{-6}	1.4055×10^{-5}	3.3371	2.0345	6.6527

5.1.4 HEU Epithermal Systems

5.1.4.1 Intermediate Heterogeneous Assembly with Highly Enriched Uranium Dioxide and Sand/Water Radial Reflector

An experiment was performed at the RRC "Kurchatov Institute" to investigate accidental sand and water immersion criticality safety of the thermionic intermediate reactor-converter with highly enriched fuel

(approximately 96% U^{235}), zirconium hydride moderator, and end beryllium reflectors (p. 1, Ref. 7.3, HEU-COMP-INTER-002 (HCI-002)). Described in this category are five configurations of the critical assemblies simulating water ingress into different reactor cavities, as well as surrounding the reactor with sand and water. All five configurations are considered acceptable for use as benchmark critical experiments by the evaluators. The benchmark specifications of each configuration are reported on pages 25 through 36 of Reference 7.3, HCI-002. Figures 5.1.4.1-1 through 5.1.4.1-4 (pp. 3, 5, and 33, Ref. 7.3, HCI-002) illustrate the physical dimensions of the thermionic intermediate reactor as simulated. Table 5.1.4.1-1 provides a listing of the 5 cases and the benchmark $k_{eff} \pm \sigma$. In configurations 1 and 2, wet sand is the reflector material and the rotating drums are filled with wet sand. All cavities are filled with water. The number of drums and the position of the control drums vary. In configurations 3, 4, and 5, the drum channels were removed (Figure 5.1.4.1-4), water is the radial reflector, and the number of drums and their positions vary. Tables 5.1.4.1-2 and 5.1.4.1-3 provide atom densities of the reflector and fuel respectively, used in the cases. Atom densities of the other materials used for the case are given on pages 39 and 40 of Reference 7.3, HCI-002.

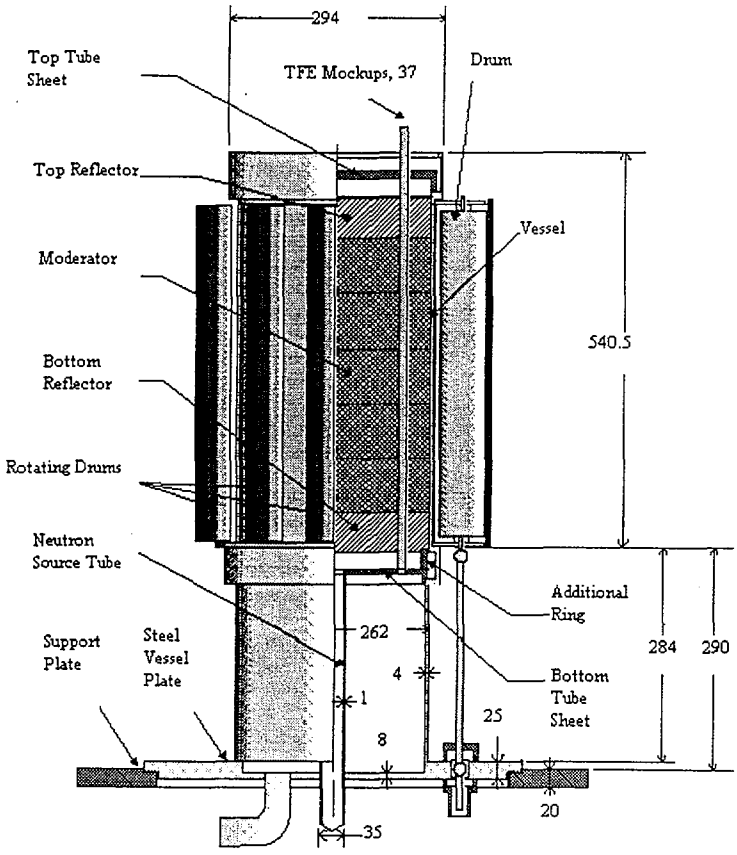

Figure 5.1.4.1-1. Axial Section of the Core with the Vessel, Rotating Drums, and End Reflectors (dimensions in cm) (p. 5, Ref. 7.3, HCI-002)

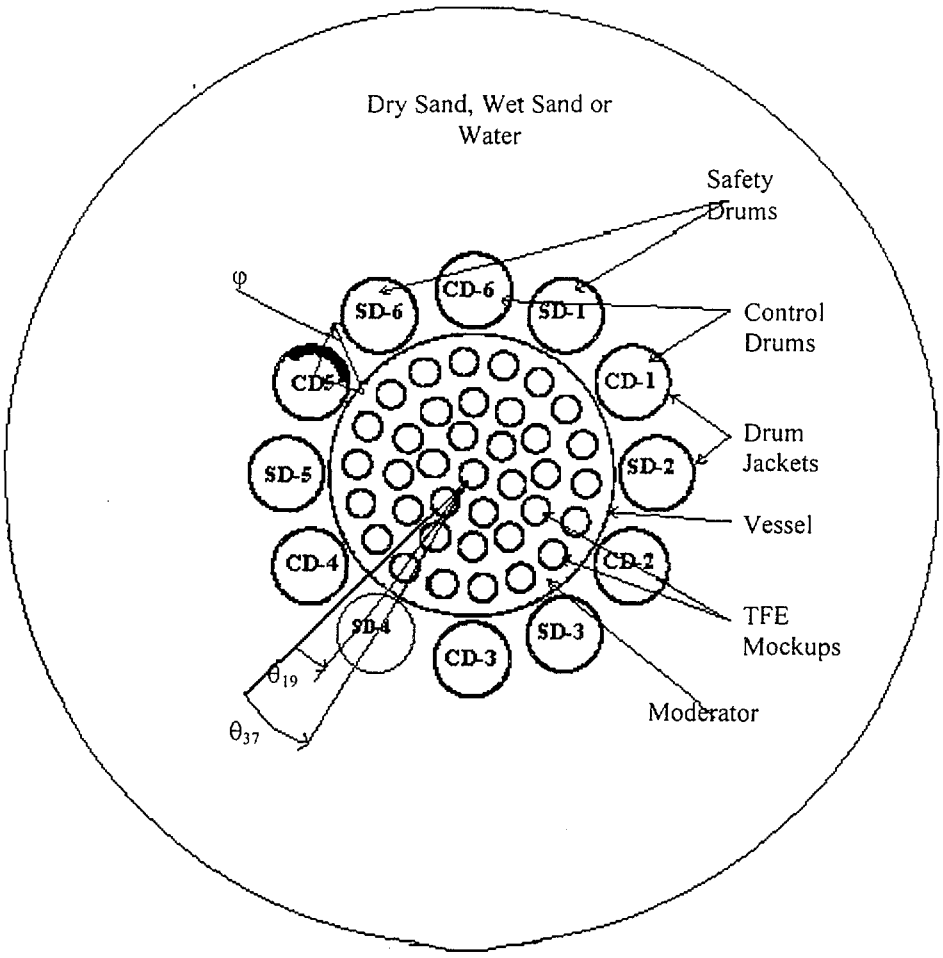

Figure 5.1.4.1-2. Cross Section of the Critical Assembly Representation Through the Core Center (φ is the angle of the drum rotation) (p. 3, Ref. 7.3, HCI-002)

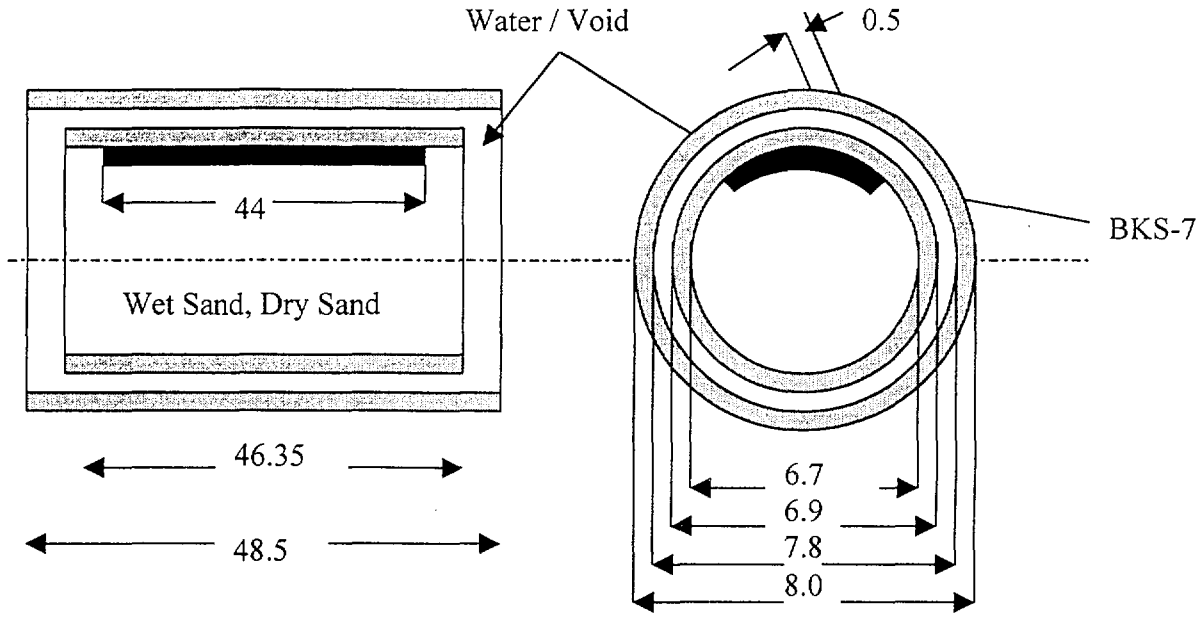

Figure 5.1.4.1-3. Schematic of the Control and Safety Drum Filled with Sand as Adopted in the Computational Simulation with Sand Radial Reflector (dimensions in cm) (p. 33, Ref. 7.3, HCI-002)

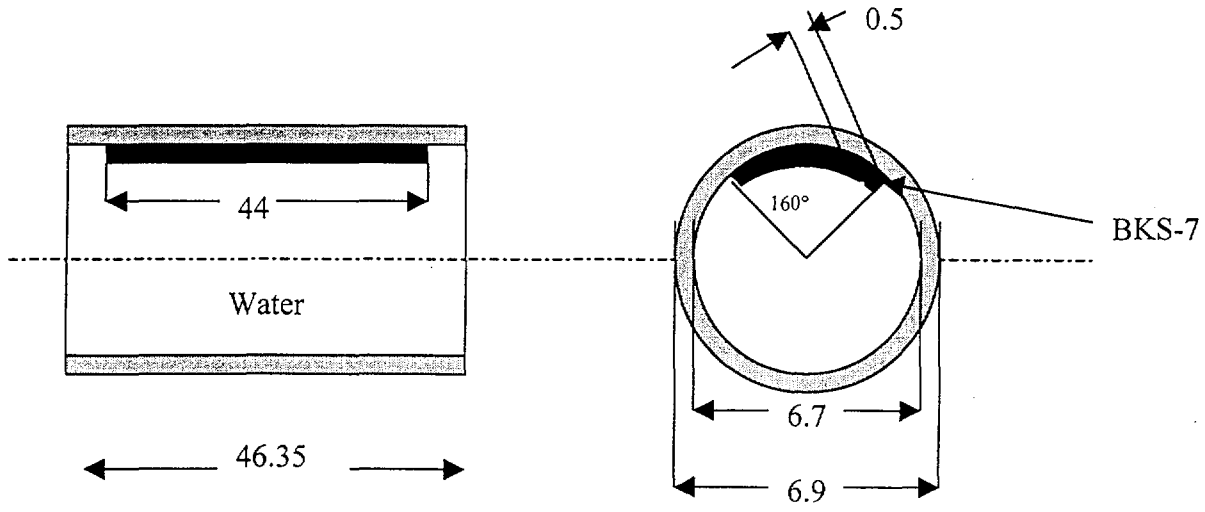

Figure 5.1.4.1-4. Schematic of the Control and Safety Drum Filled with Water as Adopted in the Computational Representation with Water Radial Reflector (dimensions in cm) (p. 33, Ref. 7.3, HCI-002)

Table 5.1.4.1-1. Configurations of Benchmark Experiments with 37 Fuel Elements in Assembly (p. 14, Ref. 7.3, HCI-002)

Handbook case name	Material		Rotating Drums		Benchmark $k_{eff} \pm \sigma$ (p. 42, Ref. 7.3, HCI-002)	H/X ratio	MCNP case name
	Radial reflector	Core cavities	Total number	Position in assemblies*			
1	SiO_2 +H_2O	H_2O	12	CD-5, φ=36° CD-1 ↑,CD-3 ↓, CD-6 ↓, the other CD and all SD ↑	1.0000± 0.0004	23.9436	hci2-1
2	SiO_2 +H_2O	H_2O	11	CD-5, φ=121° CD-3 removed, CD-1, 2, 4, 6 ↓, CD-6 ↓, all SD ↑	1.0000± 0.0004	23.9436	hci2-2
3	H_2O	H_2O	12	CD-5, φ=119.5° the other CD and all SD ↑	1.0000± 0.0004	23.9436	hci2-3
4	H_2O	H_2O	11	CD-5, φ=95.5° CD-3 removed, the other CD and all SD ↑	1.0000± 0.0004	23.9436	hci2-4
5	H_2O	H_2O	10	CD-5, φ=76° CD-3 and SD-3 removed, the other CD and all SD ↑	1.0000± 0.0004	23.9436	hci2-5

* ↑ -Control drums turned out (φ=180°),
↓ -Control drums turned in (φ=0°),
Rotation angle φ is shown in Figure 5.1.4.1-2.

Table 5.1.4.1-2. Atom Densities of the Reflector Materials in HCI-002 Experiments (p. 37, Ref. 7.3, HCI-002)

Material	Element/Isotope	Atom density (atoms/b-cm)
End reflector[a]		
Core	Be	1.2295×10^{-1}

Table 5.1.4.1-2. Atom Densities of the Reflector Materials in HCI-002 Experiments (p. 37, Ref. 7.3, HCI-002)

Material	Element/Isotope	Atom density (atoms/b-cm)
TFE[b] (BeO)	Be	6.9342×10^{-2}
	O	6.9342×10^{-2}
Radial reflector		
Water	H	6.6735×10^{-2}
	O	3.3368×10^{-2}
Dry Quartz Sand	Si	1.5639×10^{-2}
	O	3.1336×10^{-2}
	H	5.2314×10^{-6}
	B^{10}	3.4520×10^{-8}
	B^{11}	1.3983×10^{-7}
	Al	3.6973×10^{-5}
	Ti	9.8419×10^{-6}
	Fe	6.7503×10^{-6}
Wet Quartz Sand	Si	1.6134×10^{-2}
	O	4.4980×10^{-2}
	H	2.5307×10^{-2}
	B^{10}	3.5612×10^{-8}
	B^{11}	1.4425×10^{-7}
	Al	3.8143×10^{-5}
	Ti	1.0153×10^{-5}
	Fe	6.9639×10^{-6}

[a] Impurities found in the end reflectors material were included in the wt% Be. This addition was determined to be negligible in the reactivity calculation (p. 37, Ref. 7.3, HCI-002).

[b] TFE = Thermionic Fuel Elements

Table 5.1.4.1-3. Atom Densities of the Moderators and Fuel in HCI-002 Experiments (p. 38, Ref. 7.3, HCI-002)

Material	Element/Isotope	Atom density (atoms/b-cm)
ZrH_n[a]	H	6.8759×10^{-2}
	Zr	3.5848×10^{-2}
	Nb	3.3032×10^{-4}
	Hf	5.6682×10^{-7}
UO_x[b]	U^{234}	2.5363×10^{-4}
	U^{235}	2.2526×10^{-2}
	U^{236}	5.8712×10^{-5}
	U^{238}	6.4583×10^{-4}

Table 5.1.4.1-3. Atom Densities of the Moderators and Fuel in HCI-002 Experiments (p. 38, Ref. 7.3, HCI-002)

Material	Element/Isotope	Atom density (atoms/b-cm)
	O	4.7087×10^{-2}
Foil	Al	6.0262×10^{-2}

[a] See page 38 of Reference 7.3, HCI-002.

[b] Impurities found in the fuel were included in the wt% UO_x. According to page 38 of Reference 7.3, HCI-002, this has a negligible effect on system reactivity.

5.1.5 Pu Fueled Thermal Systems

5.1.5.1 FFTF Fuel Pin Array Experiments

The experimental program considered predicted critical configurations extrapolated from near critical experiments with plutonium oxide-uranium oxide fuel pins containing about 20 wt% plutonium with light water moderation and reflection (p. 1, Ref. 7.3, MIX-COMP-THERM-001 (MCT-001)). Six experiments were evaluated and are considered acceptable for use as benchmark experiments by the evaluators. These experiments were performed at the PNL Critical Mass Laboratory. The experimental configuration was comprised in an array of fast test reactor fuel pins (Figure 5.1.5.1-1) within a large tank containing water. An axial description of experimental arrangement is shown on page 4 of Reference 7.3, MCT-001. In the case, the steel grids were replaced with polypropylene grids (p. 4, Ref. 7.12). Various lattice pitches were used in the array, resulting in different numbers of fuel rods being required to obtain criticality. The fuel used for the experimental program was a mixture of PuO_2 and UO_2, with the pins comprised of either 19.84 or 24.39 wt% plutonium (p. 141, Ref. 7.12). The plutonium contained 11.5 wt% Pu^{240}, and the uranium in the PuO_2-UO_2 mixture was natural uranium. The remainder of the pin consisted of end-caps, plenum, and other types of hardware (e.g., natural UO_2 insulators and Inconel reflectors). The benchmark k_{eff} for these experiments was experimentally determined to be unity. The uncertainty associated with four of the experiments is given on page 18 of Reference 7.3, MCT-001. Table 5.1.5.1-1 provides a brief description of these experiments along with their MCNP case names. Table 5.1.5.1-2 provides the composition for the material used in the case as reported on page 9 of Reference 7.3, MCT-001. The fuel composition was established using the data in Reference 7.12. The fuel composition was established in May 1972 and the experiment took place in 1978. Therefore, a decay calculation (equation 5.1.5.1-1) was done to establish the fuel composition during the experiment.

Equation 5.1.5.1-1

$$W_i(t) = W_i(t_0)\exp\left(-\frac{t}{T_{1/2}}\ln 2\right)$$

where: $W_i(t)$ is the weight percent of isotope i at time t

$T_{1/2}$ is the half life of isotope i
t is the time at which the experiment took place (February 1978: p. 12, Ref. 7.3, MCT-001)
t_0 is the time at which the fuel composition was evaluated (April-May 1972: p. 12, Ref. 7.3, MCT-001)

Table 5.1.5.1-1. FFTF Bierman Array Critical Experiments

Experiment Number	Description (p. 7, Ref. 7.11)	H/X ratio	σ	MCNP case name
001	18 pin lattice width, 1.2588 cm lattice spacing, 279 total pins	1742.38	0.0026	fftf001
003r	36 pin lattice width, 0.7671 cm lattice spacing, 1037 total pins	555.09	0.00305	fftf003r
004	18 pin lattice width, 1.5342 cm lattice spacing, 205 total pins	11273.00	0.0032	fftf004
005	28 pin lattice width, 0.9525 cm lattice spacing, 605 total pins	835.37	0.0025	fftf005
006	14 pin lattice width, 1.9050 cm lattice spacing, 162 total pins	17210.22	0.0039	fftf006
029	28 pin lattice width, 0.9677 cm lattice spacing, 580 total pins	867.99	0.00305	fftf029

Table 5.1.5.1-2. Material Compositions for FFTF Critical Experiments

Material	Density (g/cm^3)	Element/Isotope	wt%
Stainless Steel 316L (p. 2, Ref. 7.23)	8.00 (p. 34, Ref. 7.25)	C	0.03
		Mn	2.00
		P	0.045
		S	0.03
		Si	1.00
		Cr	17.00
		Ni	12.00
		Mo	2.50
		N	0.10
		Fe	65.295 (balance)
Inconel 600 (p. 9, Ref. 7.8)	8.47	Ni	74.335
		Cr	15.50
		Fe	8.00
		C	0.15
		Mn	1.00
		S	0.015
		Si	0.500
		Cu	0.500
Stainless Steel 304[a] (p. 2, Ref. 7.24)	2.6667[b]	C	0.080
		Mn	2.000
		P	0.045
		S	0.030

Table 5.1.5.1-2. Material Compositions for FFTF Critical Experiments

Material	Density (g/cm^3)	Element/Isotope	wt%
		Si	0.750
		Cr	19.00
		Ni	9.250
		N	0.100
		Fe	68.745
Aluminum T6061 (p. 13, Ref. 7.3, LCT-001)	2.69	Si	0.6
		Fe	0.7
		Cu	0.25
		Mn	0.15
		Mg	1.0
		Cr	0.2
		Zn (added as copper)	0.25
		Ti	0.15
		Al	96.7 (balance)
Plexiglas (p. 17, Ref. 7.3, HCT-008)	1.18	H	8.06
		O	31.96
		C	59.98
Carbon Steel Grade 55 A 516 (p. 2, Ref. 7.26)	7.85 (p. 192, Ref. 7.25)	C	0.18
		Mn	0.75
		P	0.035
		S	0.035
		Si	0.275
		Fe	98.725 (balance)
Natural UO_2[c]	10.42 (p. 143, Ref. 7.12)	U^{234}	0.0048
		U^{235}	0.6267
		U^{238}	87.5183
		O	11.8502
Type 3.2 Fuel (Ref. 7.12)	9.830 (p. 143, Ref. 7.12)	Pu^{238}	0.0297
		Pu^{239}	16.9683
		Pu^{240}	2.2733
		Pu^{241}	0.3564
		Pu^{242}	0.0694
		Am^{241}	0.1395
		U^{235}	0.4853
		U^{238}	67.8638
		O	11.814
Polypropylene C_3H_6[c]	0.904 (p. 142, Ref. 7.12)	H	14.371
		C	85.629
Normal Concrete (p. M8.2.33, Ref. 7.10)	2.3	O	53.2
		Si	33.7
		Ca	4.4
		Al	3.4
		Na	2.9

Table 5.1.5.1-2. Material Compositions for FFTF Critical Experiments

Material	Density (g/cm^3)	Element/Isotope	wt%
		Fe	1.4
		H	1.0
Type 3.1 Fuel (Ref. 7.12)	9.783 (p. 143, Ref. 7.12)	Pu^{238}	0.0365
		Pu^{239}	20.8508
		Pu^{240}	2.8046
		Pu^{241}	0.4381
		Pu^{242}	0.0853
		Am^{241}	0.1715
		U^{235}	0.4547
		U^{238}	6.5857
		O	11.5728

[a] Type 304 Stainless Steel was represented, but Stainless Steel Type 302 was indicated on page 143 of Reference 7.12. This results in a negligible effect on system reactivity.

[b] Page 143 of Reference 7.12 indicates a maximum spring volume of 2.7264 cm^3, this value is believed to be in error because it is greater than the volume that the spring occupies. This region was homogenized as void and Stainless Steel 304 with a stainless steel volume fraction of 0.3333. The effect of using stainless steel over the range of 1.0 volume fraction to 0.0 volume fraction in this region is negligible. The referenced density was 8.00 g/cm^3 (p. 34, Ref. 7.25).

[c] Weight percents were calculated using equation 5.1.4.1-1

[d] This value is 0.2596 for experiment FFTF029 (p. 6, Ref. 7.11)

[e] This value is 0.0980 for experiment FFTF029 (p. 6, Ref. 7.11)

Equation 5.1.4.1-1

$$wt\%_i = \frac{at\%_i * (atomic\_mass)_i}{\sum at\%_i * (atomic\_mass)_i}$$

where: $at\%_i$ is atom percent of the isotopic species i
(atomic_mass)i is the isotopic mass of isotopic species i

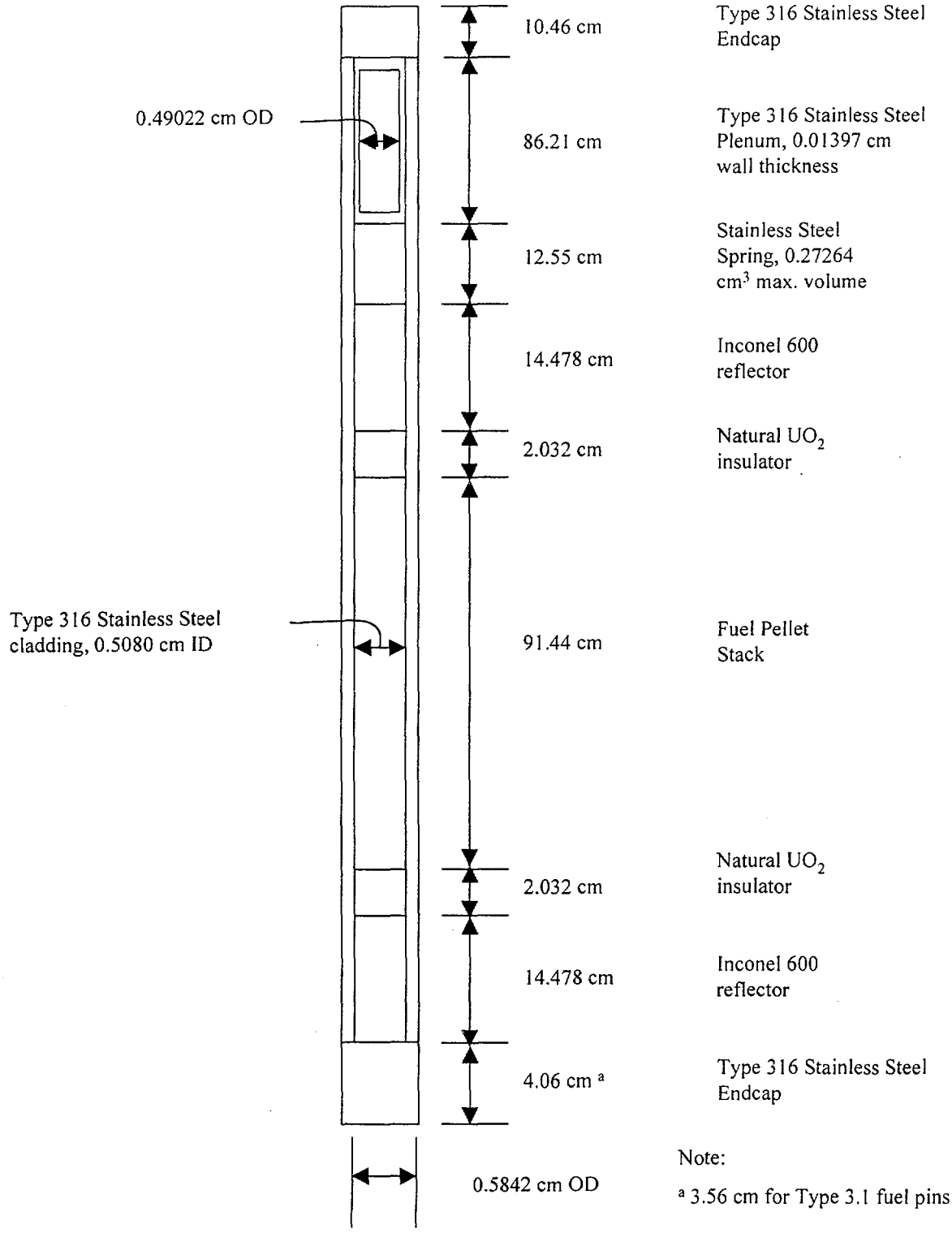

Figure 5.1.5.1-1. Type 3.2 Fast Test Reactor Fuel Pin (p. 143, Ref. 7.12)

5.1.5.2 Saxton Plutonium Program Experiment

Single and multi-region uranium and plutonium oxide fueled cores, water moderated, clean, and borated, have been used in a series of critical experiments at the Westinghouse Reactor Evaluation Center in support of the Saxton Plutonium Program. In this series of experiments, criticality was achieved entirely by varying the water level inside the core tank. The fuel used in the experiments were UO_2 fuel with 5.74 wt% U^{235} enrichment, and MOX fuel containing 6.6 wt% PuO_2 and natural enriched UO_2 (p. 231, Ref. 7.16). Figure 5.1.5.2-1 illustrates the physical dimensions of the fuel rods as used in the MCNP input decks, and Figure 5.1.5.2-2 illustrates the core tank as represented in the MCNP input decks. A description of the experiments analyzed in this calculation, and the MCNP case names is presented in Table 5.1.5.2-1. A detailed description of the experimental configuration for the MOX single-region experiments is provided on pages 4, 7, and 24 of Reference 7.3, MIX-COMP-THERM-003 (MCT-003), and a description of the multi-region and UO_2 single-region experiments is provided in Attachment B of Reference 7.22. Table 5.1.5.2-2 presents the UO_2 fuel rod specifications, Table 5.1.5.2-3 presents the MOX fuel rod specifications, and Table 5.1.5.2-4 presents the clad and end plug material compositions for the Zircaloy-4 clad. The benchmark k_{eff} values for the single-region experiments were 1.000 with an uncertainty of ± 0.0071, ± 0.0057, ± 0.0052, ± 0.0028, ± 0.0024, and ± 0.0020 for cases 3, 4, 5, 6, 7, and 8 as shown in Table 5.1.5.2-1, respectively (p. 28, Ref. 7.3, MCT-003). A benchmark k_{eff} value and associated uncertainty values for the multi-region experiments were not available and were assumed to be 1.000 and ± 0.0042, respectively. The basis of this assumption was stated in Section 3.

Table 5.1.5.2-1. Saxton Critical Experiment Descriptions (pp. 231-232, Ref. 7.16)

Single-Region Critical Experiment Description						
Reference case name	**Fuel**	**Pitch (cm)**	**Core configuration**	**Critical water height (cm)**	**Boron concentration (ppmB[a])**	**MCNP case name**
1	UO_2	1.3208	449 cylindrical	95.25	0	ssr83
2	UO_2	1.4224	19 x 19 square	83.71	0	ssr48
3	MOX	1.3208	22 x 23 square	84.56	0	ssr70
4	MOX	1.4224	19 x 19 square	82.46	0	ssr57
5	MOX	1.4224	21 x 21 square	89.70	337	ssr27
6	MOX	1.8669	13 x 13 square	70.11	0	ssr66
7	MOX	2.0117	12 x 12 square	78.43	0	ssr53
8	MOX	2.6416	11 x 11 square	81.17	0	ssr74

Multi-region Critical Experiment Description				
Reference case name	**Core configuration**	**Critical water height (cm)**	**Boron concentration (ppmB)**	**MCNP case name**
1	19 x 19 square: 11 x 11 MOX center region; UO_2 outer region	91.07	0	smr1
2	19 x 19 square: 11 x 11 MOX center region; UO_2 outer region; Al plate at the fuel interface	92.07	0	smr9
3	27 x 27 square: 19 x 19 UO_2 center region; MOX outer region	86.70	1252	smr5

Table 5.1.5.2-1. Saxton Critical Experiment Descriptions (pp. 231-232, Ref. 7.16)

Multi-region Critical Experiment Description				
Reference case name	**Core configuration**	**Critical water height (cm)**	**Boron concentration (ppmB)**	**MCNP case name**
4	27 x 27 square: 19 x 19 MOX center region; UO_2 outer region; water slot at the region boundary	99.80	1453	smr11
5	27 x 27 square: 19 x 19 MOX center region; UO_2 outer region; Al slab at the interface	106.35	1453	smr12
8	27 x 27 square: 19 x 19 MOX center region; UO_2 outer region; L shaped UO_2 insert in MOX region	92.19	1425	smr8

[a] ppmB = parts per million boron by mass

Table 5.1.5.2-2. Saxton UO_2 Fuel Rod Specifications (p. 58, Ref. 7.20)

Pellet diameter	0.90678 cm (0.357 in.)
Clad OD	0.99314 cm (0.391 in.)
Clad ID	0.91694 cm (0.361 in.)
Clad material	Type 304 Stainless Steel
% Theoretical density	93.0[a]
Fuel length	92.964 cm (36.6 in.)
Enrichment	5.74 wt% U^{235}
Theoretical density (UO_2)	10.96 g/cm^3
Fuel mass per rod (UO_2)	604.25 g
Fuel volume per rod (UO_2)	60.03556 cm^3

[a] The reported density is not consistent with the reported fuel length and mass, so a density of 10.06487 g/cm^3 was used which was calculated as follows: density = mass of fuel/ volume of fuel.

Table 5.1.5.2-3. Saxton MOX Fuel Rod Specifications

Parameter	**Value**
Pellet diameter (p. 22, Ref. 7.3, MCT-003)	0.856996 cm (0.3374 in.)
Clad O.D. (p. 22, Ref. 7.3, MCT-003)	0.99314 cm (0.391 in.)
Clad I.D. (p. 22, Ref. 7.3, MCT-003)	0.87503 cm (0.3445 in.)
Clad material (p. 22, Ref. 7.3, MCT-003)	Zircaloy-4
% Theoretical density (p. 14, Ref. 7.3, MCT-003)	94.0 ± 2.0
Fuel length (p. 22, Ref. 7.3, MCT-003)	92.964 cm (36.6 in.)
Enrichment (p. 2, Ref. 7.3, MCT-003)	6.6 wt% PuO_2
Theoretical density (PuO_2) (p. 74, Ref. 7.20)	11.46 g/cm^3
Density of MOX (PuO_2-UO_2) fuel (p. 23, Ref. 7.3, MCT-003)	10.19268 g/cm^3
Atom density Pu^{239} (p. 26, Ref. 7.3, MCT-003)	1.3526E-3 atoms/b-cm

Table 5.1.5.2-3. Saxton MOX Fuel Rod Specifications

Parameter	Value
Atom density of Pu^{240} (p. 26, Ref. 7.3, MCT-003)	1.2759E-4 atoms/b-cm
Atom density of Pu^{241} (p. 26, Ref. 7.3, MCT-003)	1.1407E-5 atoms/b-cm
Atom density of Pu^{242} (p. 26, Ref. 7.3, MCT-003)	6.0318E-7 atoms/b-cm
Atom density of Am^{241} (p. 26, Ref. 7.3, MCT-003)	1.7783E-6 atoms/b-cm
Atom density of U^{234} (p. 26, Ref. 7.3, MCT-003)	1.1688E-6 atoms/b-cm
Atom density of U^{235} (p. 26, Ref. 7.3, MCT-003)	1.5301E-4 atoms/b-cm
Atom density of U^{238} (p. 26, Ref. 7.3, MCT-003)	2.1097E-2 atoms/b-cm
Atom density of O^{16} (p. 26, Ref. 7.3, MCT-003)	4.5155E-2 atoms/b-cm
Fuel mass per rod (PuO_2-UO_2) (p. 231, Ref. 7.16)	546.576 g

Table 5.1.5.2-4. Zircaloy-4 Material Compositions (p. 26, Ref. 7.3, MCT-003)

Element	Atom Density (atoms/b-cm)
Sn	4.6590E-4
Fe	1.4148E-4
Cr	7.5977E-5
O	2.9630E-4
Zr	4.2517E-2

The moderator compositions shown in Table 5.1.5.2-5 were calculated from the formulas listed on pages 61 and 62 of Reference 7.3, MCT-003 for the multi-region critical experiments. Mass densities for the moderator in the multi-region experiments were calculated by linear interpolation and the values are listed in Table 5.1.5.2-6.

Table 5.1.5.2-5. Moderator Compositions for Saxton Experiments

Case	H/X ratio	Boron (ppmB)	H (atoms/ b-cm)	O (atoms/ b-cm)	B^{10} (atoms/ b-cm)	B^{11} (atoms/ b-cm)	Total (atoms/ b-cm)
ssr83	78.6912	0	2[a]	1[a]	0	0	0.99836[b]
ssr48	89.0526	0	2[a]	1[a]	0	0	0.99859[b]
ssr70	75.3460	0	0.066643	0.033322	0	0	0.099965
ssr57	94.7845	0	0.066781	0.033390	0	0	0.100171
ssr27[c]	10.3716	337	0.066751	0.033404	3.7338E-6	1.5029E-5	0.1001738
ssr66	174.6784	0	0.066673	0.033336	0	0	0.100009
ssr53	236.2939	0	0.066783	0.033392	0	0	0.100175
ssr74	463.5628	0	0.066737	0.033368	0	0	0.100105
smr1	99.3894	0	0.066781	0.033391	0	0	0.1001722
smr5	9.7401	1252	0.066698	0.033456	1.3901E-05	5.5953E-05	0.1002236
smr8	10.2699	1425	0.066713	0.033478	1.5834E-05	6.3734E-05	0.1002700
smr9	100.4988	0	0.066795	0.033398	0	0	0.1001927
smr11	11.0473	1453	0.066687	0.033467	1.6140E-05	6.4967E-05	0.1002349
smr12	11.7724	1453	0.066721	0.033484	1.6149E-05	6.5000E-05	0.1002860

[a] These values for the water were specified as 2 H atoms per molecule and 1 O atom per molecule.

[b] These mass densities were interpolated from the referenced data in Table 5.1.5.2-6 for temperatures of 19.2 and 18.0°C.

[c] These compositions are from page 27 of Reference 7.3, MCT-003.

Table 5.1.5.2-6. Moderator Density for Multi-Region Critical Experiments

Reference temperature (°C)[a]	Referenced density (g/cm^3)[a]	Experiment temperature (°C)	Interpolated density (g/cm^3)	Experiment name
15.75	0.998982	16.2	0.998905	smr1
16.1	0.998922	15.0	0.999110	smr9
17.0	0.998772	20.0	0.998201	smr5
18.0	0.998593	18.0	0.998593	smr11
19.9	0.998224	17.8	0.998629	smr12
24.1	0.997269	18.5	0.998496	smr8
25.8	0.996831	--	--	--

[a] These values are from page 12 of Reference 7.3, MCT-003.

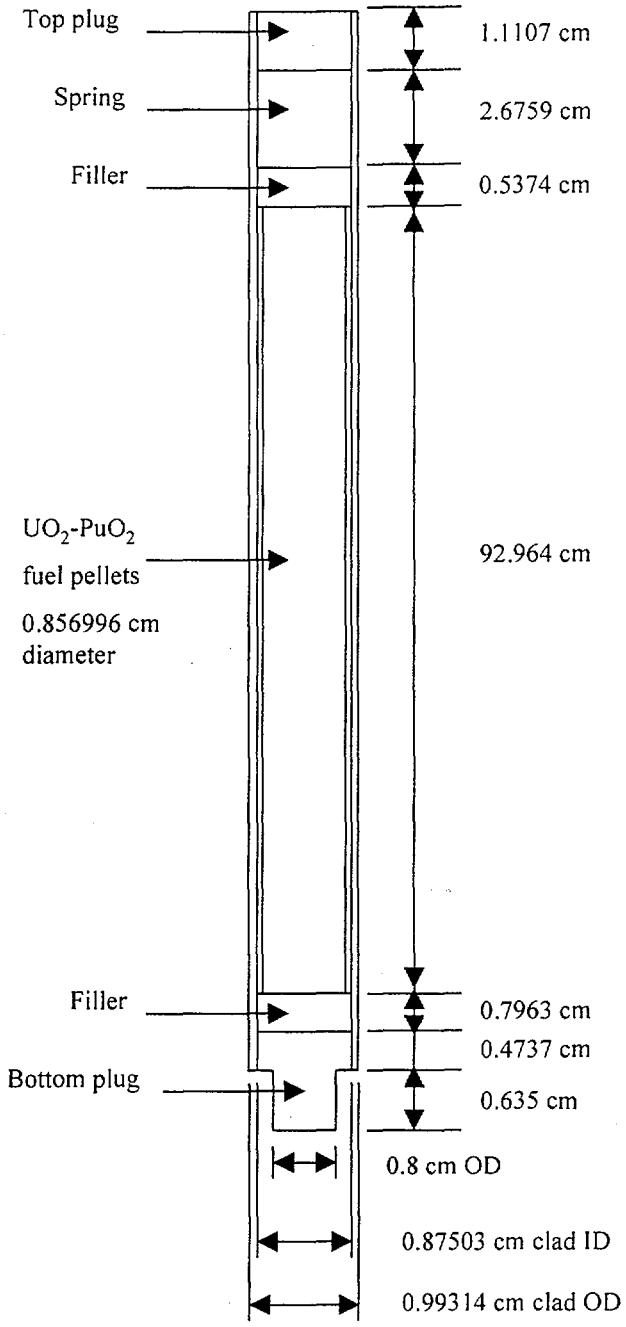

Figure 5.1.5.2-1. Saxton Experiment Fuel Rod (pp. 9, 22, 23, Ref. 7.3, MCT-003)

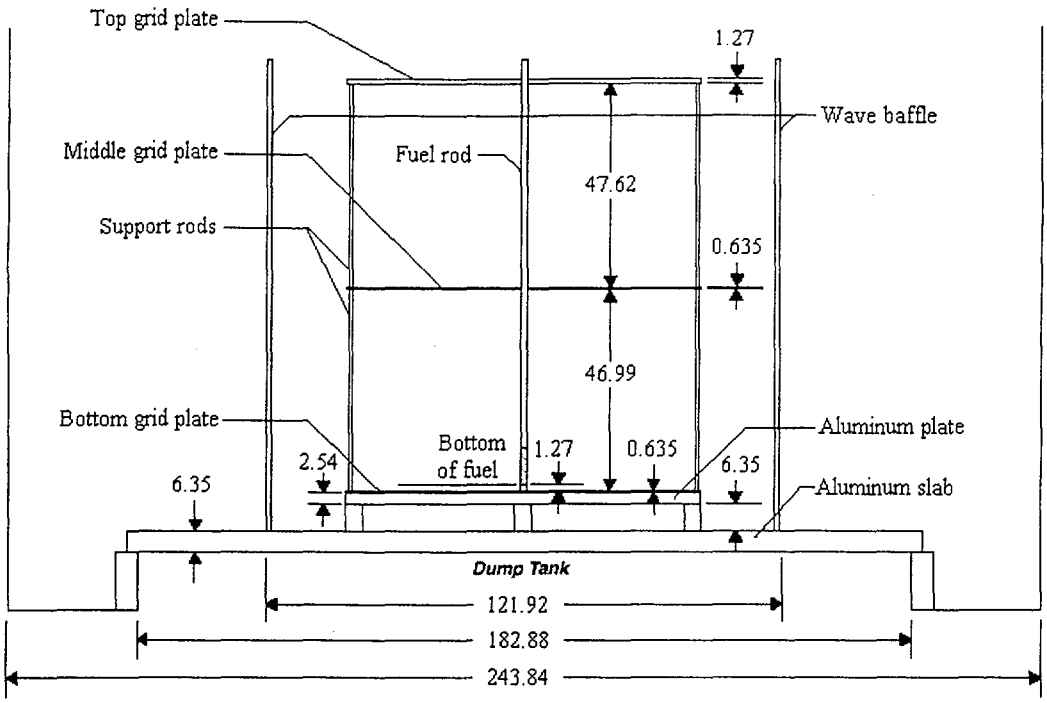

Figure 5.1.5.2-2. Core Tank Side View (p. 22, Ref. 7.22, p. 4, Ref. 7.3, MCT-003) (dimensions in cm)

5.1.6 Homogenous Solution Calculations

5.1.6.1 LCE Reactivity Calculation for UO_3-H_2O Solution Experiments

This set of experiments is described in Section 5.1.1.3.

5.1.6.2 Unreflected UO_2F_2+H_2O Cylindrical Assembly Sheba-II

SHEBA-II (Solution High Energy Burst Assembly-II) is a critical assembly experiment that was operated at the Los Alamos Critical Experiments Facility. A schematic of the critical assembly is shown in Figure 1 on page 2 of Reference 7.3, LEU-SOL-THERM-001 (LST-001). It is a bare assembly fueled with an aqueous solution of about 5 wt% enriched uranyl fluoride that is stored in four critically safe steel tanks. Reactivity control is accomplished by varying the solution level, and a safety rod may be inserted in a thimble along the central axis of the cylindrical assembly vessel (CAV) for fast shutdown. The simple geometry provided by this cylindrical system allows for easily applied calculational methods, and thus SHEBA-II is ideally suited for use as a criticality safety benchmark experiment (p. 1, Ref. 7.3, LST-001). Benchmark dimensions are shown in Figure 5.1.6.2-1 and Table 5.1.6.2-1. The benchmark $k_{eff} \pm \sigma$ value was 0.9991 $\pm$ 0.0029 (p. 19, Ref. 7.3, LST-001). Descriptions of the experimental representation materials are given in Table 5.1.6.2-2. The H/X ratio for this experiment was calculated as 453.898.

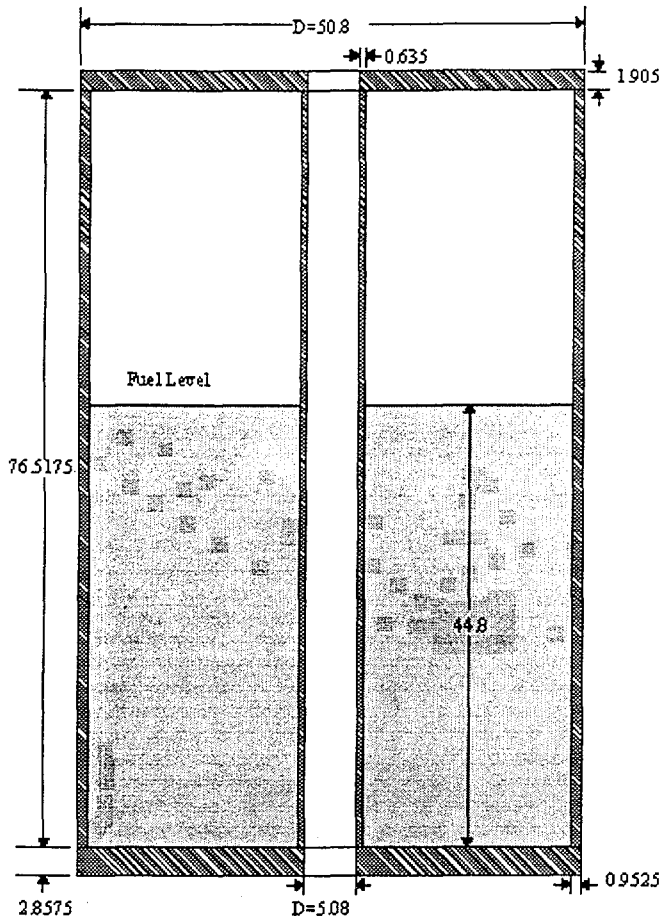

Figure 5.1.6.2-1. SHEBA-II Critical Assembly (dimensions in cm) (p. 17, Ref. 7.3, LST-001)

Table 5.1.6.2-1. Case Dimensions for SHEBA-II Assembly (p. 18, Ref. 7.3, LST-001)

Region	Inner radius (cm)	Outer radius (cm)	Height (cm)	Material
Vessel Bottom	2.5400	25.4000	2.8575	SS304L
Central Void	0.0000	2.5400	81.2800	Air
Thimble	2.5400	3.1750	76.5175	SS304L
Fuel	3.1750	24.4475	44.8000	Fuel Solution
Above Fuel	3.1750	24.4475	31.7175	Air
Outer Tank	24.4475	25.4000	76.5175	SS304L
Cover	2.5400	25.4000	1.9050	SS304L

Table 5.1.6.2-2. Material Compositions for LST-001 Experiments (p. 19, Ref. 7.3, LST-001)

Material	Element/Isotope	Atom density (atoms/b-cm)
SS304L	Cr	1.6348×10^{-2}
	Mn	1.7192×10^{-3}

Table 5.1.6.2-2. Material Compositions for LST-001 Experiments (p. 19, Ref. 7.3, LST-001)

Material	Element/Isotope	Atom density (atoms/b-cm)
	Fe	6.0038×10^{-2}
	Ni	7.2418×10^{-3}
Air	N	3.5214×10^{-5}
	O	1.5092×10^{-5}
Fuel Solution	H	5.6179×10^{-2}
	O	3.2967×10^{-2}
	F	5.1035×10^{-3}
	U^{234}	6.7855×10^{-7}
	U^{235}	1.2377×10^{-4}
	U^{236}	1.2085×10^{-6}
	U^{238}	10^{-3}

5.1.6.3 Full and Truncated Bare Spheres of 10% Enriched Uranyl Nitrate Water Solutions

A series of critical experiments with aqueous uranyl nitrate solutions with uranium enriched to 10 wt% U^{235} was performed at the Solution Critical Facility of the Institute of Physics and Power Engineering, Obninsk, Russia. Nine critical experiment measurements were made with solutions in thin-wall spherical tanks without reflectors. Spheres with outer diameters of 66 cm, 88 cm, and 120 cm were used. A schematic of the critical assembly is shown in Figure 5.1.6.3-1 (p. 2, Ref. 7.3, LEU-SOL-THERM-003 (LST-003)). Criticality was achieved at two partial fillings of each sphere and at full fillings. One experiment differed from another in geometry, size, and in uranium concentration in the solution. Descriptions of the experiments are given in Table 5.1.6.3-1. All nine experiments presented here are considered to be acceptable for use as benchmark experiments by the evaluators. Descriptions of the experimental case materials are given in Tables 5.1.6.3-2 and 5.1.6.3-3.

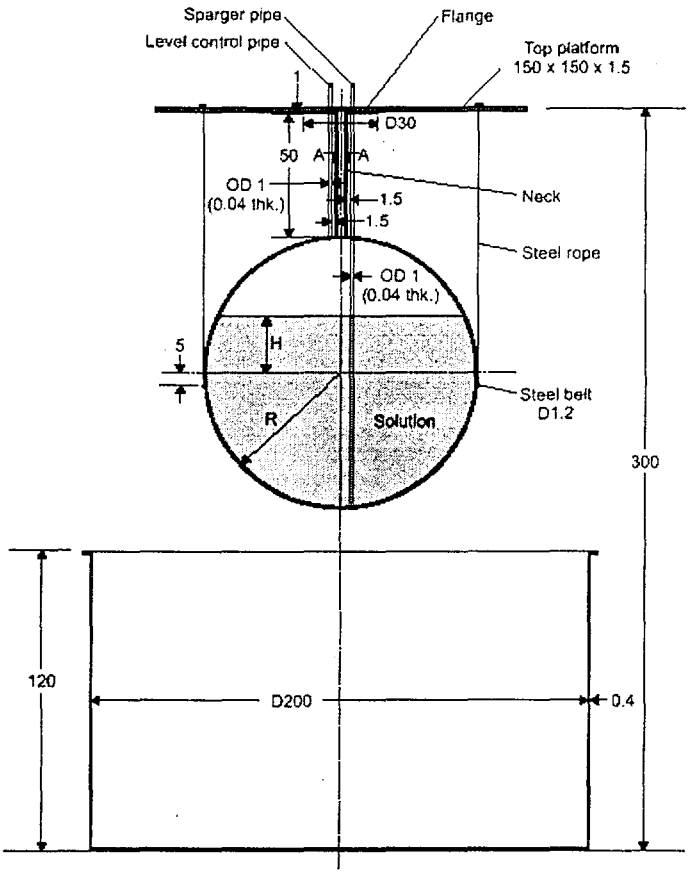

Figure 5.1.6.3-1. Critical Assembly Schematic (dimensions in cm) (p. 2, Ref. 7.3, LST-003)

Table 5.1.6.3-1. Configurations of LST-003 Experiments (p. 12, Ref. 7.3, LST-003)

Handbook case name	Spherical shell inner radius (cm)	Spherical shell thickness (cm)	Solution height (cm)	Benchmark $k_{eff} \pm$ standard deviation (p. 15, Ref. 7.3, LST-003)	H/X ratio	MCNP case name
1	32.9537	0.15	16.4073	0.9997 ± 0.0039	770.3100	lst3-1
2	32.9537	0.15	25.1548	0.9993 ± 0.0042	877.6000	lst3-2
3	32.9537	0.15	32.9537	0.9995 ± 0.0042	897.0000	lst3-3
4	43.6303	0.19	3.9656	0.9995 ± 0.0042	913.2500	lst3-4
5	43.6303	0.19	28.0537	0.9997 ± 0.0048	1173.3800	lst3-5
6	43.6303	0.19	43.6303	0.9999 ± 0.0049	1213.1000	lst3-6
7	59.8897	0.21	4.6151	0.9994 ± 0.0049	1239.7970	lst3-7
8	59.8897	0.21	41.9340	0.9993 ± 0.0052	1411.6400	lst3-8
9	59.8897	0.21	59.8897	0.9996 ± 0.0052	1437.5057	lst3-9

Table 5.1.6.3-2. Solution Atom Densities in atoms/b-cm for LST-003 Experiments (p. 13, Ref. 7.3, LST-003)

Case name	U^{234}	U^{235}	U^{238}	N	O	H
1	6.7481×10^{-7}	7.6403×10^{-5}	6.7271×10^{-4}	2.3185×10^{-3}	3.7473×10^{-2}	5.8854×10^{-2}
2	6.0186×10^{-7}	6.8143×10^{-5}	5.9998×10^{-4}	2.0540×10^{-3}	3.7042×10^{-2}	5.9802×10^{-2}
3	5.9274×10^{-7}	6.7111×10^{-5}	5.9089×10^{-4}	1.9856×10^{-3}	3.7040×10^{-2}	6.0199×10^{-2}
4	5.8134×10^{-7}	6.5820×10^{-5}	5.7953×10^{-4}	1.9783×10^{-3}	3.6939×10^{-2}	6.0110×10^{-2}
5	4.6279×10^{-7}	5.2398×10^{-5}	4.6135×10^{-4}	1.5764×10^{-3}	3.6225×10^{-2}	6.1483×10^{-2}
6	4.4911×10^{-7}	5.0849×10^{-5}	4.4771×10^{-4}	1.5340×10^{-3}	3.6175×10^{-2}	6.1685×10^{-2}
7	4.3999×10^{-7}	4.9817×10^{-5}	4.3862×10^{-4}	1.5077×10^{-3}	3.6117×10^{-2}	6.1763×10^{-2}
8	3.8984×10^{-7}	4.4138×10^{-5}	3.8862×10^{-4}	1.3661×10^{-3}	3.5868×10^{-2}	6.2307×10^{-2}
9	3.8300×10^{-7}	4.3364×10^{-5}	3.8181×10^{-4}	1.3569×10^{-3}	3.5837×10^{-2}	6.2336×10^{-2}

5.1.6.4 Graphite Reflected Uranyl Sulphate (20.9 at% U^{235}) Solutions

The purpose of these experiments, performed at the RRC "Kurchatov Institute" in 1980-1981, was to investigate nuclear safety issues for a special-purpose compact reactor with an aqueous solution of uranyl-sulphate (~20.9 at% (see footnote p. 59) U^{235}) and graphite reflector (p. 1, Ref. 7.3, IEU-SOL-THERM-001 (IST-001)). Four configurations of critical assemblies with different concentrations of uranium in the solution were involved in this work. These configurations are described in sufficient detail and are considered acceptable for use as benchmark critical experiments by the evaluators. Schematics of the critical assembly with the main structures of the facility are presented through Figures 1, 2, and 3 on pages 2, 3, and 5 of Reference 7.3, IST-001, which also give all the necessary dimensions of the experimental configuration. Table 5.1.6.4-1 provides a listing of the 4 cases and the benchmark k_{eff} values in the experimental configurations. Descriptions of the experimental cases are given in Figures 5.1.6.4-1 through 5.1.6.4-2. The spiral was simulated using two half torus. Further details are given on pages 1 through 5 of Reference 7.3, IST-001. Descriptions of the experimental case materials are given in Tables 5.1.6.4-2 through 5.1.6.4-3.

Table 5.1.6.4-1. Configurations of IST-001 Experiments (p. 20, Ref. 7.3, IST-001)

Handbook case name	Description	Benchmark $k_{eff} \pm \sigma$ (p. 29, Ref. 7.3, IST-001)	H/X ratio	MCNP case name
1	Core height 49.24 cm Core thickness 0.5cm	1.000 ± 0.0052	444.0300	ist1-1
2	Core height 33.498 cm Core thickness 0.5cm	1.000 ± 0.0052	297.3818	ist1-2
3	Core height 32.251 cm Core thickness 0.3cm	1.000 ± 0.0052	297.3818	ist1-3
4	Core height 29.056 cm Core thickness 0.5cm	1.000 ± 0.0052	217.3670	ist1-4

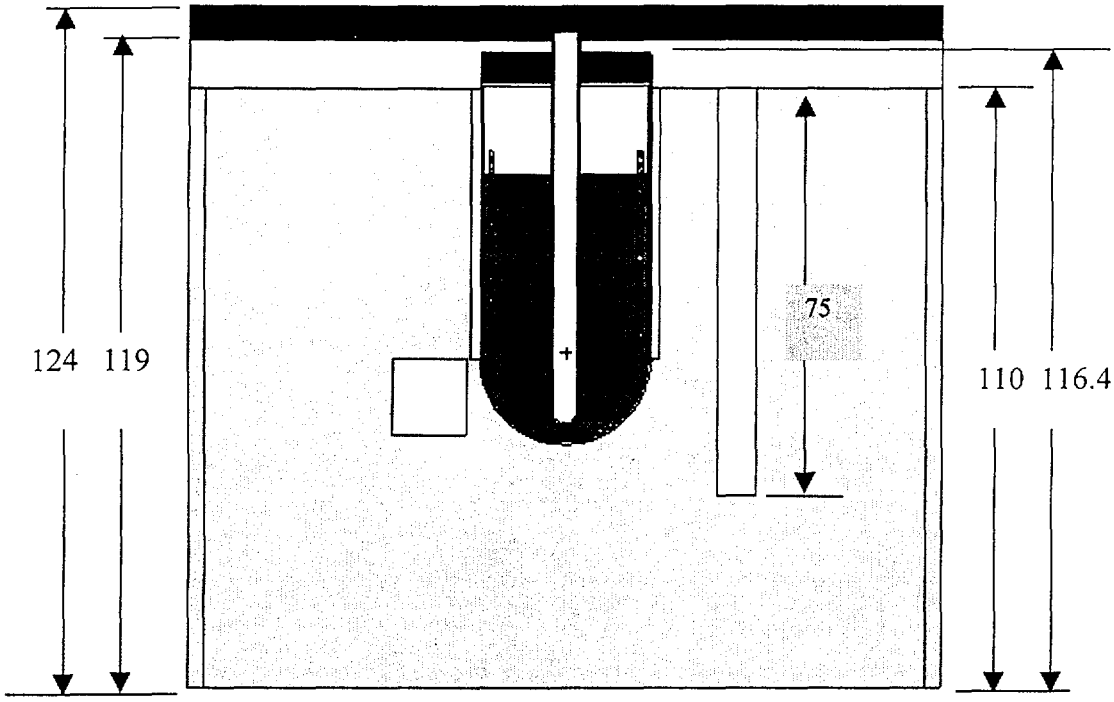

Figure 5.1.6.4-1. Longitudinal Section of the Benchmark Representation (dimensions in cm)

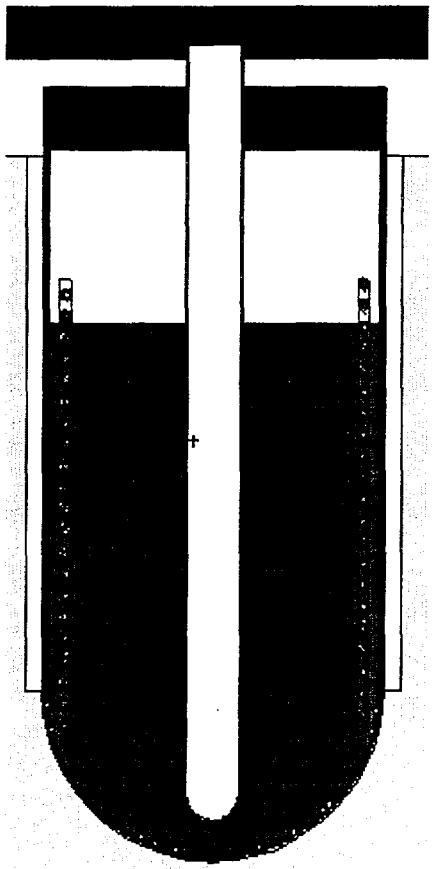

Figure 5.1.6.4-2. Longitudinal Cross Section of the Core

Table 5.1.6.4-2. Fuel Material Atom Densities (atoms/b-cm) for IST-001 Experiments (p. 27, Ref. 7.3, IST-001)

Case	U^{234} ($\times 10^{-6}$)	U^{235} ($\times 10^{-4}$)	U^{236} ($\times 10^{-6}$)	U^{238} ($\times 10^{-4}$)	H ($\times 10^{-2}$)	O ($\times 10^{-2}$)	S ($\times 10^{-4}$)
1	1.0419	1.3972	1.4092	5.2571	6.2040	3.5118	6.9799
2	1.5124	2.0281	2.0456	7.6310	6.0312	3.6063	9.9959
3	1.5124	2.0281	2.0456	7.6310	6.0312	3.6063	9.9959
4	1.9983	2.6798	2.7028	10.083	5.8250	3.6901	13.111

Table 5.1.6.4-3. Material Compositions for IST-001 Experiments (pp. 28, 29, Ref. 7.3, IST-001)

Material	Element/Isotope	Atom density (atoms/b-cm)
Water	H	6.6735×10^{-2}
	O	3.3367×10^{-2}
Graphite Reflector	C	8.5235×10^{-2}
Borated Polyethylene	B^{10}	3.1268×10^{-4}
	B^{11}	1.2665×10^{-3}
	C	3.9354×10^{-2}
	H	7.8708×10^{-2}
Stainless Steel 0X18H10T	C	3.1687×10^{-4}
	Si	1.3551×10^{-3}
	Mn	1.7319×10^{-3}
	Cr	1.6469×10^{-2}
	Ni	8.1061×10^{-3}
	Ti	4.9681×10^{-4}
	S	2.9669×10^{-5}
	P	5.3759×10^{-5}
	Cu	2.2460×10^{-4}
	Fe	153×10^{-2}

5.1.7 Fast Metal Systems

Reactivity calculations involving Fast Metal Fuel are presented in this section. In the two following sections, a series of critical experiments performed by the Institute for Experimental Physics of the Russian Federal Nuclear Center (VNIIEF) at Arzamas-16 and the Institute for Technical Physics of the Russian Federal Nuclear Center (VNIITF) at Chelyabinsk-70 are described. Detailed experimental configurations and material compositions for these experiments are included in Reference 7.3. The series of experiments studied in this report include uranium metal systems of intermediate enrichment, high enrichment, and plutonium systems reflected by the following materials: depleted uranium, steel, aluminum, graphite, and polyethylene. Tables 5.1.7.1-1, 5.1.7.2-1 and 5.1.7.3-2 provide a listing of the Reference 7.3 identifier numbers, some information about the experiment, the benchmark k_{eff} value, and the MCNP case names. The steel diaphragm was not modeled in the MCNP representations for the PMF experiments based on Assumption 3.5.

5.1.7.1 HEU Fast Metal Fuel Experiments

Table 5.1.7.1-1. Russian Criticality Safety Benchmark Experiments (p. 244, Ref. 7.15)

Handbook identifier	U^{235} wt% or Pu^{239} at%	Core dimensions (cm)		Reflector material	Reflector thickness (cm)	Benchmark k_{eff}	MCNP case name
		Radius	Height				
HEU-MET-FAST-008	90	10.150	--	None	--	0.9989 ± 0.0016	HMF8
HEU-MET-FAST-011	90	7.550	--	Polyethylene	13.230	0.9989 ± 0.0015	HMF11
HEU-MET-FAST-012	90	9.150	--	Aluminum	0.850, 2.850	0.9992 ± 0.0018	HMF12
HEU-MET-FAST-013	90	8.350	--	Steel	3.650	0.9990 ± 0.0015	HMF13
HEU-MET-FAST-014	90	7.750	--	Depleted U	4.650	0.9989 ± 0.0017	HMF14
HEU-MET-FAST-015	96	9.995	11.130	None	--	0.9996 ± 0.0017	HMF15
HEU-MET-FAST-018	90	9.150	--	None	--	1.0000 ± 0.0014	HMF18
HEU-MET-FAST-019	90	9.150	--	Graphite	3.450	1.0000 ± 0.0028	HMF19
HEU-MET-FAST-020	90	8.350	--	Polyethylene	1.450	1.0000 ± 0.0028	HMF20
HEU-MET-FAST-021	90	7.550	--	Steel	9.700	1.0000 ± 0.0024	HMF21
HEU-MET-FAST-022	90	8.350	--	Duralumin	3.900	1.0000 ± 0.0019	HMF22
HEU-MET-FAST-024	90	7.550	--	Steel, polyethylene	0.850, 2.850	0.9990 ± 0.0015	HMF24

5.1.7.2 Plutonium Fueled Fast Metal Systems

Table 5.1.7.2-1. Russian Criticality Safety Benchmark Experiments (p. 244, Ref. 7.15)

Handbook identifier	U^{235} wt% or Pu^{239} at%	Core dimensions (cm)		Reflector material	Reflector thickness (cm)	Benchmark k_{eff}	MCNP case name
		Radius	Height				
PU-MET-FAST-020	89	5.350	--	Depleted U	7.650	0.9987 ± 0.0017	PMF20
PU-MET-FAST-022	98	6.670	--	None	--	1.0000 ± 0.0020	PMF22
PU-MET-FAST-023	98	6.000	--	Graphite	2.350	1.0000 ± 0.0020	PMF23
PU-MET-FAST-024	98	6.000	--	Polyethylene	1.550	1.0000 ± 0.0020	PMF24
PU-MET-FAST-025	98	6.000	--	Steel	1.550	1.0000 ± 0.0020	PMF25

Table 5.1.7.2-1. Russian Criticality Safety Benchmark Experiments (p. 244, Ref. 7.15)

Handbook identifier	U^{235} wt% or Pu^{239} at%	Core dimensions (cm)		Reflector material	Reflector thickness (cm)	Benchmark k_{eff}	MCNP case name
		Radius	Height				
PU-MET-FAST-026	98	5.350	--	Steel	11.900	1.0000 ± 0.0024	PMF26
PU-MET-FAST-027	89	5.350	--	Polyethylene	5.580	1.0000 ± 0.0022	PMF27
PU-MET-FAST-028	89	5.350	--	Steel	19.650	1.0000 ± 0.0022	PMF28
PU-MET-FAST-029	88	6.670	--	None	--	1.0000 ± 0.0019	PMF29
PU-MET-FAST-030	88	4.660	--	Graphite	4.490	1.0000 ± 0.0021	PMF30
PU-MET-FAST-031	88	4.660	--	Polyethylene	3.690	1.0000 ± 0.0021	PMF31
PU-MET-FAST-032	88	4.660	--	Steel	4.490	1.0000 ± 0.0020	PMF32

5.1.7.3 IEU Fast Metal Fuel Systems

5.1.7.3.1 The Early Jemima Experiments: Bare Cylindrical Configurations of Enriched and Natural Uranium

The purpose of the early Aunt Jemima experiments, performed at the Pajarito critical assembly facility at Los Alamos (1952-1954), was to determine critical conditions for bare uranium cylinders of intermediate enrichment. A schematic of the experimental assembly is shown on page 2 of Reference 7.3, IEU-MET-FAST-002 (IMF-002). Vertical cylindrical columns were constructed by stacking thin disks of enriched uranium (oralloy, or Oy, 93.4 wt% U^{235}) and natural uranium (tuballoy, or Tu) in different orders. A total of five critical cylindrical configurations of uranium disks, partial disks (in the shape of 45° circular sectors), and layers of rectangular blocks were assembled. Documentation and detailed drawings of these experiments are shown on pages 16 through 37 of Reference 7.3 IEU-MET-FAST-001 (IMF-001). The evaluators considered that four of the experiments (involving only the disks and sectors) qualified as benchmark experiments. For each of the four acceptable experiments, two benchmark cases, referenced as detailed and idealized, were developed in this evaluation. The MCNP input filenames that correspond to these representations are named IMF1-1, IMF1-2, IMF1-3, and IMF1-4 (for the detailed case), and IMF1-5, IMF1-6, IMF1-7, and IMF1-8 (for the idealized case), for configurations 1 through 4, respectively. The specifications for components in the detailed cases and idealized cases are presented on pages 35 and 37 of Reference 7.3, IMF-001, respectively. The material compositions for these cases are presented in Tables 12, 13, and 14 on pages 39, 40, and 41 of Reference 7.3, IMF-001, respectively. The benchmark $k_{eff} \pm \sigma$ values for the cases are presented in Table 5.1.7.3-1.

Table 5.1.7.3-1. Benchmark $k_{eff} \pm \sigma$ values for IMF-001 Experiments (p. 42, Ref. 7.3, IMF-001)

Configuration No.	Detailed case	Idealized case
1	0.9988 ± 0.0012	0.9989 ± 0.0012

Table 5.1.7.3-1. Benchmark $k_{eff} \pm \sigma$ values for IMF-001 Experiments (p. 42, Ref. 7.3, IMF-001)

Configuration No.	Detailed case	Idealized case
2	0.9988 ± 0.0012	0.9997 ± 0.0012
3	0.9990 ± 0.0010	0.9993 ± 0.0010
4	0.9990 ± 0.0010	1.0002 ± 0.0010

5.1.7.3.2 Natural Uranium Reflected Assembly of Enriched and Natural Uranium Plates

This critical experiment was a cylindrical assembly with a core of alternating plates of enriched and natural uranium surrounded by a natural uranium reflector. The core average enrichment was 16 wt% U^{235} (p. 1, Ref. 7.3, IMF-002). This experiment was performed at the Los Alamos Pajarito critical assembly facility and can be considered an extension of the earlier " Jemima" experiments that determined the critical conditions of bare natural and enriched uranium disks of combined intermediate enrichments (29 - 94 wt% U^{235}; p. 1, Ref. 7.3, IMF-002). This experiment was judged to be an acceptable criticality-safety benchmark by the evaluators. Detailed descriptions of the experiment are given on pages 2 through 4, and 8 of Reference 7.3, IMF-002. The benchmark keff value was 1.000 ± 0.003 (p. 9, Ref. 7.3, IMF-002) for this experiment.

5.1.7.3.3 Spherical Assembly of U^{235} (36 wt%)

A series of critical experiments with a spherical assembly of U^{235} (36 wt%) was performed over the course of several years (1993-1996) by the Institute for Experimental Physics of the Russian Federal Nuclear Center (VNIIEF). All of these experiments were consider acceptable for use as benchmark critical experiments by the evaluators. Figure 5.1.7.3-1 shows a sectional view of the assembly on the critical test facility (CTF). The assembly core included different layers of fissile material (lower core limit) and could be covered by different layers of graphite, steel or duralumin (upper core limit). The upper core layers are the reflector layers. Table 5.1.7.3-1 shows the description of each experiment and the benchmark k_{eff} value for the experimental configuration.

Table 5.1.7.3-2. Experimental Description

Handbook case name	Description	Benchmark $k_{eff} \pm \sigma$	MCNP case name
IEU-MET-FAST-003	Bare Spherical Assembly (detailed)	1.0000 ± 0.0017[a]	IMF3-1
	Bare Spherical Assembly (simplified)	1.0000 ± 0.0019[a]	IMF3-2
IEU-MET-FAST-004	Graphite Reflected Spherical Assembly (detailed)	1.0000 ± 0.003[b]	IMF4-1
	Graphite Reflected Spherical Assembly (simplified)	1.0000 ± 0.0032[b]	IMF4-2
IEU-MET-FAST-005	Steel Reflected Spherical Assembly (detailed)	1.0000 ± 0.0021[c]	IMF5-1
	Steel Reflected Spherical Assembly (simplified)	1.0000 ± 0.0023[c]	IMF5-2
IEU-MET-FAST-006	Duralumin Reflected Spherical Assembly (detailed)	1.0000 ± 0.0023[d]	IMF6-1
	Duralumin Reflected Spherical Assembly (simplified)	1.0000 ± 0.0025[d]	IMF6-2
IEU-MET-FAST-008	Uranium Depleted Reflected Spherical Assembly	1.0000 ± 0.0018[e]	IMF8

[a] p. 14, Ref 7.3, IEU-MET-FAST-003 (IMF-003)

[b] p. 13, Ref 7.3, IEU-MET-FAST-004 (IMF-004)

[c] p. 13, Ref 7.3, IEU-MET-FAST-005 (IMF-005)

[d] p. 14, Ref 7.3, IEU-MET-FAST-006 (IMF-006)

[e] p. 14, Ref 7.3, IEU-MET-FAST-007 (IMF-008)

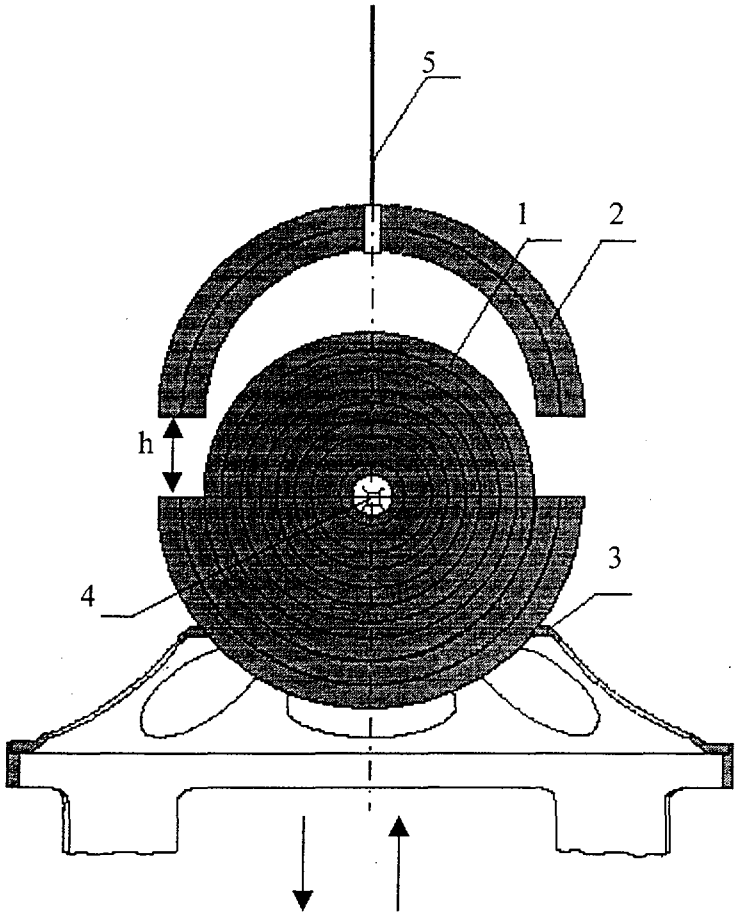

1 - lower core unit
2 - upper core unit
3 - lower support
4 - neutron source
5 - cable

Figure 5.1.7.3-1. Sectional View of the Assembly on the CTF (p. 2, Ref. 7.3, IMF-003)

5.1.7.3.4 Bare Spherical Assembly of U^{235} (36%)

A criticality measurement of a bare spherical assembly of U^{235} (36 wt%) was performed. Figure 5.1.7.3-1 shows a schematic sectional view of the assembly on the CTF. The CTF is described in detail on page 2 of Reference 7.3, IMF-003. The assembly had a core of U^{235} (36 wt%) incorporating 10 spherical layers of fissile material. The experimentally determined k_{eff} value in the experimental configuration was 1.0000 ± 0.0017 (p. 14, Ref. 7.3, IMF-003). Two benchmark cases, one detailed and one simplified were developed for this experiment. Characteristics of these cases are presented in Table 5.1.7.3-2. Descriptions of the experimental case materials are given in Table 5.1.7.3-3.

Table 5.1.7.3-2. Dimensions and Mass Characteristics of the IMF-003 Critical Assembly (p. 12, Ref. 7.3, IMF-003)

Detailed 10 shell case			
Layer no.	Radius (cm)		Layer mass (g)
	Inner	Outer	
1	0.00	2.00	623.29
2	2.00	6.00	16256
3	6.00	7.55	16630
4	7.55	9.15	25864
5	9.15	11.00	43638
6	11.00	12.25	39021
7	12.25	13.25	37156
8	13.25	14.00	31449
9	14.00	15.00	48363
10	15.00	15.324	17128
Simplified 10 shell case			
Layer no.	Radius (cm)		Layer mass (g)
	Inner	Outer	
1	0.00	15.324	277312

Table 5.1.7.3-3. Atom Densities (atoms/b-cm) of the IMF-003 Critical Assembly (p. 13, Ref. 7.3, IMF-003)

Detailed 10 shell case								
Layer no.	U^{234} ($\times 10^{-4}$)	U^{235} ($\times 10^{-2}$)	U^{238} ($\times 10^{-2}$)	C ($\times 10^{-4}$)	Fe ($\times 10^{-4}$)	W ($\times 10^{-6}$)	Cu ($\times 10^{-4}$)	Ni ($\times 10^{-4}$)
1	1.2743	1.7093	2.9308	5.5181	2.5713	6.0083	12.1830	13.1910
2	1.5814	1.7321	2.9785	4.6687	1.6066	12.2000	1.6315	1.7665
3	1.5677	1.7194	2.9508	3.7026	1.5926	12.0950	2.7440	2.9710
4	1.5581	1.7174	2.9235	5.5201	1.5829	12.0210	2.0893	2.2621
5	1.3256	1.7141	2.9417	7.3802	1.1904	12.0540	1.9423	2.1030
6	1.6004	1.7121	2.9159	5.5031	0.9863	5.9920	3.3673	3.6459
7	1.7235	1.6958	2.8806	9.0767	0.97607	11.8600	3.5934	3.8907
8	1.4729	1.6779	2.8482	6.2781	0.96445	5.8593	3.8989	4.2215
9	1.4996	1.7018	2.9013	13.697	1.3748	11.9310	4.0157	4.3479
10	1.3891	1.6796	2.8748	6.3157	7.7618	5.8944	14.3890	15.5790

Table 5.1.7.3-3. Atom Densities (atoms/b-cm) of the IMF-003 Critical Assembly (p. 13, Ref. 7.3, IMF-003)

Simplified 10 shell case								
1	1.5272	1.7118	2.9211	7.7389	1.2058	10.0870	3.8133	4.1288

5.1.7.3.5 Graphite-Reflected Spherical Assembly of U^{235} (36 wt%)

A criticality measurement of graphite reflected spherical assembly of U^{235} (36 wt%) was performed. Figure 5.1.7.3-1 shows a schematic sectional view of the assembly on the CTF. The CTF is described in detail on page 2 of Reference 7.3, IMF-003. The assembly core had a central cavity of 2-cm radius and incorporated 7 spherical layers of fissile material. Characteristics of these core layers are presented in Table 5.1.7.3-4. The graphite reflector was a single spherical layer with an outer radius of 17.2 cm. The k_{eff} value for the experimental configuration was 1.0000 ± 0.0030 (p. 13, Ref. 7.3, IMF-004). Two benchmark cases, one detailed and one simplified were developed for this experiment. Descriptions of the experimental case materials are given in Table 5.1.7.3-5.

Table 5.1.7.3-4. Dimensions and Mass Characteristics of the IMF-004 Critical Assembly (p. 11, Ref. 7.3, IMF-004)

Detailed 8 shell case			
Layer no.	**Radius (cm)**		**Layer mass (g)**
	Inner	**Outer**	
Fuel			
1	2.788 [(a)]	6.000	15267
2	6.000	7.550	16791
3	7.550	9.150	26169
4	9.150	11.000	44087
5	11.000	12.250	39542
6	12.250	13.250	37804
7	13.250	14.000	32214
Graphite reflector			
1	14.000	17.200	15222
Simplified case			
Layer no.	**Radius (cm)**		**Layer mass (g)**
	Inner	**Outer**	
Fuel			
1	2.788[a]	14.00	212080
Graphite reflector			
1	14.00	17.20	15222

[a] p. 11, Ref. 7.3, IMF-004

Table 5.1.7.3-5. Atom Densities (atoms/b-cm) of the IMF-004 Critical Assembly (p. 12, Ref. 7.3, IMF-004)

Detailed 8 shell case						
Layer no.	U^{234}	U^{235}	U^{238}	C	Fe	W
Fuel						
1	1.5926×10^{-4}	1.7443×10^{-2}	2.9996×10^{-2}	4.7018×10^{-4}	1.6180×10^{-4}	1.2287×10^{-5}
2	1.5878×10^{-4}	1.7415×10^{-2}	2.9887×10^{-2}	3.7502×10^{-4}	1.6131×10^{-4}	1.2250×10^{-5}
3	1.5803×10^{-4}	1.7418×10^{-2}	2.9651×10^{-2}	5.5986×10^{-4}	1.6054×10^{-4}	1.2192×10^{-5}
4	1.3423×10^{-4}	1.7356×10^{-2}	2.9786×10^{-2}	7.4727×10^{-4}	1.2054×10^{-4}	1.2205×10^{-5}
5	1.6281×10^{-4}	1.7417×10^{-2}	2.9663×10^{-2}	5.5983×10^{-4}	1.0034×10^{-4}	6.0956×10^{-6}
6	1.7609×10^{-4}	1.7326×10^{-2}	2.9432×10^{-2}	9.2737×10^{-4}	9.9725×10^{-5}	1.2117×10^{-2}
7	1.5156×10^{-4}	1.7266×10^{-2}	2.9309×10^{-2}	6.4604×10^{-4}	9.9245×10^{-5}	6.0294×10^{-6}
Graphite reflector						
1				7.7716×10^{-2}		
Simplified case						
Layer no.	**U^{234}**	**U^{235}**	**U^{238}**	**C**	**Fe**	**W**
Fuel						
1	1.5652×10^{-4}	1.7384×10^{-2}	2.9662×10^{-2}	6.5752×10^{-4}	1.2098×10^{-4}	1.0121×10^{-5}
Graphite reflector						
1				7.7716×10^{-2}		

5.1.7.3.6 Steel-Reflected Spherical Assembly of U^{235} (36 wt%)

A criticality measurement for a steel reflected spherical assembly of U^{235} (36 wt%) was performed. Figure 5.1.7.3-1 shows a schematic sectional view of the assembly on the CTF. The CTF is described in detail on page 2 of Reference 7.3, IMF-003. The assembly core had a central cavity of 2.686-cm radius and incorporated 6 spherical layers of fissile material. Characteristics of these core layers are presented in Table 5.1.7.3-6. Five spherical layers that differ slightly in density represented the steel reflector. The outermost layer had an outer radius of 21.5 cm. The k_{eff} value for the experimental configuration was 1.0000 ± 0.0021 (p. 13, Ref. 7.3, IMF-005). Two benchmark cases, one detailed and one simplified, were developed for this experiment. The reflector was represented in both cases as 2 spherical layers that differ slightly in density. Descriptions of the experimental case materials are given in Table 5.1.7.3-7.

Table 5.1.7.3-6. Dimension and Mass Characteristics of the IMF-005 Critical Assembly (p. 11, Ref. 7.3, IMF-005)

Detailed 8 shell case			
Layer no.	Radius (cm)		Layer mass (g)
	Inner	Outer	
Fuel			
1	2.686[a]	6.000	15366
2	6.000	7.550	16630
3	7.550	9.150	25864

Table 5.1.7.3-6. Dimension and Mass Characteristics of the IMF-005 Critical Assembly (p. 11, Ref. 7.3, IMF-005)

Detailed 8 shell case			
	Radius (cm)		
4	9.150	11.000	43638
5	11.000	12.250	39021
6	12.250	13.250	37156
	Inner	Outer	
Steel reflector			
1	13.250	15.000	32860
2	15.000	21.500	208500
Simplified case			
Layer no.	Radius (cm)		Layer mass (g)
	Inner	Outer	
Fuel			
1	2.686[a]	13.250	177997
Steel reflector			
1	13.250	15.000	32860
2	15.000	21.500	208500

[a] p. 11, Ref. 7.3, IMF-005

Table 5.1.7.3-7. Atom Densities (atoms/b-cm) of the IMF-005 Critical Assembly (p. 12, Ref. 7.3, IMF-005)

Detailed 8 shell case								
Fuel								
Layer no.	U^{234} ($\times 10^{-4}$)	U^{235} ($\times 10^{-2}$)	U^{238} ($\times 10^{-2}$)	C ($\times 10^{-4}$)	Fe ($\times 10^{-4}$)	W ($\times 10^{-5}$)	Cu ($\times 10^{-4}$)	Ni ($\times 10^{-4}$)
1	1.5823	1.7320	2.9783	4.6685	1.6065	1.2200	4.6685	1.7665
2	1.5677	1.7194	2.9508	3.7026	1.5926	1.2095	3.7026	2.9710
3	1.5581	1.7174	2.9235	5.5201	1.5829	1.2021	5.5201	2.2621
4	1.3256	1.7141	2.9417	7.3802	1.1904	1.2054	7.3802	2.1030
5	1.6004	1.7121	2.9159	5.5031	0.9863	5.9920	5.5031	3.6459
6	1.7235	1.6958	2.8806	9.0767	0.97607	1.1860	9.0767	3.8907
Steel reflector								
Layer no.	Fe ($\times 10^{-2}$)	C ($\times 10^{-3}$)	Si ($\times 10^{-4}$)	Cr ($\times 10^{-4}$)	Mn ($\times 10^{-4}$)	Ni ($\times 10^{-4}$)	Cu ($\times 10^{-4}$)	
1	7.9285	1.1251	1.6038	2.5989	3.2796	2.3025	2.1265	
2	8.0388	1.1407	1.6261	2.6351	3.3253	2.3345	2.1561	
Simplified case								
Fuel								

Table 5.1.7.3-7. Atom Densities (atoms/b-cm) of the IMF-005 Critical Assembly (p. 12, Ref. 7.3, IMF-005)

Layer no.	U^{234} ($\times 10^{-4}$)	U^{235} ($\times 10^{-2}$)	U^{238} ($\times 10^{-2}$)	C ($\times 10^{-4}$)	Fe ($\times 10^{-4}$)	W ($\times 10^{-5}$)	Cu ($\times 10^{-4}$)	Ni ($\times 10^{-4}$)
1	1.5511	1.7154	2.9297	6.4945	1.2324	1.0711	2.6791	2.9008
Steel reflector								
Layer no.	**Fe ($\times 10^{-2}$)**	**C ($\times 10^{-3}$)**	**Si ($\times 10^{-4}$)**	**Cr ($\times 10^{-4}$)**	**Mn ($\times 10^{-4}$)**	**Ni ($\times 10^{-4}$)**	**Cu ($\times 10^{-4}$)**	
1	7.9285	1.1251	1.6038	2.5989	3.2796	2.3025	2.1265	
2	8.0388	1.1407	1.6261	2.6351	3.3253	2.3345	2.1561	

5.1.7.3.7 Duralumin-Reflected Spherical Assembly of U^{235} (36 wt%)

A criticality measurement for a duralumin reflected spherical assembly of U^{235} (36 wt%) was performed. Figure 5.1.6.3-1 shows a schematic sectional view of the assembly on the CTF. The CTF is described in detail on page 2 of Reference 7.3, IMF-003. The assembly core had a central cavity of 2.1 cm radius and incorporated 6 spherical layers of fissile material. Characteristics of these core layers are presented in Table 5.1.7.3-8. Seven spherical layers that differ slightly in density represented the duralumin reflector. The outermost layer had an outer radius of 25 cm. The k_{eff} value for the experimental configuration was 1.0000 ± 0.0023 (p. 14, Ref. 7.3, IMF-006). Two benchmark cases, one detailed and one simplified, were developed for this experiment. The reflector was represented in both cases as 2 spherical layers that differ slightly in density. Descriptions of the experimental case materials are given in Table 5.1.7.3-9.

Table 5.1.7.3-8. Dimensions and Mass Characteristics of the IMF-006 Critical Assembly (pp. 12, 13, Ref. 7.3, IMF-006)

Detailed 8 shell case			
Layer no.	**Radius (cm)**		**Layer mass (g)**
	Inner	**Outer**	
Fuel			
1	2.10[a]	6.00	16157
2	6.00	7.55	16630
3	7.55	9.15	25864
4	9.15	11.00	43638
5	11.00	12.25	39021
6	12.25	13.25	37156
Duralumin reflector			
1	13.25	15.00	11150
2	15.00	25.00	129550
Simplified case			
Layer no.	**Radius (cm)**		**Layer mass (g)**
	Inner	**Outer**	
Fuel			
1	2.10[a]	13.25	178853

Table 5.1.7.3-8. Dimensions and Mass Characteristics of the IMF-006 Critical Assembly (pp. 12, 13, Ref. 7.3, IMF-006)

Duralumin reflector			
1	13.25	15.00	11150
2	15.00	25.00	129550

[a] p. 11, Ref. 7.3, IMF-006

Table 5.1.7.3-9. Atom Densities (atoms/b-cm) of the IMF-006 Critical Assembly (pp. 13, 14, Ref. 7.3, IMF-006)

Detailed 8 shell case								
Fuel								
Layer no.	U^{234} ($\times10^{-4}$)	U^{235} ($\times10^{-2}$)	U ($\times10^{-2}$)	C ($\times10^{-4}$)	Fe ($\times10^{-4}$)	W ($\times10^{-5}$)	Cu ($\times10^{-4}$)	Ni ($\times10^{-4}$)
1	1.5813	1.7320	2.9784	4.6685	1.6065	1.2200	4.6685	1.7665
2	1.5677	1.7194	2.9508	3.7026	1.5926	1.2095	3.7026	2.9710
3	1.5581	1.7174	2.9235	5.5201	1.5829	1.2021	5.5201	2.2621
4	1.3256	1.7141	2.9417	7.3802	1.1904	1.2054	7.3802	2.1030
5	1.6004	1.7121	2.9159	5.5031	0.9863	5.9920	5.5031	3.6459
6	1.7235	1.6958	2.8806	9.0767	0.97607	1.1860	9.0767	3.8907
Duralumin reflector								
Layer no.		Al ($\times10^{-2}$)		Fe ($\times10^{-4}$)			Cu ($\times10^{-4}$)	
1		5.2342		9.5788			9.8614	
2		5.2067		9.5286			9.8097	
Simplified case								
Fuel								
Layer no.	U^{234} ($\times10^{-4}$)	U^{235} ($\times10^{-2}$)	U^{238} ($\times10^{-2}$)	C ($\times10^{-4}$)	Fe ($\times10^{-4}$)	W ($\times10^{-5}$)	Cu ($\times10^{-4}$)	Ni ($\times10^{-4}$)
1	1.5518	1.7161	2.9310	6.4888	1.2345	1.0721	2.6755	2.8969
Duralumin reflector								
Layer no.		Al ($\times10^{-2}$)		Fe ($\times10^{-4}$)			Cu ($\times10^{-4}$)	
1		5.2342		9.5788			9.8614	
2		5.2067		9.5286			9.8097	

5.1.7.3.8 Depleted Uranium-Reflected Spherical Assembly of U^{235} (36 wt%)

A criticality measurement for a depleted uranium reflected spherical assembly of U^{235} (36 wt%) was performed. Figure 5.1.6.3-1 shows a schematic sectional view of the assembly on the CTF. The CTF is described in detail on page 2 of Reference 7.3, IMF-003. The assembly core had a central cavity of 2 cm radius and incorporated 6 spherical layers of fissile material. Characteristics of these core layers are presented in Table 5.1.7.3-10. Three spherical layers that differ slightly in density represented the depleted uranium reflector. The outermost layer had an outer radius of 16.5 cm. The $k_{eff} \pm \sigma$ value for

the experimental configuration was 1.0000 ± 0.0018 (p. 14, Ref. 7.3, IMF-008). Descriptions of the experimental case materials are given in Table 5.1.7.3-11.

Table 5.1.7.3-10. Dimensions and Mass Characteristics of the IMF-008 Critical Assembly (p. 12, Ref. 7.3, IMF-008)

Detailed 9 shells case			
Layer no.	Radius (cm)		Layer mass (g)
	Inner	Outer	
Fuel			
0	1.40[a]	2.00	395.7
1	2.00	6.00	16256
2	6.00	7.55	16630
3	7.55	9.15	25864
4	9.15	11.00	43638
5	11.00	12.25	39021
6	12.25	13.25	37156
Depleted uranium reflector			
1	13.25	14.00	31510
2	14.00	15.00	48390
3	15.00	16.50	85890

[a] p. 11, Ref. 7.3, IMF-008

Table 5.1.7.3-11. Atom Densities (atoms/b-cm) of the IMF-008 Critical Assembly (p. 13, Ref. 7.3, IMF-008)

Detailed 9 shells case								
Fuel								
Layer no.	U^{234} ($\times10^{-4}$)	U^{235} ($\times10^{-2}$)	U^{238} ($\times10^{-2}$)	C ($\times10^{-4}$)	Fe ($\times10^{-4}$)	W ($\times10^{-5}$)	Cu ($\times10^{-4}$)	Ni ($\times10^{-4}$)
1	1.2314	1.6517	2.8320	5.3321	2.4847	0.58058	11.7720	12.7460
2	1.5814	1.7194	2.9508	3.7026	1.5926	1.2095	3.7026	2.9710
3	1.5677	1.7174	2.9235	5.5201	1.5829	1.2021	5.5201	2.2621
4	1.3256	1.7141	2.9417	7.3802	1.1904	1.2054	7.3802	2.1030
5	1.6004	1.7121	2.9159	5.5031	0.9863	5.9920	5.5031	3.6459
6	1.7235	1.6958	2.8806	9.0767	0.97607	1.1860	9.0767	3.8907
Depleted uranium reflector								
Layer no.	U^{235} ($\times10^{-2}$)		U^{238} ($\times10^{-2}$)		Fe ($\times10^{-4}$)		W ($\times10^{-5}$)	
1	2.0298×10^{-4}		4.5120×10^{-2}		3.6889×10^{-4}		2.7985×10^{-3}	
2	2.1577×10^{-4}		4.5870×10^{-2}		3.7509×10^{-4}		2.8456×10^{-3}	
3	2.0692×10^{-4}		4.5997×10^{-2}		3.7606×10^{-4}		2.8529×10^{-3}	

5.2 LCE MCNP Material Descriptions

5.2.1 LCE MCNP Cross Section Libraries

The MCNP cross section libraries utilized in the reactivity calculations are one of the primary components of the calculation that determines whether or not the neutronic behavior of the system is simulated correctly. Table 5.2.1-1 lists all of the MCNP cross section library identifiers (ZAID's) utilized in the LCE reactivity calculations documented in this calculation file. The MCNP ZAID's are used to identify the cross section libraries. The ZAID consists of a 5-integer element and isotope identifier followed by a cross section library designation suffix. The first one or two integers in the ZAID refer to the atomic number of the corresponding element. The three integers preceding the decimal always refer to the isotopic mass number. The ZAID suffixes presented in Table 5.2.1-1 correspond to libraries compiled from either ENDF/B-V, ENDF/B-VI, LANL/T-2, or LLNL evaluated cross section data sets. The atom percent in nature of the various isotopes presented in Table 5.2.1-1 were obtained from Reference 7.5. The temperatures, library names, and data sources were obtained from Appendix G of Reference 7.1.

Table 5.2.1-1. MCNP Cross Section Libraries Used in the LCE Reactivity Calculations

Element/ Isotope	MCNP ZAID	Atom % in nature	Atomic wt. ratio [1]	Temp. (K)	Library name	Data source
H-1	1001.50c	99.985	0.9992	294.0	rmccs	ENDF/B-V.0
H-1	1001.60c	99.985	0.9992	294.0	endf60	ENDF/B-VI.1
H-2	1002.55c	0.015	1.9968	294.0	rmccs	LANL/T-2
H-2	1002.60c	0.015	1.9968	294.0	endf60	ENDF/B-VI.0
Be-9	4009.50c	100.0	8.9348	294.0	rmccs	ENDF/B-V.0
Be-9	4009.60c	100.0	8.9348	294.0	endf60	ENDF/B-VI.0
B-10	5010.50c	19.400 [2]	9.9269	294.0	rmccs	ENDF/B-V.0
B-10	5010.60c	19.400 [2]	9.9269	294.0	endf60	ENDF/B-VI.1
B-11	5011.56c	80.600 [2]	10.9147	294.0	newxs	LANL/T-2
B-11	5011.60c	80.600 [2]	10.9147	294.0	endf60	ENDF/B-VI.0
C-nat	6000.50c	100.0	11.8969	294.0	rmccs	ENDF/B-V.0
C-nat	6000.60c	100.0	11.8980	294.0	endf60	ENDF/B-VI.1
C-12	6012.50c	98.90	11.8969	294.0	rmccs	ENDF/B-V.0
N-14	7014.50c	99.630	13.8830	294.0	rmccs	ENDF/B-V.0
N-14	7014.60c	99.630	13.8828	294.0	endf60	LANL/T-2
N-15	7015.55c	0.37	14.8710	294.0	rmccsa	LANL/T-2
N-15	7015.60c	0.37	14.8710	294.0	endf60	ENDF/B-VI.0
O-16	8016.50c	99.760	15.8580	294.0	rmccs	ENDF/B-V.0
O-16	8016.60c	99.760	15.8532	294.0	endf60	ENDF/B-VI.0

Table 5.2.1-1. MCNP Cross Section Libraries Used in the LCE Reactivity Calculations

Element/ Isotope	MCNP ZAID	Atom % in nature	Atomic wt. ratio [1]	Temp. (K)	Library name	Data source
O-17	8017.60c	0.04	16.8531	294.0	endf60	ENDF/B-VI.0
Mg-nat	12000.50c	100.0	24.0963	294.0	endf5u	ENDF/B-V.0
Mg-nat	12000.60c	100.0	24.0963	294.0	endf60	ENDF/B-VI.0
Al-27	13027.50c	100.0	26.7500	294.0	rmccs	ENDF/B-V.0
Al-27	13027.60c	100.0	26.7500	294.0	endf60	ENDF/B-VI.0
Si-nat	14000.50c	100.0	27.8440	294.0	endf5p	ENDF/B-V.0
Si-nat	14000.60c	100.0	27.8440	294.0	endf60	ENDF/B-VI.0
P-31	15031.50c	100.0	30.7080	294.0	endf5u	ENDF/B-V.0
P-31	15031.60c	100.0	30.7080	294.0	endf60	ENDF/B-VI.0
S-32	16032.50c	95.02	31.6970	294.0	endf5u	ENDF/B-V.0
S-32	16032.60c	95.02	31.6970	294.0	endf60	ENDF/B-VI.0
Ca-nat	20000.50c	100.0	39.7360	294.0	endf5u	ENDF/B-V.0
Ca-nat	20000.60c	100.0	39.7360	294.0	endf60	ENDF/B-VI.0
Ti-nat	22000.50c	100.0	47.4676	294.0	endf5u	ENDF/B-V.0
Ti-nat	22000.60c	100.0	47.4676	294.0	endf60	ENDF/B-VI.0
V-nat	23000.50c	100.0	50.5040	294.0	endf5u	ENDF/B-V.0
V-nat	23000.60c	100.0	50.5040	294.0	endf60	ENDF/B-VI.0
Cr-nat	24000.50c	100.0	51.5490	294.0	rmccs	ENDF/B-V.0
Cr-50	24050.60c	4.345	49.5170	294.0	endf60	ENDF/B-VI.1
Cr-52	24052.60c	83.790	51.4940	294.0	endf60	ENDF/B-VI.1
Cr-53	24053.60c	9.500	52.4860	294.0	endf60	ENDF/B-VI.1
Cr-54	24054.60c	2.365	53.4760	294.0	endf60	ENDF/B-VI.1
Mn-55	25055.50c	100.0	54.4661	294.0	endf5u	ENDF/B-V.0
Mn-55	25055.60c	100.0	54.4661	294.0	endf60	ENDF/B-VI.0
Fe-nat	26000.55c	100.0	55.3650	294.0	rmccs	LANL/T-2
Fe-54	26054.60c	5.900	53.4760	294.0	endf60	ENDF/B-VI.1
Fe-56	26056.60c	91.720	55.4540	294.0	endf60	ENDF/B-VI.1
Fe-57	26057.60c	2.100	56.4460	294.0	endf60	ENDF/B-VI.1
Fe-58	26058.60c	0.280	57.4360	294.0	endf60	ENDF/B-VI.1
Ni-nat	28000.50c	100.0	58.1826	294.0	rmccs	ENDF/B-V.0
Ni-58	28058.60c	68.270	57.4380	294.0	endf60	ENDF/B-VI.1
Ni-60	28060.60c	26.100	59.4160	294.0	endf60	ENDF/B-VI.1
Ni-61	28061.60c	1.130	60.4080	294.0	endf60	ENDF/B-VI.1

Table 5.2.1-1. MCNP Cross Section Libraries Used in the LCE Reactivity Calculations

Element/ Isotope	MCNP ZAID	Atom % in nature	Atomic wt. ratio [1]	Temp. (K)	Library name	Data source
Ni-62	28062.60c	3.590	61.3960	294.0	endf60	ENDF/B-VI.1
Ni-64	28064.60c	0.910	63.3790	294.0	endf60	ENDF/B-VI.1
Cu-nat	29000.50c	100.0	63.5460	294.0	rmccs	ENDF/B-V.0
Cu-63	29063.60c	69.170	62.3890	294.0	endf60	ENDF/B-VI.2
Cu-65	29065.60c	30.830	64.3700	294.0	endf60	ENDF/B-VI.2
Ga-nat	31000.50c	100.0	69.1211	294.0	rmccs	ENDF/B-V.0
Ga-nat	31000.60c	100.0	69.1211	294.0	endf60	ENDF/B-VI.0
Zr-nat	40000.56c	100.0	90.4360	294.0	misc5xs	ENDF/B-V: XTM
Zr-nat	40000.60c	100.0	90.4360	294.0	endf60	ENDF/B-VI.1
Nb-93	41093.50c	100.0	92.1051	294.0	endf5p	ENDF/B-V.0
Nb-93	41093.60c	100.0	92.1051	294.0	endf60	ENDF/B-VI.1
Mo-nat	42000.50c	100.0	95.1160	294.0	endf5u	ENDF/B-V.0
Mo-nat	42000.60c	100.0	95.1160	294.0	endf60	ENDF/B-VI.0
Cd-nat	48000.50c	100.0	111.4600	294.0	endf5u	ENDF/B-V.0
Gd-152	64152.50c	0.2	150.6150	294.0	endf5u	ENDF/B-V.0
Gd-152	64152.60c	0.2	150.6150	294.0	endf60	ENDF/B-VI.0
Gd-154	64154.50c	2.18	152.5990	294.0	endf5u	ENDF/B-V.0
Gd-154	64154.60c	2.18	152.5990	294.0	endf5u	ENDF/B-V.0
Gd-155	64155.50c	14.80	153.5920	294.0	endf5u	ENDF/B-V.0
Gd-155	64155.60c	14.80	153.5920	294.0	endf5u	ENDF/B-V.0
Gd-156	64156.50c	20.47	154.5830	294.0	endf5u	ENDF/B-V.0
Gd-156	64156.60c	20.47	154.5830	294.0	endf5u	ENDF/B-V.0
Gd-157	64157.50c	15.65	155.5760	294.0	endf5u	ENDF/B-V.0
Gd-157	64157.60c	15.65	155.5760	294.0	endf5u	ENDF/B-V.0
Gd-158	64158.50c	24.84	156.5670	294.0	endf5u	ENDF/B-V.0
Gd-158	64158.60c	24.84	156.5670	294.0	endf5u	ENDF/B-V.0
Gd-160	64160.50c	21.86	158.5530	294.0	endf5u	ENDF/B-V.0
Gd-160	64160.60c	21.86	158.5530	294.0	endf60	ENDF/B-V.0
W-nat	74000.55c	100.0	182.2770	294.0	rmccs	ENDF/B-V.2
W-182	74182.60c	26.3	180.3900	294.0	endf60	ENDF/B-VI.0
W-183	74183.60c	14.28	181.3800	294.0	endf60	ENDF/B-VI.0

Table 5.2.1-1. MCNP Cross Section Libraries Used in the LCE Reactivity Calculations

Element/ Isotope	MCNP ZAID	Atom % in nature	Atomic wt. ratio [1]	Temp. (K)	Library name	Data source
W-184	74184.60c	30.7	182.3700	294.0	endf60	ENDF/B-VI.0
W-186	74186.60c	28.6	184.3600	294.0	endf60	ENDF/B-VI.0
U-234	92234.50c	0.0055	232.0300	294.0	endf5p	ENDF/B-V.0
U-234	92234.60c	0.0055	232.0300	294.0	endf60	ENDF/B-VI.0
U-235	92235.50c	0.7200	233.0250	294.0	rmccs	ENDF/B-V.0
U-235	92235.60c	0.7200	233.0250	294.0	endf60	ENDF/B-VI.2
U-236	92236.50c	0.0	234.0180	294.0	endf5p	ENDF/B-V.0
U-236	92236.60c	0.0	234.0180	294.0	endf60	ENDF/B-VI.0
U-238	92238.50c	99.2745	236.0060	294.0	rmccs	ENDF/B-V.0
U-238	92238.60c	99.2745	236.0060	294.0	endf60	ENDF/B-VI.2
Pu-238	94238.50c	0.0	236.1670	294.0	endf5p	ENDF/B-VI.0
Pu-238	94238.60c	0.0	236.0045	294.0	endf60	ENDF/B-V.0
Pu-239	94239.55c	0.0	236.9990	294.0	rmccs	ENDF/B-V.2
Pu-239	94239.60c	0.0	236.9986	294.0	endf60	ENDF/B-VI.2
Pu-240	94240.50c	0.0	237.9920	294.0	rmccs	ENDF/B-V.0
Pu-240	94240.60c	0.0	237.9920	294.0	endf60	ENDF/B-VI.2
Pu-241	94241.50c	0.0	238.9780	294.0	endf5p	ENDF/B-V.0
Pu-241	94241.60c	0.0	238.9780	294.0	endf60	ENDF/B-VI.1
Pu-242	94242.50c	0.0	239.9790	294.0	endf5p	ENDF/B-V.0
Pu-242	94242.60c	0.0	239.9790	294.0	endf60	ENDF/B-VI.0
Am-241	95241.50c	0.0	238.9860	294.0	endf5u	ENDF/B-V.0
Am-241	95241.60c	0.0	238.9860	294.0	endf60	LANL/T-2

[1] The atomic weight ratio presented for each isotope/element is the ratio of the isotope/element mass to the mass of a neutron. The mass of a neutron is 1.008664904 amu (p. 57, Ref. 7.5). The atomic weight ratio values are obtained from the "xsdir" file for MCNP as identified on page III-2 of Reference 7.4.

[2] The atom percent in nature of B-10 and B-11 varies significantly between different geographical regions of the world. The atom percents in nature that are listed in Table 5.2.1-1 for B-10 and B-11 were obtained from page 232 of Reference 7.6.

6. Results

This calculation file documents the LCE reactivity evaluations that were performed for benchmark calculations. Sections 6.1 through 6.6 present the k_{eff} results for each of the LCE evaluations. The k_{eff} results represent the average combined collision, absorption, and track-length estimator from the MCNP calculations. The standard deviation (σ) represents the standard deviation of k_{eff} about the average combined collision, absorption, and track-length estimate due to the Monte Carlo calculation statistics. Also presented in Sections 6.1 through 6.6 are tables of the $\Delta k_{eff} \pm 2$ standard deviations (2σ). These values were calculated using Equations 6.1 and 6.2.

Equation 6.1 $\Delta k = \text{Experimental k} - \text{Calculated k}$

Equation 6.2 $$2\sigma = \sqrt{(2\sigma)^2_{experimental} + (2\sigma)^2_{calculated}}$$

6.1 LEU System Results

6.1.1 LCT-001 Results

Table 6.1.1-1 presents the MCNP calculation results for ENDF/B-V, WPO Selected, and ENDF/B-VI cross section libraries for the LCT-001 set of critical experiments, which are also illustrated in Figure 6.1.1-1. Table 6.1.1-3 presents the AENCF values for the LCT-001 set of critical experiments. As presented in Figure 6.1.1-1 and Table 6.1.1-2, it can be seen that all of the calculated results are slightly less than the benchmark k_{eff} value. All of the cross section sets under-predict the k_{eff} value, with the ENDF/B-VI library being the least conservative. Similar behavior of under-predicting k_{eff} was also observed in the evaluators' KENO results.

Table 6.1.1-1. LCE Reactivity Calculation Results for LCT-001 Experiments

MCNP case name	KENO[a] $k_{eff} \pm \sigma$	ENDF/B-V $k_{eff} \pm \sigma$	WPO selected $k_{eff} \pm \sigma$	ENDF/B-VI $k_{eff} \pm \sigma$
Case_1	0.9914 ± 0.0011	0.9987 ± 0.00191	0.99436 ± 0.00167	0.99248 ± 0.00153
Case_2	0.9904 ± 0.0016	0.99557 ± 0.00185	0.99445 ± 0.00158	0.9923 ± 0.00161
Case_3	0.9888 ± 0.0016	0.9957 ± 0.00175	0.99982 ± 0.00159	0.99637 ± 0.00172
Case_4	0.9962 ± 0.0016	0.99907 ± 0.00144	0.99313 ± 0.00161	0.98949 ± 0.00156
Case_5	0.9890 ± 0.0017	0.99313 ± 0.00157	0.9931 ± 0.00169	0.99429 ± 0.00172
Case_6	0.9931 ± 0.0015	0.99882 ± 0.00143	0.99831 ± 0.00158	0.99161 ± 0.00158
Case_7	0.9919 ± 0.0017	0.99677 ± 0.00143	0.99261 ± 0.00138	0.99578 ± 0.00155
Case_8	0.9906 ± 0.0016	1.00246 ± 0.00162	0.99888 ± 0.00151	0.99597 ± 0.00149

[a] These values are sample calculation results using KENO and 27-Group ENDF/B-IV cross section libraries. Reported values are from page 26 of Reference 7.3, LCT-001.

Table 6.1.1-2. Δk Between Experimental k_{eff} and MCNP Calculated k_{eff} for LCT-001 Experiments

MCNP case name	ENDF/B-V $\Delta k_{eff} \pm 2\sigma$	WPO selected $\Delta k_{eff} \pm 2\sigma$	ENDF/B-VI $\Delta k_{eff} \pm 2\sigma$
Case_1	0.00110 ± 0.00728	0.00544 ± 0.00704	0.00732 ± 0.00691
Case_2	0.00423 ± 0.00722	0.00535 ± 0.00696	0.00750 ± 0.00699
Case_3	0.00410 ± 0.00712	-0.00002 ± 0.00318	0.00343 ± 0.00486
Case_4	0.00073 ± 0.00684	0.00667 ± 0.00699	0.01031 ± 0.00694
Case_5	0.00667 ± 0.00695	0.00670 ± 0.00706	0.00551 ± 0.00709
Case_6	0.00098 ± 0.00683	0.00149 ± 0.00696	0.00819 ± 0.00696
Case_7	0.00303 ± 0.00683	0.00719 ± 0.00679	0.00402 ± 0.00693
Case_8	-0.00266 ± 0.00700	0.00092 ± 0.00316	0.00383 ± 0.00485

Table 6.1.2-3. AENCF for LCT-001 Experiments (MeV)

MCNP case name	ENDF/B-V	ENDF/B-VI	WPO selected
Case1	0.1239	0.1227	0.1229
Case2	0.1208	0.1210	0.1223
Case3	0.1220	0.1221	0.1200
Case4	0.1208	0.1207	0.1222
Case5	0.1218	0.1187	0.1204
Case6	0.1208	0.1219	0.1221
Case7	0.1186	0.1176	0.1211
Case8	0.1201	0.1214	0.1209

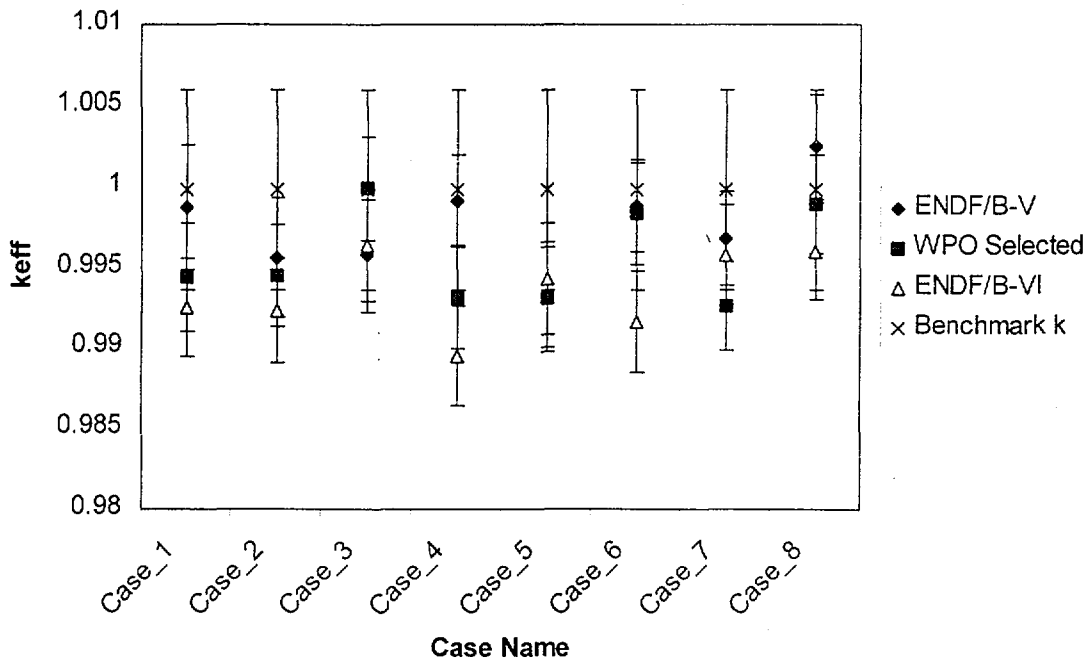

Figure 6.1.1-1. LCE Calculation Results for LCT-001 Experiments

6.1.2 LCE Calculation Results for MKIA Experiments

Table 6.1.2-1 presents the MCNP calculation results for ENDF/B-V, WPO Selected, and ENDF/B-VI cross section libraries for the MKIA set of critical experiments, which are also illustrated in Figure 6.1.2-1. Table 6.1.2-3 presents the AENCF values for the MKIA set of critical experiments. As presented in Figure 6.1.2-1 and Table 6.1.2-2, it can be seen that all of the results over-predict the benchmark k_{eff} value.

Table 6.1.2-1. LCE Reactivity Calculation Results for MKIA Experiments

MCNP case name	Reference MCNP $k_{eff} \pm \sigma$[a]	ENDF/B-V $k_{eff} \pm \sigma$	WPO selected $k_{eff} \pm \sigma$	ENDF/B-VI $k_{eff} \pm \sigma$
subc2p8h	1.0088 ± 0.0021	1.0048 ± 0.00294	1.00887 ± 0.00320	1.01057 ± 0.00335
subc3p1h	1.0392 ± 0.0018	1.03902 ± 0.00248	1.0335 ± 0.00287	1.04014 ± 0.00310
subc3p4h	1.0232 ± 0.0019	1.02088 ± 0.00277	1.01929 ± 0.00238	1.01971 ± 0.00266

[a] Values were calculated with MCNP and a continuous energy cross section library (p. A-6, Ref. 7.17), and are from page 52 of Reference 7.17.

Table 6.1.2-2. Δk Between Experimental k_{eff} and MCNP Calculated k_{eff} for MKIA Experiments

MCNP case name	ENDF/B-V $\Delta k_{eff} \pm 2\sigma$	WPO selected $\Delta k_{eff} \pm 2\sigma$	ENDF/B-VI $\Delta k_{eff} \pm 2\sigma$
subc2p8h	-0.00480 ± 0.01160	-0.00887 ± 0.01094	-0.01057 ± 0.01251
subc3p1h	-0.03902 ± 0.01116	-0.03350 ± 0.03399	-0.04014 ± 0.04062
subc3p4h	-0.02088 ± 0.01143	-0.01929 ± 0.01987	-0.01971 ± 0.02042

Table 6.1.2-3. AENCF for MKIA Experiments (MeV)

MCNP case name	ENDF/B-V	ENDF/B-VI	WPO selected
SUBC2P8H	0.4085	0.4005	0.4085
SUBC3P1H	0.3516	0.3447	0.3417
SUBC3P4H	0.3145	0.3165	0.3153

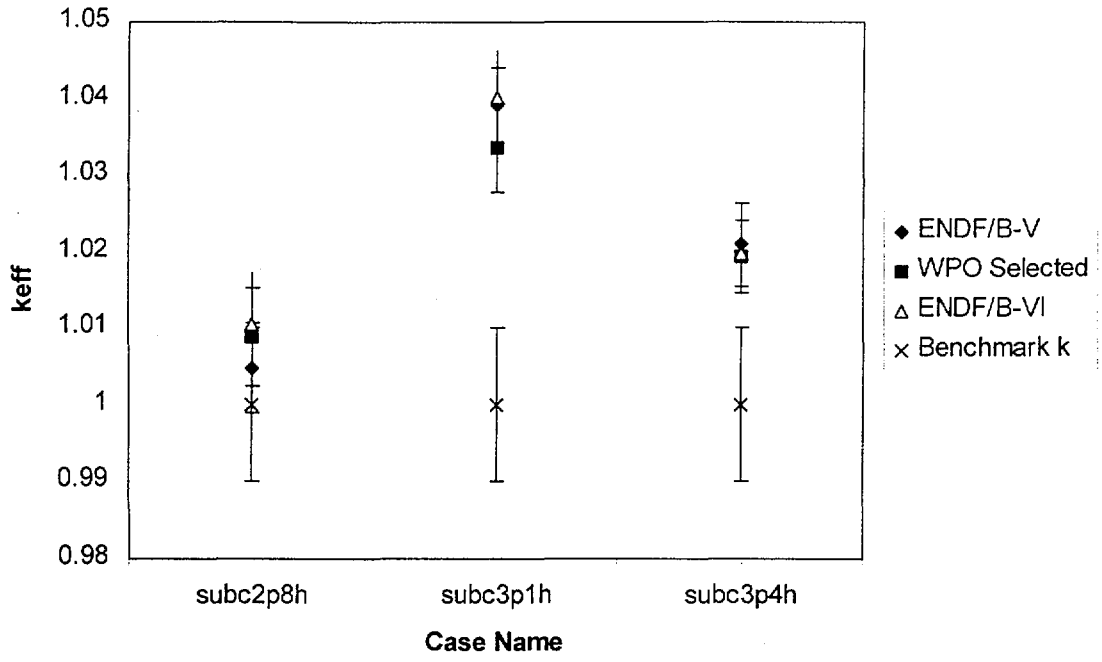

Figure 6.1.2-1. LCE Calculation Results for MKIA Experiments

6.2 IEU System Results

6.2.1 TRIGA Fuel Rod Experiments

Table 6.2.1-1 presents the MCNP calculation results for ENDF/B-V, WPO Selected, and ENDF/B-VI cross section libraries for the TRIGA set of critical experiments, which are also illustrated in Figure 6.2.1-1. Table 6.2.1-3 presents the AENCF values for the TRIGA set of critical experiments. As presented in Figure 6.2.1-1 and Table 6.2.1-2, it can be seen that both of the calculated results are slightly greater than the benchmark k_{eff} value. All of the cross section sets over-predict the k_{eff} value, with the WPO Selected library being the most conservative. Similar behavior of under-predicting k_{eff} was also observed in the evaluators' KENO results.

Table 6.2.1-1. LCE Reactivity Calculation Results for TRIGA Experiments

MCNP case name	KENO[a] $k_{eff} \pm \sigma$	ENDF/B-V[b] $k_{eff} \pm \sigma$	WPO selected $k_{eff} \pm \sigma$	ENDF/B-VI $k_{eff} \pm \sigma$
tri17	1.0191 ± 0.0014	1.00737 ± 0.00129	1.00897 ± 0.00141	1.00740 ± 0.00132
tri18	1.0201 ± 0.0013	1.00921 ± 0.00132	1.01314 ± 0.00126	1.01195 ± 0.00143

[a] These values are sample calculation results using KENO and 27-Group ENDF/B-IV cross section libraries. Reported values are from page 10 of Reference 7.14.

[b] The values calculated for the ENDF/B-V and ENDF/B-VI cross section libraries were within the statistical uncertainty of the sample MCNP values using the ENDF/B-V and ENDF/B-VI libraries reported on page 10 of Reference 7.14.

Table 6.2.1-2. Δk Between Experimental k_{eff} and MCNP Calculated k_{eff} for TRIGA Experiments

MCNP case name	ENDF/B-V $\Delta k_{eff} \pm 2\sigma$	WPO selected $\Delta k_{eff} \pm 2\sigma$	ENDF/B-VI $\Delta k_{eff} \pm 2\sigma$
tri17	-0.00872 ± 0.00261	-0.01032 ± 0.01070	-0.00875 ± 0.00914
tri18	-0.00641 ± 0.00267	-0.01034 ± 0.01064	-0.00915 ± 0.00959

Table 6.2.1-3. AENCF for TRIGA Experiments (MeV)

MCNP case name	ENDF/B-V	WPO selected	ENDF/B-VI
tri17	0.0233	0.0236	0.0236
tri18	0.0234	0.0240	0.0238

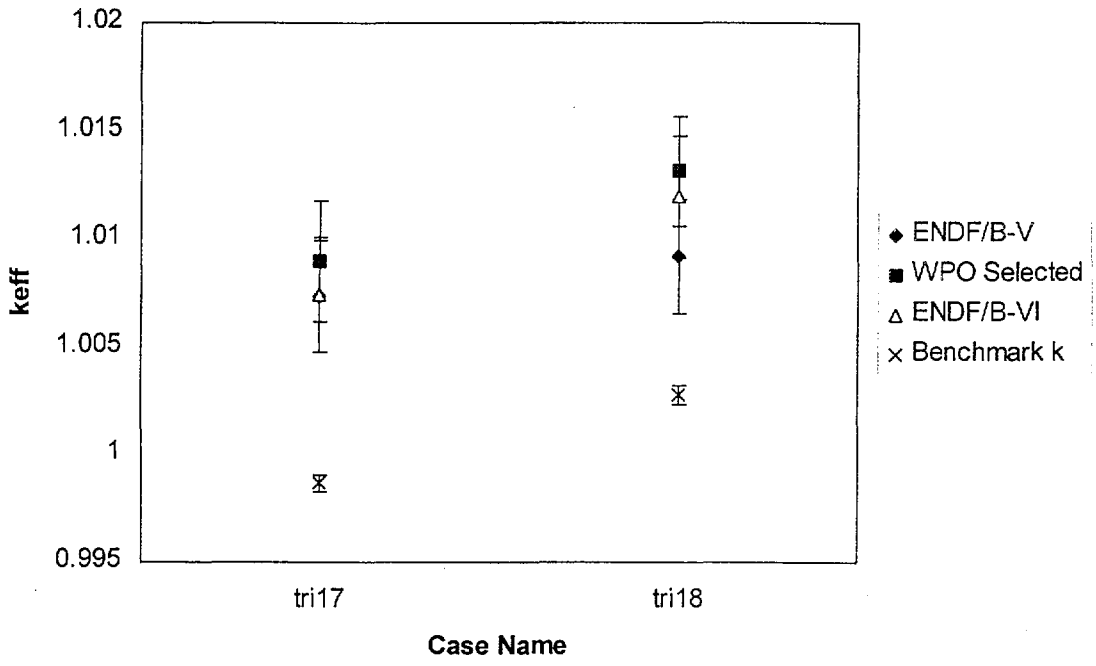

Figure 6.2.1-1. LCE Calculation Results for TRIGA Experiments

6.3 HEU Thermal System Results

6.3.1 HTM-006 Results

Table 6.3.1-1 presents the MCNP calculation results for ENDF/B-V, WPO Selected, and ENDF/B-VI cross section libraries for the SPERT-D Fuel set of critical experiments, which are also illustrated in Figure 6.3.1-1. Table 6.3.1-3 presents the AENCF values for the SPERT-D Fuel set of critical

experiments. As presented in Figure 6.3.1-1 and Table 6.3.1-2, it can be seen that all of the calculated results are slightly greater than or slightly less than the benchmark k_{eff} value. In this set of experiments the WPO Selected results were the same as the ENDF/B-V results. The calculated k_{eff} for SPERT13 was significantly higher than the benchmark k_{eff} for no apparent reason. This behavior was also observed in the sample calculations provided by the evaluator and stated on page 29 of Reference 7.3, HMT-006.

Table 6.3.1-1. LCE Reactivity Calculation Results for HMT-006

MCNP case name	KENO[a] $k_{eff} \pm \sigma$	ENDF/B-V $k_{eff} \pm \sigma$	WPO selected $k_{eff} \pm \sigma$	ENDF/B-VI $k_{eff} \pm \sigma$
spert1	0.9958 ± 0.0013	0.99792 ± 0.00184	0.99792 ± 0.00184	0.99727 ± 0.00176
spert2	0.9990 ± 0.0012	0.99952 ± 0.0019	0.99952 ± 0.0019	0.99732 ± 0.00186
spert3	1.0062 ± 0.0012	1.00676 ± 0.00114	1.00676 ± 0.00114	1.00384 ± 0.00095
spert4	0.9924 ± 0.0012	0.99542 ± 0.00173	0.99542 ± 0.00173	0.98908 ± 0.00179
spert5	0.9997 ± 0.0011	1.00104 ± 0.00162	1.00104 ± 0.00162	1.00072 ± 0.00183
spert6	1.0035 ± 0.0011	1.00133 ± 0.00168	1.00133 ± 0.00168	0.99683 ± 0.00152
spert7	0.9975 ± 0.0011	0.99923 ± 0.00163	0.99923 ± 0.00163	0.9952 ± 0.00147
spert8	0.9925 ± 0.0011	0.99843 ± 0.00154	0.99843 ± 0.00154	0.99009 ± 0.0015
spert9	0.9935 ± 0.0011	1.00003 ± 0.00143	1.00003 ± 0.00143	0.99697 ± 0.00149
spert10	1.0064 ± 0.0013	1.00608 ± 0.00177	1.00608 ± 0.00177	1.00534 ± 0.0019
spert11	1.0036 ± 0.0012	1.00565 ± 0.00163	1.00565 ± 0.00163	1.00283 ± 0.00171
spert12	1.0064 ± 0.0011	1.00676 ± 0.00156	1.00676 ± 0.00156	1.00466 ± 0.00175
spert13	1.0265 ± 0.0012	1.03289 ± 0.00181	1.03289 ± 0.00181	1.02936 ± 0.00189
spert14	0.9977 ± 0.0012	0.99451 ± 0.00158	0.99451 ± 0.00158	0.99427 ± 0.00159
spert15	0.9933 ± 0.0011	0.99355 ± 0.00107	0.99355 ± 0.00107	0.99179 ± 0.00103
spert16	1.0054 ± 0.0013	1.00791 ± 0.00175	1.00791 ± 0.00175	1.00549 ± 0.00183
spert17	1.0050 ± 0.0013	1.00569 ± 0.00188	1.00569 ± 0.00188	1.00206 ± 0.00179
spert18	1.0065 ± 0.0014	1.00028 ± 0.00198	1.00028 ± 0.00198	1.00615 ± 0.00181
spert19	0.9929 ± 0.0011	0.99482 ± 0.00148	0.99482 ± 0.00148	0.98982 ± 0.00158
spert20	0.9945 ± 0.0011	0.99652 ± 0.00158	0.99652 ± 0.00158	0.99315 ± 0.00166
spert21	0.9966 ± 0.0011	1.00113 ± 0.00186	1.00113 ± 0.00186	1.00086 ± 0.00178
spert22	0.9994 ± 0.0011	1.00272 ± 0.00194	1.00272 ± 0.00194	0.9984 ± 0.00175
spert23	1.0011 ± 0.0010	1.00695 ± 0.0011	1.00695 ± 0.00110	1.00426 ± 0.00099

[a] These values are sample calculation results using KENO and 27-Group ENDF/B-IV cross section libraries. Reported values are from page 30 of Reference 7.3, HMT-006.

Table 6.3.1-2. Δk Between Experimental k_{eff} and MCNP Calculated k_{eff} for HMT-006 Experiments

MCNP case name	ENDF/B-V $\Delta k_{eff} \pm 2\sigma$	WPO selected $\Delta k_{eff} \pm 2\sigma$	ENDF/B-VI $\Delta k_{eff} \pm 2\sigma$
spert1	0.00208 ± 0.00881	0.00208 ± 0.00881	0.00273 ± 0.00874
spert2	0.00048 ± 0.00886	0.00048 ± 0.00886	0.00268 ± 0.00882
spert3	-0.00676 ± 0.00832	-0.00676 ± 0.00832	-0.00384 ± 0.00822

Table 6.3.1-2. Δk Between Experimental k_{eff} and MCNP Calculated k_{eff} for HMT-006 Experiments

MCNP case name	ENDF/B-V $\Delta k_{eff} \pm 2\sigma$	WPO selected $\Delta k_{eff} \pm 2\sigma$	ENDF/B-VI $\Delta k_{eff} \pm 2\sigma$
spert4	0.00458 ± 0.00872	0.00458 ± 0.00872	0.01092 ± 0.00876
spert5	-0.00104 ± 0.00863	-0.00104 ± 0.00863	-0.00072 ± 0.00880
spert6	-0.00133 ± 0.00868	-0.00133 ± 0.00868	0.00317 ± 0.00856
spert7	0.00077 ± 0.00864	0.00077 ± 0.00864	0.00480 ± 0.00852
spert8	0.00157 ± 0.00857	0.00157 ± 0.00857	0.00991 ± 0.00854
spert9	-0.00003 ± 0.00850	-0.00003 ± 0.00850	0.00303 ± 0.00854
spert10	-0.00608 ± 0.00875	-0.00608 ± 0.00875	-0.00534 ± 0.00886
spert11	-0.00565 ± 0.00864	-0.00565 ± 0.00864	-0.00283 ± 0.00870
spert12	-0.00676 ± 0.00859	-0.00676 ± 0.00859	-0.00466 ± 0.00873
spert13	-0.03289 ± 0.00878	-0.03289 ± 0.00878	-0.02936 ± 0.00885
spert14	0.00549 ± 0.00860	0.00549 ± 0.00860	0.00573 ± 0.00861
spert15	0.00645 ± 0.00828	0.00645 ± 0.00828	0.00821 ± 0.00826
spert16	-0.00791 ± 0.00873	-0.00791 ± 0.00873	-0.00549 ± 0.00880
spert17	-0.00569 ± 0.00884	-0.00569 ± 0.00682	-0.00206 ± 0.00413
spert18	-0.00028 ± 0.00893	-0.00028 ± 0.00397	-0.00615 ± 0.00714
spert19	0.00518 ± 0.00853	0.00518 ± 0.00853	0.01018 ± 0.00860
spert20	0.00348 ± 0.00860	0.00348 ± 0.00860	0.00685 ± 0.00866
spert21	-0.00113 ± 0.00882	-0.00113 ± 0.00882	-0.00086 ± 0.00876
spert22	-0.00272 ± 0.00889	-0.00272 ± 0.00889	0.00160 ± 0.00873
spert23	-0.00695 ± 0.00830	-0.00695 ± 0.00830	-0.00426 ± 0.00824

Table 6.3.1-3. AENCF for HMT-006 Experiments

MCNP case name	ENDF/B-V	ENDF/B-VI	WPO selected
spert1	0.0147	0.0140	0.0147
spert2	0.0126	0.0125	0.0126
spert3	0.0117	0.0112	0.0117
spert4	0.0110	0.0113	0.0110
spert5	0.0105	0.0110	0.0105
spert6	0.0102	0.0098	0.0102
spert7	0.0097	0.0104	0.0097
spert8	0.0098	0.0096	0.0098
spert9	0.0099	0.0098	0.0099
spert10	0.0147	0.0140	0.0147
spert11	0.0115	0.0113	0.0115
spert12	0.0101	0.0102	0.0101
spert13	0.0143	0.0141	0.0143
spert14	0.0106	0.0107	0.0106
spert15	0.0106	0.0105	0.0106
spert16	0.0120	0.0118	0.0120
spert17	0.0131	0.0133	0.0131

Table 6.3.1-3. AENCF for HMT-006 Experiments

MCNP case name	ENDF/B-V	ENDF/B-VI	WPO selected
spert18	0.0140	0.0135	0.0140
spert19	0.0097	0.0090	0.0097
spert20	0.0114	0.0115	0.0114
spert21	0.0126	0.0127	0.0124
spert22	0.0133	0.0131	0.0133
spert23	0.0132	0.0131	0.0133

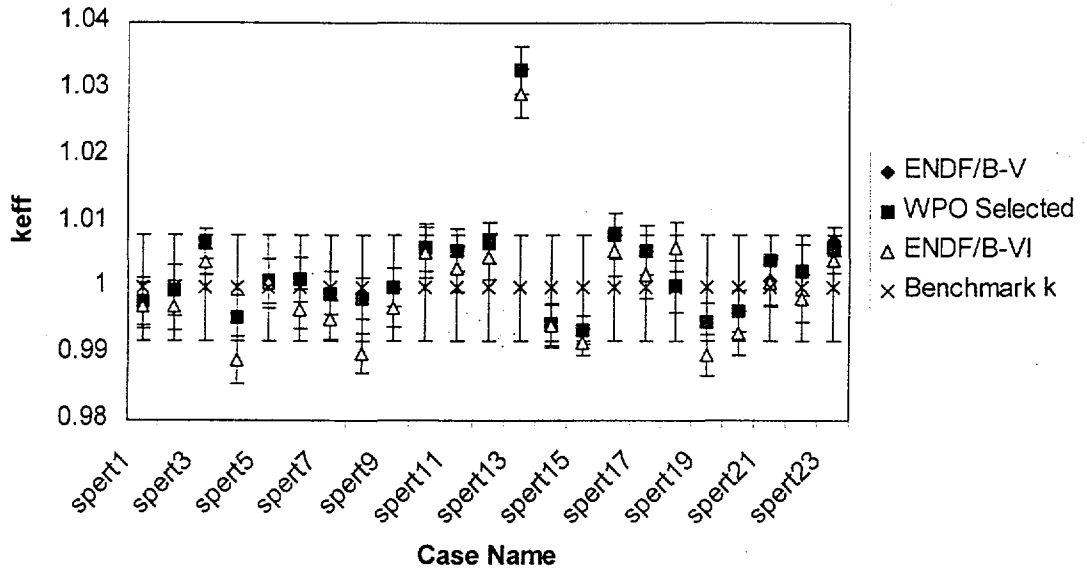

Figure 6.3.1-1. LCE Calculation Results for HMT-006 Experiments

6.3.2 Water-Moderated Hexagonally Pitched Lattices of Highly Enriched Fuel Rods of Cross-Shaped Cross Section Results

Table 6.3.2-1 presents the MCNP calculation results for ENDF/B-V, WPO Selected, and ENDF/B-VI cross section libraries for the HCT-003, 004, 005, 006, 007, and 008 set of critical experiments, which are also illustrated in Figures 6.3.2-1 through 6.3.2-5. Table 6.3.2-3 presents the AENCF for the HCT-003, 004, 005, 006, 007, and 008 set of critical experiments. As presented in Figure 6.3.2-1 and in Table 6.3.2-2, it can be seen that arrays with middle-spaced lattice in the peripheral zone (hct3-6 through hct3-11) gave high results. Arrays with a closely spaced lattice in the peripheral zone tended to give results less than the benchmark value (cases hct3-1 through hct3-4, hct3-12, and hct3-13), with the exception of the WPO selected library in case hct3-4 being greater than the benchmark value. Figure 6.3.2-2 shows all of the calculated results in the hct-004 set of experiments as being less than the benchmark value. Two cases were used to describe HCT-005 and HCT-007 experiments. In the first one (hct5-1, hct7-1, hct7-2, and hct7-3), the fuel rod was assumed to be cylindrical and in the second (hct5-2, hct7-4, hct7-5,

and hct7-6) the cross-shaped fuel rod was represented. There is up to 0.9% difference between the k_{eff} obtained using a cylindrical fuel rod and a cross-shaped fuel rod. Figures 6.3.2-3 and 6.3.2-5 show the HCT-005 and HCT-007 results respectively. Figure 6.3.2-4 shows the HCT-006 and HCT-008 results.

Table 6.3.2-1. LCE Reactivity Calculation Results for HCT-003, 004, 005, 006, 007, and 008 Experiments

MCNP case name	ENDF/B-V[a] $k_{eff} \pm \sigma$	WPO selected $k_{eff} \pm \sigma$	ENDF/B-VI $k_{eff} \pm \sigma$
hct3-1	0.99381 ± 0.00136	0.99475 ± 0.0015	0.99473 ± 0.00138
hct3-2	0.99746 ± 0.00144	0.99147 ± 0.00152	0.9956 ± 0.00144
hct3-3	0.99637 ± 0.00144	0.99699 ± 0.00132	0.99473 ± 0.00149
hct3-4	0.99796 ± 0.00148	1.00159 ± 0.00141	0.99688 ± 0.00148
hct3-5	1.00253 ± 0.00137	1.00175 ± 0.00146	1.0006 ± 0.00151
hct3-6	1.00616 ± 0.00152	1.00947 ± 0.00153	1.00706 ± 0.0016
hct3-7	1.01132 ± 0.00143	1.01327 ± 0.00144	1.009 ± 0.00145
hct3-8	1.00988 ± 0.00155	1.01001 ± 0.0015	1.01081 ± 0.00143
hct3-9	1.01309 ± 0.00154	1.01332 ± 0.00147	1.01355 ± 0.00145
hct3-10	1.00962 ± 0.0014	1.01014 ± 0.00143	1.01004 ± 0.00149
hct3-11	1.0133 ± 0.0014	1.01347 ± 0.00137	1.01317 ± 0.00152
hct3-12	0.98956 ± 0.00133	0.9933 ± 0.00136	0.98921 ± 0.00135
hct3-13	0.99677 ± 0.00119	1.00022 ± 0.00126	0.99588 ± 0.00126
hct3-14	1.005 ± 0.00157	1.00853 ± 0.00143	1.00682 ± 0.0015
hct3-15	1.00775 ± 0.00142	1.00648 ± 0.00128	1.003 ± 0.00141
hct4-1	0.98756 ± 0.00122	0.98875 ± 0.00126	0.99143 ± 0.00122
hct4-2	0.9889 ± 0.0012	0.98977 ± 0.00124	0.99042 ± 0.00123
hct4-3[b]	0.99157 ± 0.00119	0.99049 ± 0.00123	0.99272 ± 0.00121
hct4-4[b]	0.99116 ± 0.00114	0.99036 ± 0.00118	0.98934 ± 0.00122
hct5-1[c]	0.98467 ± 0.00118	0.98653 ± 0.0012	0.98829 ± 0.00117
hct5-2[c]	0.98455 ± 0.00128	0.98493 ± 0.0018	0.988871 ± 0.00115
hct6-t1	0.98952 ± 0.00137	0.99034 ± 0.00125	0.99212 ± 0.00136
hct6-t2	1.0104 ± 0.0013	1.01252 ± 0.00127	1.00798 ± 0.00128
hct6-t3	0.99557 ± 0.00095	0.9993 ± 0.001	0.99612 ± 0.00099
hct7-1	0.99271 ± 0.00155	0.99497 ± 0.00148	0.99909 ± 0.00149
hct7-2	0.9947 ± 0.00153	0.99633 ± 0.00142	0.99394 ± 0.00151
hct7-3	0.99196 ± 0.00144	0.99374 ± 0.00151	0.99499 ± 0.00154
hct7-4	0.99932 ± 0.00164	1.00086 ± 0.00149	0.99992 ± 0.00148
hct7-5	0.99492 ± 0.00156	0.99902 ± 0.00164	0.99969 ± 0.00152
hct7-6	0.99487 ± 0.00154	0.99556 ± 0.00154	0.99545 ± 0.00159
hct8-1[d]	0.99042 ± 0.00106	0.98915 ± 0.0011	0.99281 ± 0.00108
hct8-2[d]	0.98954 ± 0.00112	0.99273 ± 0.00108	0.99117 ± 0.00116

[a] The values calculated for the ENDF/B-V cross section libraries were within the statistical uncertainty of the sample MCNP values using the ENDF/B-V libraries reported in Reference 7.3 on p. 25 HCT-003

and p. 18 HCT-006. The calculated values for hct3-7 and hct3-15 were not within the statistical uncertainty of the sample MCNP values which used the ENDF/B-V libraries, and the reason for the differences could not be determined with the existing information.

[b] The values calculated using ENDF/B-V cross section libraries for hct4-3 and hct4-4 were not within the statistical uncertainty of the sample MCNP value which used the ENDF/B-V libraries reported on p. 20 of Reference 7.3, HCT-004. The reason is most likely due to the use of natural Sm as the absorber material in the sample calculation, and the use of Sm isotopes in this analysis. This calculation used the Sm isotopes because the natural Sm cross section data was unavailable.

[c] The evaluator noticed that in this experiment k_{eff} was strongly sensitive to the pitch values of the fuel-rod and narrow cluster arrays. Moreover, the sensitivity was a positive one; that is, the greater the pitch, the greater was k_{eff}. Additionally, the lattices were so close-spaced (maximally) that any deviations during the experiment of the dimensions that could have influence on the pitch (the fuel rod outer diameters, curve of the fuel rods, inner dimension of the cluster clads) would lead only to the increase of the pitches and, accordingly, to the increase of k_{eff}. Therefore, the absence of control of precise spacing of the arrays can be the reason for the calculated results underestimating k_{eff} (p. 16, Ref. 7.3, HCT-005). However, the experimental benchmark shows that MCNP code is able to predict the criticality within the uncertainty associated with the calculation and the experiments (Table 6.1.2-2). This result is independent of the cross section library used.

[d] The values calculated using ENDF/B-V cross section libraries for hct8-1 and hct8-2 were not within the statistical uncertainty of the sample MCNP value which used the ENDF/B-V libraries reported on p. 19 of Reference 7.3, HCT-008. The reason is most likely due to errors in the sample inputs provided by the evaluator which were corrected in this analysis.

Table 6.3.2-2. Δk Between Experimental k_{eff} and MCNP Calculated k_{eff} for HCT-003, 004, 005 006, 007, and 008 Experiments

MCNP case name	ENDF/B-V $\Delta k_{eff} \pm 2\sigma$	WPO selected $\Delta k_{eff} \pm 2\sigma$	ENDF/B-VI $\Delta k_{eff} \pm 2\sigma$
hct3-1	0.00619 ± 0.00921	0.00525 ± 0.00930	0.00527 ± 0.00922
hct3-2	0.00254 ± 0.00926	0.00853 ± 0.00931	0.00440 ± 0.00926
hct3-3	0.00363 ± 0.00926	0.00301 ± 0.00919	0.00527 ± 0.00929
hct3-4	0.00204 ± 0.00928	-0.00159 ± 0.00924	0.00312 ± 0.00928
hct3-5	-0.00253 ± 0.00922	-0.00175 ± 0.00927	-0.00060 ± 0.00930
hct3-6	-0.00616 ± 0.00931	-0.00947 ± 0.00932	-0.00706 ± 0.00936
hct3-7	-0.01132 ± 0.00925	-0.01327 ± 0.00926	-0.00900 ± 0.00927
hct3-8	-0.00988 ± 0.00933	-0.01001 ± 0.00930	-0.01081 ± 0.00925
hct3-9	-0.01309 ± 0.00932	-0.01332 ± 0.00928	-0.01355 ± 0.00927
hct3-10	-0.00962 ± 0.00923	-0.01014 ± 0.00925	-0.01004 ± 0.00929
hct3-11	-0.01330 ± 0.00923	-0.01347 ± 0.00922	-0.01317 ± 0.00931
hct3-12	0.01044 ± 0.00919	0.00670 ± 0.00921	0.01079 ± 0.00920
hct3-13	0.00323 ± 0.00912	-0.00022 ± 0.00915	0.00412 ± 0.00915
hct3-14	-0.00500 ± 0.00934	-0.00853 ± 0.00925	-0.00682 ± 0.00930
hct3-15	-0.00775 ± 0.00925	-0.00648 ± 0.00916	-0.00300 ± 0.00924

Table 6.3.2-2. Δk Between Experimental k_{eff} and MCNP Calculated k_{eff} for HCT-003, 004, 005 006, 007, and 008 Experiments

MCNP case name	ENDF/B-V $\Delta k_{eff} \pm 2\sigma$	WPO selected $\Delta k_{eff} \pm 2\sigma$	ENDF/B-VI $\Delta k_{eff} \pm 2\sigma$
hct4-1	0.01244 ± 0.00798	0.01125 ± 0.01153	0.00857 ± 0.00891
hct4-2	0.01110 ± 0.00816	0.01023 ± 0.00818	0.00958 ± 0.00818
hct4-3	0.00843 ± 0.00777	0.00951 ± 0.00780	0.00728 ± 0.00779
hct4-4	0.00884 ± 0.00793	0.00964 ± 0.00992	0.01066 ± 0.01094
hct5-1	0.01533 ± 0.018948	0.01171 ± 0.0190	0.01347 ± 0.0190
hct5-2	0.01545 ± 0.018973	0.01129 ± 0.0189	0.01507 ± 0.0191
hct6-t1	0.01048 ± 0.01192	0.00966 ± 0.01187	0.00788 ± 0.01191
hct6-t2	-0.01040 ± 0.00477	-0.01252 ± 0.00474	-0.00798 ± 0.00475
hct6-t3	0.00443 ± 0.00979	0.00070 ± 0.00981	0.00388 ± 0.00980
hct7-1	0.00729 ± 0.004675	0.00091 ± 0.00761	0.00503 ± 0.0076
hct7-2	0.0053 ± 0.005116	0.00606 ± 0.00874	0.00367 ± 0.0087
hct7-3	0.00804 ± 0.005175	0.00501 ± 0.00913	0.00626 ± 0.0091
hct7-4	0.00068 ± 0.004797	8E-05 ± 0.0076	-0.0009 ± 0.0076
hct7-5	0.00508 ± 0.005152	0.00031 ± 0.00875	0.00098 ± 0.0088
hct7-6	0.00513 ± 0.005289	0.00455 ± 0.00917	0.00444 ± 0.0091
hct8-1	0.00958 ± 0.01120	0.01085 ± 0.01122	0.00719 ± 0.01121
hct8-2	0.01046 ± 0.01142	0.00727 ± 0.01141	0.00883 ± 0.01144

Table 6.3.2-3. AENCF For HCT-003, 004, 005, 006, 007, and 008 Experiments (MeV)

MCNP case name	ENDF/B-V	ENDF/B-VI	WPO selected
hct3-1	0.0467	0.0460	0.0466
hct3-2	0.0404	0.0405	0.0417
hct3-3	0.0337	0.0333	0.0330
hct3-4	0.0259	0.0261	0.0262
hct3-5	0.0202	0.0199	0.0207
hct3-6	0.0405	0.0398	0.0419
hct3-7	0.0339	0.0339	0.0345
hct3-8	0.0329	0.0334	0.0342
hct3-9	0.0263	0.0260	0.0265
hct-310	0.0209	0.0200	0.0202
hct3-11	0.0177	0.0173	0.0177
hct3-12	0.0265	0.0265	0.0263
hct3-13	0.0139	0.0133	0.0140
hct3-14	0.0300	0.0301	0.0305
hct3-15	0.0183	0.0179	0.0185
hct4-1	0.0744	0.0735	0.0740
hct4-2	0.0736	0.0716	0.0732
hct4-3	0.0756	0.0747	0.0765
hct4-4	0.0742	0.0729	0.0748
hct5-1	0.0779	0.0762	0.0781

Table 6.3.2-3. AENCF For HCT-003, 004, 005, 006, 007, and 008 Experiments (MeV)

MCNP case name	ENDF/B-V	ENDF/B-VI	WPO selected
hct5-2	0.0764	0.0765	0.0776
hct6-t1	0.0720	0.0718	0.0715
hct6-t2	0.0232	0.0229	0.0231
hct6-t3	0.0104	0.0106	0.0106
hct7-1	0.0347	0.0335	0.0345
hct7-2	0.0455	0.0451	0.0450
hct7-3	0.0485	0.0473	0.0495
hct7-4	0.0339	0.0334	0.0340
hct7-5	0.0458	0.0445	0.0448
hct7-6	0.0475	0.0470	0.0486
hct8-1	0.0882	0.0856	0.0882
hct8-2	0.0922	0.0912	0.0919

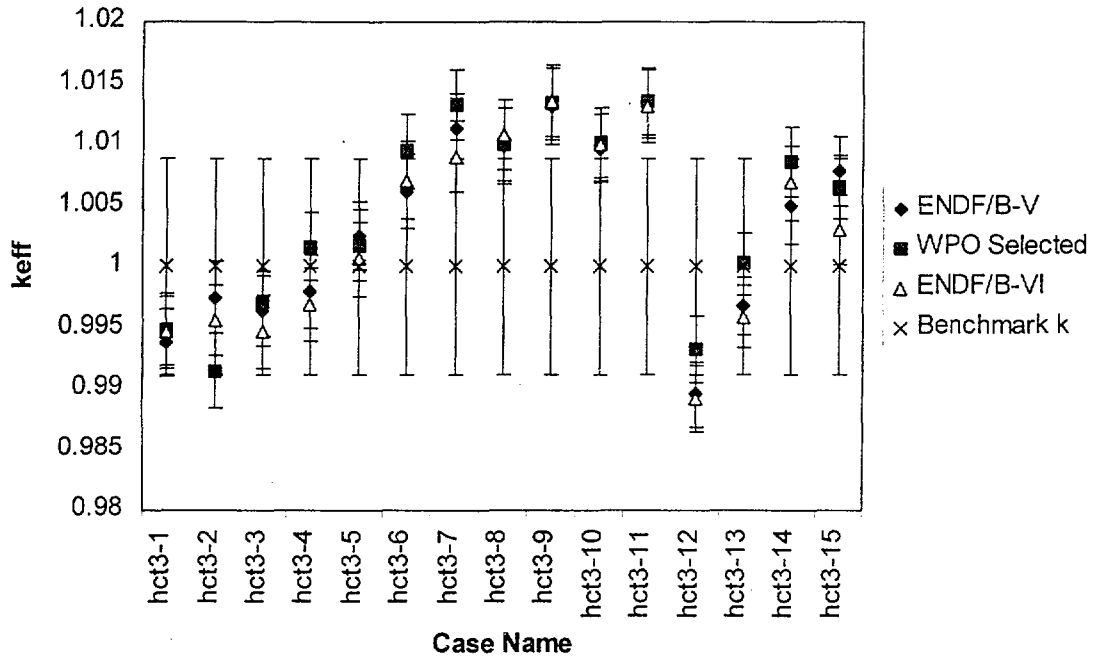

Figure 6.3.2-1. LCE Calculation Results for HCT-003 Experiments

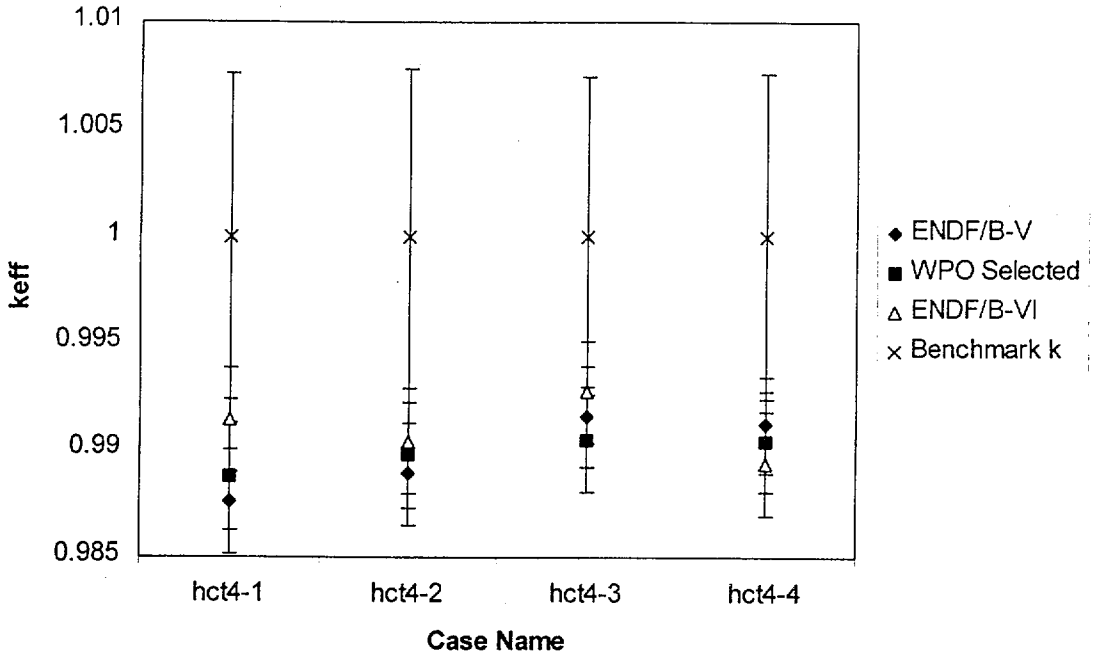

Figure 6.3.2-2. LCE Calculation Results for HCT-004 Experiments

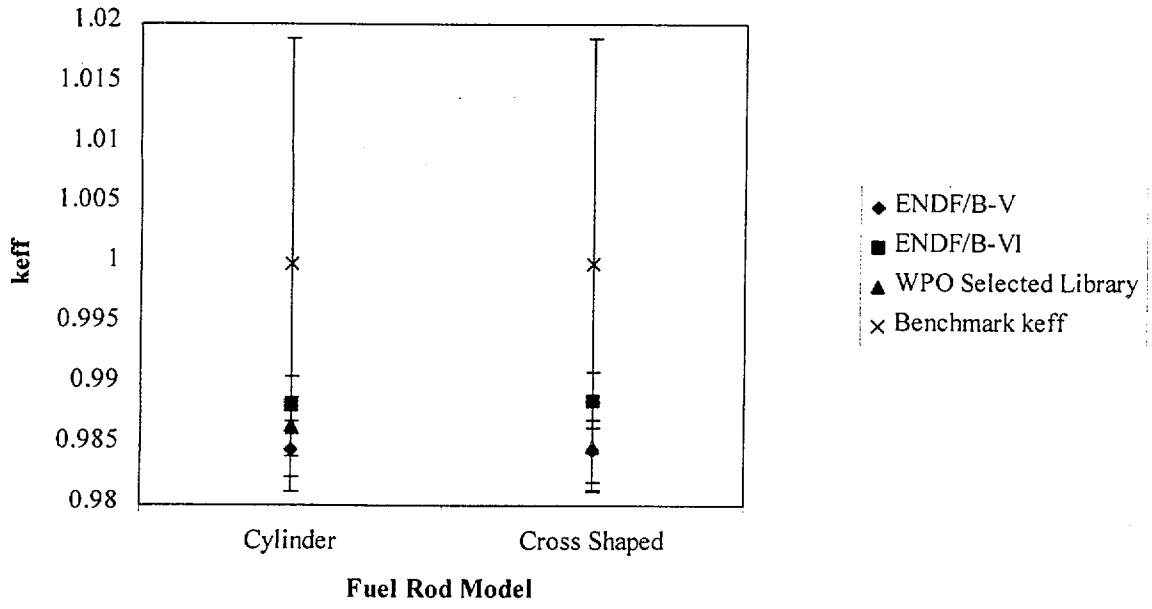

Figure 6.3.2-3. LCE Calculation Results for HCT-005 Experiments

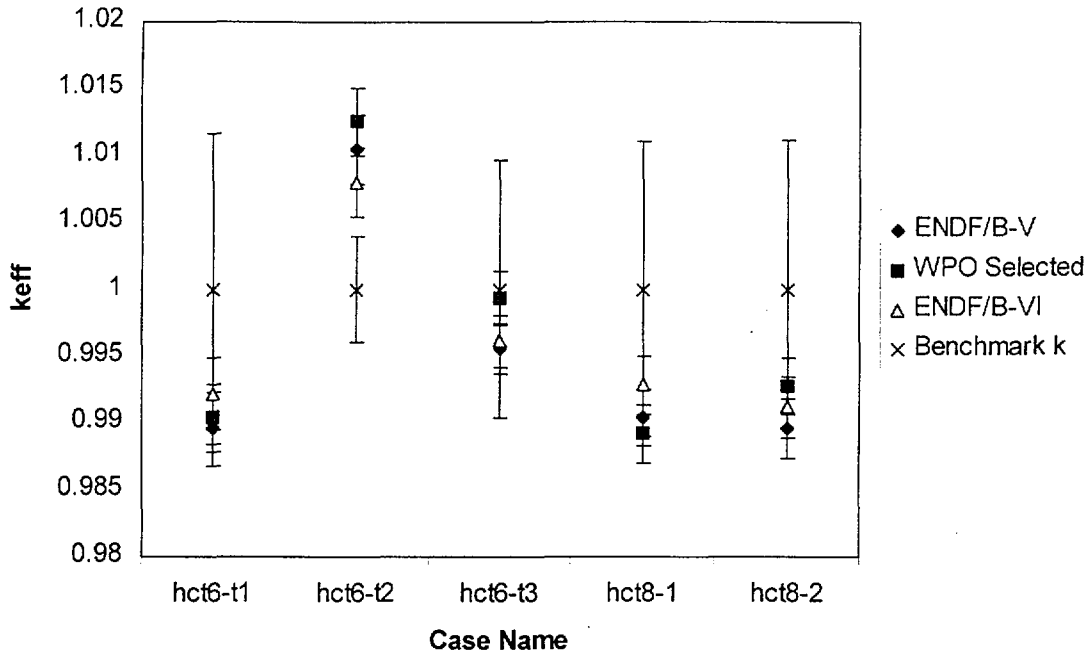

Figure 6.3.2-4. LCE Calculation Results for HCT-006 and HCT-008 Experiments

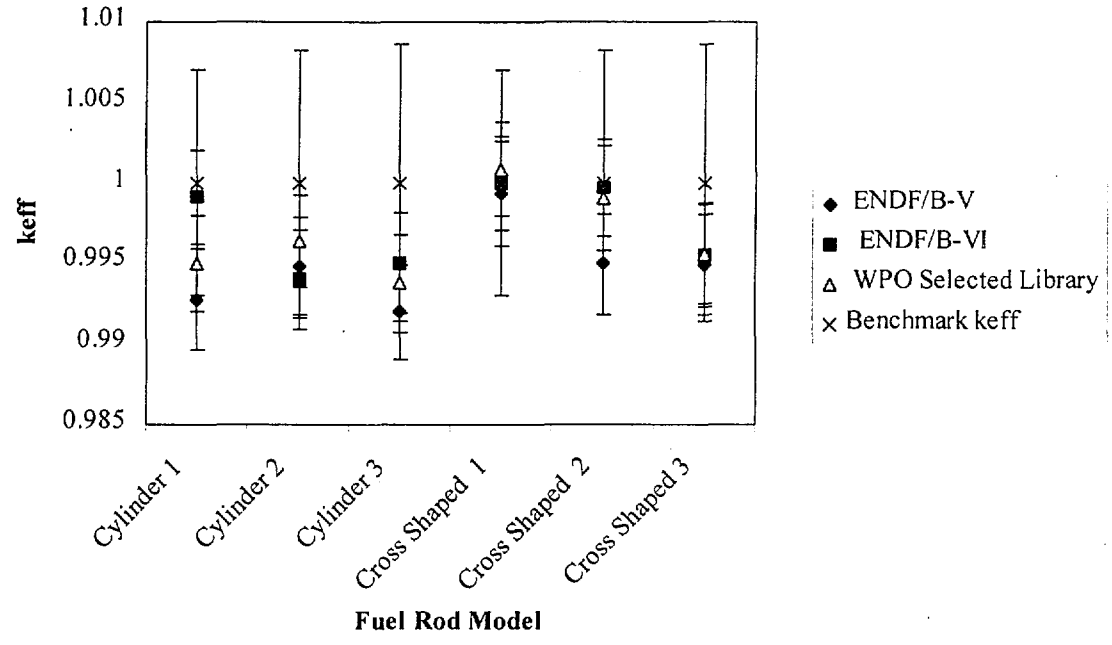

Figure 6.3.2-5. LCE Calculation Results for HCT-007 Experiments

6.3.3 Intermediate Heterogeneous Assembly with Highly Enriched Uranium Dioxide and Sand/Water Radial Reflector

Table 6.3.3-1 and Figure 6.3.3-1 present the MCNP calculation results for ENDF/B-V, WPO Selected, and ENDF/B-VI cross section libraries for the HCI-002 set of critical experiments. Table 6.3.3-2 shows the difference between referenced k_{eff} results and the MCNP calculated results, and Table 6.3.3-3 shows the AENCF for the HCI-002 set of critical experiments. The experimental benchmark shows that the MCNP code is able to predict the criticality of this experiment with a precision not worse than 0.68% (Table 6.3.3-2). This result is independent of the cross section library used. The MCNP calculations using the ENDF/B-VI library tended to over estimate k_{eff} and the MCNP calculations using the ENDF/B-V and the WPO Selected libraries tended to under estimate k_{eff}.

Table 6.3.3-1. LCE Reactivity Calculation Results for HCI-002 Experiments

MCNP case name	MCU[a]	MCNP		
	ABBN, LIPAR,VESTA $k_{eff} \pm \sigma$	ENDF/B-V $k_{eff} \pm \sigma$	ENDF/B-VI $k_{eff} \pm \sigma$	WPO selected $k_{eff} \pm \sigma$
hci2-1	0.99250 ± 0.0010	0.99236 ± 0.00081	0.99933 ± 0.00081	0.99627 ± 0.00079
hci2-2	0.99250 ± 0.0009	0.99339 ± 0.00107	1.00136 ± 0.00085	0.99614 ± 0.00082
hci2-3	0.99360 ± 0.0010	0.99603 ± 0.00101	1.00422 ± 0.00087	0.99871 ± 0.00083
hci2-4	0.99330 ± 0.0010	0.99676 ± 0.00101	1.00469 ± 0.00081	0.99892 ± 0.00083
hci2-5	0.99260 ± 0.0010	0.99736 ± 0.001	1.00278 ± 0.00081	1.00059 ± 0.00078

[a] Sample calculation results using MCU as reported by the evaluator on page 43 of Reference 7.3, HCI-002. MCU is a general purpose, continuous energy, general combinatorial geometry Monte Carlo code for solving criticality problems (p. 45, Ref. 7.3, HCI-002).

Table 6.3.3-2. Δk Between Experimental k_{eff} and MCNP Calculated k_{eff} for HCI-002 Experiments

MCNP case name	ENDF/B-V $\Delta k_{eff} \pm 2\sigma$	ENDF/B-VI $\Delta k_{eff} \pm 2\sigma$	WPO selected $\Delta k_{eff} \pm 2\sigma$
hci2-1	0.00764 ± 0.001807	0.00067 ± 0.0023	0.00373 ± 0.0023
hci2-2	0.00661 ± 0.002285	-0.00140 ± 0.0023	0.00386 ± 0.0023
hci2-3	0.00397 ± 0.002173	-0.00420 ± 0.0024	0.00129 ± 0.0023
hci2-4	0.00324 ± 0.002173	-0.00470 ± 0.0023	0.00108 ± 0.0023
hci2-5	0.00264 ± 0.002154	-0.00280 ± 0.0023	-0.00060 ± 0.0023

Table 6.3.3-3. AENCF for HCI-002 Experiments

MCNP case name	ENDF/B-V	ENDF/B-VI	WPO selected
hci2-1	0.2430	0.2354	0.2422
hci2-2	0.2439	0.2357	0.2413
hci2-3	0.2377	0.2313	0.2381
hci2-4	0.2394	0.2312	0.2376
hci2-5	0.2391	0.2313	0.2376

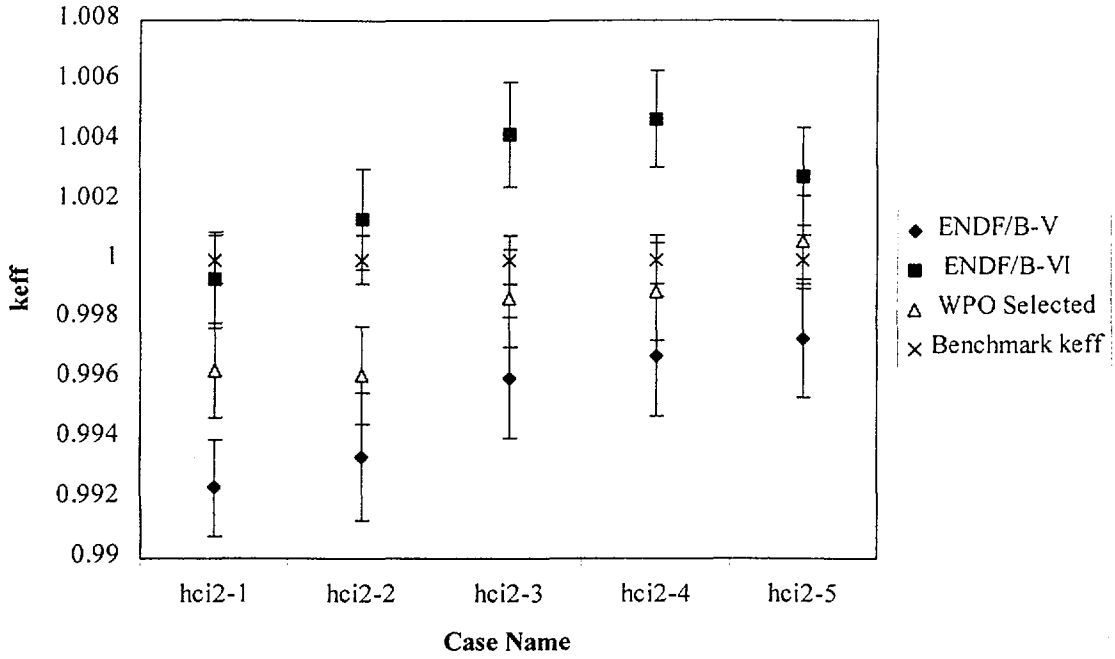

Figure 6.3.3-1. Intermediate Heterogeneous Assembly with Highly Enriched Uranium Dioxide k_{eff} Calculation Results

6.3.4 Critical Experiments of EBOR Fuel Pins in Water

Table 6.3.4-1 and Figure 6.3.4-1 present the MCNP calculation results for ENDF/B-V, WPO Selected, and ENDF/B-VI cross section libraries for the HCT-010 set of critical experiments. Table 6.3.4-2 shows the difference between experimental k_{eff} results and MCNP calculated results, and Table 6.3.4-3 shows the AENCF for the HCT-010 set of critical experiments. MCNP continuous energy simulations produced k_{eff} values that were within 1% of 1.0, with the exception of cases 1 and 2 as the evaluators also noticed (p. 28, Ref. 7.3, HCT-010).

Table 6.3.4-1. LCE Reactivity Calculation Results for HCT-010 Experiments

MCNP case name	MCNP[a] ENDF/B-V $k_{eff} \pm \sigma$	MCNP		
		ENDF/B-V $k_{eff} \pm \sigma$	ENDF/B-VI $k_{eff} \pm \sigma$	WPO selected $k_{eff} \pm \sigma$
hct101	0.9858 ± 0.0013	0.98716 ± 0.00118	0.98784 ± 0.00112	0.98849 ± 0.00121
hct102	0.9841 ± 0.0012	0.98361 ± 0.00115	0.98632 ± 0.00117	0.98532 ± 0.00116
hct103	0.9927 ± 0.0011	0.99328 ± 0.00125	0.98998 ± 0.00117	0.99428 ± 0.00127
hct104	0.9966 ± 0.0012	0.99468 ± 0.00125	0.99397 ± 0.00126	0.99478 ± 0.00119
hct105	0.9983 ± 0.0012	0.99734 ± 0.00119	0.99568 ± 0.00113	0.99679 ± 0.00115
hct106	0.9941 ± 0.0012	0.99239 ± 0.00121	0.99419 ± 0.00113	0.99644 ± 0.00113
hct107	0.9992 ± 0.0011	0.99976 ± 0.00105	0.99841 ± 0.00113	0.99679 ± 0.00115
hct108	1.0008 ± 0.0011	0.9991 ± 0.00122	0.99853 ± 0.00121	1.00263 ± 0.00108

Table 6.3.4-1. LCE Reactivity Calculation Results for HCT-010 Experiments

MCNP case name	MCNP[a] ENDF/B-V $k_{eff} \pm \sigma$	MCNP		
		ENDF/B-V $k_{eff} \pm \sigma$	ENDF/B-VI $k_{eff} \pm \sigma$	WPO selected $k_{eff} \pm \sigma$
hct109	0.9976 ± 0.0012	0.99777 ± 0.00109	0.99798 ± 0.00116	0.99882 ± 0.00113
hct110	1.0053 ± 0.0011	1.00198 ± 0.00104	1.00261 ± 0.00102	1.00461 ± 0.00106
hct111	0.9999 ± 0.0011	0.99913 ± 0.00109	0.99882 ± 0.00111	1.00002 ± 0.00115
hct112	0.9977 ± 0.0010	1.00052 ± 0.00105	0.99642 ± 0.00107	1.00103 ± 0.00111
hct113	1.0037 ± 0.0011	1.00237 ± 0.001	1.0006 ± 0.0010	1.00366 ± 0.00102
hct114	1.0008 ± 0.0012	1.00112 ± 0.00112	0.99823 ± 0.00113	1.00135 ± 0.00114
hct115	1.0017 ± 0.0011	1.00059 ± 0.00113	0.99844 ± 0.00115	1.00368 ± 0.00113
hct116	1.0044 ± 0.0011	1.00378 ± 0.00114	0.99892 ± 0.00115	1.00594 ± 0.00109
hct117	1.0038 ± 0.0011	1.00377 ± 0.0011	1.00117 ± 0.00124	1.00448 ± 0.00107
hct118	1.0039 ± 0.0011	1.0018 ± 0.00117	0.99989 ± 0.0012	1.00267 ± 0.00116
hct119	1.0028 ± 0.0012	1.00151 ± 0.00105	0.99935 ± 0.00126	1.0037 ± 0.00108
hct120	1.0051 ± 0.0009	1.0024 ± 0.001	1.00295 ± 0.00096	1.00489 ± 0.00101
hct121	1.0044 ± 0.0011	1.00416 ± 0.0011	1.00250 ± 0.00111	1.00342 ± 0.00115

[a] Sample Calculation result using MCNP and ENDF/B-V cross section library as reported by the evaluator on page 28 of Reference 7.3, HCT-010. The calculated results in this analysis were within two standard deviations of the evaluator calculations.

Table 6.3.4-2. Δk Between Experimental k_{eff} and MCNP Calculated k_{eff} for HCT-010 Experiments

MCNP case name	ENDF/B-V $\Delta k_{eff} \pm 2\sigma$	ENDF/B-VI $\Delta k_{eff} \pm 2\sigma$	WPO selected $\Delta k_{eff} \pm 2\sigma$
hct101	0.01284 ± 0.010275	0.01216 ± 0.0103	0.01151 ± 0.0103
hct102	0.01639 ± 0.010261	0.01368 ± 0.0103	0.01468 ± 0.0103
hct103	0.00672 ± 0.010308	0.01002 ± 0.0103	0.00572 ± 0.0103
hct104	0.00532 ± 0.010308	0.00603 ± 0.0103	0.00522 ± 0.0103
hct105	0.00266 ± 0.010279	0.00432 ± 0.0103	0.00321 ± 0.0103
hct106	0.00761 ± 0.010289	0.00581 ± 0.0103	0.00356 ± 0.0103
hct107	0.00024 ± 0.010218	0.00159 ± 0.0103	0.00321 ± 0.0103
hct108	0.0009 ± 0.010293	0.00147 ± 0.0103	-0.0026 ± 0.0102
hct109	0.00223 ± 0.010235	0.00202 ± 0.0103	0.00118 ± 0.0103
hct110	-0.00198 ± 0.010214	-0.0026 ± 0.0102	-0.0046 ± 0.0102
hct111	0.00087 ± 0.010235	0.00118 ± 0.0102	-2E-05 ± 0.0103
hct112	-0.00052 ± 0.010218	0.00358 ± 0.0102	-0.001 ± 0.0102
hct113	-0.00237 ± 0.010198	-0.0006 ± 0.0102	-0.0037 ± 0.0102
hct114	-0.00112 ± 0.010248	0.00177 ± 0.0103	-0.0013 ± 0.0103
hct115	-0.00059 ± 0.010252	0.00156 ± 0.0103	-0.0037 ± 0.0103
hct116	-0.00378 ± 0.009091	0.00108 ± 0.0091	-0.0059 ± 0.0091
hct117	-0.00377 ± 0.014963	-0.0012 ± 0.0150	-0.0045 ± 0.0150

Table 6.3.4-2. Δk Between Experimental k_{eff} and MCNP Calculated k_{eff} for HCT-010 Experiments

MCNP case name	ENDF/B-V $\Delta k_{eff} \pm 2\sigma$	ENDF/B-VI $\Delta k_{eff} \pm 2\sigma$	WPO selected $\Delta k_{eff} \pm 2\sigma$
hct118	-0.0018 ± 0.014984	0.00011 ± 0.0150	-0.0027 ± 0.0150
hct119	-0.00151 ± 0.014948	0.00065 ± 0.0150	-0.0037 ± 0.0150
hct120	-0.0024 ± 0.00961	-0.00295 ± 0.00959	-0.00489 ± 0.00962
hct121	-0.00416 ± 0.015358	-0.0025 ± 0.0097	-0.0034 ± 0.0097

Table 6.3.4-3. AENCF for HCT-010 Experiments (MeV)

MCNP case name	ENDF/B-V	ENDF/B-VI	WPO selected
hct101	0.0797	0.0783	0.0793
hct102	0.0797	0.0800	0.0799
hct103	0.0557	0.0551	0.0555
hct104	0.0431	0.0423	0.0439
hct105	0.0360	0.0358	0.0357
hct106	0.0361	0.0358	0.0359
hct107	0.0308	0.0307	0.0357
hct108	0.0315	0.0309	0.0320
hct109	0.0314	0.0310	0.0316
hct110	0.0287	0.0282	0.0288
hct111	0.0291	0.0283	0.0285
hct112	0.0262	0.0257	0.0262
hct113	0.0250	0.0244	0.0252
hct114	0.0281	0.0280	0.0284
hct115	0.0289	0.0286	0.0288
hct116	0.0289	0.0281	0.0282
hct117	0.0293	0.0281	0.0286
hct118	0.0287	0.0283	0.0288
hct119	0.0295	0.0294	0.0296
hct120	0.0234	0.0228	0.0229
hct121	0.0278	0.0272	0.0277

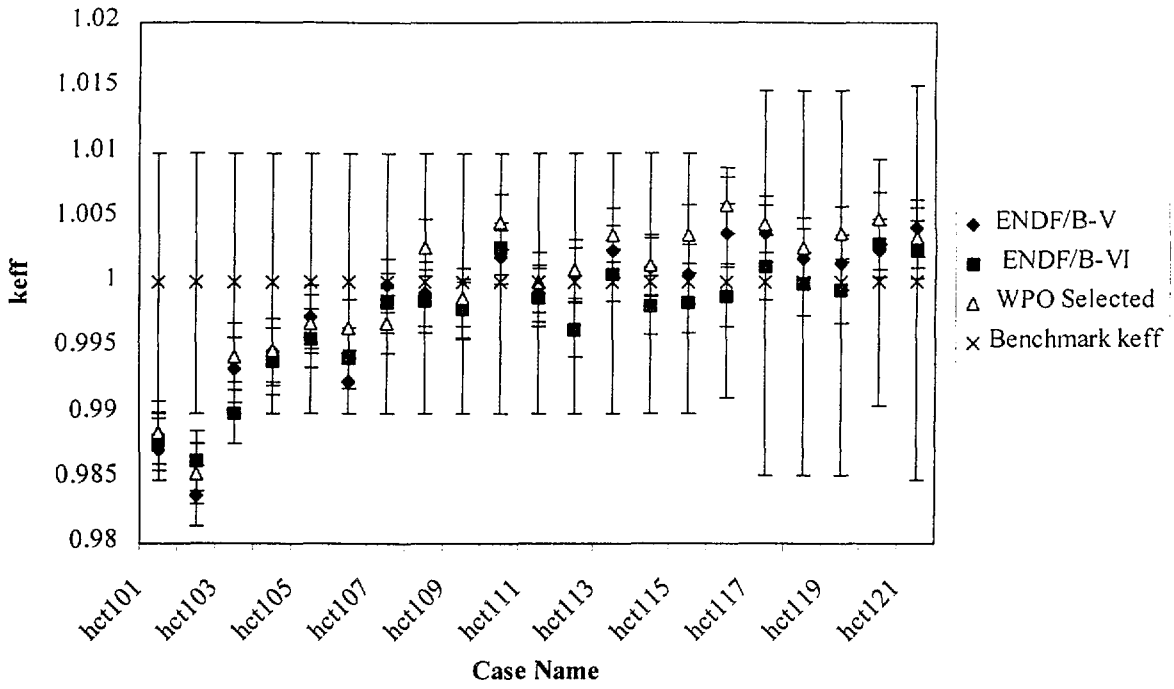

Figure 6.3.4-1. LCE Calculation Results for HCT-010 Experiments

6.4 Pu Fueled Thermal System Results

6.4.1 LCE Reactivity Calculation Results for FFTF Experiments

Table 6.4.1-1 presents the MCNP calculation results for ENDF/B-V, WPO Selected, and ENDF/B-VI cross section libraries for the FFTF set of critical experiments, which are also illustrated in Figure 6.4.1-1. Table 6.4.1-3 presents the AENCF values for the FFTF set of critical experiments. As presented in Figure 6.4.1-1 and Table 6.4.1-2, it can be seen that ENDF/B-VI results are slightly less than the benchmark k_{eff} value. The ENDF/B-V results were all greater than the benchmark value, and the WPO selected results were greater than the benchmark value except for case FFTF005.

Table 6.4.1-1. LCE Reactivity Calculation Results for FFTF Experiments

MCNP case name	ENDF/B-V $k_{eff} \pm \sigma$	WPO selected $k_{eff} \pm \sigma$	ENDF/B-VI $k_{eff} \pm \sigma$
fftf001	1.00567±0.00342	1.00557 ± 0.00355	0.99485 ± 0.00344
fftf003r	0.98913±0.00307	0.99049 ± 0.00276	0.99388 ± 0.00371
fftf004	0.99333±0.00348	1.00635 ± 0.00361	1.00137 ± 0.00337
fftf005	0.99582±0.00361	1.00373 ± 0.0031	0.99835 ± 0.00316
fftf006	1.01291±0.00285	1.00558 ± 0.00313	0.99947 ± 0.00313
fftf029	0.99891±0.00323	0.99776 ± 0.00278	0.9985 ± 0.0032

Table 6.4.1-2. Δk Between Experimental k_{eff} and MCNP Calculated k_{eff} for FFTF Experiments

MCNP case name	ENDF/B-V $\Delta k_{eff} \pm 2\sigma$	ENDF/B-VI $\Delta k_{eff} \pm 2\sigma$	WPO selected $\Delta k_{eff} \pm 2\sigma$
fftf001	-0.00567 ± 0.02102	0.00515 ± 0.00862	-0.00557 ± 0.00880
fftf003r	0.01087 ± 0.02081	0.00612 ± 0.00961	0.00951 ± 0.00823
fftf004	0.00667 ± 0.02106	-0.00137 ± 0.00929	-0.00635 ± 0.00965
fftf005	0.00418 ± 0.02115	0.00165 ± 0.00806	-0.00373 ± 0.00796
fftf006	-0.01291 ± 0.02068	0.00053 ± 0.01000	-0.00558 ± 0.01000
fftf029	0.00109 ± 0.02090	0.0015 ± 0.00884	0.00224 ± 0.00825

Table 6.4.1-3. AENCF for FFTF Experiments (MeV)

MCNP case name	ENDF/B-V	ENDF/B-VI	WPO selected
fftf001	0.1044	0.1043	0.1015
fftf003r	0.2447	0.2388	0.2453
fftf004	0.0816	0.0779	0.0819
fftf005	0.1717	0.1727	0.1728
fftf006	0.0635	0.0646	0.0609
fftf029	0.1694	0.1661	0.1647

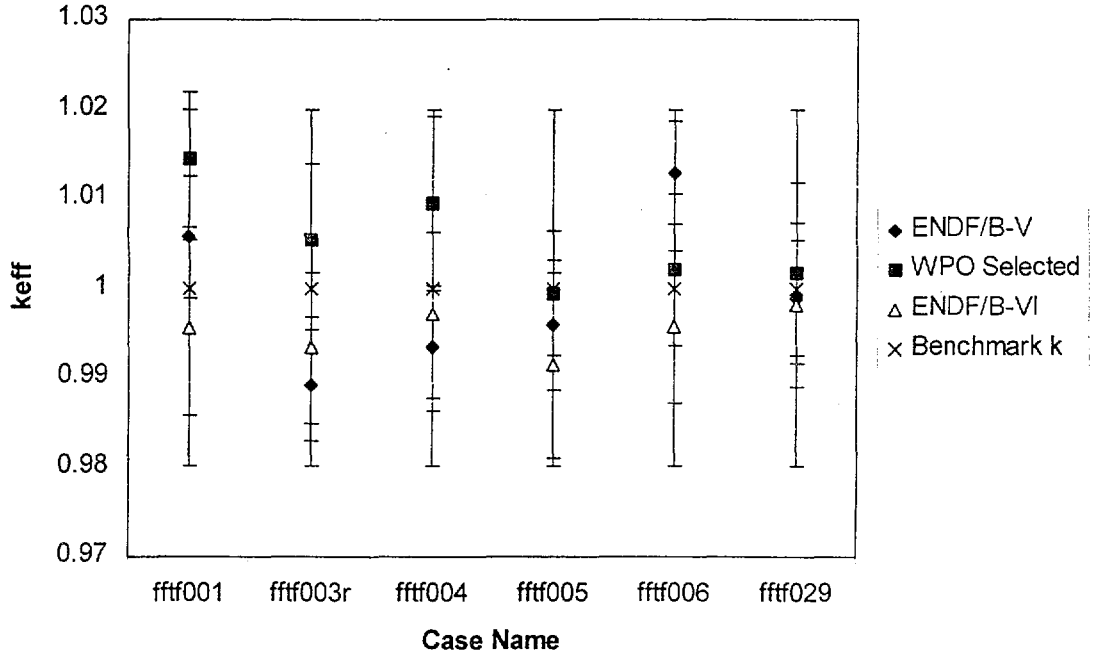

Figure 6.4.1-1. LCE Calculation Results for FFTF Experiments

6.4.2 LCE Reactivity Calculation Results for the Saxton Experiments

Table 6.4.2-1 presents the MCNP calculation results for ENDF/B-V, WPO Selected, and ENDF/B-VI cross section libraries for the Saxton set of critical experiments, which are also illustrated in Figure 6.4.2-1. Table 6.4.2-3 presents the AENCF values for the Saxton set of critical experiments. As presented in Figure 6.4.2-1 and Table 6.4.2-2, it can be seen that most of the multi-region experiment results are slightly below the benchmark value, and the single-region results are within 1% of the benchmark values. In all of the cases the ENDF/B-VI results were the least conservative.

Table 6.4.2-1. LCE Reactivity Calculation Results for the Saxton Experiments

MCNP case name	ENDF/B-V[a] $k_{eff} \pm \sigma$	WPO selected $k_{eff} \pm \sigma$	ENDF/B-VI $k_{eff} \pm \sigma$
smr1	0.99627 ± 0.00072	0.99783 ± 0.00073	0.99302 ± 0.00072
smr5	0.99442 ± 0.00072	0.99349 ± 0.00073	0.99087 ± 0.00074
smr8	0.99861 ± 0.00064	0.99956 ± 0.00068	0.99444 ± 0.00058
smr9	0.99468 ± 0.00072	0.99683 ± 0.00078	0.99151 ± 0.00074
smr11	0.99833 ± 0.00072	0.99783 ± 0.00078	0.99247 ± 0.00079
smr12	0.99869 ± 0.00073	0.99992 ± 0.0008	0.99358 ± 0.00077
ssr27	0.99728 ± 0.00077	0.99881 ± 0.00082	0.99195 ± 0.00077
ssr48	0.99396 ± 0.00074	0.9939 ± 0.00071	0.99136 ± 0.00072
ssr53	1.0034 ± 0.00065	1.00454 ± 0.00066	0.99503 ± 0.00074
ssr57	0.99673 ± 0.00076	0.99807 ± 0.00075	0.99009 ± 0.00072
ssr66	1.00272 ± 0.00074	1.00308 ± 0.00073	0.99383 ± 0.00073
ssr70	0.99369 ± 0.00074	0.99543 ± 0.00072	0.98936 ± 0.00071
ssr74	1.00551 ± 0.00066	1.00505 ± 0.00068	0.99858 ± 0.00072
ssr83	0.9928 ± 0.00069	0.99299 ± 0.00074	0.98821 ± 0.00073

[a] The values calculated for the ENDF/B-V cross section libraries for the MOX single region configurations were within the statistical uncertainty of the sample MCNP values using the ENDF/B-V libraries reported on page 30 of Reference 7.3, MCT-003, with the exception of ssr27, which was within 2 standard deviations. The reason for the slight difference in values for this case could not be determined at this time. Sample values were not available for the multi-region cores.

Table 6.4.2-2. Δk Between Experimental k_{eff} and MCNP Calculated k_{eff} for Saxton Experiments

MCNP case name	ENDF/B-V $\Delta k_{eff} \pm 2\sigma$	WPO selected $\Delta k_{eff} \pm 2\sigma$	ENDF/B-VI $\Delta k_{eff} \pm 2\sigma$
smr1	0.00373 ± 0.00852	0.00217 ± 0.00853	0.00698 ± 0.00852
smr5	0.00558 ± 0.00852	0.00651 ± 0.00853	0.00913 ± 0.00853
smr8	0.00139 ± 0.00850	0.00044 ± 0.00851	0.00556 ± 0.00848
smr9	0.00532 ± 0.00852	0.00317 ± 0.00854	0.00849 ± 0.00853
smr11	0.00167 ± 0.00852	0.00217 ± 0.00854	0.00753 ± 0.00855
smr12	0.00131 ± 0.00853	0.00008 ± 0.00855	0.00642 ± 0.00854
ssr27	0.00272 ± 0.01051	0.00119 ± 0.01053	0.00805 ± 0.01051
ssr48	0.00604 ± 0.00853	0.00610 ± 0.00852	0.00864 ± 0.00852

Table 6.4.2-2. Δk Between Experimental k_{eff} and MCNP Calculated k_{eff} for Saxton Experiments

MCNP case name	ENDF/B-V $\Delta k_{eff} \pm 2\sigma$	WPO selected $\Delta k_{eff} \pm 2\sigma$	ENDF/B-VI $\Delta k_{eff} \pm 2\sigma$
ssr53	-0.00340 ± 0.00497	-0.00454 ± 0.00498	0.00497 ± 0.00502
ssr57	0.00327 ± 0.01150	0.00193 ± 0.01150	0.00991 ± 0.01149
ssr66	-0.00272 ± 0.00579	-0.00308 ± 0.00579	0.00617 ± 0.00579
ssr70	0.00631 ± 0.01428	0.00457 ± 0.01427	0.01064 ± 0.01427
ssr74	-0.00551 ± 0.00421	-0.00505 ± 0.00422	0.00142 ± 0.00425
ssr83	0.00720 ± 0.00851	0.00701 ± 0.00853	0.01179 ± 0.00853

Table 6.4.2-3. AENCF for Saxton Experiments (MeV)

MCNP case name	ENDF/B-V	ENDF/B-VI	WPO selected
smr1	0.1707	0.1705	0.1715
smr5	0.1928	0.1919	0.1919
smr8	0.2045	0.2037	0.2051
smr9	0.1683	0.1667	0.1673
smr11	0.2049	0.2027	0.0205
smr12	0.2041	0.2024	0.2049
ssr27	0.2013	0.2017	0.2015
ssr48	0.1564	0.15464	0.155676
ssr53	0.1063	0.1064	0.1065
ssr57	0.1933	0.1928	0.1938
ssr66	0.1182	0.1189	0.1183
ssr70	0.2294	0.2290	0.2295
ssr74	0.0799	0.0800	0.0790
ssr83	0.1821	0.181145	0.181971

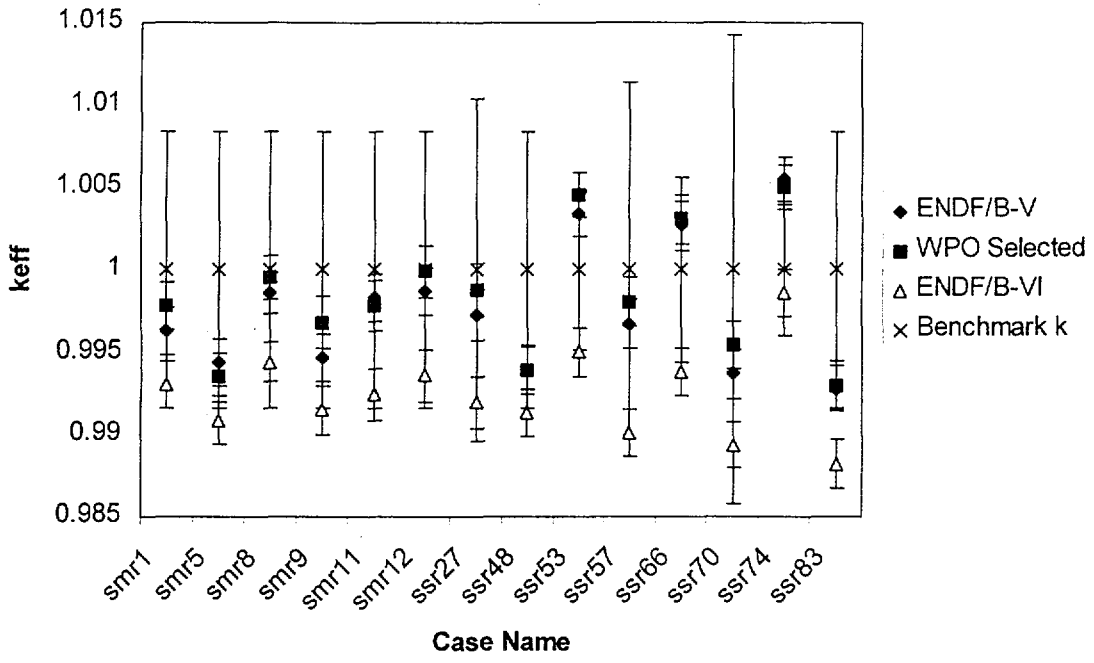

Figure 6.4.2-1. LCE Calculation Results for Saxton Experiments

6.5 Homogeneous Solution Results

6.5.1 LCE Reactivity Calculation Results for UO_3-H_2O Solution Experiments

Table 6.5.1-1 presents the MCNP calculation results for ENDF/B-V, WPO Selected, and ENDF/B-VI cross section libraries for the UO_3-H_2O solution set of critical experiments, which are also illustrated in Figure 6.5.1-1. Table 6.5.1-3 presents the AENCF values for the UO_3-H_2O solution set of critical experiments. In this set of experiments the ENDF/B-V and WPO Selected results were the same. As presented in Figure 6.5.1-1 and Table 6.5.1-2, it can be seen that the ENDF/B-VI results were the least conservative.

Table 6.5.1-1. LCE Reactivity Calculation Results for UO_3-H_2O Solution Experiments

MCNP case name	Reference MCNP $k_\infty \pm \sigma$[a]	ENDF/B-V $k_\infty \pm \sigma$	WPO selected $k_\infty \pm \sigma$	ENDF/B-VI $k_\infty \pm \sigma$
sphu9a	0.9898 ± 0.0015	0.99004 ± 0.00249	0.99004 ± 0.00249	0.98665 ± 0.00293
sphu9b	0.9945 ± 0.0015	0.99269 ± 0.00249	0.99269 ± 0.00249	0.98518 ± 0.00271
sphu9c	0.9830 ± 0.0017	0.97871 ± 0.00256	0.97871 ± 0.00256	0.97958 ± 0.00190
sphu9d	0.9761 ± 0.0015	0.97914 ± 0.00242	0.97914 ± 0.00242	0.97132 ± 0.00233
sphu9e	0.9680 ± 0.0014	0.96607 ± 0.00163	0.96607 ± 0.00163	0.96429 ± 0.00221
sphu9f	1.0125 ± 0.0017	1.00952 ± 0.00261	1.00952 ± 0.00261	1.00009 ± 0.00306
sphu9g	1.0103 ± 0.0017	1.0136 ± 0.00246	1.01360 ± 0.00246	1.00763 ± 0.00235
sphu9h	0.9964 ± 0.0016	0.99713 ± 0.00198	0.99713 ± 0.00198	0.99364 ± 0.00224

Table 6.5.1-1. LCE Reactivity Calculation Results for UO_3-H_2O Solution Experiments

MCNP case name	Reference MCNP $k_\infty \pm \sigma$[a]	ENDF/B-V $k_\infty \pm \sigma$	WPO selected $k_\infty \pm \sigma$	ENDF/B-VI $k_\infty \pm \sigma$
sphu9i	1.0358 ± 0.0014	1.03372 ± 0.00274	1.03372 ± 0.00274	1.03156 ± 0.00233
sphu9j	1.0412 ± 0.0014	1.04207 ± 0.00224	1.04207 ± 0.00224	1.03178 ± 0.00240
sphu9k	1.0311 ± 0.0016	1.02951 ± 0.00216	1.02951 ± 0.00216	1.02122 ± 0.00206
sphu9l	1.0240 ± 0.0015	1.02281 ± 0.0021	1.02281 ± 0.00210	1.01910 ± 0.00237

[a] Values were calculated with MCNP and a continuous energy cross section library (p. A-6, Ref. 7.17), and are from page 42 of Reference 7.17.

Table 6.5.1-2. Δk Between Experimental k_∞ and MCNP Calculated k_∞ Results for UO_3-H_2O Solution Experiments

MCNP case name	ENDF/B-V $\Delta k_{eff} \pm 2\sigma$	WPO selected $\Delta k_{eff} \pm 2\sigma$	ENDF/B-VI $\Delta k_{eff} \pm 2\sigma$
sphu9a	0.00196 ± 0.01299	0.00196 ± 0.00535	0.00535 ± 0.00793
sphu9b	-0.00019 ± 0.01117	-0.00019 ± 0.00498	0.00732 ± 0.00911
sphu9c	0.00879 ± 0.01268	0.00879 ± 0.01017	0.00792 ± 0.00878
sphu9d	0.00296 ± 0.01183	0.00296 ± 0.00567	0.01078 ± 0.01174
sphu9e	0.00413 ± 0.01437	0.00413 ± 0.00526	0.00591 ± 0.00738
sphu9f	-0.00322 ± 0.01551	-0.00322 ± 0.00613	0.00621 ± 0.00872
sphu9g	-0.00720 ± 0.01636	-0.00720 ± 0.00872	-0.00123 ± 0.00486
sphu9h	-0.00143 ± 0.01283	-0.00143 ± 0.00421	0.00206 ± 0.00493
sphu9i	-0.00392 ± 0.01247	-0.00392 ± 0.00674	-0.00176 ± 0.00498
sphu9j	-0.00907 ± 0.01114	-0.00907 ± 0.01012	0.00122 ± 0.00495
sphu9k	0.00179 ± 0.00772	0.00179 ± 0.00468	0.01008 ± 0.01089
sphu9l	-0.00191 ± 0.01103	-0.00191 ± 0.00461	0.00180 ± 0.00507

Table 5.1.6-1. AENCF for UO_3-H_2O Solution Experiments (MeV)

MCNP case name	ENDF/B-V	ENDF/B-VI	WPO selected
sphu9a	0.2541	0.2562	0.2541
sphu9b	0.2163	0.2155	0.2163
sphu9c	0.1883	0.1839	0.1883
sphu9d	0.1737	0.1740	0.1737
sphu9e	0.1591	0.1660	0.1591
sphu9f	0.2511	0.2543	0.2511
sphu9g	0.1839	0.1906	0.1839
sphu9h	0.1651	0.1642	0.1651
sphu9i	0.2495	0.2499	0.2495
sphu9j	0.1783	0.1760	0.1783
sphu9k	0.1661	0.1670	0.1661
sphu9l	0.1549	0.1545	0.1549

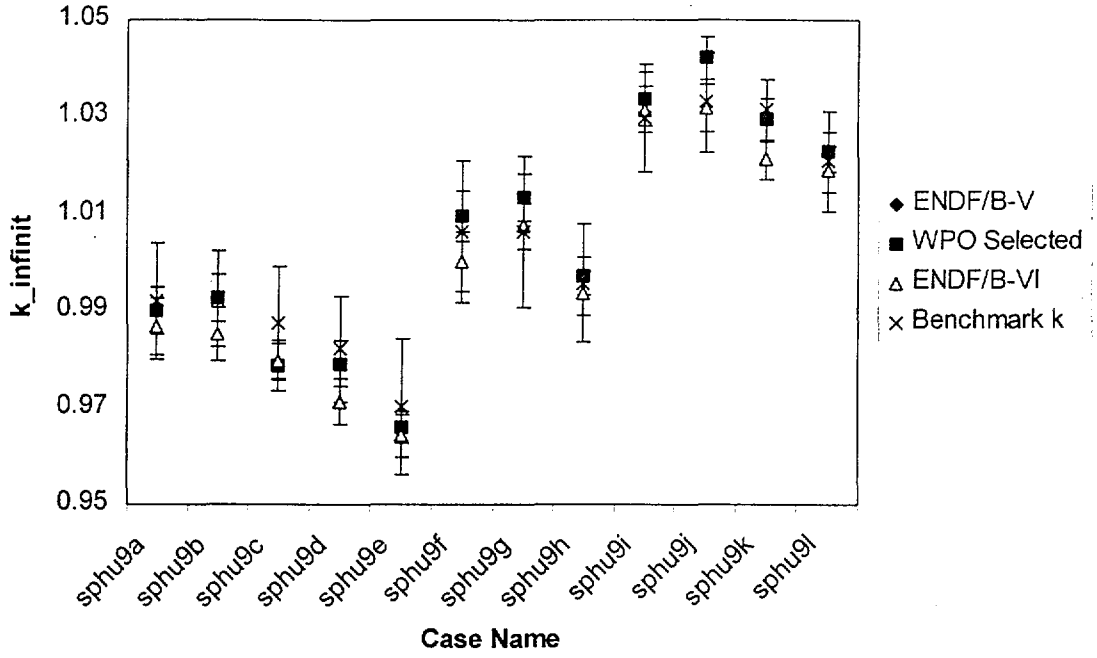

Figure 6.5.1-1. LCE Calculation Results for H_3O-UO_2 Experiments

6.5.2 Unreflected UO_2F_2+H_2O Cylindrical Assembly Sheba-II

Table 6.5.2-1 and Figure 6.5.2-1 present the MCNP calculation results for ENDF/B-V, WPO Selected, and ENDF/B-VI cross section libraries for the UO_2F_2+H_2O solution set of critical experiments. Table 6.5.2-2 shows the differences between experimental k_{eff} results and the MCNP calculated results, Table 6.5.2-3 shows the AENCF values for the UO_2F_2+H_2O solution set of critical experiments. The MCNP continuous energy simulations produced k_{eff} values that were about 1.4% higher than the benchmark values.

Table 6.5.2-1. LCE Reactivity Calculation Results for LST-001 Experiments

MCNP case name	MCNP[a] ENDF/B-V $k_{eff} \pm \sigma$	MCNP		
		ENDF/B-V $k_{eff} \pm \sigma$	ENDF/B-VI $k_{eff} \pm \sigma$	WPO selected $k_{eff} \pm \sigma$
lst1-1	1.0139 ± 0.0010	1.01182 ± 0.00101	1.00714 ± 0.00092	1.01069 ± 0.00085

[a] Sample calculation result using MCNP and ENDF/B-V cross section library as reported by the evaluator on page 20 of Reference 7.3, LST-001. The calculated results in this analysis using ENDF/B-V cross sections were within two standard deviations of the evaluator calculation.

Table 6.5.2-2. Δk Between Experimental k_{eff} and MCNP Calculated k_{eff} Results for LST-001 Experiments

MCNP case name	ENDF/B-V $\Delta k_{eff} \pm 2\sigma$	ENDF/B-VI $\Delta k_{eff} \pm 2\sigma$	WPO selected $\Delta k_{eff} \pm 2\sigma$
lst1-1	-0.01272 ± 0.006142	-0.00804 ± 0.00608	-0.01160 ± 0.00604

Table 6.5.2-3. AENCF for LST-001 Experiment (MeV)

MCNP case name	ENDF/B-V	ENDF/B-VI	WPO selected
lst1-1	0.1884	0.0514	0.0523

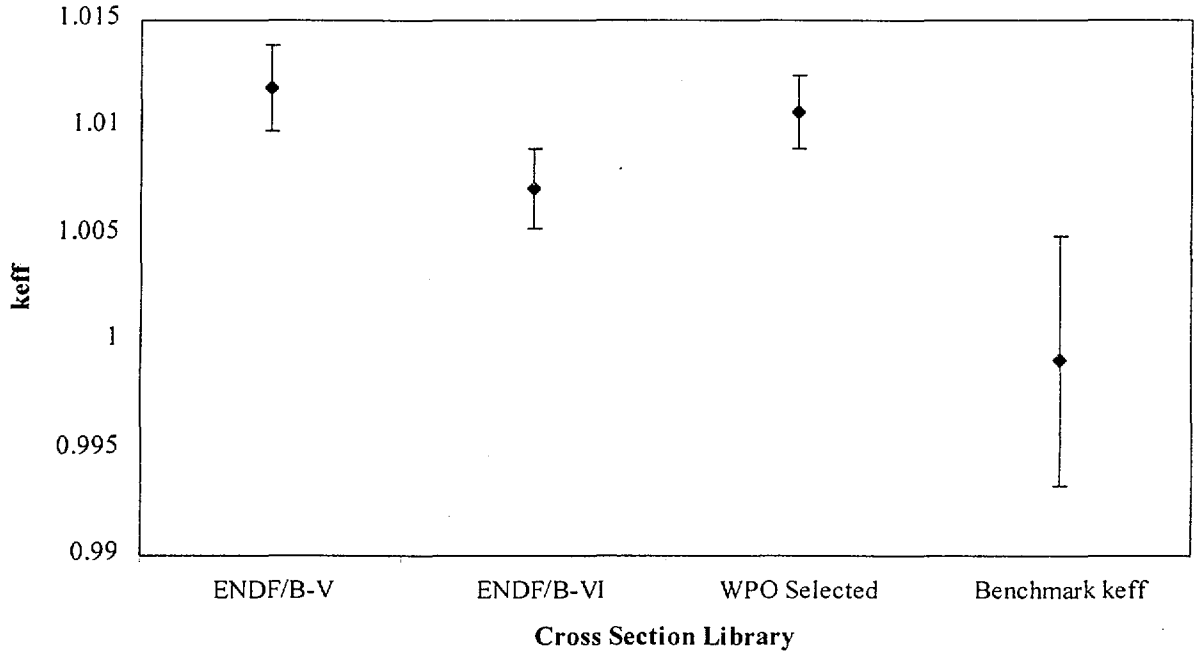

Figure 6.5.2-1. LCE Calculation Results for LST-001 Experiments

6.5.3 Full and Truncated Bare Spheres of 10% Enriched Uranyl Nitrate Water Solutions

Table 6.5.3-1 and Figure 6.5.3-1 present the MCNP calculation results for ENDF/B-V, WPO Selected, and ENDF/B-VI cross section libraries for the LST-003 set of critical experiments. Table 6.5.3-2 shows the differences between experimental k_{eff} results and the MCNP calculated results, and Table 6.5.3-3 shows the AENCF values for the LST-003 set of critical experiments. The MCNP continuous energy representations produced k_{eff} values that were within 0.7% of 1.0. Calculations based on the ENDF/B-VI cross section library resulted in a more non-conservative k_{eff} than the calculations using the ENDF/B-V and WPO Selected libraries.

Table 6.5.3-1. LCE Reactivity Calculations for LST-003 Experiments

MCNP case name	MCNP[a]	MCNP		
	ENDF/B-V $k_{eff} \pm \sigma$	ENDF/B-V $k_{eff} \pm \sigma$	ENDF/B-VI $k_{eff} \pm \sigma$	WPO selected $k_{eff} \pm \sigma$
lst3-1	0.9994 ± 0.0004	0.9993 ± 0.0004	0.99274 ± 0.00067	0.99784 ± 0.00069
lst3-2	0.9981 ± 0.0004	0.99705 ± 0.00038	0.99335 ± 0.00066	0.99898 ± 0.00068
lst3-3	1.0016 ± 0.0004	1.00151 ± 0.00037	0.99701 ± 0.00065	1.00141 ± 0.00066
lst3-4	0.9943 ± 0.0004	0.99536 ± 0.00038	0.98964 ± 0.00063	0.99406 ± 0.00061
lst3-5	0.9983 ± 0.0003	0.99897 ± 0.00031	0.99468 ± 0.00056	0.99799 ± 0.00056
lst3-6	0.9987 ± 0.0003	0.99924 ± 0.0003	0.99507 ± 0.00053	0.99935 ± 0.00053
lst3-7	0.9969 ± 0.0003	0.99716 ± 0.0003	0.99397 ± 0.00051	0.99917 ± 0.0005
lst3-8	1.0000 ± 0.0003	1.00079 ± 0.00025	0.99637 ± 0.00045	1.00116 ± 0.00044
lst3-9	0.9979 ± 0.0003	0.99732 ± 0.00025	0.99603 ± 0.00041	0.99779 ± 0.00048

[a] Sample calculation results using MCNP and the ENDF/B-V cross section library as reported by the evaluator on page 16 of Reference 7.3, LST-003.

Table 6.5.3-2. Δk Between Experimental k_{eff} and MCNP Calculated k_{eff} Results for LST-003 Experiments

MCNP case name	ENDF/B-V $\Delta k_{eff} \pm 2\sigma$	ENDF/B-VI $\Delta k_{eff} \pm 2\sigma$	WPO selected $\Delta k_{eff} \pm 2\sigma$
lst3-1	0.0004 ± 0.00784	0.00696 ± 0.00791	0.00186 ± 0.00792
lst3-2	0.00225 ± 0.00843	0.00595 ± 0.00850	0.00032 ± 0.00851
lst3-3	-0.00201 ± 0.00843	0.00249 ± 0.00850	-0.0019 ± 0.00850
lst3-4	0.00414 ± 0.00843	0.00986 ± 0.00849	0.00544 ± 0.00849
lst3-5	0.00073 ± 0.00962	0.00502 ± 0.00967	0.00171 ± 0.00967
lst3-6	0.00066 ± 0.00982	0.00483 ± 0.00986	0.00055 ± 0.00986
lst3-7	0.00224 ± 0.00982	0.00543 ± 0.00985	0.00023 ± 0.00985
lst3-8	-0.00149 ± 0.01041	0.00293 ± 0.01044	-0.0019 ± 0.01044
lst3-9	0.00228 ± 0.01041	0.00357 ± 0.01043	0.00181 ± 0.01044

Table 6.5.3-3. AENCF for LST-003 Experiments (MeV)

MCNP case name	ENDF/B-V	ENDF/B-VI	WPO selected
lst3-1	0.0186	0.0186	0.0185
lst3-2	0.0166	0.0165	0.0165
lst3-3	0.0164	0.0161	0.0164
lst3-4	0.0162	0.0161	0.0160
lst3-5	0.0133	0.0128	0.0131
lst3-6	0.0129	0.0126	0.0130
lst3-7	0.0127	0.0124	0.0126
lst3-8	0.0114	0.0113	0.0115
lst3-9	0.0114	0.0112	0.0114

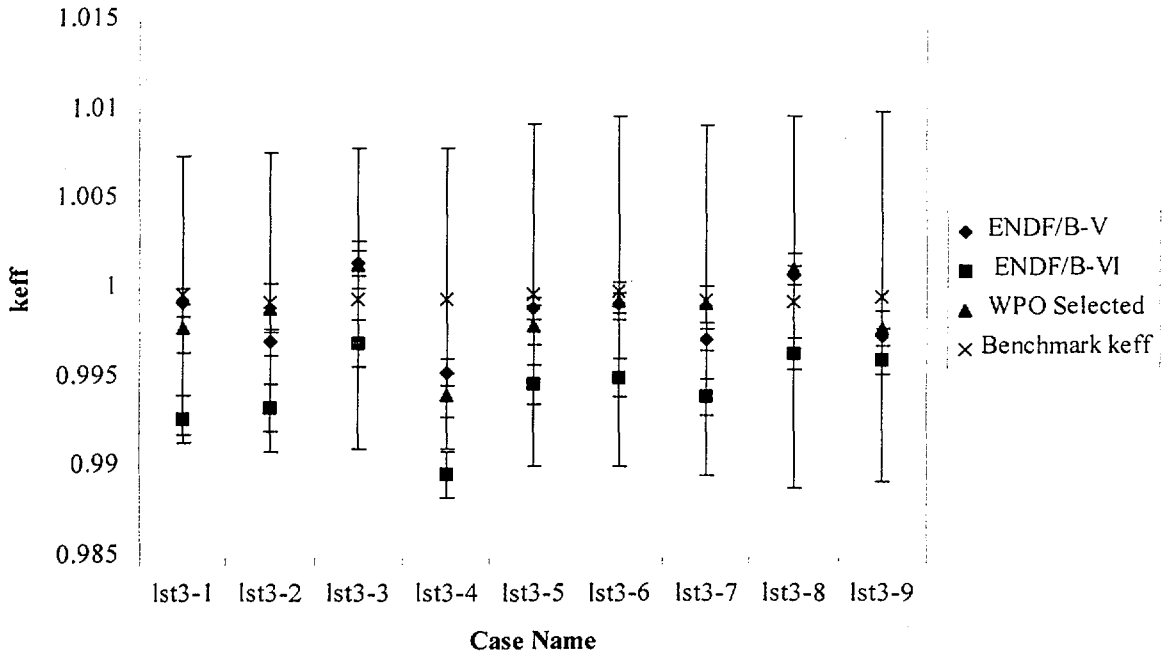

Figure 6.5.3-1. LCE Calculation Results LST-003 Experiments

6.5.4 Graphite-Reflected Uranyl Sulfate (20.9%) Solutions

Table 6.5.4-1 and Figure 6.5.4-1 present the MCNP calculation results for ENDF/B-V, WPO Selected, and ENDF/B-VI cross section libraries for the IST-001 set of critical experiments. Table 6.5.4-2 shows the difference between referenced k_{eff} results and MCNP calculated results, and Table 6.5.4-3 shows the AENCF values for the IST-001 set of critical experiments. It should be noted that the calculational results for all four cases were considerably lower than the benchmark k_{eff} values. The MCNP calculated k_{eff} values range from about 1.5% to 3.2% below the benchmark k_{eff} values. The evaluator also observed similar behavior of under-predicting k_{eff} (p. 30, Ref. 7.3, IST-001). The reason for the differences could not be determined with the existing information.

Table 6.5.4-1. LCE Calculation Results for IST-001 Experiments

MCNP case name	MCU[a]	MCNP		
	Continuous energy MCU-LIB $k_{eff} \pm \sigma$	ENDF/B-V $k_{eff} \pm \sigma$	ENDF/B-VI $k_{eff} \pm \sigma$	WPO selected $k_{eff} \pm \sigma$
ist1-1	0.9855 ± 0.0013	0.98074 ± 0.00108	0.97915 ± 0.00106	0.98509 ± 0.00111
ist1-2	0.9807 ± 0.0013	0.97596 ± 0.00121	0.97348 ± 0.00118	0.97695 ± 0.00120
ist1-3	0.9777 ± 0.0013	0.97222 ± 0.00119	0.97079 ± 0.00117	0.97306 ± 0.00113
ist1-4	0.9735 ± 0.0014	0.97105 ± 0.00124	0.96757 ± 0.00126	0.97124 ± 0.00126

[a] Sample calculation results using MCU and MCU cross section library as reported by the evaluator on page 30 of Reference 7.3, IST-001. The calculations in this analysis were within two standard deviations of the evaluator calculations.

Table 6.5.4-2. Δk Between Experimental k_{eff} and MCNP Calculated k_{eff} for IST-001 Experiments

MCNP case name	ENDF/B-V $\Delta k_{eff} \pm 2\sigma$	ENDF/B-VI $\Delta k_{eff} \pm 2\sigma$	WPO selected $\Delta k_{eff} \pm 2\sigma$
ist1-1	0.01926 ± 0.01062	0.02085 ± 0.010614	0.01491 ± 0.010634
ist1-2	0.02404 ± 0.01068	0.02652 ± 0.010664	0.02305 ± 0.010673
ist1-3	0.02778 ± 0.01067	0.02921 ± 0.01066	0.02694 ± 0.010643
ist1-4	0.02895 ± 0.01069	0.03243 ± 0.010701	0.03243 ± 0.010701

Table 6.5.4-3. AENCF for IST-001 Experiments (MeV)

MCNP case name	ENDF/B-V	ENDF/B-VI	WPO selected
ist1-1	0.0149	0.0146	0.0150
ist1-2	0.0207	0.0208	0.0209
ist1-3	0.0205	0.0208	0.0207
ist1-4	0.0275	0.0271	0.0273

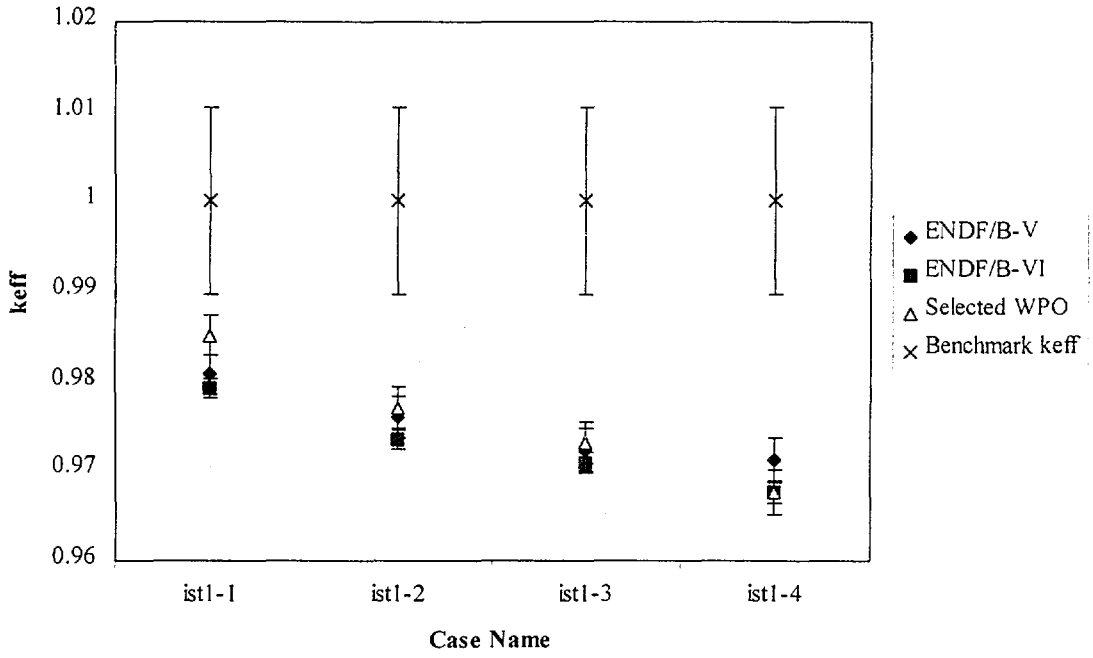

Figure 6.5.4-1. LCE Calculation Results for IST-001 Experiments

6.6 Fast Metal Fuel Results

6.6.1 HEU Fast Metal Fuel (HMF) System Results

Table 6.6.1-1 presents the MCNP calculation results for ENDF/B-V, WPO Selected, and ENDF/B-VI cross section libraries for the HEU Russian Criticality set of experiments, which are also illustrated in Figure 6.6.1-1. Table 6.6.1-3 presents the AENCF values for the HEU Russian Criticality set of

experiments. As presented in Figure 6.5.1-5 and Table 6.5.1-2, it can be seen that all of the results are within 1.5% of the benchmark values.

Table 6.6.1-1. LCE Reactivity Calculation Results for HMF Experiments[a]

MCNP case name	ENDF/B-V $k_{eff} \pm \sigma$	WPO selected $k_{eff} \pm \sigma$	ENDF/B-VI $k_{eff} \pm \sigma$
HMF8	0.9951 ± 0.00058	0.99477 ± 0.00059	0.99281 ± 0.00059
HMF11	0.99348 ± 0.00079	0.99264 ± 0.00078	0.99717 ± 0.00081
HMF12	0.99399 ± 0.00043	0.99446 ± 0.00044	0.9944 ± 0.00043
HMF13	0.99997 ± 0.00061	0.9962 ± 0.00061	0.99478 ± 0.00063
HMF14	0.99831 ± 0.00062	0.99773 ± 0.00058	0.99501 ± 0.00063
HMF15	0.99263 ± 0.00056	0.9936 ± 0.00062	0.99172 ± 0.00061
HMF18	0.99805 ± 0.00056	0.9978 ± 0.00056	0.99837 ± 0.00058
HMF19	1.00277 ± 0.0006	1.00306 ± 0.0006	1.00328 ± 0.0006
HMF20	0.99574 ± 0.00061	0.99643 ± 0.0006	0.99839 ± 0.00069
HMF21	1.00192 ± 0.0006	0.99727 ± 0.0006	0.99463 ± 0.00061
HMF22	0.99272 ± 0.0006	0.99252 ± 0.00064	0.99188 ± 0.0006
HMF24	0.99521 ± 0.00109	0.99401 ± 0.00108	0.99443 ± 0.00109

[a] The values calculated for the ENDF/B-V and ENDF/B-VI cross section libraries were within the statistical uncertainty of the sample MCNP values using the ENDF/B-V and ENDF/B-VI libraries reported on page 244 of Reference 7.15.

Table 6.6.1-2. Δk Between Experimental k_{eff} and MCNP Calculated k_{eff} for HMF Experiments

MCNP case name	ENDF/B-V $\Delta k_{eff} \pm 2\sigma$	WPO selected $\Delta k_{eff} \pm 2\sigma$	ENDF/B-VI $\Delta k_{eff} \pm 2\sigma$
HMF8	0.00490 ± 0.00340	0.00523 ± 0.00341	0.00719 ± 0.00341
HMF11	0.00542 ± 0.00339	0.00626 ± 0.00338	0.00173 ± 0.00341
HMF12	0.00601 ± 0.00370	0.00554 ± 0.00371	0.00560 ± 0.00370
HMF13	-0.00037 ± 0.00324	0.00340 ± 0.00324	0.00482 ± 0.00325
HMF14	0.00169 ± 0.00362	0.00227 ± 0.00359	0.00499 ± 0.00363
HMF15	0.00737 ±0.00358	0.00640 ± 0.00362	0.00828 ± 0.00361
HMF18	0.00085 ± 0.00302	0.00110 ± 0.00302	0.00053 ± 0.00303
HMF19	-0.00407 ± 0.00573	-0.00436 ± 0.00573	-0.00458 ± 0.00573
HMF20	0.00426 ±0 .00573	0.00357 ± 0.00573	0.00161 ± 0.00577
HMF21	-0.00292 ± 0.00495	0.00173 ± 0.00495	0.00437 ± 0.00495
HMF22	0.00728 ± 0.00398	0.00748 ± 0.00401	0.00812 ± 0.00398
HMF24	0.00479 ± 0.00371	0.00599 ± 0.00370	0.00557 ± 0.00371

Table 6.6.1-2. AENCF for HMF Experiments (MeV)

MCNP case name	ENDF/B-V	ENDF/B-VI	WPO selected
HMF8	1.5501	1.4766	1.5503
HMF11	1.1607	1.1026	1.1620

Table 6.6.1-2. AENCF for HMF Experiments (MeV)

MCNP case name	ENDF/B-V	ENDF/B-VI	WPO selected
HMF12	1.5237	1.4486	1.5222
HMF13	1.4838	1.4155	1.4860
HMF14	1.5465	1.4893	1.5443
HMF15	1.5813	1.5000	1.5808
HMF18	1.5515	1.4753	1.5522
HMF19	1.4793	1.4018	1.4765
HMF20	1.4341	1.3635	1.4333
HMF21	1.4431	1.3807	1.4481
HMF22	1.5049	1.4299	1.5039
HMF24	1.2553	1.1917	1.2504

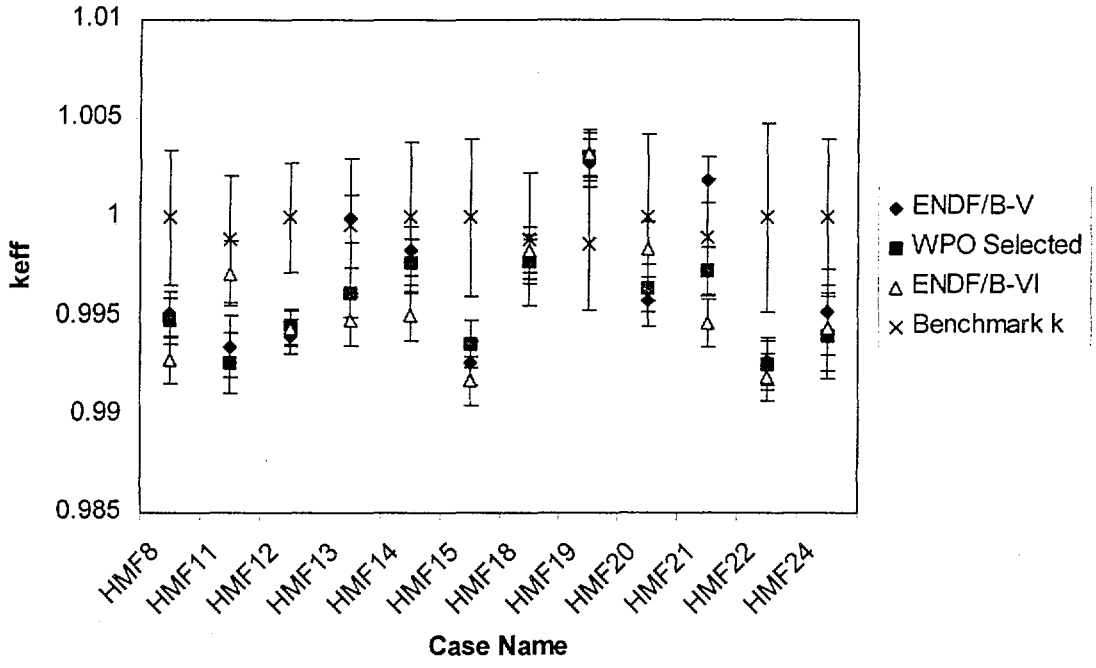

Figure 6.6.1-1. LCE Calculation Results for Russian Criticality Benchmark Experiments

6.6.2 IEU Fast Metal Fuel (IMF) System Results

6.6.2.1 The Early Jemima Experiments: Bare Cylindrical Configurations of Enriched and Natural Uranium

Table 6.6.2.1-1 and Figure 6.6.2.1-1 presents the MCNP calculation results for ENDF/B-V, WPO Selected, and ENDF/B-VI cross section libraries for some of the IEU Russian Criticality set of experiments. Table 6.6.2.1-2 shows the difference between experimental k_{eff} results and MCNP calculated results, and Table 6.6.2.1-3 shows the AENCF values for the IEU Russian Criticality set of

experiments. The use of a simplified case results in a slightly higher k_{eff} than the one calculated using the reference case (the difference is not more than 0.12%). Overall, the experimental benchmark shows that the MCNP code is able to predict the criticality of this experiment with a precision not worse than 0.57% (Table 6.6.2.1-2). This result is independent of the cross section library used. However, k_{eff} obtained using the ENDF/B-VI cross section library under-estimates the experimental k_{eff}. The k_{eff} obtained using ENDF/B-V and the WPO Selected libraries over-estimates the experimental k_{eff}.

Table 6.6.2.1-1. LCE Calculation Results for IMF-001 Experiments

MCNP case name	MCNP[a] (Continuous energy ENDF/B-V)	ENDF/B-V $k_{eff} \pm \sigma$	ENDF/B-VI $k_{eff} \pm \sigma$	WPO selected $k_{eff} \pm \sigma$
imf1-1	1.0018 ± 0.00028[b]	1.00224 ± 0.00029	0.99714 ± 0.00028	1.00183 ± 0.00028
imf1-2	1.0020 ± 0.00028	1.00225 ± 0.00028	0.99666 ± 0.00027	1.00254 ± 0.00028
imf1-3	1.0041 ± 0.00028	1.00401 ± 0.00029	0.9986 ± 0.00028	1.004 ± 0.00027
imf1-4	1.0043 ± 0.00028	1.00477 ± 0.00028	0.999 ± 0.00026	1.00459 ± 0.00028
imf1-5	1.0019 ± 0.00028	1.00175 ± 0.00026	0.99683 ± 0.00028	1.00153 ± 0.00027
imf1-6	1.0029 ± 0.00028	1.0024 ± 0.00027	0.99709 ± 0.00028	1.00197 ± 0.00026
imf1-7	1.0044 ± 0.00028	1.00374 ± 0.00028	0.99876 ± 0.00028	1.00398 ± 0.00028
imf1-8	1.0055 ± 0.00028	1.005 ± 0.00026	0.99988 ± 0.00028	1.00513 ± 0.00027

[a] Sample calculation results using MCNP and ENDF/B-V cross section library as reported by the evaluator on page 43 of Reference 7.3, IMF-001. The calculations in this analysis were within the statistical uncertainty of the evaluator calculations.

[b] Standard deviations were between 0.00027 and 0.00029 (p. 43, Ref. 7.3, IMF-001)

Table 6.6.2.1-2. Δk Between Experimental k_{eff} Results and MCNP Calculated k_{eff} Results for the IMF-001 Experiments

MCNP case name	ENDF/B-V $\Delta k_{eff} \pm 2\sigma$	ENDF/B-VI $\Delta k_{eff} \pm 2\sigma$	WPO selected $\Delta k_{eff} \pm 2\sigma$
imf1-1	-0.00344 ± 0.002469	0.00166 ± 0.00246	-0.003 ± 0.00246
imf1-2	-0.00345 ± 0.002464	0.00214 ± 0.00246	-0.0037 ± 0.00246
imf1-3	-0.00501 ± 0.002082	0.0004 ± 0.00208	-0.005 ± 0.00207
imf1-4	-0.00577 ± 0.002077	0 ± 0.00207	-0.0056 ± 0.00208
imf1-5	-0.00285 ± 0.002456	0.00207 ± 0.00246	-0.0026 ± 0.00246
imf1-6	-0.0027 ± 0.00246	0.00261 ± 0.00246	-0.0023 ± 0.00246
imf1-7	-0.00444 ± 0.002077	0.00054 ± 0.00208	-0.0047 ± 0.00208
imf1-8	-0.0048 ± 0.002066	0.00032 ± 0.00208	-0.0049 ± 0.00207

Table 6.6.2.1-3. AENCF for the IMF-001 Experiments (MeV)

MCNP case name	ENDF/B-V	ENDF/B-VI	WPO selected
imf1-1	1.4394	1.3910	1.4395
imf1-2	1.4398	1.3919	1.4403
imf1-3	1.3860	1.3515	1.3862

Table 6.6.2.1-3. AENCF for the IMF-001 Experiments (MeV)

MCNP case name	ENDF/B-V	ENDF/B-VI	WPO selected
imf1-4	1.3859	1.3495	1.3848
imf1-5	1.4401	1.3922	1.4395
imf1-6	1.4398	1.3911	1.4394
imf1-7	1.3865	1.3509	1.3869
imf1-8	1.3861	1.3498	1.3852

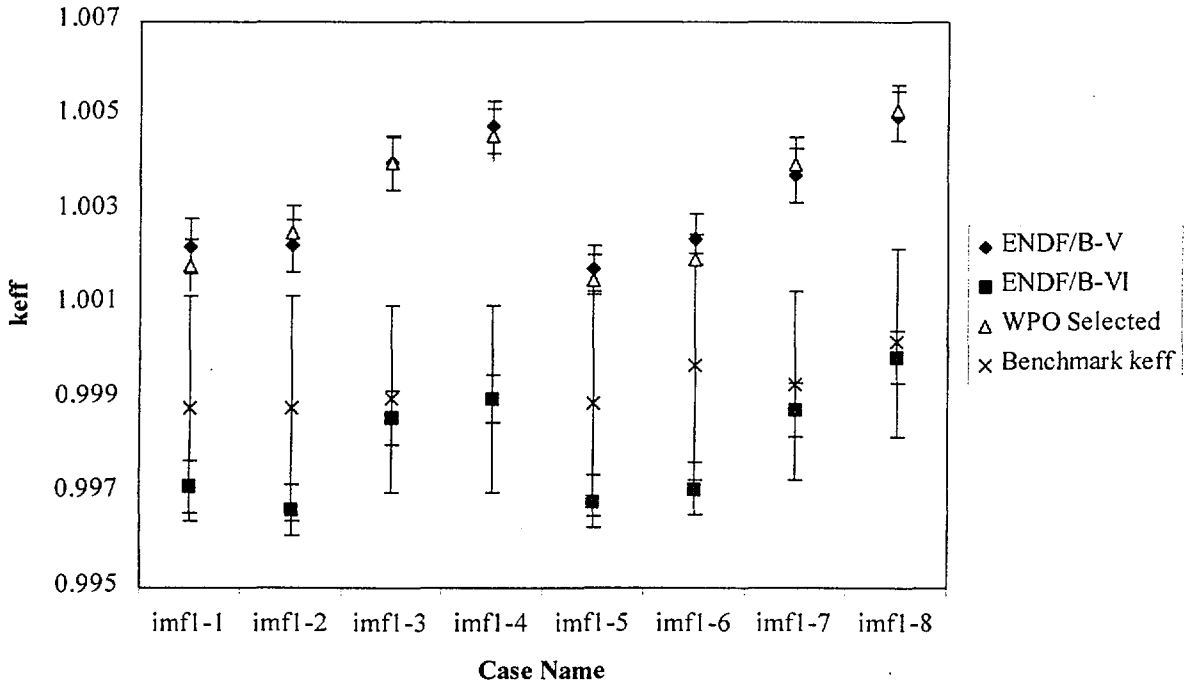

Figure 6.6.2.1-1. LCE Calculation Results for IMF Experiments

6.6.2.2 Natural Uranium Reflected Assembly of Enriched and Natural Uranium Plates

Table 6.6.2.2-1 and Figure 6.6.2.2-1 presents the MCNP calculation results for ENDF/B-V, WPO Selected, and ENDF/B-VI cross section libraries for one of the IEU Russian Criticality set of experiments. Table 6.6.2.2-2 shows the difference between experimental k_{eff} results and MCNP calculated results, and Table 6.6.2.2-3 shows the AENCF values. In this experiment, the only material used for both the core and the reflector was uranium. The cross sections used for this material in the WPO Selected libraries are identical to the ones used in the ENDF/B-V library. Therefore both calculations give exactly the same k_{eff} results. Overall, the experimental benchmark shows that the MCNP code is able to predict the criticality of this experiment with a precision not worse than 0.6% (Table 6.6.2.2-2). This result is independent of the cross section library used. However, calculations based on the ENDF/B-VI cross section library resulted in a lower k_{eff} than the calculation based on the ENDF/B-V and WPO Selected libraries.

Table 6.6.2.2-1. LCE Calculation Results for the IMF-002 Experiment

MCNP case name	MCNP[a]	MCNP		
	ENDF/B-V $k_{eff} \pm \sigma$	ENDF/B-V $k_{eff} \pm \sigma$	ENDF/B-VI $k_{eff} \pm \sigma$	WPO selected $k_{eff} \pm \sigma$
imf2-1	1.0059 ± 0.0006	1.00594 ± 0.0006	1.00327 ± 0.00056	1.00594 ± 0.0006

[a] Sample calculation result using MCNP and ENDF/B-V Cross Section Library as reported by the evaluator on page 10 of Reference 7.3, IMF-002. The calculation in this analysis was within two standard deviations of the evaluator calculation.

Table 6.6.2.2-2. Δk Between Experimental k_{eff} and MCNP Calculated k_{eff} for IMF-002 Experiment

MCNP case name	ENDF/B-V $\Delta k_{eff} \pm 2\sigma$	ENDF/B-VI $\Delta k_{eff} \pm 2\sigma$	WPO selected $\Delta k_{eff} \pm 2\sigma$
imf2-1	-0.0059 ± 0.0061	-0.00327 ± 0.0061	-0.0059 ± 0.0061

Table 6.6.2.2-3. AENCF for IMF-002 Experiment (MeV)

MCNP case name	ENDF/B-V	ENDF/B-VI	WPO selected
imf2-1	1.2784	1.2650	1.2784

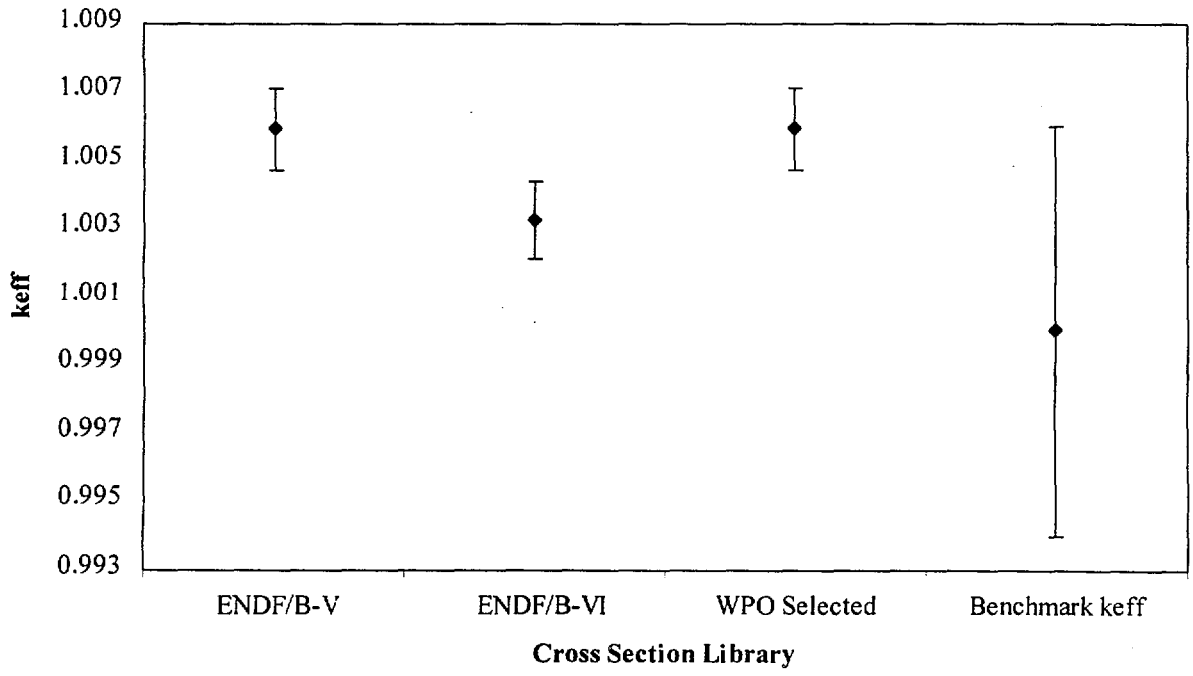

Figure 6.6.2.2-1. LCE Calculation Results for IMF-002 Experiments

6.6.2.3 Spherical Assembly of U^{235} (36 wt%)

Table 6.6.2.3-1 and Figure 6.6.2.3-1 presents the MCNP calculation results for ENDF/B-V, WPO Selected, and ENDF/B-VI cross section libraries for some of the IEU Russian Criticality set of experiments. Table 6.6.2.3-2 shows the difference between experimental k_{eff} results and MCNP calculated results, and Table 6.6.2.3-3 shows the AENCF values. The use of a simplified case results in a slightly different k_{eff} than the one calculated using the detailed case (the difference is not worse than 0.4%). Overall, the experimental benchmark calculation shows that the MCNP code is able to predict the criticality of this experiment with a precision not worse than 1.3% (Table 6.6.2.3-2). This result is independent of the cross section library used. However, calculations based on the ENDF/B-VI cross section library resulted in a more non-conservative k_{eff} than the calculations based on the ENDF/B-V and WPO Selected libraries.

Table 6.6.2.3-1. LCE Calculation Results for IMF-003, 004, 005, 006, and 008 Experiments

MCNP case name	Evaluator $k_{eff} \pm \sigma$	ENDF/B-V $k_{eff} \pm \sigma$	ENDF/B-VI $k_{eff} \pm \sigma$	WPO selected $k_{eff} \pm \sigma$
Bare sphere				
imf3-1	0.9943±0.0008[a]	0.99925 ± 0.00076	0.99539 ± 0.00076	1.00096 ± 0.0008
imf3-2	0.9954±0.0008[a]	1.00559 ± 0.00078	0.99881 ± 0.00078	1.00467 ± 0.00083
Graphite reflected sphere				
imf4-1	1.0095 ± 0.0006[b]	1.01048 ± 0.00084	1.00446 ± 0.00081	1.00884 ± 0.00078
imf4-2	1.0094 ± 0.0006[b]	1.00999 ± 0.00088	1.00592 ± 0.00083	1.01001± 0.00085
Steel reflected sphere				
imf5-1	1.0138 ± 0.0006[c]	1.00881 ± 0.00079	1.00053 ± 0.00081	1.00632 ± 0.00082
imf5-2	1.0135 ± 0.0006[c]	1.00951 ± 0.00085	0.99897 ± 0.00082	1.00584 ± 0.00082
Duralumin reflected sphere				
imf6-1	0.9964 ± 0.0006[d]	0.99597 ± 0.00081	0.99173 ± 0.00083	0.99727 ± 0.00083
imf6-2	0.9972 ± 0.0006[d]	0.99613 ± 0.00086	0.99191 ± 0.00079	0.99768 ± 0.00082
Uranium depleted reflected sphere				
imf8-1	0.9957 ± 0.0008[e]	1.0087 ± 0.00084	1.0038 ± 0.00081	1.00845 ± 0.00079

[a] KENO–16 Group Hansen Roach (pp. 15, 16, Ref. 7.3, IMF-003)

[b] MCNP Continuous Energy ENDF/B-V (pp. 14, 15, Ref. 7.3, IMF-004)

[c] MCNP Continuous Energy ENDF/B-V (pp. 15, 16, Ref. 7.3, IMF-005)

[d] MCNP Continuous Energy ENDF/B-V (pp. 15, 16, Ref. 7.3, IMF-006)

[e] KENO–16 Group Hansen Roach (p. 15, Ref. 7.3, IMF-008)

Table 6.6.2.3-2. Δk Between Experimental k_{eff} and MCNP Calculated k_{eff} Results for IMF-003, 004, 005, 006, and 008 Experiments

MCNP case name	ENDF/B-V $\Delta k_{eff} \pm 2\sigma$	ENDF/B-VI $\Delta k_{eff} \pm 2\sigma$	WPO selected $\Delta k_{eff} \pm 2\sigma$
Bare sphere			
imf3-2	0.00075 ± 0.003724	0.00119 ± 0.00374	-0.0047 ± 0.00378
imf3-1	-0.00559 ± 0.003741	0.00461 ± 0.00372	-0.001 ± 0.00376
Graphite reflected sphere			
imf4-2	-0.01048 ± 0.006231	-0.00592 ± 0.00623	-0.01 ± 0.00624
imf4-1	-0.00999 ± 0.006253	-0.00446 ± 0.00621	0.0088 ± 0.00620
Steel reflected sphere			
imf5-2	-0.00881 ± 0.004487	0.00103 ± 0.00428	-0.0058 ± 0.00428
imf5-1	-0.00951 ± 0.004531	-0.00053 ± 0.00428	-0.0063 ± 0.00428
Duralumin reflected sphere			
imf6-2	0.00403 ± 0.004877	0.00809 ± 0.00467	0.00232 ± 0.00467
imf6-1	0.00387 ± 0.004911	0.00827 ± 0.00467	0.00273 ± 0.00467
Uranium depleted reflected sphere			
imf8-1	-0.0087 ± 0.003973	-0.0038 ± 0.00369	-0.0085 ± 0.00369

Table 6.6.2.3-3. AENCF for IMF-003, 004, 005, 006, and 008 Experiments (MeV)

MCNP case name	ENDF/B-V	ENDF/B-VI	WPO selected
imf3-2	1.3535	1.3162	1.3507
imf3-1	1.3502	1.3242	1.3526
imf4-2	1.3062	1.2777	1.3058
imf4-1	1.3071	1.2768	1.3076
imf5-2	1.2822	1.2583	1.2889
imf5-1	1.2852	1.2597	1.2872
imf6-2	1.2905	1.2568	1.2912
imf6-1	1.2892	1.2610	1.2915
imf8-1	1.3650	1.3337	1.3639

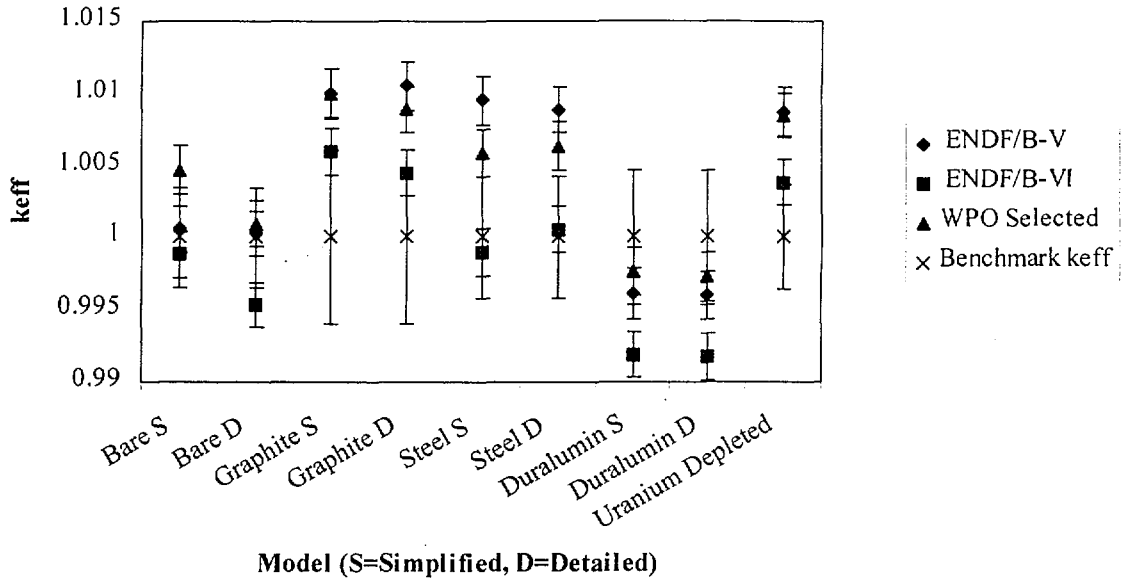

Figure 6.6.2.3-1. Spherical Assembly of U^{235} with various Reflectors k_{eff} Calculation Results

6.6.3 Pu Fast Metal Fuel (PMF) System Results

Table 6.6.3-1 presents the MCNP calculation results for ENDF/B-V, WPO Selected, and ENDF/B-VI cross section libraries for the Pu fueled Russian Criticality set of experiments, which are also illustrated in Figure 6.6.3-1. Table 6.6.3-3 presents the AENCF values for the Pu fueled Russian Criticality set of experiments. As presented in Figure 6.5.1-5 and Table 6.5.1-2, it can be seen that all of the results are within 1.5% of the benchmark values.

Table 6.6.3-1. LCE Reactivity Calculation Results for PMF Experiments[a]

MCNP case name	ENDF/B-V $k_{eff} \pm \sigma$	WPO selected $k_{eff} \pm \sigma$	ENDF/B-VI $k_{eff} \pm \sigma$
PMF20	1.00085 ± 0.00064	0.99968 ± 0.00065	0.99878 ± 0.00062
PMF22	0.99627 ± 0.00057	0.99459 ± 0.00055	0.99707 ± 0.00051
PMF23	0.99742 ± 0.00059	0.99681 ± 0.00058	0.99869 ± 0.00061
PMF24	0.99781 ± 0.00065	0.99756 ± 0.00066	1.00122 ± 0.00064
PMF25	0.99835 ± 0.00062	0.99601 ± 0.00057	0.9971 ± 0.00064
PMF26	1.00167 ± 0.00059	0.99551 ± 0.00064	0.99754 ± 0.00057
PMF27	1.00178 ± 0.00078	1.00113 ± 0.00076	1.00258 ± 0.00073
PMF28	1.00324 ± 0.00063	0.99739 ± 0.00065	0.99891 ± 0.0006
PMF29	0.99309 ± 0.00056	0.9933 ± 0.00055	0.99463 ± 0.00058
PMF30	1.00078 ± 0.00066	1.00129 ± 0.00063	1.00176 ± 0.00057
PMF31	1.00208 ± 0.00073	1.00104 ± 0.0007	1.00305 ± 0.00074

Table 6.6.3-1. LCE Reactivity Calculation Results for PMF Experiments[a]

MCNP case name	ENDF/B-V $k_{eff} \pm \sigma$	WPO selected $k_{eff} \pm \sigma$	ENDF/B-VI $k_{eff} \pm \sigma$
PMF32	0.99938 ± 0.0006	0.99667 ± 0.00061	0.9964 ± 0.00065

[a] The values calculated for the ENDF/B-V and ENDF/B-VI cross section libraries were within the statistical uncertainty of the sample MCNP values using the ENDF/B-V and ENDF/B-VI libraries reported on page 244 of Reference 7.15.

Table 6.6.3-2. Δk Between Experimental k_{eff} and MCNP Calculated k_{eff} for PMF Experiments

MCNP case name	ENDF/B-V $\Delta k_{eff} \pm 2\sigma$	WPO selected $\Delta k_{eff} \pm 2\sigma$	ENDF/B-VI $\Delta k_{eff} \pm 2\sigma$
PMF20	-0.00165 ± 0.00363	-0.00048 ± 0.00139	0.00042 ± 0.00131
PMF22	0.00373 ± 0.00416	0.00541 ± 0.00552	0.00293 ± 0.00310
PMF23	0.00258 ± 0.00417	0.00319 ± 0.00339	0.00131 ± 0.00179
PMF24	0.00219 ± 0.00421	0.00244 ± 0.00277	-0.00122 ± 0.00177
PMF25	0.00165 ± 0.00419	0.00399 ± 0.00415	0.00290 ± 0.00317
PMF26	-0.00167 ± 0.00494	0.00449 ± 0.00467	0.00246 ± 0.00271
PMF27	-0.00278 ± 0.00467	-0.00213 ± 0.00262	-0.00358 ± 0.00387
PMF28	-0.00434 ± 0.00458	0.00151 ± 0.00199	-0.00001 ± 0.00120
PMF29	0.00691 ± 0.00396	0.00670 ± 0.00679	0.00537 ± 0.00549
PMF30	-0.00078 ± 0.00440	-0.00129 ± 0.00180	-0.00176 ± 0.00210
PMF31	-0.00208 ± 0.00445	-0.00104 ± 0.00174	-0.00305 ± 0.00339
PMF32	0.00062 ± 0.00418	0.00333 ± 0.00355	0.00360 ± 0.00383

Table 6.6.3-3. AENCF for PMF Experiments (MeV)

MCNP case name	ENDF/B-V	ENDF/B-VI	WPO selected
PMF20	1.8895	1.8960	1.8886
PMF22	1.8914	1.9004	1.8932
PMF23	1.7988	1.8070	1.8011
PMF24	1.7418	1.7414	1.7421
PMF25	1.8293	1.8431	1.8316
PMF26	1.7250	1.7407	1.7318
PMF27	1.4726	1.4768	1.4768
PMF28	1.7100	1.7229	1.7166
PMF29	1.9154	1.9254	1.9188
PMF30	1.8138	1.8213	1.8152
PMF31	1.6057	1.6082	1.6059
PMF32	1.8113	1.8263	1.8192

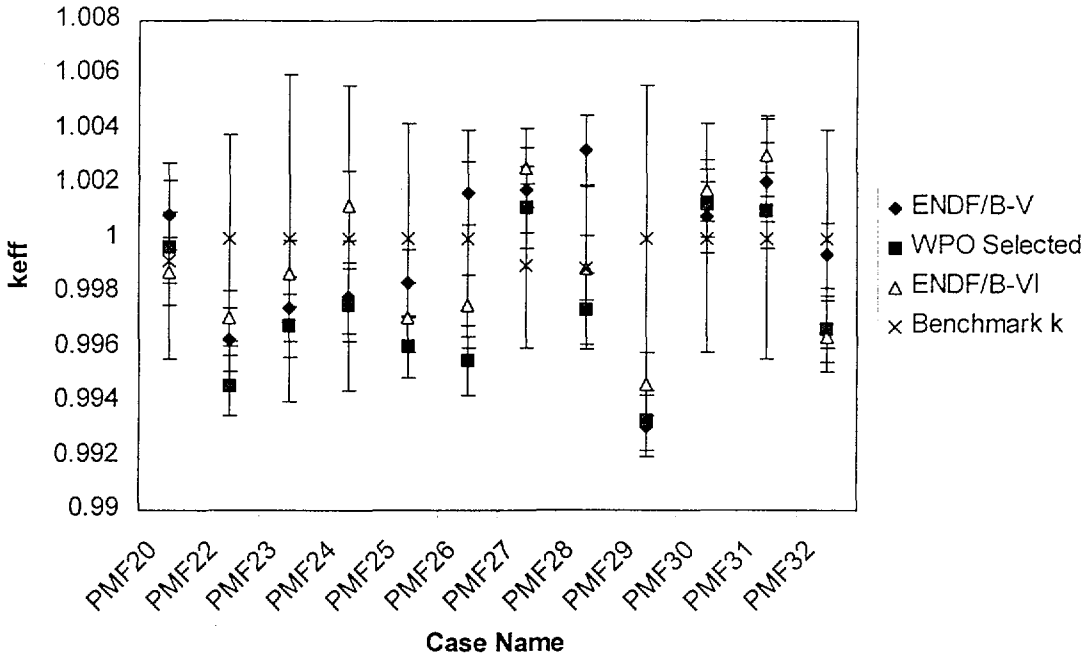

Figure 6.6.3-1. LCE Calculation Results for PMF Experiments

6.7 Regression Analysis Results

The following section presents the results of a regression calculation performed on the LCE k_{eff} results. Each regression calculation was performed on LCE's having the similar fuel characteristics. Figures 1 through 42 in Attachment VII illustrate the plots of k_{eff} and the regression of k_{eff} against AENCF and H/X ratio. The linear coefficient was used to numerically evaluate the "goodness of fit". The linear coefficient (noted as r^2) is a quantitative measure of the degree to which a linear relationship exists between two variables. The closer r^2 approaches the value of 1, the better the fit of the data to the linear equation (Ref. 7.9). Table 6.7-1 and 6.7-2 show the linear coefficient and the coefficients of the linear equation for each regression of k_{eff} against AENCF and H/X ratio calculation, respectively.

Table 6.7-1. Equation and Linear Correlation Coefficient of the Regression of k_{eff} Against AENCF

Experiment type	r^2			Equation y=ax+b					
				x variable (a values)			y-intercept (b values)		
	ENDF /B-V	ENDF /B-VI	WPO selected	ENDF/ B-V	ENDF/ B-VI	WPO selected	ENDF/ B-V	ENDF/ B-VI	WPO selected
HMF	0.0189	0.0436	0.0815	0.0038	-0.0056	0.0066	0.9911	1.0033	0.9863
PMF	0.4063	0.5613	0.3698	0.0146	-0.0153	-0.0127	1.0251	1.0261	1.0201
IMF	0.1087	0.0790	0.1109	-0.0198	-0.0193	-0.0171	1.0316	1.0249	1.0276
HEU Thermal	0.6557	0.1858	0.3409	-0.2096	-0.1413	-0.2047	1.0063	1.0030	1.0070
HEU Epithermal	0.7557	0.7644	0.8581	-0.7047	-0.8063	-0.8011	1.1647	1.1903	1.1899

Table 6.7-1. Equation and Linear Correlation Coefficient of the Regression of k_{eff} Against AENCF

Experiment type	r^2			Equation y=ax+b					
				x variable (a values)			y-intercept (b values)		
	ENDF /B-V	ENDF /B-VI	WPO selected	ENDF/ B-V	ENDF/ B-VI	WPO selected	ENDF/ B-V	ENDF/ B-VI	WPO selected
LEU	0.5173	0.6981	0.5528	0.0921	0.1311	0.1042	0.9856	0.9752	0.9814
Solution k_{eff}	0.1398	0.0079	0.0033	0.1008	0.0993	0.0678	0.9899	0.9872	0.9917
Solution k_∞	0.0079	0.0024	0.0013	0.0575	0.0315	0.0220	0.9934	0.99293	0.9998
Pu Thermal	0.5311	0.4930	0.4551	-0.0741	-0.0444	-0.0485	1.0106	1.0016	1.0073

Table 6.7-2. Equation and Linear Correlation Coefficient of the Regression of k_{eff} Against H/X Ratio

Experiment type	r^2			Equation y=ax+b					
				x variable (a values)			y-intercept (b values)		
	ENDF/ B-V	ENDF/ B-VI	WPO selected	ENDF/ B-V	ENDF/ B-VI	WPO selected	ENDF/ B-V	ENDF/ B-VI	WPO selected
HMF	N/A	N/A	N/A	N/A	N/A	N/A	N/A	N/A	N/A
PMF	N/A	N/A	N/A	N/A	N/A	N/A	N/A	N/A	N/A
IMF	N/A	N/A	N/A	N/A	N/A	N/A	N/A	N/A	N/A
HEU Thermal	0.1059	0.0375	0.1122	0.0000	0.0000	0.0000	0.9959	0.9966	0.9966
HEU Epithermal	N/A	N/A	N/A	N/A	N/A	N/A	N/A	N/A	N/A
LEU	0.7260	0.7228	0.8445	0.0000	0.0000	0.0000	0.9885	0.9822	0.9855
Solution k_{eff}	0.4234	0.4520	0.4448	0.0000	0.0000	0.0000	0.9770	0.9739	0.9769
Solution k_∞	0.2260	0.1866	0.2007	0.0000	-0.0001	-0.0001	1.0498	1.0394	1.0457
Pu Thermal	0.1911	0.6264	0.2391	0.0000	0.0000	0.0000	0.9977	0.9936	0.9991

Attachments I, III, and V, (the attachment CD has been moved to Reference 7.28) contain the MCNP input files for the ENDF/B-V, ENDF/B-VI, and WPO Selected cross section libraries, respectively. Attachments II, IV, and VI (moved to Reference 7.28) contain the MCNP output files for the ENDF/B-V, ENDF/B-VI, and WPO Selected cross section libraries, respectively.

7. References

7.1 Breismeister, Judith F., Ed. 1997. *MCNP—A General Monte Carlo N-Particle Transport Code.* User manual, Report Number: LA-12625-M, Version 4B. Los Alamos National Laboratory: Los Alamos, New Mexico. TIC: 241044

7.2 Civilian Radioactive Waste Management System (CRWMS) Management and Operating Contractor (M&O) 1998. *Selection of MCNP Cross Section Libraries.* B00000000-01717-5705-00099 REV 00. Las Vegas, Nevada: M&O. ACC: MOL.19980722.0042

7.3 Organization for Economic Cooperation and Development-Nuclear Energy Agency (OECD-NEA) 1997. *International Handbook of Evaluated Criticality Safety Benchmark Experiments.* NEA/NSC/DOC(95)03, September 1997 Edition. Paris, France: OECD. TIC: 243013

7.4 CRWMS M&O 1998. *Software Qualification Report for MCNP Version 4B2, A General Monte Carlo N-Particle Transport Code.* Document Identifier 30033-2003 REV 01; CSCI: 30033 V4B2LV; MI: 30055-M72-001, 30056-M03-001. Las Vegas, Nevada: M&O. ACC: MOL.19980622.0637

7.5 General Electric Company 1989. *Nuclides and Isotopes Fourteenth Edition: Chart of the Nuclides.* San Jose, California: General Electric Company. TIC: 201637

7.6 U. S. Public Health Service 1970. *Radiological Health Handbook.* Report Number: PB230846. Washington, DC. TIC: 214902

7.7 [Reserved]

7.8 Inco Alloys International 1988. *Inco Alloys International Product Handbook.* Huntington, West Virginia: Inco Alloys International, Inc. TIC: 239397

7.9 Kimball, K.D.; Trumble, E.F. 1997. Statistical Methods for Accurately Determining Criticality Code Bias. *Proceedings of the Topical Meeting on Criticality Safety Challenges in the Next Decade, Meeting of the Nuclear Criticality Safety Division American Nuclear Society, September 7-11*, pp. 247-254. ISBN: O-89448-618-7. La Grange Park, Illinois: American Nuclear Society. TIC: 238734

7.10 Oak Ridge National Laboratory 1995. *SCALE 4.3, RSIC COMPUTER CODE COLLECTION, (CCC-545).* Report Number: NUREG/CR-0200, REV 5. Oak Ridge, Tennessee. TIC: 235920

7.11 Schwinkendorf, K.N.; Wittekind, W.D.; Toffer, H. 1991. *Calculation of the Fast Flux Test Facility Fuel Pin Tests with the WIMS-E and MCNP Codes.* WHC-SA-1379-FP. Washington, DC: Department of Energy. TIC: 240988

7.12 Bierman, S.R.; Durst, B.M.; Clayton, E.D.; Scherpelz, R.I.; Kerr, H.T. 1979. Critical Experiments with Fast Test Reactor Fuel Pins in Water. *Nuclear Technology*, vol. 44, pp. 141-151. American Nuclear Society. TIC: 239579

7.13 [Reserved]

7.14 Mele, I.; Ravnik, M.; Trkov, A. 1994. TRIGA Mark II Benchmark Experiment, Part I: Steady-State Operation. *Nuclear Technology*, vol. 105, pp. 37-51. American Nuclear Society. TIC: 240865

7.15 Capell, B.M.; Mosteller, R.D.; Pelowitz, D. B. 1997. ENDF/B-V and ENDF/B-VI Results for the Russian Criticality-Safety Benchmarks. *Transactions of the American Nuclear Society.* ISSN: 0003-018X, Volume 76, June. TIC: 242665

7.16 Radulescu, G.; Abdurrahman, N.M. 1997. MCNP Criticality Benchmark Calculations of the Saxton Plutonium Program Experiments. *Transactions of the American Nuclear Society*. ISSN: 0003-018X, Volume 76, June. TIC: 242666

7.17 Wittekind, W.D. 1992. *K Basin Criticality Evaluation for Irradiated Fuel Canisters in Sludge*. WHC-SD-NR-CSER-001 Rev. 0. Westinghouse Hanford Company: Richland, Washington. TIC: 240971

7.18 Schmittroth, F. 1996. *MCNP Criticality Validation and Bias for LEU Systems*. WHC-SD-SNF-ANAL-013 Rev. 0. Richland, Washington: Department of Energy. TIC: 241004

7.19 Brown, C.L.; Lloyd, R.C.; Bierman, S.R.; Clayton, E.D. 1965. *Exponential Experiments and Neutron Multiplication Measurements with 1.25 wt% Enriched N-Reactor Fuel Elements in Light Water*. BNWL-52. Richland, Washington: Pacific Northwest Laboratory. TIC: 241005

7.20 DeHart, M.D. and Bowman, S.M. 1995. *Analysis of Fresh Fuel Critical Experiments Appropriate for Burnup Credit Validation*. ORNL/TM-12959. Oak Ridge, Tennessee: Oak Ridge National Laboratory. TIC: 240899

7.21 [Reserved]

7.22 Taylor, E.G. 1965. *Saxton Plutonium Program Critical Experiments for the Saxton Partial Plutonium Core*. WCAP-3385-54 (EURAEC-1493). Westinghouse Electric Corporation: Atomic Power Division. Pittsburgh, Pennsylvania. TIC: 223286

7.23 American Society for Testing and Materials (ASTM) 1997. *Standard Specification for Heat-Resisting Chromium and Chromium-Nickel Stainless Steel Plate, Sheet, and Strip for Pressure Vessels*. ASTM A 240/A 240M-97a. West Conshohocken, Pennsylvania: ASTM. TIC: 239431

7.24 ASTM 1997. *Standard Specification for Stainless Steel Bars and Shapes*. ASTM A 276-97. Philadelphia, Pennsylvania: ASTM. TIC: 240987

7.25 American Society for Metals (ASM) 1980. *Metals Handbook Ninth Edition, Properties and Selection: Stainless Steels, Tool Materials and Special-Purpose Metals*. LC Call Number: TA459.A5. ISBN: 0-87170009-3. Metals Park, Ohio: ASM. TIC: 209801

7.26 ASTM 1990. *Standard Specification for Pressure Vessel Plates, Carbon Steel, for Moderate- and Lower-Temperature Service*. ASTM A 516/A 516M-90. Philadelphia, Pennsylvania: ASTM. TIC: 237681

7.27 Hintze, J.L. 1997. *NCSS 97 - User's Guide-I, Statistical System for Windows*. Kaysville, Utah: Number Cruncher Statistical Systems. TIC: 240515

7.28 CRWMS M&O 1999. *Two (2) Compact Discs for LCE for Research Reactor Benchmark Calculations, Attachments I through VI*. B00000000-01717-0210-00034 REV 00. Las Vegas, Nevada: M&O. ACC: MOL.19990311.0479

8. Attachments

Table 8-1 presents the attachment specifications for this calculation file.

Table 8-1. Attachment Listing

Attachment #	# of Pages	Creation Date	Description
I	5 (Hard-copy listing of CD content)	03/05/99	MCNP input decks using ENDF/B-V cross section library for the LCE benchmark calculations (attachment CD moved to Reference 7.28)
II	5 (Hard-copy listing of CD content)	03/05/99	MCNP output files using ENDF/B-V cross section library for the LCE benchmark calculations (attachment CD moved to Reference 7.28)
III	5 (Hard-copy listing of CD content)	03/05/99	MCNP input decks using ENDF/B-VI cross section library for the LCE benchmark calculations (attachment CD moved to Reference 7.28)
IV	5 (Hard-copy listing of tape content)	03/05/99	MCNP output files using ENDF/B-VI cross section library for the LCE benchmark calculations (attachment CD moved to Reference 7.28)
V	4 (Hard-copy listing of CD content)	03/05/99	MCNP input decks using WPO Selected cross section libraries for the LCE benchmark calculations (attachment CD moved to Reference 7.28)
VI	4 (Hard-copy listing of CD content)	03/05/99	MCNP output files using WPO Selected cross section libraries for the LCE benchmark calculations (attachment CD moved to Reference 7.28)
VII	22	N/A	k_{eff} regression analysis plots
VIII	17	N/A	Normality test plots

This attachment contains the MCNP input files for the LCE benchmark calculations that were performed using the ENDF/B-V cross section library. The input files are contained on an attachment CD of this calculation file (the attachment CD has been moved to Reference 7.28). The information contained in this hard-copy representation of Attachment I is a listing of the various MCNP input deck files and their attributes. The CD containing Attachment I was written using the Hewlett Packard (HP) CD-Writer Plus model 7200e external CD-rewritable drive for personal computers.

Filename	File Type	File Size (bytes)	File Date and Time	
Case_1	ASCII	3,032	2/24/99	1:25p
Case_2	ASCII	3,507	2/24/99	1:25p
Case_3	ASCII	3,510	2/24/99	3:33p
Case_4	ASCII	3,514	2/24/99	1:25p
Case_5	ASCII	3,499	2/24/99	1:25p
Case_6	ASCII	3,512	2/24/99	1:25p
Case_7	ASCII	3,508	2/24/99	1:25p
Case_8	ASCII	3,514	2/24/99	3:33p
FFTF001	ASCII	19,539	2/24/99	1:25p
FFTF003R	ASCII	21,436	2/24/99	1:25p
FFTF004	ASCII	21,642	2/24/99	1:25p
FFTF005	ASCII	20,361	2/24/99	1:25p
FFTF006	ASCII	20,361	2/24/99	1:25p
FFTF029	ASCII	20,363	2/24/99	1:25p
hci2-1	ASCII	24,297	3/3/99	1:04p
hci2-2	ASCII	24,293	3/3/99	1:04p
hci2-3	ASCII	24,071	3/3/99	1:04p
hci2-4	ASCII	24,066	3/3/99	1:04p
hci2-5	ASCII	24,049	3/3/99	1:04p
hct101	ASCII	2,817	3/3/99	1:04p
hct102	ASCII	3,326	3/3/99	1:04p
hct103	ASCII	2,815	3/3/99	1:04p
hct104	ASCII	3,359	3/3/99	1:04p
hct105	ASCII	2,767	3/3/99	1:04p
hct106	ASCII	3,299	3/3/99	1:04p
hct107	ASCII	2,689	3/3/99	1:04p
hct108	ASCII	3,178	3/3/99	1:04p
hct109	ASCII	3,323	3/3/99	1:04p
hct110	ASCII	2,853	3/3/99	1:04p
hct111	ASCII	3,301	3/3/99	1:04p
hct112	ASCII	3,328	3/3/99	1:04p
hct113	ASCII	3,329	3/3/99	1:04p
hct114	ASCII	3,093	3/3/99	1:04p
hct115	ASCII	3,543	3/3/99	1:04p
hct116	ASCII	3,021	3/3/99	1:04p
hct117	ASCII	3,086	3/3/99	1:04p
hct118	ASCII	3,094	3/3/99	1:04p

Filename	File Type	File Size (bytes)	File Date and Time	
hct119	ASCII	3,086	3/3/99	1:04p
hct120	ASCII	2,201	3/3/99	1:04p
hct121	ASCII	2,286	3/3/99	1:04p
hct3-1	ASCII	7,816	2/24/99	1:25p
hct3-2	ASCII	7,998	2/24/99	1:25p
hct3-3	ASCII	8,315	2/24/99	1:25p
hct3-4	ASCII	8,705	2/24/99	1:25p
hct3-5	ASCII	9,043	2/24/99	1:25p
hct3-6	ASCII	8,307	2/24/99	1:25p
hct3-7	ASCII	8,625	2/24/99	1:25p
hct3-8	ASCII	8,587	2/24/99	1:25p
hct3-9	ASCII	8,716	2/24/99	1:25p
hct310	ASCII	8,872	2/24/99	1:25p
hct311	ASCII	8,934	2/24/99	1:25p
hct312	ASCII	8,777	2/24/99	1:25p
hct313	ASCII	10,366	2/24/99	1:25p
hct314	ASCII	8,653	2/24/99	1:25p
hct315	ASCII	9,544	2/24/99	1:25p
hct4-1	ASCII	7,196	2/24/99	3:33p
hct4-2	ASCII	6,224	2/24/99	1:25p
hct4-3	ASCII	6,727	2/24/99	1:25p
hct4-4	ASCII	7,337	2/24/99	3:33p
hct5-1	ASCII	4,337	2/24/99	1:25p
hct5-2	ASCII	5,197	2/24/99	1:25p
hct6-t1	ASCII	5,767	2/24/99	1:25p
hct6-t2	ASCII	6,077	2/24/99	1:25p
hct6-t3	ASCII	6,351	2/24/99	1:25p
hct7-1	ASCII	8,898	2/24/99	1:26p
hct7-2	ASCII	9,927	2/24/99	1:26p
hct7-3	ASCII	9,914	2/24/99	1:26p
hct7-4	ASCII	9,829	2/24/99	1:26p
hct7-5	ASCII	10,844	2/24/99	1:26p
hct7-6	ASCII	10,843	2/24/99	1:26p
hct8-1	ASCII	7,602	2/24/99	1:26p
hct8-2	ASCII	8,158	2/24/99	1:26p
HMF11	ASCII	989	3/3/99	1:04p
HMF12	ASCII	1,286	3/3/99	1:04p
HMF13	ASCII	1,131	3/3/99	1:04p
HMF14	ASCII	1,474	3/3/99	1:04p
HMF15	ASCII	1,327	3/3/99	1:04p
HMF18	ASCII	3,091	3/3/99	1:04p
HMF19	ASCII	2,391	3/3/99	1:04p
HMF20	ASCII	3,089	3/3/99	1:04p
HMF21	ASCII	3,048	3/3/99	1:04p

Filename	File Type	File Size (bytes)	File Date and Time	
HMF22	ASCII	3,002	3/3/99	1:04p
HMF24	ASCII	1,239	3/3/99	1:04p
HMF8	ASCII	1,693	3/3/99	1:04p
imf1-1	ASCII	6,674	2/24/99	1:26p
imf1-2	ASCII	5,218	2/24/99	1:26p
imf1-3	ASCII	8,194	2/24/99	1:26p
imf1-4	ASCII	6,219	2/24/99	1:26p
imf1-5	ASCII	4,527	2/24/99	1:26p
imf1-6	ASCII	4,179	2/24/99	1:26p
imf1-7	ASCII	5,040	2/24/99	1:26p
imf1-8	ASCII	5,025	2/24/99	1:26p
imf2-1	ASCII	477	2/24/99	1:26p
imf3-1	ASCII	3,035	2/24/99	1:26p
imf3-2	ASCII	406	2/24/99	1:26p
imf4-1	ASCII	2,114	2/24/99	1:26p
imf4-2	ASCII	711	2/24/99	1:26p
imf5-1	ASCII	2,766	2/24/99	1:26p
imf5-2	ASCII	1,237	2/24/99	1:26p
imf6-1	ASCII	2,533	2/24/99	1:26p
imf6-2	ASCII	1,079	2/24/99	1:26p
imf8-1	ASCII	2,869	2/24/99	1:26p
ist1-1	ASCII	5,355	2/24/99	1:26p
ist1-2	ASCII	5,354	2/24/99	1:26p
ist1-3	ASCII	5,354	2/24/99	1:26p
ist1-4	ASCII	5,356	2/24/99	1:26p
lst1-1	ASCII	962	2/24/99	1:26p
lst3-1	ASCII	578	2/24/99	1:26p
lst3-2	ASCII	581	2/24/99	1:26p
lst3-3	ASCII	545	2/24/99	1:26p
lst3-4	ASCII	581	2/24/99	1:26p
lst3-5	ASCII	580	2/24/99	1:26p
lst3-6	ASCII	543	2/24/99	1:26p
lst3-7	ASCII	579	2/24/99	1:26p
lst3-8	ASCII	578	2/24/99	1:26p
lst3-9	ASCII	543	2/24/99	1:26p
PMF20	ASCII	1,205	3/3/99	1:04p
PMF22	ASCII	1,442	3/3/99	1:04p
PMF23	ASCII	1,359	3/3/99	1:04p
PMF24	ASCII	1,663	3/3/99	1:04p
PMF25	ASCII	1,667	3/3/99	1:04p
PMF26	ASCII	1,771	3/3/99	1:04p
PMF27	ASCII	1,720	3/3/99	1:04p
PMF28	ASCII	1,635	3/3/99	1:04p
PMF29	ASCII	1,744	3/3/99	1:04p

Filename	File Type	File Size (bytes)	File Date and Time	
PMF30	ASCII	1,857	3/3/99	1:04p
PMF31	ASCII	1,676	3/3/99	1:04p
PMF32	ASCII	1,752	3/3/99	1:04p
smr1.i	ASCII	13,232	2/24/99	1:26p
smr11.i	ASCII	13,301	2/24/99	1:26p
smr12.i	ASCII	14,766	2/24/99	1:26p
smr5.i	ASCII	13,494	2/24/99	1:26p
smr8.i	ASCII	13,876	2/24/99	1:26p
smr9.i	ASCII	14,579	2/24/99	1:26p
spert1	ASCII	5,134	2/24/99	1:26p
spert10	ASCII	5,743	2/24/99	1:26p
spert11	ASCII	5,046	2/24/99	1:26p
spert12	ASCII	4,381	2/24/99	1:26p
spert13	ASCII	5,442	2/24/99	1:26p
spert14	ASCII	4,648	2/24/99	1:26p
spert15	ASCII	3,705	2/24/99	1:26p
spert16	ASCII	5,029	2/24/99	1:26p
spert17	ASCII	5,743	2/24/99	3:33p
spert18	ASCII	6,061	2/24/99	3:33p
spert19	ASCII	5,703	2/24/99	1:26p
spert2	ASCII	5,891	2/24/99	1:26p
spert20	ASCII	5,819	2/24/99	1:26p
spert21	ASCII	5,046	2/24/99	1:26p
spert22	ASCII	5,860	2/24/99	1:26p
spert23	ASCII	4,762	2/24/99	1:26p
spert3	ASCII	4,149	2/24/99	1:26p
spert4	ASCII	11,664	2/24/99	1:26p
spert5	ASCII	5,890	2/24/99	1:26p
spert6	ASCII	5,891	2/24/99	1:26p
spert7	ASCII	5,854	2/24/99	1:26p
spert8	ASCII	6,004	2/24/99	1:26p
spert9	ASCII	5,250	2/24/99	1:26p
SPHU9A	ASCII	3,907	2/24/99	3:33p
SPHU9B	ASCII	3,907	2/24/99	3:33p
SPHU9C	ASCII	3,907	2/24/99	3:33p
SPHU9D	ASCII	3,907	2/24/99	3:33p
SPHU9E	ASCII	3,907	2/24/99	3:33p
SPHU9F	ASCII	3,907	2/24/99	3:33p
SPHU9G	ASCII	3,907	2/24/99	3:33p
SPHU9H	ASCII	3,907	2/24/99	3:33p
SPHU9I	ASCII	3,907	2/24/99	3:33p
SPHU9J	ASCII	3,907	2/24/99	3:33p
SPHU9K	ASCII	3,907	2/24/99	3:33p
SPHU9L	ASCII	3,907	2/24/99	3:33p

Filename	File Type	File Size (bytes)	File Date and Time	
ssr27.i	ASCII	12,262	2/24/99	1:26p
ssr48.i	ASCII	12,281	2/24/99	1:26p
ssr53.i	ASCII	12,131	2/24/99	1:26p
ssr57.i	ASCII	14,109	2/24/99	1:26p
ssr66.i	ASCII	15,322	2/24/99	1:26p
ssr70.i	ASCII	19,955	2/24/99	1:26p
ssr74.i	ASCII	14,584	2/24/99	1:26p
ssr83.i	ASCII	18,832	2/24/99	1:26p
SUBC2P8H	ASCII	86,796	2/24/99	3:33p
SUBC3P1H	ASCII	86,796	2/24/99	3:33p
SUBC3P4H	ASCII	86,796	2/24/99	3:33p
tri17	ASCII	39,099	2/24/99	3:33p
tri18	ASCII	39,098	2/24/99	3:33p

This attachment contains the MCNP output files for the LCE benchmark calculations that were performed using the ENDF/B-V cross section library. The output files are contained on an attachment CD of this calculation file (the attachment CD has been moved to Reference 7.28). The information contained in this hard-copy representation of Attachment II is a listing of the various MCNP output files and their attributes. The CD containing Attachment II was written using the Hewlett Packard (HP) CD-Writer Plus model 7200e external CD-rewritable drive for personal computers.

Filename	File Type	File Size (bytes)	File Date	File Time
2P8H.O[1]	ASCII	369,271	3/2/99	2:31p
3P1H.O[2]	ASCII	369,314	3/2/99	2:31p
3P4H.O[3]	ASCII	369,308	3/2/99	2:31p
Case_1.O	ASCII	211,842	3/2/99	11:05a
Case_2.O	ASCII	215,834	3/2/99	11:05a
Case_3.O	ASCII	215,834	3/2/99	11:05a
Case_4.O	ASCII	215,834	3/2/99	11:05a
Case_5.O	ASCII	215,834	3/2/99	11:05a
Case_6.O	ASCII	215,941	3/2/99	11:05a
Case_7.O	ASCII	215,941	3/2/99	11:05a
Case_8.O	ASCII	216,019	3/2/99	11:05a
FF001.O	ASCII	146,068	3/2/99	11:05a
FF003R.O	ASCII	335,090	3/2/99	11:05a
FF004.O	ASCII	151,002	3/2/99	11:05a
FF005.O	ASCII	146,822	3/2/99	11:05a
FF006.O	ASCII	146,890	3/2/99	11:05a
FF029.O	ASCII	146,828	3/2/99	11:05a
hci2-1.O	ASCII	656,906	3/2/99	10:10a
hci2-2.O	ASCII	480,706	3/2/99	10:10a
hci2-3.O	ASCII	480,496	3/2/99	10:10a
hci2-4.O	ASCII	480,123	3/2/99	10:10a
hci2-5.O	ASCII	479,735	3/2/99	10:10a
hct101.O	ASCII	318,443	3/2/99	10:10a
hct102.O	ASCII	440,864	3/2/99	10:10a
hct103.O	ASCII	318,031	3/2/99	10:09a
hct104.O	ASCII	404,248	3/2/99	10:10a
hct105.O	ASCII	317,650	3/2/99	10:10a
hct106.O	ASCII	397,978	3/2/99	10:10a
hct107.O	ASCII	317,647	3/2/99	10:10a
hct108.O	ASCII	393,268	3/2/99	10:10a
hct109.O	ASCII	396,907	3/2/99	10:10a
hct110.O	ASCII	317,914	3/2/99	10:10a
hct111.O	ASCII	396,678	3/2/99	10:09a
hct112.O	ASCII	396,716	3/2/99	10:09a
hct113.O	ASCII	397,595	3/2/99	10:09a
hct114.O	ASCII	395,700	3/2/99	10:09a
hct115.O	ASCII	429,392	3/2/99	10:09a

Filename	File Type	File Size (bytes)	File Date	File Time
hct116.O	ASCII	318,924	3/2/99	10:09a
hct117.O	ASCII	319,418	3/2/99	10:09a
hct118.O	ASCII	319,319	3/2/99	10:09a
hct119.O	ASCII	319,513	3/2/99	10:09a
hct120.O	ASCII	380,830	3/2/99	10:09a
hct121.O	ASCII	390,407	3/2/99	10:09a
hct3-1.O	ASCII	348,616	3/2/99	11:05a
hct3-2.O	ASCII	346,875	3/2/99	11:05a
hct3-3.O	ASCII	347,255	3/2/99	11:05a
hct3-4.O	ASCII	347,313	3/2/99	11:05a
hct3-5.O	ASCII	347,885	3/2/99	11:05a
hct3-6.O	ASCII	347,352	3/2/99	11:05a
hct3-7.O	ASCII	347,728	3/2/99	11:05a
hct3-8.O	ASCII	383,566	3/2/99	11:05a
hct3-9.O	ASCII	418,728	3/2/99	11:05a
hct310.O	ASCII	348,263	3/2/99	11:05a
hct311.O	ASCII	348,167	3/2/99	11:05a
hct312.O	ASCII	348,207	3/2/99	11:05a
hct313.O	ASCII	349,975	3/2/99	11:05a
hct314.O	ASCII	432,490	3/2/99	11:05a
hct315.O	ASCII	348,932	3/2/99	11:05a
hct4-1O	ASCII	523,695	3/2/99	11:05a
hct4-2O	ASCII	521,069	3/2/99	11:05a
hct4-3O	ASCII	520,941	3/2/99	11:05a
hct4-4O	ASCII	523,187	3/2/99	11:05a
hct5-1.O	ASCII	520,691	3/3/99	7:53a
hct5-2.O	ASCII	701,201	3/3/99	7:53a
hct6-t1O	ASCII	434,807	3/2/99	11:05a
hct6-t2O	ASCII	429,791	3/2/99	11:05a
hct6-t3O	ASCII	429,974	3/2/99	11:05a
hct7-1O	ASCII	351,884	3/2/99	11:05a
hct7-2O	ASCII	350,550	3/2/99	11:05a
hct7-3O	ASCII	350,647	3/2/99	11:05a
hct7-4O	ASCII	356,623	3/2/99	11:05a
hct7-5O	ASCII	355,584	3/2/99	11:05a
hct7-6O	ASCII	355,485	3/2/99	11:05a
hct8-1O	ASCII	302,478	3/2/99	11:05a
hct8-2O	ASCII	302,962	3/2/99	11:05a
HMF11.O	ASCII	970,880	3/3/99	2:38p
HMF12.O	ASCII	967,678	3/3/99	2:38p
HMF13.O	ASCII	969,158	3/3/99	2:38p
HMF14.O	ASCII	970,972	3/3/99	2:37p
HMF15.O	ASCII	518,903	3/2/99	10:10a
HMF18.O	ASCII	352,167	3/2/99	10:10a

Filename	File Type	File Size (bytes)	File Date	File Time
HMF19.O	ASCII	348,947	3/2/99	10:10a
HMF20.O	ASCII	350,578	3/2/99	10:09a
HMF21.O	ASCII	352,712	3/2/99	10:10a
HMF22.O	ASCII	352,048	3/2/99	10:10a
HMF24.O	ASCII	519,964	3/3/99	2:37p
HMF8.O	ASCII	969,512	3/3/99	2:38p
imf1-1.O	ASCII	639,986	3/2/99	10:11a
imf1-2.O	ASCII	606,909	3/2/99	10:11a
imf1-3.O	ASCII	680,469	3/2/99	10:11a
imf1-4.O	ASCII	630,025	3/2/99	10:11a
imf1-5.O	ASCII	594,003	3/2/99	10:11a
imf1-6.O	ASCII	592,279	3/2/99	10:11a
imf1-7.O	ASCII	612,853	3/2/99	10:11a
imf1-8.O	ASCII	614,253	3/2/99	10:11a
imf2-1.O	ASCII	182,850	3/2/99	10:11a
imf3-1.O	ASCII	329,502	3/2/99	10:11a
imf3-2.O	ASCII	317,946	3/2/99	10:11a
imf4-1.O	ASCII	325,696	3/2/99	10:11a
imf4-2.O	ASCII	319,607	3/2/99	10:11a
imf5-1.O	ASCII	328,585	3/2/99	10:11a
imf5-2.O	ASCII	322,561	3/2/99	10:11a
imf6-1.O	ASCII	327,676	3/2/99	10:11a
imf6-2.O	ASCII	321,448	3/2/99	10:11a
imf8-1.O	ASCII	328,848	3/2/99	10:11a
ist1-1.O	ASCII	602,281	3/2/99	10:11a
ist1-2.O	ASCII	603,462	3/2/99	10:11a
ist1-3.O	ASCII	604,119	3/2/99	10:11a
ist1-4.O	ASCII	604,098	3/2/99	10:11a
lst1-1.O	ASCII	284,347	3/2/99	10:11a
lst3-1.O	ASCII	1,450,928	3/2/99	10:11a
lst3-2.O	ASCII	1,450,361	3/2/99	10:11a
lst3-3.O	ASCII	1,449,550	3/2/99	10:11a
lst3-4.O	ASCII	1,451,777	3/2/99	10:11a
lst3-5.O	ASCII	1,451,209	3/2/99	10:11a
lst3-6.O	ASCII	1,451,885	3/2/99	10:11a
lst3-7.O	ASCII	1,451,601	3/2/99	10:11a
lst3-8.O	ASCII	1,452,721	3/2/99	10:11a
lst3-9.O	ASCII	1,452,513	3/2/99	10:11a
PMF20.O	ASCII	963,052	3/2/99	10:10a
PMF22.O	ASCII	344,800	3/2/99	10:10a
PMF23.O	ASCII	343,421	3/2/99	10:10a
PMF24.O	ASCII	345,534	3/2/99	10:09a
PMF25.O	ASCII	344,952	3/2/99	10:10a
PMF26.O	ASCII	345,232	3/2/99	10:10a

Filename	File Type	File Size (bytes)	File Date	File Time
PMF27.O	ASCII	345,369	3/2/99	10:10a
PMF28.O	ASCII	345,051	3/2/99	10:10a
PMF29.O	ASCII	343,348	3/2/99	10:10a
PMF30.O	ASCII	346,002	3/2/99	10:10a
PMF31.O	ASCII	344,340	3/2/99	10:10a
PMF32.O	ASCII	344,995	3/2/99	10:09a
smr1.O	ASCII	389,173	3/2/99	11:05a
smr11.O	ASCII	389,190	3/2/99	11:05a
smr12.O	ASCII	393,918	3/2/99	11:05a
smr5.O	ASCII	390,004	3/2/99	11:05a
smr8.O	ASCII	390,669	3/2/99	11:05a
smr9.O	ASCII	395,474	3/2/99	11:05a
spert10O	ASCII	308,334	3/2/99	11:05a
spert11O	ASCII	293,283	3/2/99	11:05a
spert12O	ASCII	292,415	3/2/99	11:05a
spert13O	ASCII	307,600	3/2/99	11:05a
spert14O	ASCII	297,564	3/2/99	11:05a
spert15O	ASCII	310,363	3/2/99	11:05a
spert16O	ASCII	312,540	3/2/99	11:05a
spert17O	ASCII	295,399	3/2/99	11:05a
spert18O	ASCII	305,140	3/2/99	11:05a
spert19O	ASCII	292,203	3/2/99	11:05a
spert1O	ASCII	283,256	3/2/99	11:05a
spert20O	ASCII	302,312	3/2/99	11:05a
spert21O	ASCII	294,266	3/2/99	11:05a
spert22O	ASCII	309,060	3/2/99	11:05a
spert23O	ASCII	301,581	3/2/99	11:05a
spert2O	ASCII	291,519	3/2/99	11:05a
spert3O	ASCII	284,550	3/2/99	11:05a
spert4O	ASCII	318,824	3/2/99	11:05a
spert5O	ASCII	291,131	3/2/99	11:05a
spert6O	ASCII	291,131	3/2/99	11:05a
spert7O	ASCII	296,125	3/2/99	11:05a
spert8O	ASCII	305,167	3/2/99	11:05a
spert9O	ASCII	305,670	3/2/99	11:05a
SPHU9A.O	ASCII	63,074	2/24/99	3:45p
SPHU9B.O	ASCII	63,074	2/24/99	3:45p
SPHU9C.O	ASCII	63,031	2/24/99	3:45p
SPHU9D.O	ASCII	63,068	2/24/99	3:45p
SPHU9E.O	ASCII	63,095	2/24/99	3:45p
SPHU9F.O	ASCII	63,206	2/24/99	3:45p
SPHU9G.O	ASCII	63,074	2/24/99	3:45p
SPHU9H.O	ASCII	63,068	2/24/99	3:45p
SPHU9I.O	ASCII	63,031	2/24/99	3:45p

Filename	File Type	File Size (bytes)	File Date	File Time
SPHU9J.O	ASCII	63,111	2/24/99	3:45p
SPHU9K.O	ASCII	63,074	2/24/99	3:45p
SPHU9L.O	ASCII	63,111	2/24/99	3:45p
ssr27.O	ASCII	382,093	3/2/99	11:05a
ssr48.O	ASCII	380,597	3/2/99	11:05a
ssr53.O	ASCII	381,423	3/2/99	11:05a
ssr57.O	ASCII	384,495	3/2/99	11:05a
ssr66.O	ASCII	405,265	3/2/99	11:05a
ssr70.O	ASCII	414,022	3/2/99	11:05a
ssr74.O	ASCII	384,516	3/2/99	11:05a
ssr83.O	ASCII	366,766	3/2/99	11:05a
tri17.O	ASCII	923,097	3/2/99	11:05a
tri18.O	ASCII	922,999	3/2/99	11:05a

[1] Output file for SUBC2P8H
[2] Output file for SUBC3P1H
[3] Output file for SUBC3P4H

This attachment contains the MCNP input files for the LCE benchmark calculations that were performed using the ENDF/B-V cross section library. The input files are contained on an attachment CD of this calculation file (the attachment CD has been moved to Reference 7.28). The information contained in this hard-copy representation of Attachment III is a listing of the various MCNP input deck files and their attributes. The CD containing Attachment III was written using the Hewlett Packard (HP) CD-Writer Plus model 7200e external CD-rewritable drive for personal computers.

Filename	File Type	File Size (bytes)	File Date	File Time
Case_1	ASCII	3,928	8/19/98	8:33a
Case_2	ASCII	4,369	8/19/98	8:33a
Case_3	ASCII	4,365	1/26/99	9:40a
Case_4	ASCII	4,378	8/19/98	8:33a
Case_5	ASCII	4,362	8/19/98	8:33a
Case_6	ASCII	4,377	8/19/98	8:33a
Case_7	ASCII	4,370	8/19/98	8:33a
Case_8	ASCII	4,369	1/26/99	9:40a
FFTF001	ASCII	20,866	10/8/98	9:43a
FFTF003R	ASCII	22,755	10/8/98	9:58a
FFTF004	ASCII	22,969	10/8/98	9:43a
FFTF005	ASCII	21,681	10/8/98	9:43a
FFTF006	ASCII	21,681	10/8/98	9:43a
FFTF029	ASCII	21,685	10/8/98	9:43a
hci2-1	ASCII	24,722	10/8/98	9:34a
hci2-2	ASCII	24,689	10/8/98	9:34a
hci2-3	ASCII	24,504	10/8/98	9:34a
hci2-4	ASCII	24,496	10/8/98	9:34a
hci2-5	ASCII	24,438	10/8/98	9:34a
hct101	ASCII	3,338	10/8/98	9:35a
hct102	ASCII	3,832	10/8/98	9:35a
hct103	ASCII	3,333	10/8/98	9:35a
hct104	ASCII	3,856	10/8/98	9:35a
hct105	ASCII	3,286	10/8/98	9:35a
hct106	ASCII	3,805	10/8/98	9:35a
hct107	ASCII	3,208	10/8/98	9:35a
hct108	ASCII	3,682	10/8/98	9:35a
hct109	ASCII	3,828	10/8/98	9:35a
hct110	ASCII	3,288	10/8/98	9:35a
hct111	ASCII	3,807	10/8/98	9:35a
hct112	ASCII	3,833	10/8/98	9:35a
hct113	ASCII	3,834	10/8/98	9:35a
hct114	ASCII	3,599	10/8/98	9:35a
hct115	ASCII	4,079	10/8/98	9:35a
hct116	ASCII	3,841	10/8/98	9:35a
hct117	ASCII	3,948	10/8/98	9:35a
hct118	ASCII	3,950	10/8/98	9:35a

Filename	File Type	File Size (bytes)	File Date	File Time
hct119	ASCII	3,949	10/8/98	9:35a
hct120	ASCII	3,048	1/28/99	11:19a
hct121	ASCII	3,135	10/8/98	9:35a
hct3-1	ASCII	8,442	8/19/98	9:05a
hct3-2	ASCII	8,742	8/19/98	9:05a
hct3-3	ASCII	9,059	8/19/98	9:05a
hct3-4	ASCII	9,447	8/19/98	8:26a
hct3-5	ASCII	9,787	8/19/98	8:26a
hct3-6	ASCII	9,053	8/19/98	8:26a
hct3-7	ASCII	9,369	8/19/98	8:26a
hct3-8	ASCII	9,328	8/19/98	8:26a
hct3-9	ASCII	9,456	8/19/98	8:26a
hct310	ASCII	9,597	8/19/98	9:05a
hct311	ASCII	9,673	8/19/98	9:05a
hct312	ASCII	9,516	8/19/98	9:05a
hct313	ASCII	11,128	8/19/98	9:05a
hct314	ASCII	9,392	8/19/98	9:05a
hct315	ASCII	10,282	8/19/98	9:05a
hct4-1	ASCII	8,366	1/26/99	9:34a
hct4-2	ASCII	7,403	8/19/98	8:26a
hct4-3	ASCII	7,910	8/19/98	8:26a
hct4-4	ASCII	8,475	1/26/99	9:34a
hct5-1	ASCII	4,944	10/8/98	9:34a
hct5-2	ASCII	5,800	10/8/98	9:34a
hct6-t1	ASCII	6,369	8/20/98	1:10p
hct6-t2	ASCII	6,681	8/20/98	1:10p
hct6-t3	ASCII	6,953	8/20/98	1:10p
hct7-1	ASCII	9,743	10/8/98	9:34a
hct7-2	ASCII	10,771	10/8/98	9:34a
hct7-3	ASCII	10,759	10/8/98	9:34a
hct7-4	ASCII	10,671	10/8/98	9:34a
hct7-5	ASCII	11,686	10/8/98	9:34a
hct7-6	ASCII	11,688	10/8/98	9:34a
hct8-1	ASCII	8,247	8/20/98	1:10p
hct8-2	ASCII	8,803	8/20/98	1:10p
HMF11	ASCII	1,473	8/19/98	8:39a
HMF12	ASCII	1,891	8/19/98	8:39a
HMF13	ASCII	1,947	8/19/98	8:39a
HMF14	ASCII	2,079	8/19/98	8:39a
HMF15	ASCII	1,710	8/19/98	8:39a
HMF18	ASCII	4,268	8/19/98	8:39a
HMF19	ASCII	3,228	8/19/98	8:39a
HMF20	ASCII	4,161	8/19/98	8:39a
HMF21	ASCII	4,746	8/19/98	8:39a

Filename	File Type	File Size (bytes)	File Date	File Time
HMF22	ASCII	4,194	8/19/98	8:39a
HMF24	ASCII	1,993	8/19/98	8:39a
HMF8	ASCII	2,471	8/19/98	8:39a
imf1-1	ASCII	7,103	10/8/98	9:31a
imf1-2	ASCII	5,647	10/8/98	9:31a
imf1-3	ASCII	8,624	10/8/98	9:31a
imf1-4	ASCII	6,652	10/8/98	9:31a
imf1-5	ASCII	4,957	10/8/98	9:31a
imf1-6	ASCII	4,608	10/8/98	9:31a
imf1-7	ASCII	5,469	10/8/98	9:31a
imf1-8	ASCII	5,454	10/8/98	9:31a
imf2-1	ASCII	604	10/8/98	9:32a
imf3-1	ASCII	6,934	10/8/98	9:32a
imf3-2	ASCII	889	10/8/98	9:32a
imf4-1	ASCII	3,658	10/8/98	9:32a
imf4-2	ASCII	1,003	10/8/98	9:32a
imf5-1	ASCII	5,860	10/8/98	9:33a
imf5-2	ASCII	2,443	10/8/98	9:33a
imf6-1	ASCII	5,161	10/8/98	9:33a
imf6-2	ASCII	1,785	10/8/98	9:33a
imf8-1	ASCII	5,926	10/8/98	9:33a
PMF20	ASCII	1,665	8/19/98	8:39a
ist1-1	ASCII	5,784	10/8/98	9:33a
ist1-2	ASCII	5,783	10/8/98	9:33a
ist1-3	ASCII	5,784	10/8/98	9:33a
ist1-4	ASCII	5,785	10/8/98	9:33a
lst1-1	ASCII	1,365	10/8/98	9:35a
lst3-1	ASCII	1,031	10/8/98	9:35a
lst3-2	ASCII	1,034	10/8/98	9:35a
lst3-3	ASCII	998	10/8/98	9:35a
lst3-4	ASCII	1,034	10/8/98	9:35a
lst3-5	ASCII	1,033	10/8/98	9:35a
lst3-6	ASCII	996	10/8/98	9:35a
lst3-7	ASCII	1,032	10/8/98	9:35a
lst3-8	ASCII	1,031	10/8/98	9:35a
lst3-9	ASCII	996	10/8/98	9:35a
PMF22	ASCII	2,944	8/19/98	8:39a
PMF23	ASCII	2,621	8/19/98	8:39a
PMF24	ASCII	3,150	8/19/98	8:39a
PMF25	ASCII	3,545	8/19/98	8:39a
PMF26	ASCII	3,760	8/19/98	8:39a
PMF27	ASCII	2,983	8/19/98	8:39a
PMF28	ASCII	3,274	8/19/98	8:39a
PMF29	ASCII	2,362	8/19/98	8:39a

Filename	File Type	File Size (bytes)	File Date	File Time
PMF30	ASCII	2,466	8/19/98	8:39a
PMF31	ASCII	2,175	8/19/98	8:39a
PMF32	ASCII	2,630	8/19/98	8:39a
smr1.i	ASCII	14,062	9/8/98	8:03a
smr11.i	ASCII	14,133	9/10/98	4:47p
smr12.i	ASCII	15,598	9/8/98	8:03a
smr5.i	ASCII	14,326	9/8/98	8:03a
smr8.i	ASCII	14,708	9/8/98	8:03a
smr9.i	ASCII	15,409	9/8/98	8:03a
spert1	ASCII	5,134	8/24/98	10:17a
spert10	ASCII	5,743	8/24/98	10:17a
spert11	ASCII	5,046	8/24/98	10:17a
spert12	ASCII	4,381	8/24/98	10:17a
spert13	ASCII	5,442	8/24/98	10:17a
spert14	ASCII	4,648	8/24/98	10:17a
spert15	ASCII	3,705	8/24/98	10:17a
spert16	ASCII	5,029	8/24/98	10:17a
spert17	ASCII	5,800	1/26/99	10:07a
spert18	ASCII	6,078	1/26/99	10:08a
spert19	ASCII	5,703	8/24/98	10:17a
spert2	ASCII	5,891	8/24/98	10:17a
spert20	ASCII	5,819	8/24/98	10:17a
spert21	ASCII	5,046	8/24/98	10:17a
spert22	ASCII	5,860	8/24/98	10:17a
spert23	ASCII	4,762	8/24/98	10:17a
spert3	ASCII	4,149	8/24/98	10:17a
spert4	ASCII	11,664	8/24/98	10:17a
spert5	ASCII	5,890	8/24/98	10:17a
spert6	ASCII	5,891	8/24/98	10:17a
spert7	ASCII	5,854	8/24/98	10:17a
spert8	ASCII	6,004	8/24/98	10:17a
spert9	ASCII	5,250	8/24/98	10:17a
SPHU9A	ASCII	4,044	1/26/99	9:34a
SPHU9B	ASCII	4,044	1/26/99	9:34a
SPHU9C	ASCII	4,044	1/26/99	9:34a
SPHU9D	ASCII	4,044	1/26/99	9:34a
SPHU9E	ASCII	4,044	1/26/99	9:34a
SPHU9F	ASCII	4,044	1/26/99	9:34a
SPHU9G	ASCII	4,044	1/26/99	9:34a
SPHU9H	ASCII	4,044	1/26/99	9:34a
SPHU9I	ASCII	4,044	1/26/99	9:34a
SPHU9J	ASCII	4,044	1/26/99	9:34a
SPHU9K	ASCII	4,044	1/26/99	9:34a
SPHU9L	ASCII	4,044	1/26/99	9:34a

Filename	File Type	File Size (bytes)	File Date	File Time
ssr27.i	ASCII	13,094	9/8/98	8:03a
ssr48.i	ASCII	13,112	9/8/98	8:03a
ssr53.i	ASCII	12,961	9/8/98	8:03a
ssr57.i	ASCII	14,938	9/8/98	8:03a
ssr66.i	ASCII	16,151	9/8/98	8:03a
ssr70.i	ASCII	20,785	9/8/98	8:03a
ssr74.i	ASCII	15,414	9/8/98	8:03a
ssr83.i	ASCII	19,662	9/8/98	8:03a
SUBC2P8H	ASCII	87,006	1/26/99	1:32p
SUBC3P1H	ASCII	87,006	1/26/99	1:32p
SUBC3P4H	ASCII	87,006	1/26/99	1:32p
tri17	ASCII	39,390	1/26/99	9:34a
tri18	ASCII	39,389	1/26/99	9:34a

This attachment contains the MCNP output files for the LCE benchmark calculations that were performed using the ENDF/B-VI cross section library. The output files are contained on an attachment CD of this calculation file (the attachment CD has been moved to Reference 7.28). The information contained in this hard-copy representation of Attachment IV is a listing of the various MCNP output files and their attributes. The CD containing Attachment IV was written using the Hewlett Packard (HP) CD-Writer Plus model 7200e external CD-rewritable drive for personal computers.

Filename	File Type	File Size (bytes)	File Date	File Time
Case_1O	ASCII	218,046	8/19/98	12:00a
3P1H.O[1]	ASCII	370,077	1/28/99	9:28a
Case_2O	ASCII	222,201	8/19/98	12:00a
Case_4O	ASCII	222,279	8/19/98	12:00a
Case_5O	ASCII	222,094	8/19/98	12:00a
Case_6O	ASCII	222,201	8/19/98	12:00a
Case_7O	ASCII	222,279	8/19/98	12:00a
FFTF01.O	ASCII	152,143	10/8/98	10:08a
FFTF04.O	ASCII	156,962	10/8/98	10:08a
FFTF05.O	ASCII	152,827	10/8/98	10:08a
FFTF06.O	ASCII	152,827	10/8/98	10:08a
FFTF29.O	ASCII	169,170	10/8/98	10:08a
FFTF3R.O	ASCII	187,281	10/8/98	10:08a
hci2-1.O	ASCII	652,606	10/8/98	10:13a
hci2-2.O	ASCII	652,418	10/8/98	10:13a
hci2-3.O	ASCII	652,500	10/8/98	10:13a
hci2-4.O	ASCII	651,926	10/8/98	10:13a
hci2-5.O	ASCII	651,675	10/8/98	10:13a
hct101.O	ASCII	317,689	10/8/98	10:15a
hct102.O	ASCII	441,921	10/8/98	10:15a
hct103.O	ASCII	317,407	10/8/98	10:15a
hct104.O	ASCII	406,181	10/8/98	10:15a
hct105.O	ASCII	317,006	10/8/98	10:15a
hct106.O	ASCII	399,603	10/8/98	10:15a
hct107.O	ASCII	316,797	10/8/98	10:14a
hct108.O	ASCII	394,965	10/8/98	10:14a
hct109.O	ASCII	398,451	10/8/98	10:14a
hct110.O	ASCII	317,006	10/8/98	10:14a
hct111.O	ASCII	398,415	10/8/98	10:14a
hct112.O	ASCII	398,543	10/8/98	10:14a
hct113.O	ASCII	398,328	10/8/98	10:14a
hct114.O	ASCII	397,346	10/8/98	10:14a
hct115.O	ASCII	430,752	10/8/98	10:14a
hct116.O	ASCII	319,624	10/8/98	10:14a
hct117.O	ASCII	319,887	10/8/98	10:14a
hct118.O	ASCII	319,903	10/8/98	10:14a
hct119.O	ASCII	319,685	10/8/98	10:14a

Filename	File Type	File Size (bytes)	File Date	File Time
hct121.O	ASCII	394,622	1/25/99	10:49a
hct3-1O	ASCII	368,361	8/19/98	12:00a
hct3-2O	ASCII	347,800	8/19/98	12:00a
hct3-3O	ASCII	387,124	8/19/98	12:00a
hct3-4O	ASCII	348,958	8/19/98	12:00a
hct3-5O	ASCII	349,232	8/19/98	12:00a
hct3-6O	ASCII	349,013	8/19/98	12:00a
hct3-7O	ASCII	349,173	8/19/98	12:00a
hct3-8O	ASCII	364,407	8/19/98	12:00a
hct3-9O	ASCII	349,453	8/19/98	12:00a
hct310O	ASCII	348,799	8/19/98	12:00a
hct311O	ASCII	348,992	8/19/98	12:00a
hct312O	ASCII	349,022	8/19/98	12:00a
hct313O	ASCII	350,676	8/19/98	12:00a
hct314O	ASCII	348,829	8/19/98	12:00a
hct315O	ASCII	350,051	8/19/98	12:00a
hct4-2O	ASCII	521,648	8/19/98	12:00a
hct4-3O	ASCII	521,692	8/19/98	12:00a
hct5-1.O	ASCII	516,373	10/8/98	10:13a
hct5-2.O	ASCII	522,825	10/8/98	10:13a
hct6-t1O	ASCII	551,946	8/20/98	12:00a
hct6-t2O	ASCII	428,984	8/20/98	12:00a
hct6-t3O	ASCII	429,271	8/20/98	12:00a
hct7-1.O	ASCII	351,223	10/8/98	10:14a
hct7-2.O	ASCII	350,001	10/8/98	10:14a
hct7-3.O	ASCII	350,001	10/8/98	10:14a
hct7-4.O	ASCII	356,322	10/8/98	10:14a
hct7-5.O	ASCII	355,100	10/8/98	10:14a
hct7-6.O	ASCII	355,100	10/8/98	10:14a
hct8-1O	ASCII	303,170	8/20/98	12:00a
hct8-2O	ASCII	303,734	8/20/98	12:00a
HMF11O	ASCII	963,296	8/19/98	12:00a
HMF12O	ASCII	958,865	8/19/98	12:00a
HMF13O	ASCII	968,039	8/19/98	12:00a
HMF14O	ASCII	963,451	8/19/98	12:00a
HMF15O	ASCII	514,686	8/19/98	12:00a
HMF18O	ASCII	349,083	8/19/98	12:00a
HMF19O	ASCII	346,607	8/19/98	12:00a
HMF20O	ASCII	351,048	8/19/98	12:00a
HMF21O	ASCII	354,440	8/19/98	12:00a
HMF22O	ASCII	351,432	8/19/98	12:00a
HMF24O	ASCII	517,996	8/19/98	12:00a
HMF8O	ASCII	963,826	8/19/98	12:00a
imf1-1.O	ASCII	639,507	10/8/98	10:10a

Filename	File Type	File Size (bytes)	File Date	File Time
imf1-2.O	ASCII	605,677	10/8/98	10:10a
imf1-3.O	ASCII	679,443	10/8/98	10:10a
imf1-4.O	ASCII	629,548	10/8/98	10:10a
imf1-5.O	ASCII	593,514	10/8/98	10:10a
imf1-6.O	ASCII	590,345	10/8/98	10:10a
imf1-7.O	ASCII	611,239	10/8/98	10:10a
imf1-8.O	ASCII	613,579	10/8/98	10:10a
imf2-1.O	ASCII	181,630	10/8/98	10:10a
imf3-1.O	ASCII	337,764	10/8/98	10:11a
imf3-2.O	ASCII	317,118	10/8/98	10:11a
imf4-1.O	ASCII	327,076	10/8/98	10:11a
imf4-2.O	ASCII	317,286	10/8/98	10:11a
imf5-1.O	ASCII	335,153	10/8/98	10:11a
imf5-2.O	ASCII	324,047	10/8/98	10:11a
imf6-1.O	ASCII	332,670	10/8/98	10:11a
imf6-2.O	ASCII	321,140	10/8/98	10:11a
imf8-1.O	ASCII	335,938	10/8/98	10:12a
ist1-1.O	ASCII	615,493	10/8/98	10:12a
ist1-2.O	ASCII	616,964	10/8/98	10:12a
ist1-3.O	ASCII	617,487	10/8/98	10:12a
ist1-4.O	ASCII	617,457	10/8/98	10:12a
lst1-1.O	ASCII	283,287	10/8/98	10:30a
lst3-1.O	ASCII	544.215	10/8/98	10:31a
lst3-2.O	ASCII	544,649	10/8/98	10:31a
lst3-3.O	ASCII	543,615	10/8/98	10:31a
lst3-4.O	ASCII	544,651	10/8/98	10:31a
lst3-5.O	ASCII	545,034	10/8/98	10:30a
lst3-6.O	ASCII	543,998	10/8/98	10:30a
lst3-7.O	ASCII	545,034	10/8/98	10:30a
lst3-8.O	ASCII	544,061	10/8/98	10:30a
lst3-9.O	ASCII	543,280	10/8/98	10:30a
PMF20O	ASCII	954,868	8/19/98	12:00a
PMF22O	ASCII	344,673	8/19/98	12:00a
PMF23O	ASCII	345,329	8/19/98	12:00a
PMF24O	ASCII	346,865	8/19/98	12:00a
PMF25O	ASCII	348,600	8/19/98	12:00a
PMF26O	ASCII	349,495	8/19/98	12:00a
PMF27O	ASCII	347,042	8/19/98	12:00a
PMF28O	ASCII	346,824	8/19/98	12:00a
PMF29O	ASCII	343,935	8/19/98	12:00a
PMF30O	ASCII	342,851	8/19/98	12:00a
PMF31O	ASCII	341,911	8/19/98	12:00a
PMF32O	ASCII	345,813	8/19/98	12:00a
smr1.O	ASCII	386,969	9/8/98	8:03a

Filename	File Type	File Size (bytes)	File Date	File Time
smr11.O	ASCII	387,941	9/11/98	10:39a
smr12.O	ASCII	392,628	9/8/98	8:03a
smr5.O	ASCII	388,977	9/8/98	8:03a
smr8.O	ASCII	389,635	9/8/98	8:03a
smr9.O	ASCII	394,279	9/8/98	8:03a
spert10O	ASCII	305,414	8/25/98	12:00a
spert11O	ASCII	290,475	8/25/98	12:00a
spert12O	ASCII	289,664	8/25/98	12:00a
spert13O	ASCII	304,600	8/25/98	12:00a
spert14O	ASCII	294,678	8/25/98	12:00a
spert15O	ASCII	307,911	8/25/98	12:00a
spert16O	ASCII	309,506	8/25/98	12:00a
spert17O	ASCII	294,987	1/28/99	9:28a
spert18O	ASCII	304,798	1/28/99	9:28a
spert19O	ASCII	289,809	8/25/98	12:00a
spert1O	ASCII	280,603	8/24/98	12:00a
spert20O	ASCII	299,252	8/25/98	12:00a
spert21O	ASCII	291,342	8/25/98	12:00a
spert22O	ASCII	305,972	8/25/98	12:00a
spert23O	ASCII	299,058	8/25/98	12:00a
spert2O	ASCII	288,853	8/24/98	12:00a
spert3O	ASCII	281,763	8/24/98	12:00a
spert4O	ASCII	316,014	8/24/98	12:00a
spert5O	ASCII	288,837	8/24/98	12:00a
spert6O	ASCII	288,541	8/24/98	12:00a
spert7O	ASCII	293,458	8/24/98	12:00a
spert8O	ASCII	302,373	8/24/98	12:00a
spert9O	ASCII	302,688	8/24/98	12:00a
ssr27.O	ASCII	381,202	9/8/98	8:03a
ssr48.O	ASCII	379,911	9/8/98	8:03a
ssr53.O	ASCII	380,534	9/8/98	8:03a
ssr57.O	ASCII	383,688	9/8/98	8:03a
ssr66.O	ASCII	405,026	9/8/98	8:03a
ssr70.O	ASCII	412,452	9/8/98	8:03a
ssr74.O	ASCII	383,478	9/8/98	8:03a
ssr83.O	ASCII	367,145	9/8/98	8:03a
hct120.O	ASCII	388,980	1/28/99	1:10p
3P4H.O[2]	ASCII	370,166	1/28/99	9:28a
Case_3.O	ASCII	224,340	1/28/99	9:28a
Case_8.O	ASCII	224,262	1/28/99	9:28a
2P8H.O[3]	ASCII	370,246	1/28/99	9:28a
hct4-1.O	ASCII	528,612	1/28/99	9:28a
hct4-4.O	ASCII	528,275	1/28/99	9:28a
SPHU9A.O	ASCII	63,068	1/28/99	9:28a

Filename	File Type	File Size (bytes)	File Date	File Time
SPHU9B.O	ASCII	63,031	1/28/99	9:28a
SPHU9C.O	ASCII	63,074	1/28/99	9:28a
SPHU9D.O	ASCII	63,111	1/28/99	9:28a
SPHU9E.O	ASCII	62,595	1/28/99	9:28a
SPHU9F.O	ASCII	63,111	1/28/99	9:28a
SPHU9G.O	ASCII	63,031	1/28/99	9:28a
SPHU9H.O	ASCII	63,031	1/28/99	9:28a
SPHU9I.O	ASCII	63,074	1/28/99	9:28a
SPHU9J.O	ASCII	63,111	1/28/99	9:28a
SPHU9K.O	ASCII	63,074	1/28/99	9:28a
SPHU9L.O	ASCII	63,074	1/28/99	9:28a
tri17.O	ASCII	1,026,778	1/28/99	9:28a
tri18.O	ASCII	1,026,973	1/28/99	9:28a

[1] Output file for SUBC3P1H
[2] Output file for SUBC3P4H
[3] Output file for SUBC2P8H

This attachment contains the MCNP input files for the LCE benchmark calculations that were performed using the WPO Selected cross section library. The input files are contained on an attachment CD of this calculation file (the attachment CD has been moved to Reference 7.28). The information contained in this hard-copy representation of Attachment V is a listing of the various MCNP input files and their attributes. The CD containing Attachment V was written using the Hewlett Packard (HP) CD-Writer Plus model 7200e external CD-rewritable drive for personal computers.

Filename	File Type	File Size (Bytes)	File Date	File Time
Case_1	ASCII	3,512	8/12/98	3:32p
Case_2	ASCII	3,953	8/12/98	3:32p
Case_3	ASCII	4,364	1/26/99	10:10a
Case_4	ASCII	3,964	8/12/98	3:32p
Case_5	ASCII	3,946	8/12/98	3:32p
Case_6	ASCII	3,963	8/12/98	3:32p
Case_7	ASCII	3,955	8/12/98	3:32p
Case_8	ASCII	4,368	1/26/99	10:10a
FFTF001	ASCII	20,844	10/8/98	9:42a
FFTF003R	ASCII	22,733	10/8/98	9:42a
FFTF004	ASCII	22,947	10/8/98	9:42a
FFTF005	ASCII	21,659	10/8/98	9:42a
FFTF006	ASCII	21,659	10/8/98	9:42a
FFTF029	ASCII	21,663	10/8/98	9:51a
hci2-1	ASCII	24,732	10/8/98	1:11p
hci2-2	ASCII	24,741	10/8/98	1:11p
hci2-3	ASCII	24,514	10/8/98	1:11p
hci2-4	ASCII	24,506	10/8/98	1:10p
hci2-5	ASCII	24,498	10/8/98	1:10p
hct101	ASCII	3,334	10/8/98	1:11p
hct102	ASCII	3,830	10/8/98	1:11p
hct103	ASCII	3,331	10/8/98	1:11p
hct104	ASCII	3,854	10/8/98	1:11p
hct105	ASCII	3,284	10/8/98	1:11p
hct106	ASCII	3,803	10/8/98	1:11p
hct107	ASCII	3,206	10/8/98	1:11p
hct108	ASCII	3,680	10/8/98	1:11p
hct109	ASCII	3,826	10/8/98	1:11p
hct110	ASCII	3,286	10/8/98	1:11p
hct111	ASCII	3,805	10/8/98	1:11p
hct112	ASCII	3,831	10/8/98	1:11p
hct113	ASCII	3,832	10/8/98	1:11p
hct114	ASCII	3,597	10/8/98	1:11p
hct115	ASCII	4,077	10/8/98	1:11p
hct116	ASCII	3,866	10/8/98	1:11p
hct117	ASCII	3,946	10/8/98	1:11p
hct118	ASCII	3,930	10/8/98	1:11p

Filename	File Type	File Size (Bytes)	File Date	File Time
hct119	ASCII	3,929	10/8/98	1:11p
hct120	ASCII	3,045	1/28/99	11:12a
hct121	ASCII	3,132	10/8/98	1:11p
hct3-1	ASCII	8,427	8/12/98	3:19p
hct3-2	ASCII	8,727	8/12/98	3:19p
hct3-3	ASCII	9,044	8/12/98	3:19p
hct3-4	ASCII	9,432	8/3/98	8:37a
hct3-5	ASCII	9,772	8/3/98	8:37a
hct3-6	ASCII	9,038	8/3/98	8:37a
hct3-7	ASCII	9,354	8/3/98	8:37a
hct3-8	ASCII	9,313	8/3/98	8:40a
hct3-9	ASCII	9,441	8/3/98	8:41a
hct310	ASCII	9,582	8/12/98	3:19p
hct311	ASCII	9,658	8/12/98	3:19p
hct312	ASCII	9,501	8/12/98	3:19p
hct313	ASCII	11,113	8/12/98	3:19p
hct314	ASCII	9,377	8/12/98	3:19p
hct315	ASCII	10,267	8/12/98	3:19p
hct4-1	ASCII	8,352	1/26/99	10:10a
hct4-2	ASCII	7,372	8/3/98	8:42a
hct4-3	ASCII	7,870	8/3/98	8:42a
hct4-4	ASCII	8,468	1/26/99	10:10a
hct5-1	ASCII	4,941	10/8/98	1:11p
hct5-2	ASCII	5,797	10/8/98	1:11p
hct6-t1	ASCII	6,354	8/12/98	3:40p
hct6-t2	ASCII	6,666	8/12/98	3:40p
hct6-t3	ASCII	6,938	8/12/98	3:40p
hct7-1	ASCII	9,737	10/8/98	1:11p
hct7-2	ASCII	10,765	10/8/98	1:11p
hct7-3	ASCII	10,753	10/8/98	1:11p
hct7-4	ASCII	10,665	10/8/98	1:11p
hct7-5	ASCII	11,680	10/8/98	1:11p
hct7-6	ASCII	11,682	10/8/98	1:11p
hct8-1	ASCII	8,227	8/12/98	3:40p
hct8-2	ASCII	8,783	8/12/98	3:40p
HMF11	ASCII	1,472	8/12/98	3:18p
HMF12	ASCII	1,890	8/12/98	3:19p
HMF13	ASCII	1,947	8/12/98	3:19p
HMF14	ASCII	2,079	8/12/98	3:19p
HMF15	ASCII	1,702	8/12/98	3:19p
HMF18	ASCII	4,218	8/12/98	3:19p
HMF19	ASCII	3,192	8/12/98	3:19p
HMF20	ASCII	4,086	8/12/98	3:19p
HMF21	ASCII	4,704	8/12/98	3:19p

Filename	File Type	File Size (Bytes)	File Date	File Time
HMF22	ASCII	4,148	8/12/98	3:19p
HMF24	ASCII	2,001	8/12/98	3:19p
HMF8	ASCII	2,470	8/12/98	3:19p
imf1-1	ASCII	7,103	10/8/98	1:09p
imf1-2	ASCII	5,647	10/8/98	1:09p
imf1-3	ASCII	8,624	10/8/98	1:09p
imf1-4	ASCII	6,652	10/8/98	1:09p
imf1-5	ASCII	4,957	10/8/98	1:09p
imf1-6	ASCII	4,608	10/8/98	1:09p
imf1-7	ASCII	5,469	10/8/98	1:09p
imf1-8	ASCII	5,454	10/8/98	1:09p
imf2-1	ASCII	604	10/8/98	1:09p
imf3-1	ASCII	6,924	10/8/98	1:09p
imf3-2	ASCII	888	10/8/98	1:09p
imf4-1	ASCII	3,624	10/8/98	1:09p
imf4-2	ASCII	1,001	10/8/98	1:09p
imf5-1	ASCII	5,852	10/8/98	1:10p
imf5-2	ASCII	2,440	10/8/98	1:10p
imf6-1	ASCII	5,155	10/8/98	1:10p
imf6-2	ASCII	1,784	10/8/98	1:10p
imf8-1	ASCII	5,916	10/8/98	1:10p
ist1-1	ASCII	5,778	10/8/98	1:10p
ist1-2	ASCII	5,777	10/8/98	1:10p
ist1-3	ASCII	5,778	10/8/98	1:10p
ist1-4	ASCII	5,779	10/8/98	1:10p
lss3-1	ASCII	1,029	10/8/98	1:12p
lss3-2	ASCII	1,032	10/8/98	1:12p
lss3-3	ASCII	996	10/8/98	1:12p
lss3-4	ASCII	1,032	10/8/98	1:12p
lss3-5	ASCII	1,031	10/8/98	1:12p
lss3-6	ASCII	994	10/8/98	1:12p
lss3-7	ASCII	1,030	10/8/98	1:12p
lss3-8	ASCII	1,029	10/8/98	1:12p
lss3-9	ASCII	994	10/8/98	1:12p
lst1-1	ASCII	1,364	10/8/98	1:12p
PMF20	ASCII	1,655	8/12/98	3:19p
PMF22	ASCII	2,926	8/12/98	3:19p
PMF23	ASCII	2,605	8/12/98	3:18p
PMF24	ASCII	3,129	8/12/98	3:18p
PMF25	ASCII	3,526	8/12/98	3:18p
PMF26	ASCII	3,743	8/12/98	3:18p
PMF27	ASCII	2,959	8/12/98	3:18p
PMF28	ASCII	3,253	8/12/98	3:18p
PMF29	ASCII	2,327	8/12/98	3:18p

Filename	File Type	File Size (Bytes)	File Date	File Time
PMF30	ASCII	2,430	8/12/98	3:18p
PMF31	ASCII	2,144	8/12/98	3:18p
PMF32	ASCII	2,601	8/12/98	3:18p
smr1.i	ASCII	14,056	9/8/98	8:11a
smr11.i	ASCII	14,127	9/11/98	10:43a
smr12.i	ASCII	15,592	9/8/98	8:11a
smr5.i	ASCII	14,320	9/8/98	8:11a
smr8.i	ASCII	14,702	9/8/98	8:11a
smr9.i	ASCII	15,403	9/8/98	8:11a
SPHU9A	ASCII	4,044	1/26/99	10:10a
SPHU9B	ASCII	4,044	1/26/99	10:10a
SPHU9C	ASCII	4,044	1/26/99	10:10a
SPHU9D	ASCII	4,044	1/26/99	10:10a
SPHU9E	ASCII	4,044	1/26/99	10:10a
SPHU9F	ASCII	4,044	1/26/99	10:10a
SPHU9G	ASCII	4,044	1/26/99	10:10a
SPHU9H	ASCII	4,044	1/26/99	10:10a
SPHU9I	ASCII	4,044	1/26/99	10:10a
SPHU9J	ASCII	4,044	1/26/99	10:10a
SPHU9K	ASCII	4,044	1/26/99	10:10a
SPHU9L	ASCII	4,044	1/26/99	10:10a
ssr27.i	ASCII	13,088	9/8/98	8:11a
ssr48.i	ASCII	13,106	9/8/98	8:11a
ssr53.i	ASCII	12,955	9/8/98	8:11a
ssr57.i	ASCII	14,932	9/8/98	8:11a
ssr66.i	ASCII	16,145	9/8/98	8:11a
ssr70.i	ASCII	20,779	9/8/98	8:11a
ssr74.i	ASCII	15,408	9/8/98	8:11a
ssr83.i	ASCII	19,656	9/8/98	8:11a
SUBC2P8H	ASCII	86,986	1/26/99	1:32p
SUBC3P1H	ASCII	86,986	1/26/99	1:32p
SUBC3P4H	ASCII	86,986	1/26/99	1:32p
tri17	ASCII	39,388	1/26/99	10:10a
tri18	ASCII	39,387	1/26/99	10:10a
spert20	ASCII	5,819	10/14/98	3:07p
spert21	ASCII	5,046	10/14/98	3:07p
spert22	ASCII	5,860	10/14/98	3:07p
spert23	ASCII	4,762	10/14/98	3:07p

This attachment contains the MCNP output files for the LCE benchmark calculations that were performed using the WPO Selected cross section library. The output files are contained on an attachment CD of this calculation file (the attachment CD has been moved to Reference 7.28). The information contained in this hard-copy representation of Attachment VI is a listing of the various MCNP output files and their attributes. The CD containing Attachment VI was written using the Hewlett Packard (HP) CD-Writer Plus model 7200e external CD-rewritable drive for personal computers.

Filename	File Type	File Size (bytes)	File Date	File Time
Case_1O	ASCII	216,780	8/12/98	12:00a
3P1H.O[1]	ASCII	370,470	1/28/99	9:29a
Case_2O	ASCII	221,064	8/12/98	12:00a
Case_4O	ASCII	220,879	8/12/98	12:00a
Case_5O	ASCII	221,064	8/12/98	12:00a
Case_6O	ASCII	220,879	8/12/98	12:00a
Case_7O	ASCII	220,879	8/12/98	12:00a
FFTF01.O	ASCII	154,150	10/8/98	1:01p
FFTF04.O	ASCII	159,090	10/8/98	1:01p
FFTF05.O	ASCII	154,842	10/8/98	1:01p
FFTF06.O	ASCII	154,848	10/8/98	1:01p
FFTF29.O	ASCII	171,409	10/8/98	1:01p
FFTF3R.O	ASCII	154,916	10/8/98	1:01p
hci2-1.O	ASCII	660,161	10/8/98	1:24p
hci2-2.O	ASCII	660,168	10/8/98	1:24p
hci2-3.O	ASCII	659,524	10/8/98	1:23p
hci2-4.O	ASCII	659,150	10/8/98	1:23p
hci2-5.O	ASCII	659,286	10/8/98	1:23p
hct101.O	ASCII	320,827	10/8/98	1:07p
hct102.O	ASCII	447,027	10/8/98	1:07p
hct103.O	ASCII	320,641	10/8/98	1:07p
hct104.O	ASCII	410,637	10/8/98	1:07p
hct105.O	ASCII	320,435	10/8/98	1:07p
hct106.O	ASCII	404,367	10/8/98	1:07p
hct107.O	ASCII	320,435	10/8/98	1:07p
hct108.O	ASCII	399,565	10/8/98	1:07p
hct109.O	ASCII	403,324	10/8/98	1:07p
hct110.O	ASCII	320,034	10/8/98	1:07p
hct111.O	ASCII	402,876	10/8/98	1:07p
hct112.O	ASCII	402,780	10/8/98	1:07p
hct113.O	ASCII	403,560	10/8/98	1:07p
hct114.O	ASCII	401,990	10/8/98	1:07p
hct115.O	ASCII	435,456	10/8/98	1:07p
hct116.O	ASCII	322,777	10/8/98	1:07p
hct117.O	ASCII	322,981	10/8/98	1:07p
hct118.O	ASCII	322,981	10/8/98	1:07p

Filename	File Type	File Size (bytes)	File Date	File Time
hct119.O	ASCII	323,175	10/8/98	1:07p
hct121.O	ASCII	399,547	1/25/99	10:50a
hct3-1O	ASCII	352,216	8/12/98	12:00a
hct3-2O	ASCII	352,693	8/12/98	12:00a
hct3-3O	ASCII	352,656	8/12/98	12:00a
hct3-4O	ASCII	352,813	8/3/98	12:00a
hct3-5O	ASCII	384,310	8/3/98	12:00a
hct3-6O	ASCII	352,559	8/3/98	12:00a
hct3-7O	ASCII	353,034	8/3/98	12:00a
hct3-8O	ASCII	353,230	8/3/98	12:00a
hct3-9O	ASCII	353,098	8/3/98	12:00a
hct310O	ASCII	353,383	8/12/98	12:00a
hct311O	ASCII	353,381	8/12/98	12:00a
hct312O	ASCII	353,511	8/12/98	12:00a
hct313O	ASCII	355,380	8/12/98	12:00a
hct314O	ASCII	353,418	8/12/98	12:00a
hct315O	ASCII	354,236	8/12/98	12:00a
hct4-2O	ASCII	526,976	8/3/98	12:00a
hct4-3O	ASCII	526,724	8/3/98	12:00a
hct5-1.O	ASCII	522,162	10/8/98	1:06p
hct5-2.O	ASCII	527,643	10/8/98	1:06p
hct6-t1O	ASCII	439,104	8/12/98	12:00a
hct6-t2O	ASCII	433,550	8/12/98	12:00a
hct6-t3O	ASCII	434,059	8/12/98	12:00a
hct7-1.O	ASCII	355,303	10/8/98	1:07p
hct7-2.O	ASCII	354,068	10/8/98	1:07p
hct7-3.O	ASCII	354,068	10/8/98	1:07p
hct7-4.O	ASCII	360,141	10/8/98	1:06p
hct7-5.O	ASCII	359,224	10/8/98	1:06p
hct7-6.O	ASCII	359,323	10/8/98	1:06p
hct8-1O	ASCII	306,440	8/12/98	12:00a
hct8-2O	ASCII	307,010	8/12/98	12:00a
HMF11O	ASCII	973,753	8/12/98	12:00a
HMF12O	ASCII	969,290	8/12/98	12:00a
HMF13O	ASCII	973,058	8/12/98	12:00a
HMF14O	ASCII	979,656	8/12/98	12:00a
HMF15O	ASCII	520,332	8/12/98	12:00a
HMF18O	ASCII	355,710	8/12/98	12:00a
HMF19O	ASCII	351,639	8/12/98	12:00a
HMF20O	ASCII	355,191	8/12/98	12:00a
HMF21O	ASCII	358,619	8/12/98	12:00a
HMF22O	ASCII	355,572	8/12/98	12:00a
HMF24O	ASCII	523,968	8/12/98	12:00a
HMF8O	ASCII	974,293	8/12/98	12:00a

Filename	File Type	File Size (bytes)	File Date	File Time
imf1-1.O	ASCII	646,532	10/8/98	1:02p
imf1-2.O	ASCII	613,556	10/8/98	1:02p
imf1-3.O	ASCII	687,015	10/8/98	1:02p
imf1-4.O	ASCII	636,745	10/8/98	1:02p
imf1-5.O	ASCII	600,105	10/8/98	1:02p
imf1-6.O	ASCII	598,374	10/8/98	1:02p
imf1-7.O	ASCII	619,161	10/8/98	1:02p
imf1-8.O	ASCII	620,254	10/8/98	1:02p
imf2-1.O	ASCII	182,850	10/8/98	1:03p
imf3-1.O	ASCII	341,814	10/8/98	1:03p
imf3-2.O	ASCII	320,855	10/8/98	1:03p
imf4-1.O	ASCII	330,465	10/8/98	1:03p
imf4-2.O	ASCII	320,344	10/8/98	1:03p
imf5-1.O	ASCII	339,186	10/8/98	1:04p
imf5-2.O	ASCII	327,921	10/8/98	1:04p
imf6-1.O	ASCII	336,469	10/8/98	1:05p
imf6-2.O	ASCII	325,109	10/8/98	1:05p
imf8-1.O	ASCII	339,870	10/8/98	1:05p
ist1-1.O	ASCII	620,488	10/8/98	1:05p
ist1-2.O	ASCII	621,463	10/8/98	1:05p
ist1-3.O	ASCII	621,760	10/8/98	1:05p
ist1-4.O	ASCII	621,760	10/8/98	1:05p
lss3-1.O	ASCII	550,375	10/8/98	1:08p
lss3-2.O	ASCII	550,468	10/8/98	1:08p
lss3-3.O	ASCII	549,423	10/8/98	1:08p
lss3-4.O	ASCII	550,889	10/8/98	1:08p
lss3-5.O	ASCII	550,788	10/8/98	1:08p
lss3-6.O	ASCII	550,057	10/8/98	1:08p
lss3-7.O	ASCII	551,106	10/8/98	1:08p
lss3-8.O	ASCII	551,011	10/8/98	1:08p
lss3-9.O	ASCII	550,057	10/8/98	1:08p
lst1-1.O	ASCII	286,731	10/8/98	1:08p
PMF20O	ASCII	965,183	8/12/98	12:00a
PMF22O	ASCII	348,380	8/12/98	12:00a
PMF23O	ASCII	348,929	8/12/98	12:00a
PMF24O	ASCII	350,808	8/12/98	12:00a
PMF25O	ASCII	351,403	8/12/98	12:00a
PMF26O	ASCII	353,447	8/12/98	12:00a
PMF27O	ASCII	350,753	8/12/98	12:00a
PMF28O	ASCII	352,085	8/12/98	12:00a
PMF29O	ASCII	346,589	8/12/98	12:00a
PMF30O	ASCII	348,015	8/12/98	12:00a
PMF31O	ASCII	347,065	8/12/98	12:00a
PMF32O	ASCII	348,928	8/12/98	12:00a

Filename	File Type	File Size (bytes)	File Date	File Time
smr1.O	ASCII	392,696	9/8/98	8:11a
smr11.O	ASCII	392,706	9/11/98	10:43a
smr12.O	ASCII	398,377	9/8/98	8:11a
smr5.O	ASCII	392,476	9/8/98	8:11a
smr8.O	ASCII	394,200	9/8/98	8:11a
smr9.O	ASCII	398,874	9/8/98	8:11a
spert20O	ASCII	302,630	10/15/98	12:56p
spert21O	ASCII	294,584	10/15/98	12:56p
spert22O	ASCII	309,378	10/15/98	12:56p
spert23O	ASCII	302,535	10/15/98	12:56p
ssr27.O	ASCII	384,333	9/8/98	8:11a
ssr48.O	ASCII	384,224	9/8/98	8:11a
ssr53.O	ASCII	384,939	9/8/98	8:11a
ssr57.O	ASCII	388,127	9/8/98	8:11a
ssr66.O	ASCII	409,798	9/8/98	8:11a
ssr70.O	ASCII	415,276	9/8/98	8:11a
ssr74.O	ASCII	387,931	9/8/98	8:11a
ssr83.O	ASCII	370,316	9/8/98	8:11a
3P4H.O[2]	ASCII	370,433	1/28/99	9:29a
Case_3.O	ASCII	224,834	1/28/99	9:29a
Case_8.O	ASCII	224,727	1/28/99	9:29a
hct120.O	ASCII	389,334	1/28/99	1:11p
hct4-1.O	ASCII	528,741	1/28/99	9:30a
hct4-4.O	ASCII	528,495	1/28/99	9:30a
2P8H.O[3]	ASCII	370,513	1/28/99	9:29a
SPHU9A.O	ASCII	63,074	1/28/99	9:29a
SPHU9B.O	ASCII	63,074	1/28/99	9:29a
SPHU9C.O	ASCII	63,031	1/28/99	9:29a
SPHU9D.O	ASCII	63,068	1/28/99	9:29a
SPHU9E.O	ASCII	63,095	1/28/99	9:29a
SPHU9F.O	ASCII	63,206	1/28/99	9:29a
SPHU9G.O	ASCII	63,074	1/28/99	9:29a
SPHU9H.O	ASCII	63,068	1/28/99	9:29a
SPHU9I.O	ASCII	63,031	1/28/99	9:29a
SPHU9J.O	ASCII	63,111	1/28/99	9:29a
SPHU9K.O	ASCII	63,074	1/28/99	9:29a
SPHU9L.O	ASCII	63,111	1/28/99	9:29a
tri17.O	ASCII	1,027,111	1/28/99	9:30a
tri18.O	ASCII	1,027,306	1/28/99	9:30a

[1] Output file for SUBC3P1H
[2] Output file for SUBC3P4H
[3] Output file for SUBC2P8H

This attachment contains the plots where k_{eff} is trended against AENCF and H/X using regression analysis for the LCE benchmark calculations. The plots contained in Attachment VII were generated with the Excel 97 software routine. The information documented in Sections 5 and 6 is sufficient to provide an independent repetition of the software routine to duplicate the plots contained in Attachment VII.

Figure VII-1. Plot of keff and the Regression of keff for PMF Systems Using ENDF/B-V Cross Section Libraries

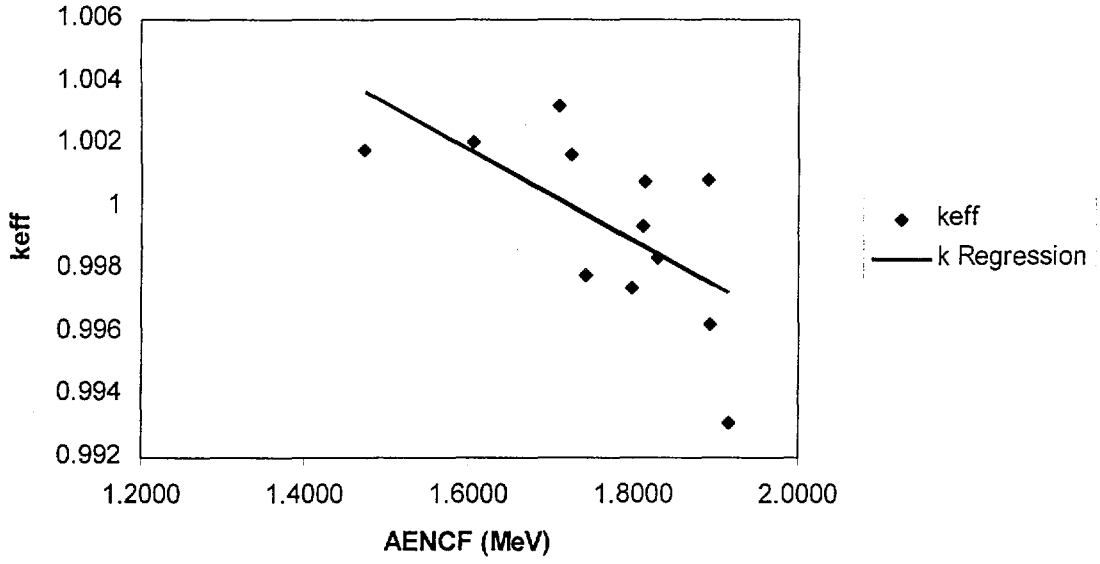

Figure VII-2. Plot of keff and the Regression of keff for PMF Systems Using ENDF/B-VI Cross Section Libraries

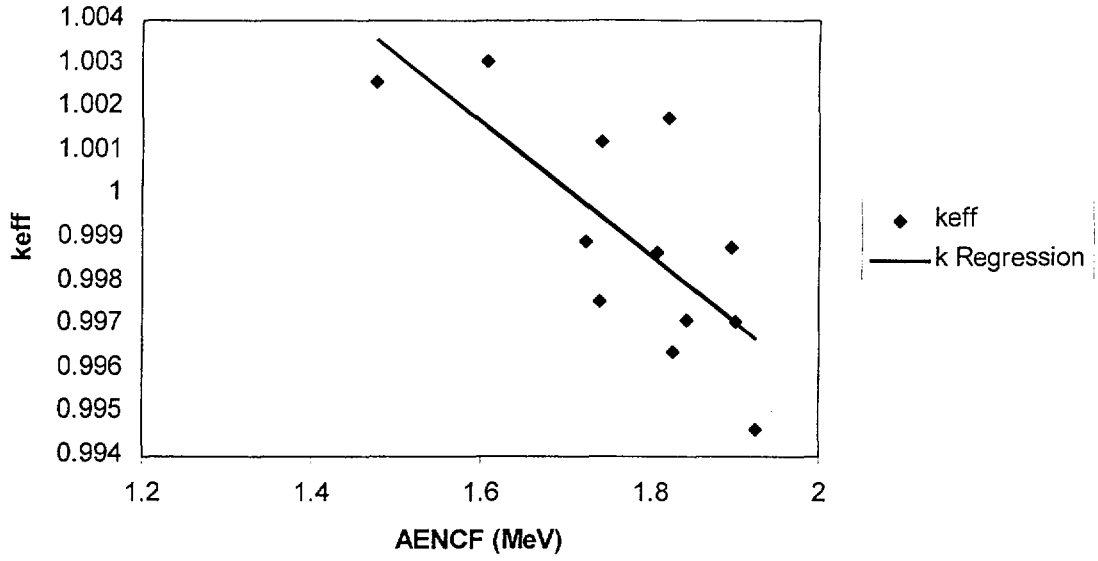

Figure VII-3. Plot of keff and the Regression of keff for PMF Results Using WPO Selected Cross Section Libraries

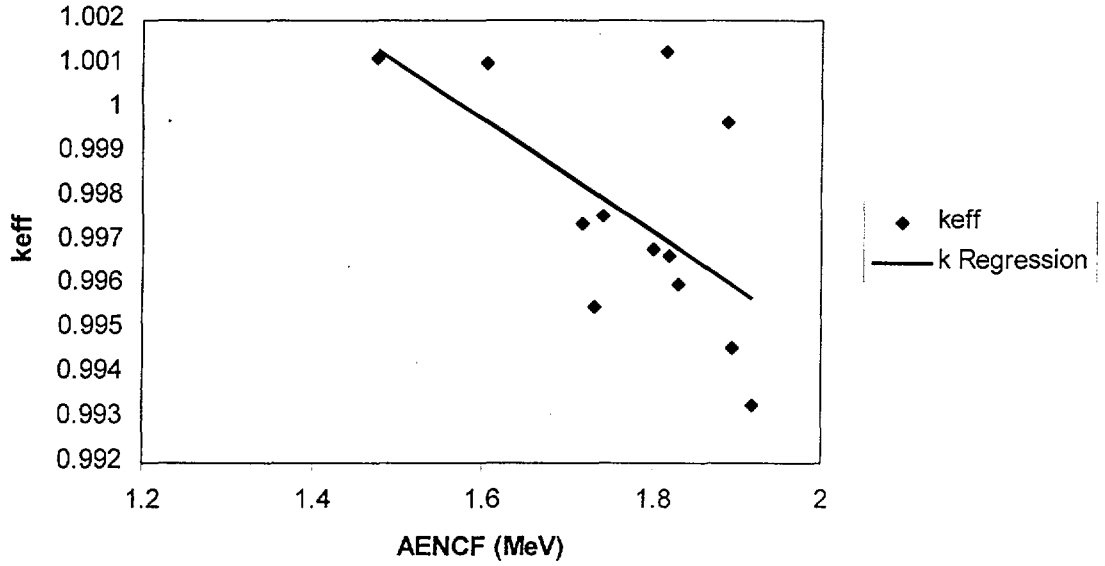

Figure VII-4. Plot of keff and the Regression of keff for HMF Systems Using ENDF/B-V Cross Section Libraries

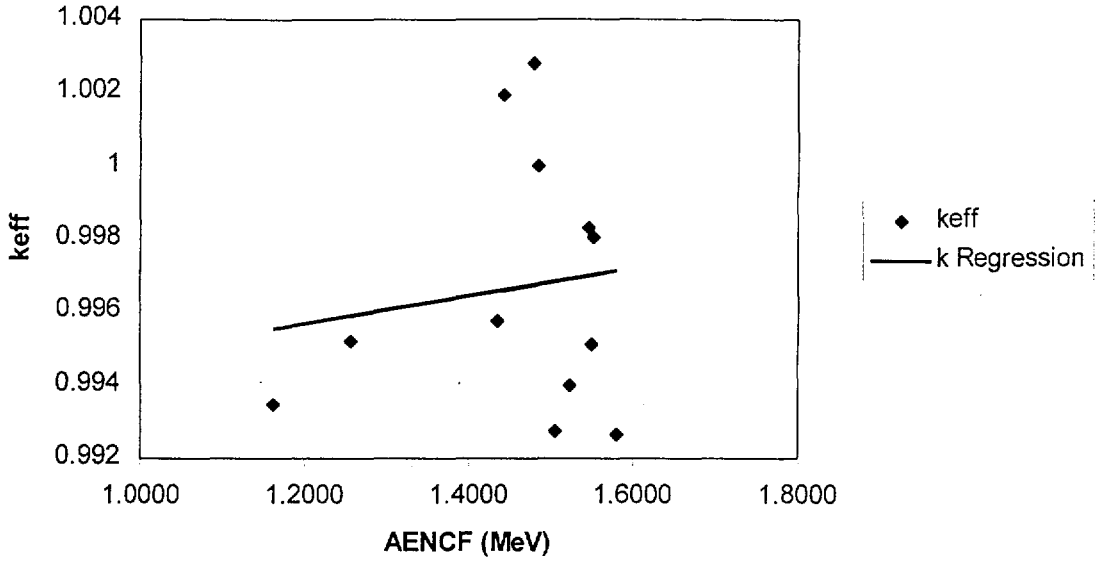

Figure VII-5. Plot of keff and the Regression of keff dor HMF Systems Using ENDF/VI Cross section Libraries

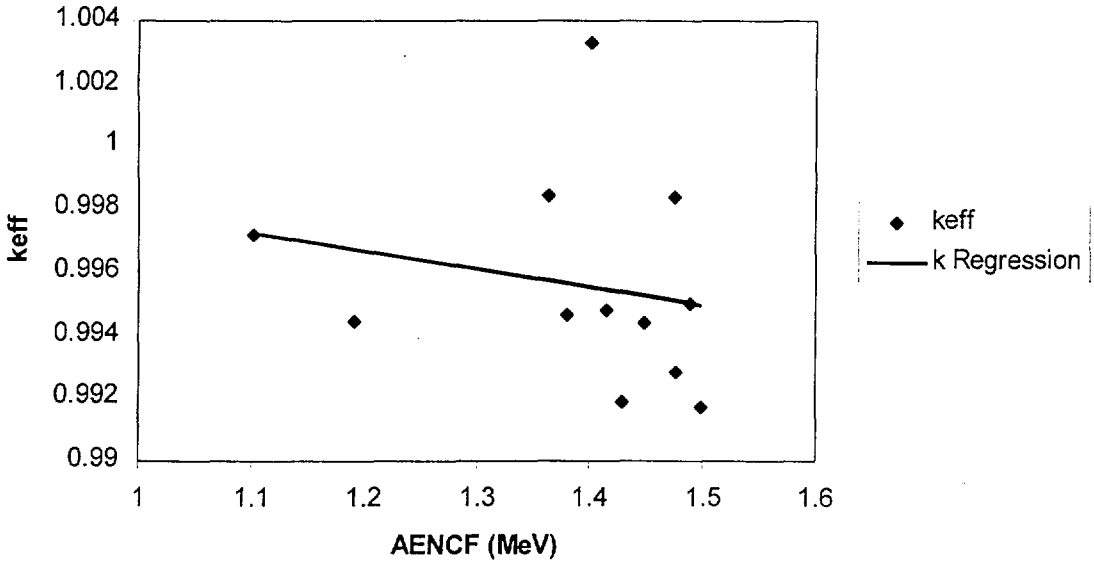

Figure VII-6. Plot of keff and the Regression of keff for HMF Systems Using WPO Selected Cross Section Libraries

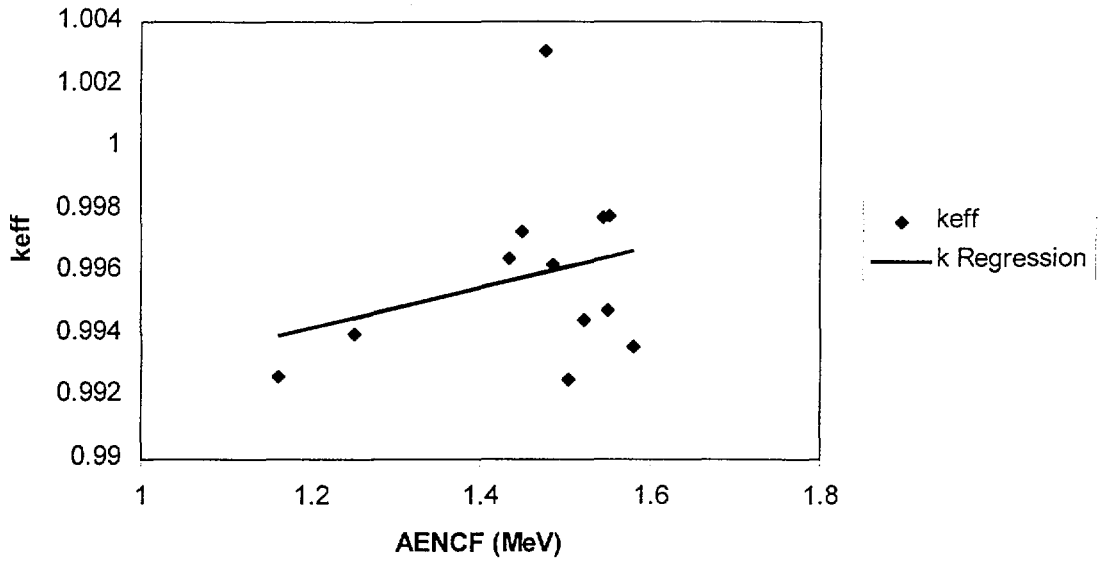

Figure VII-7. Plot of keff and the Regression of keff for IMF Systems Using ENDF/B-V Cross section Libraries

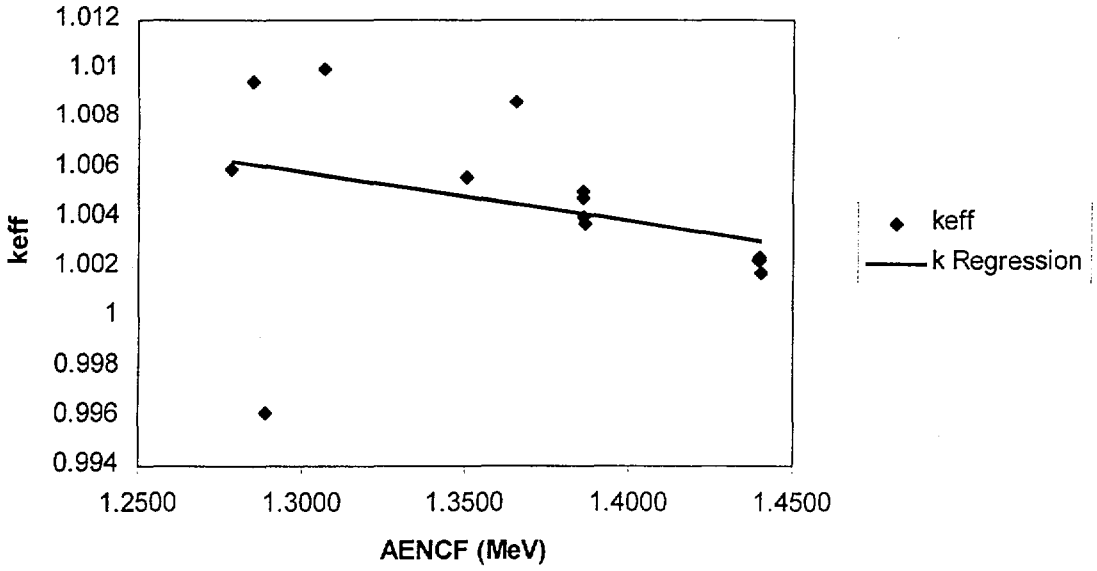

Figure VII-8. Plot of keff and the Regression of keff for IMF Systems Using ENBDF/B-VI Cross Section Libraries

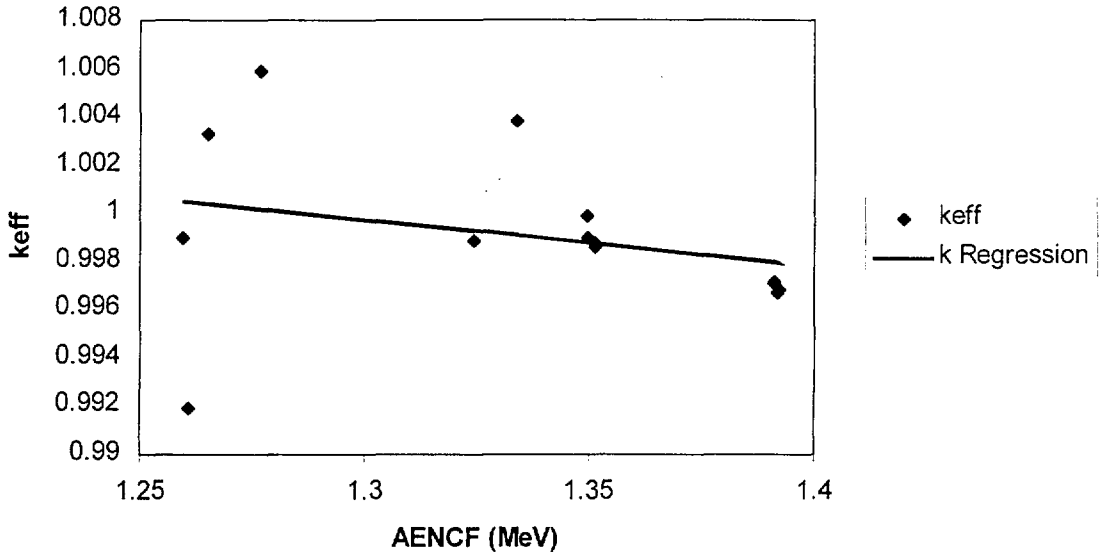

Figure VII-9. Plot of keff and the Regression of keff for IMF Systems Using WPO Selected Cross Section Libraries

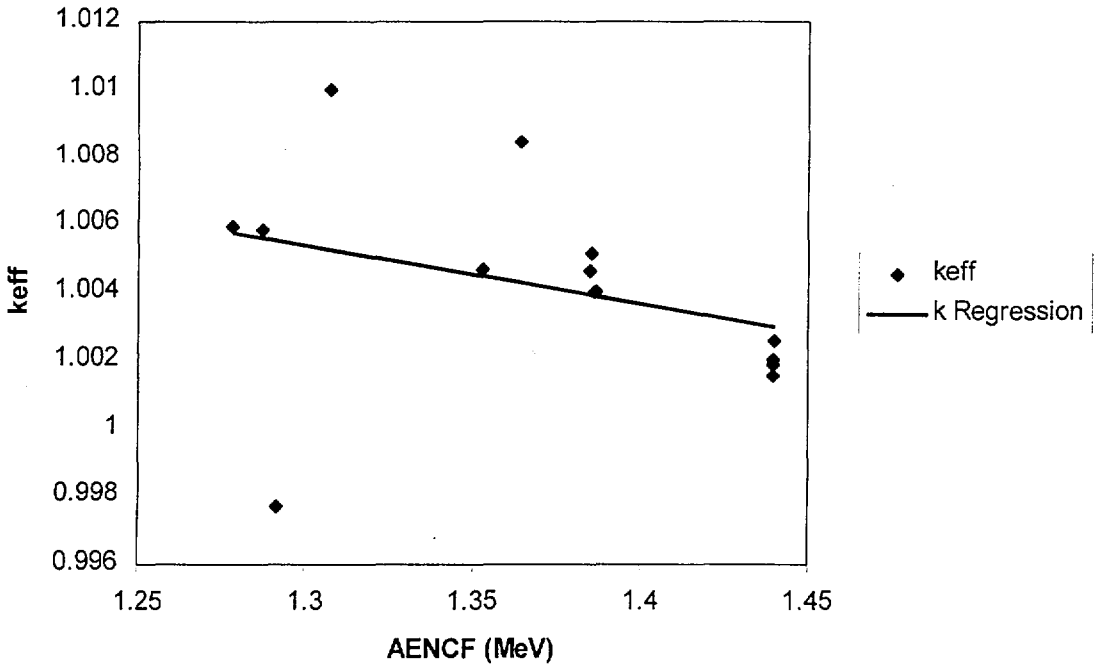

Figure VII-10. Plot of keff and the Regression of keff for HEU Thermal Systems Using ENDF/B-V Cross Section Libraries

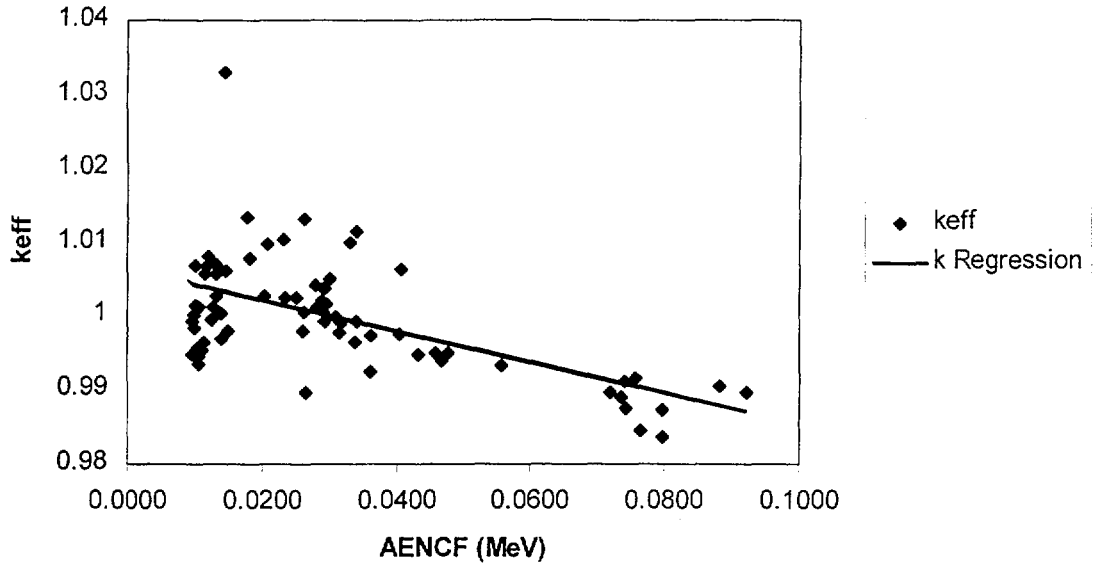

Figure VII-11. Plot of keff and the Regression of keff for HEU Thermal Systems Using ENDF/B-V Cross Section Libraries

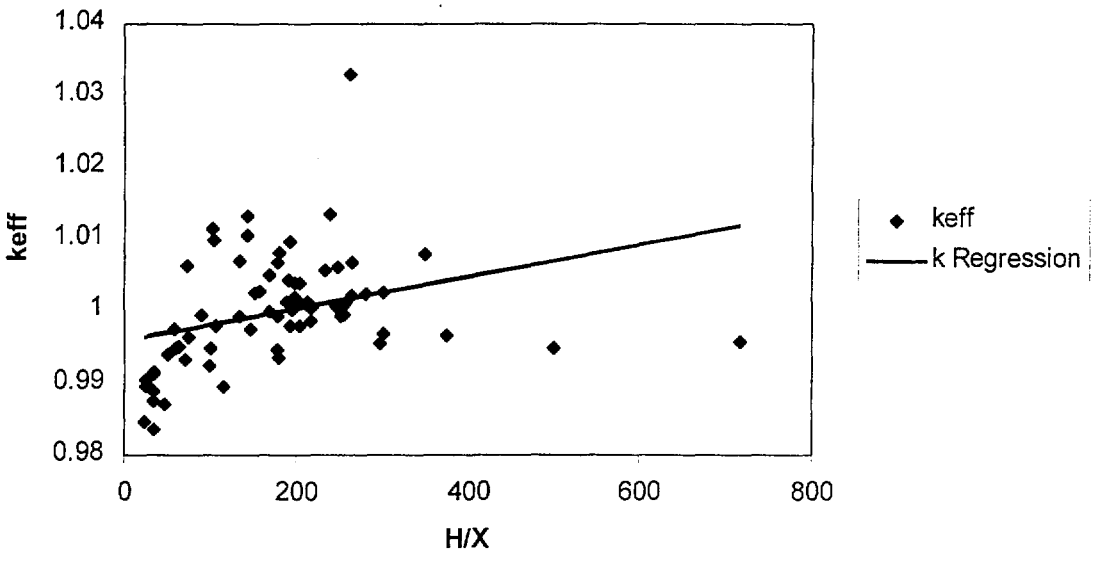

Figure VII-12. Plot of keff and the Regression of keff for HEU Thermal Systems Using ENDF/B-VI Cross Sections

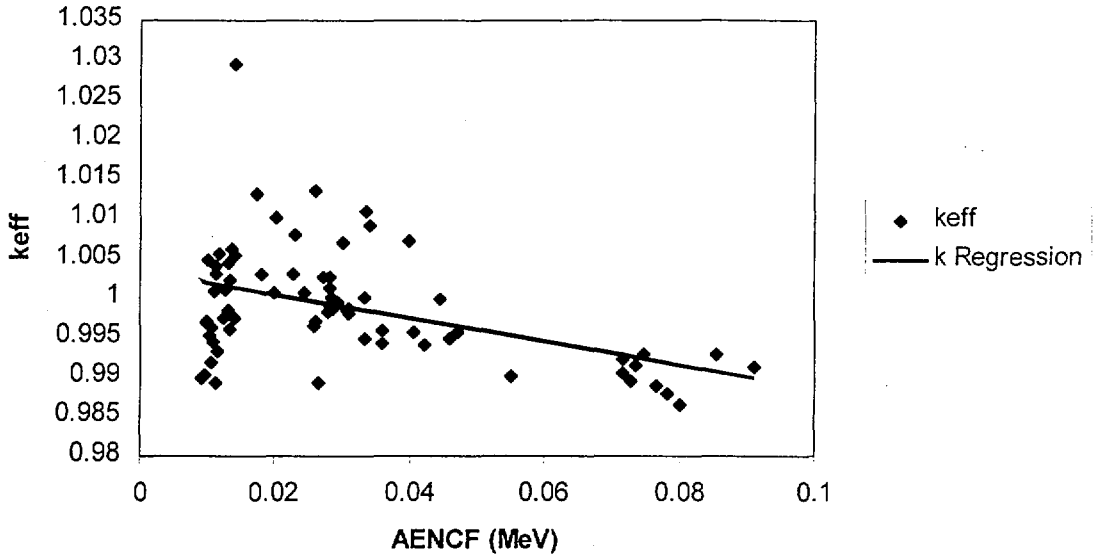

Figure VII-13. Plot of keff and the Regresion of keff for HEU Thermal Systems Using ENDF/B-VI Cross section Libraries

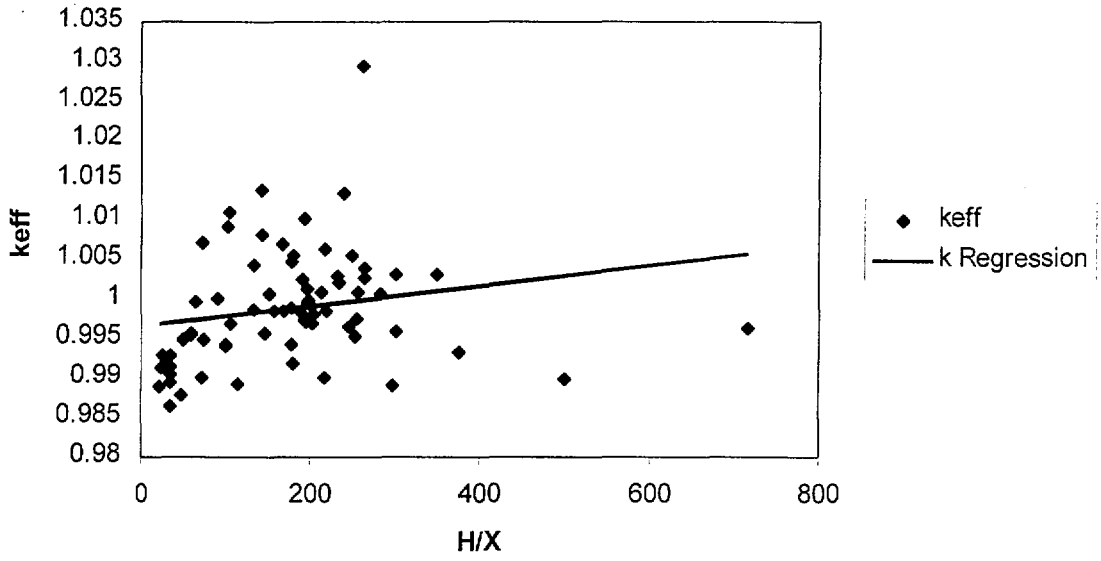

Figure VII-14. Plot of keff and the Regression of keff for HEU Thermal Systems Using WPO Selected Cross Section Libraries

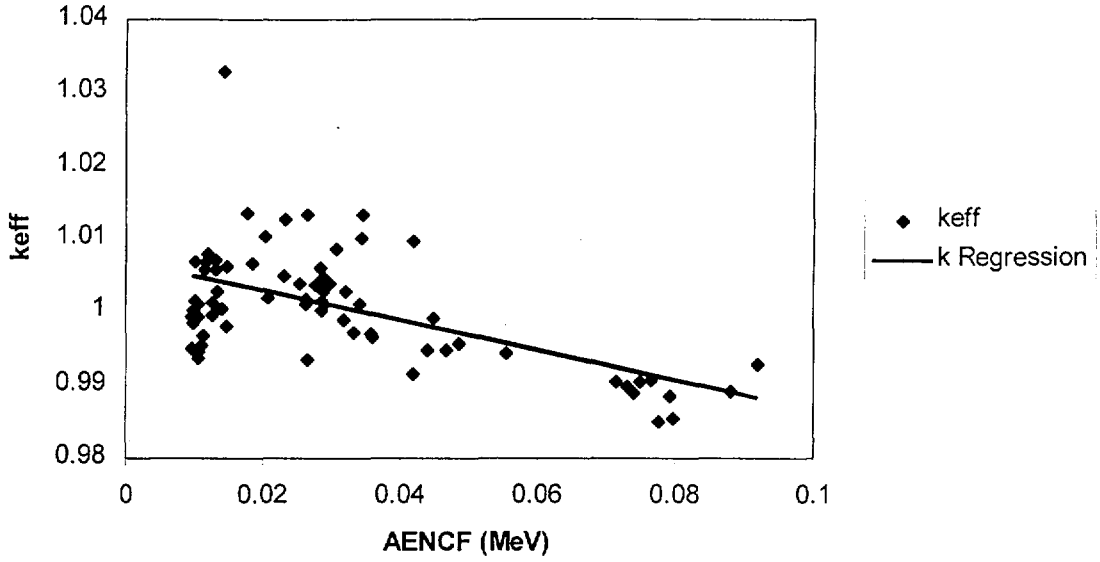

Figure VII-15. Plot of keff and the Regression of keff for HEU Thermal Systems Using WPO Selected Cross Section Libraries

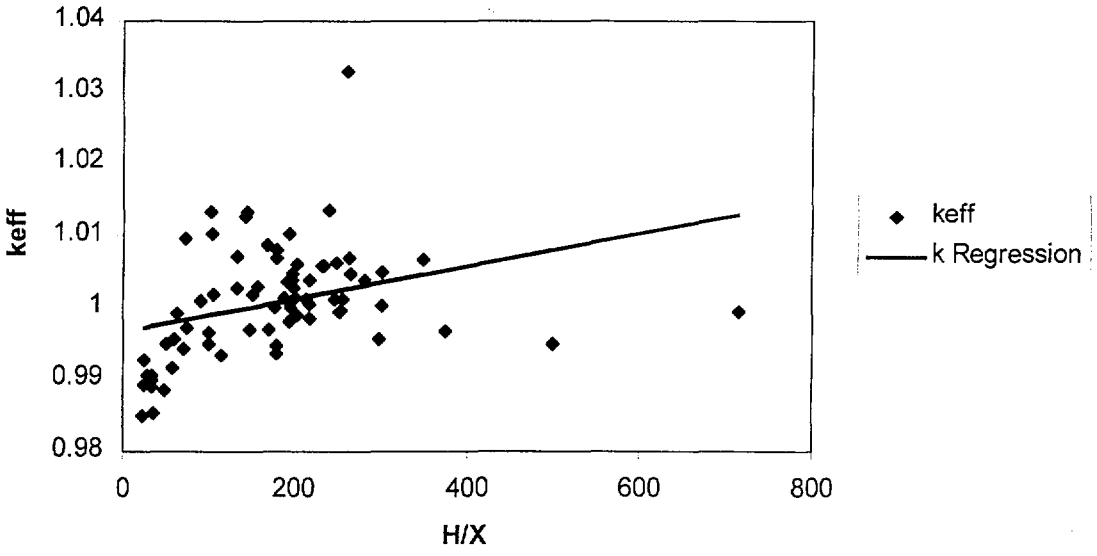

Figure VII-16. Plot of keff and the Regression of keff for HEU Epithermal Systems Using ENDF/B-V Cross Section Libraries

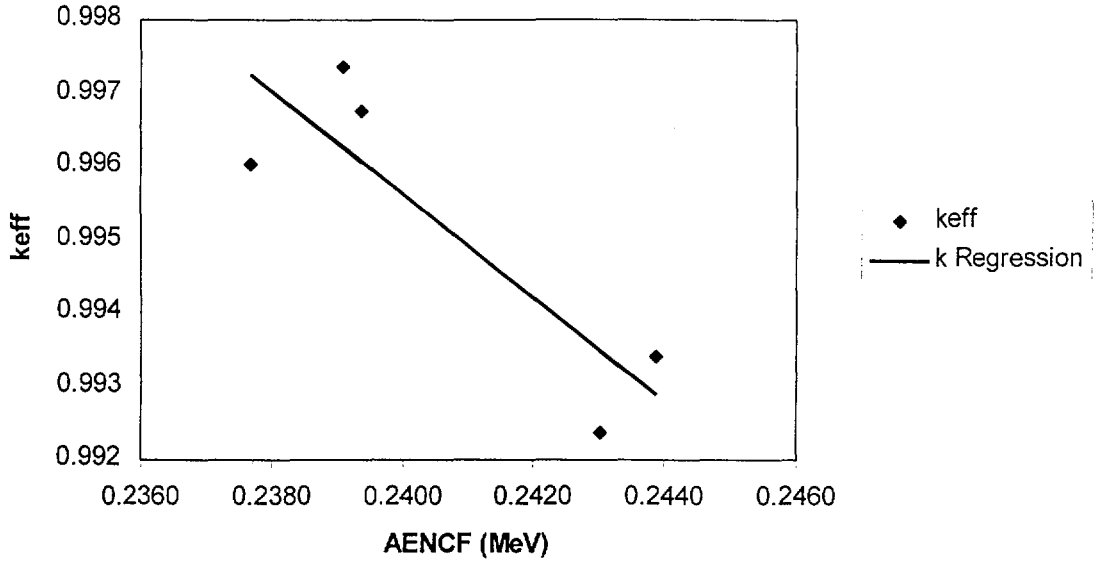

Figure VII-17. Plot of keff and the Regression of keff for HEU Epithermal Systems Using ENDF/B-VI Cross Section Libraries

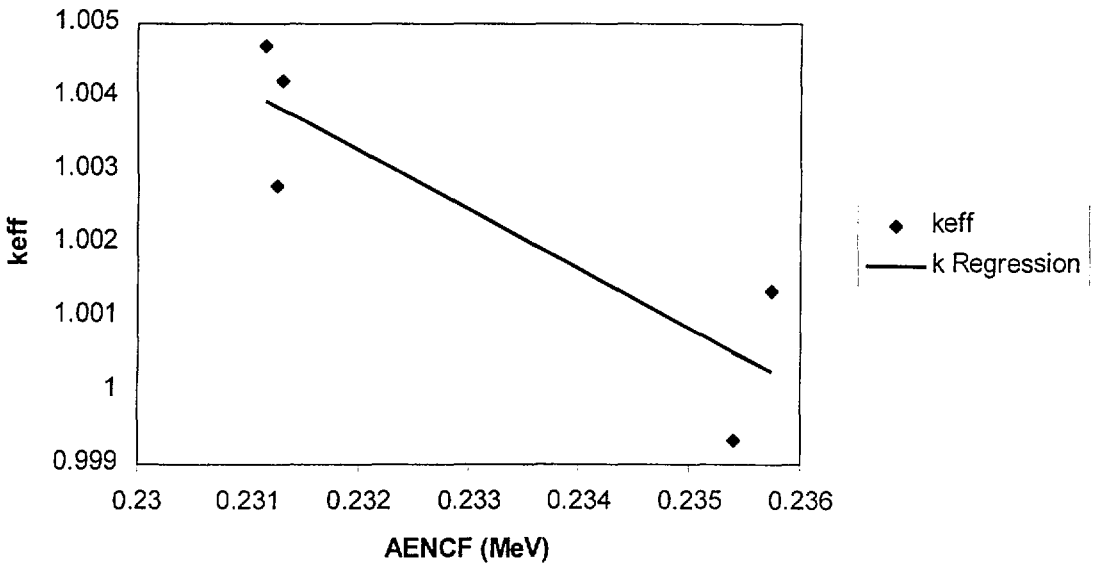

Figure VII-18. Plot of keff and the Regression of keff for HEU Epithermal Systems Using WPO Selected Cross Section Libraries

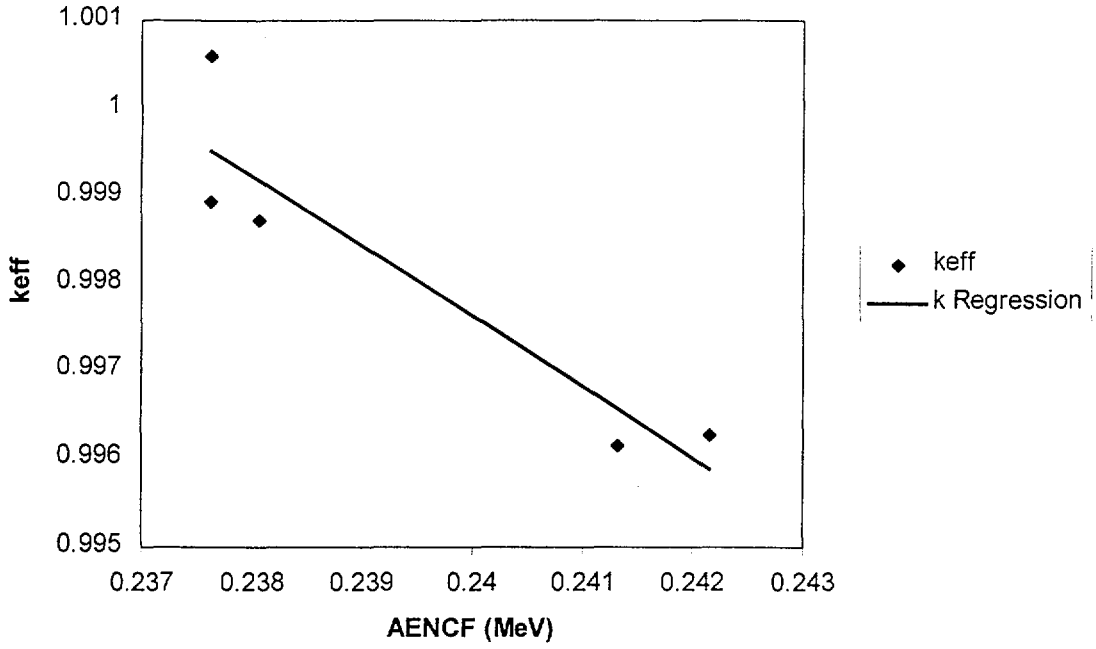

Figure VII-19. Plot of k_infinte and the Regression of k_infinite for Homogenous Critical Solutions Using ENDF/B-V Cross Section Libraries

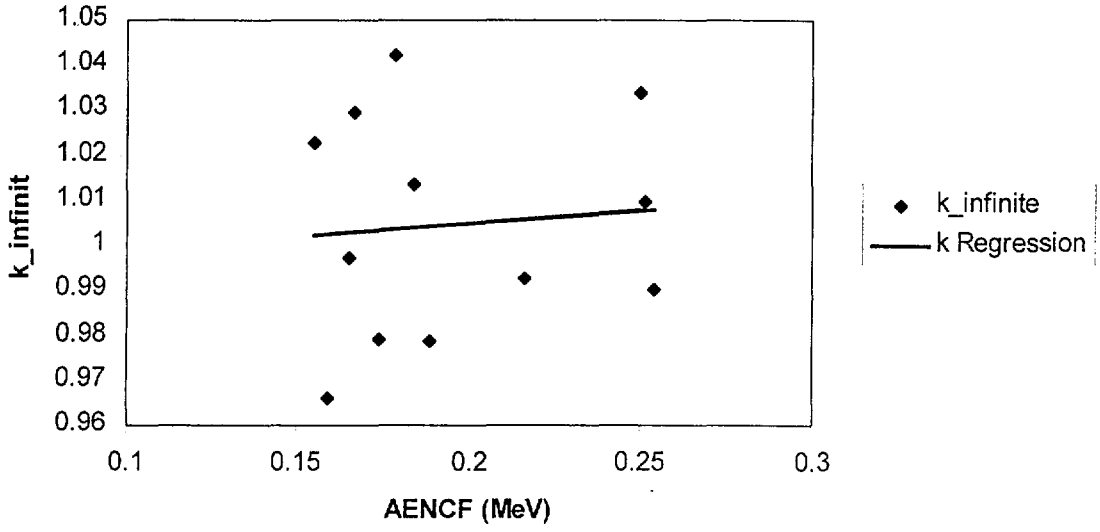

Figure VII-20. Plot of k_infinite and the Regression of k_infinite for Homogenous Critical Solutions Using ENDF/B-V Cross Section Libraries

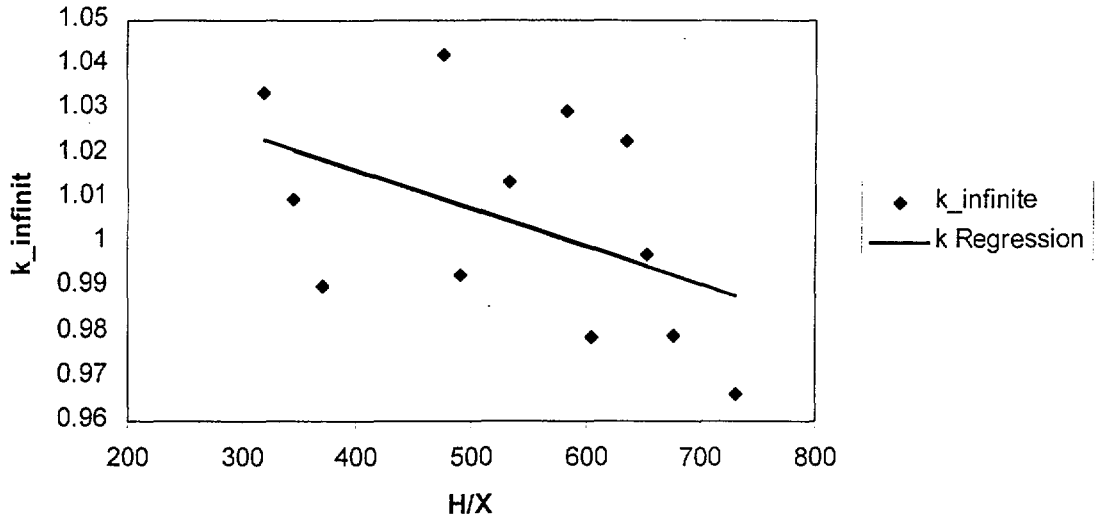

Figure VII-21. Plot of k_infinite and the Regression of k_infinite for Homogenous Critical Solutions Using ENDF/B-VI Cross Section Libraries

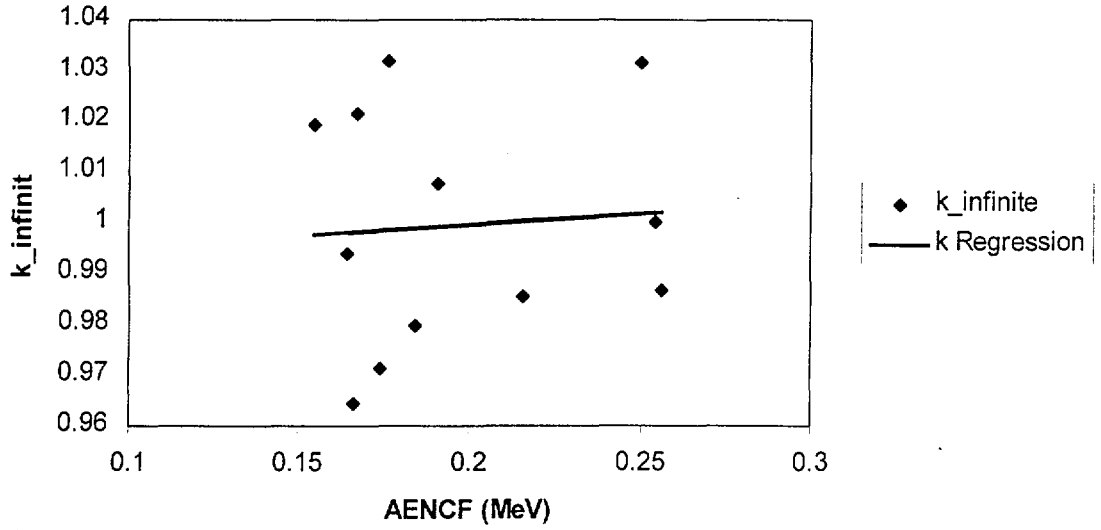

Figure VII-22. Plot of k_infinite and the Regression of k_infinite for Homogenous Critical Solutions Using ENDF/B-VI Cross Section Libraries

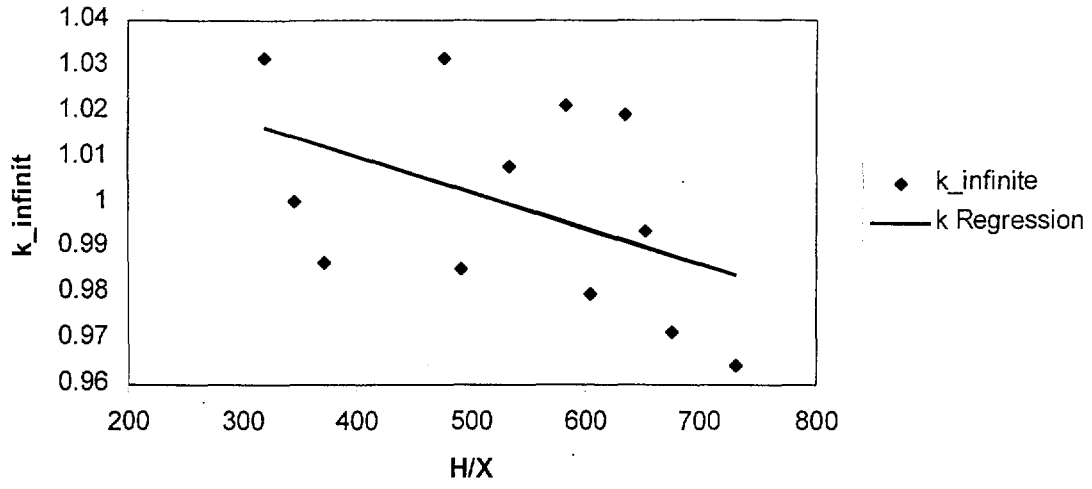

Figure VII-23. Plot of k_infinite and the Regression of k_infinite for Homogenous Critical Solutions Using WPO Selected Cross Section Libraries

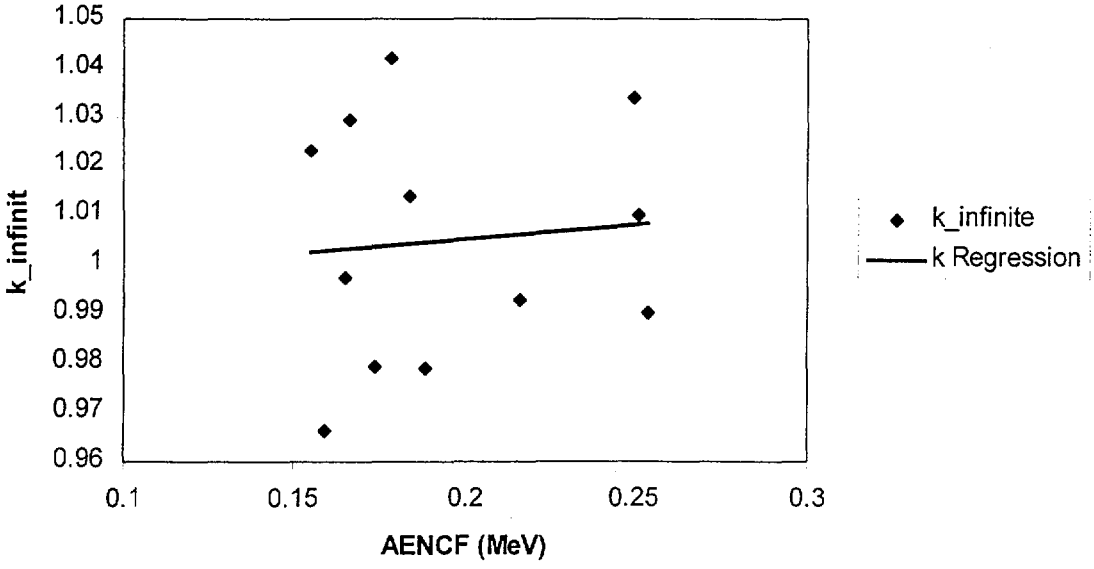

Figure VII-24. Plot of k_infinite and the Regression of k_infinite for Homogenous Critical Solutions Using WPO Selected Cross Section Libraries

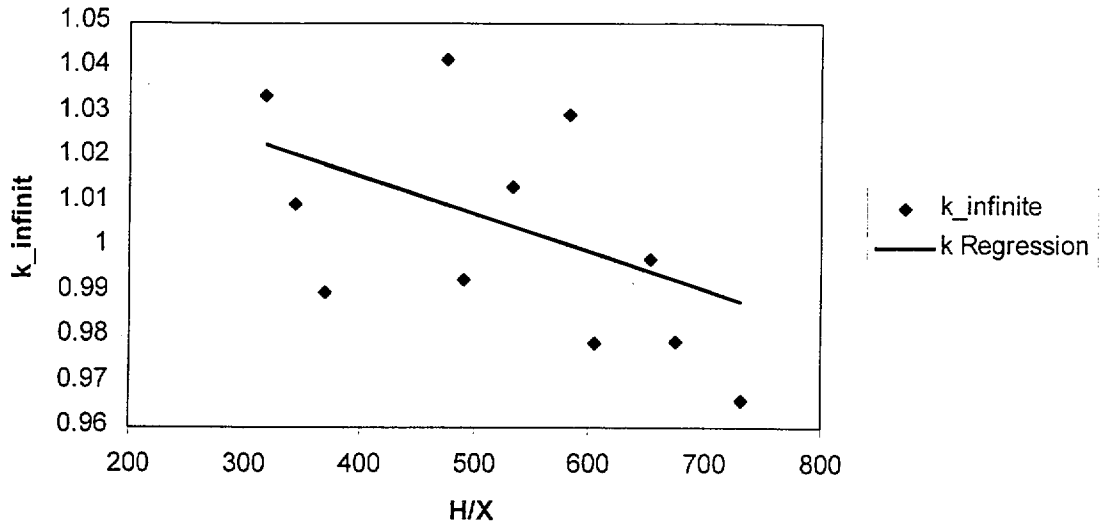

Figure VII-25. Plot of keff and the Regression of keff for LEU Systems Using ENDF/B-V Cross Section Libraries

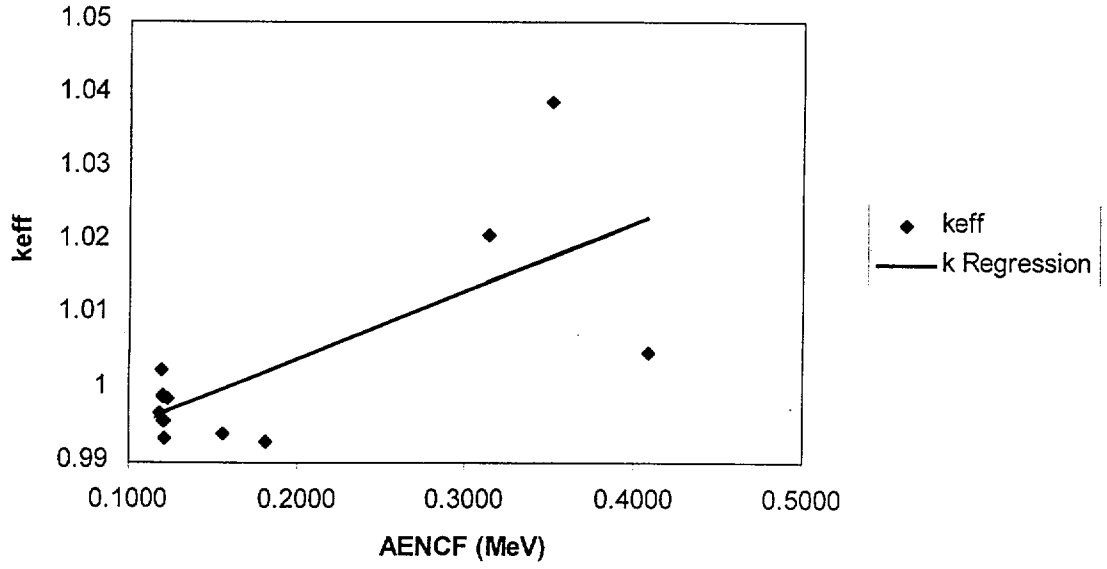

Figure VII-26. Plot of keff and the Regression of keff for LEU Systems Using ENDF/B-V Cross Section Libraries

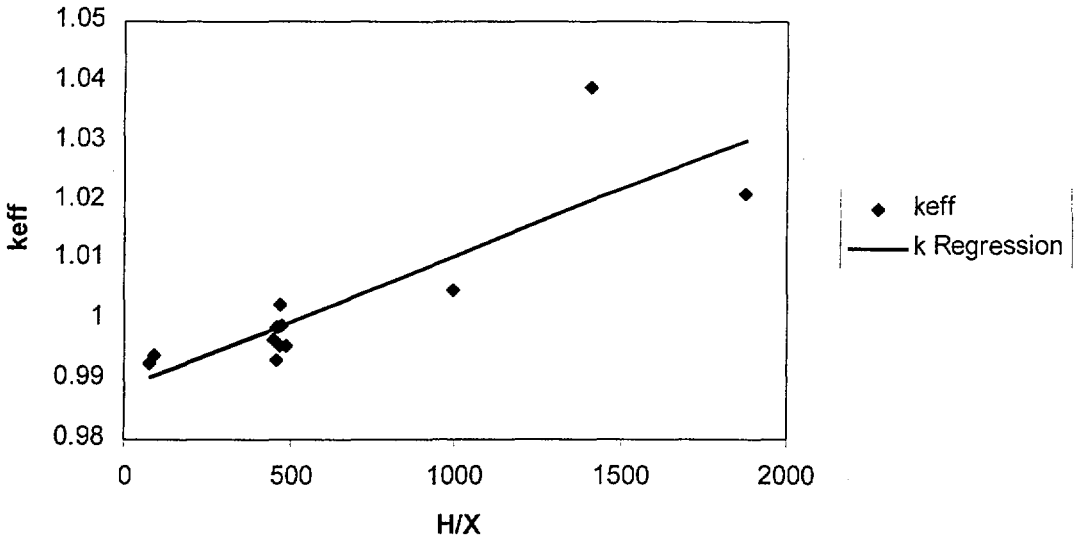

Figure VII-27. Plot of keff and the Regression of keff for LEU System Results Using ENDF/B-VI Cross Section Libraries

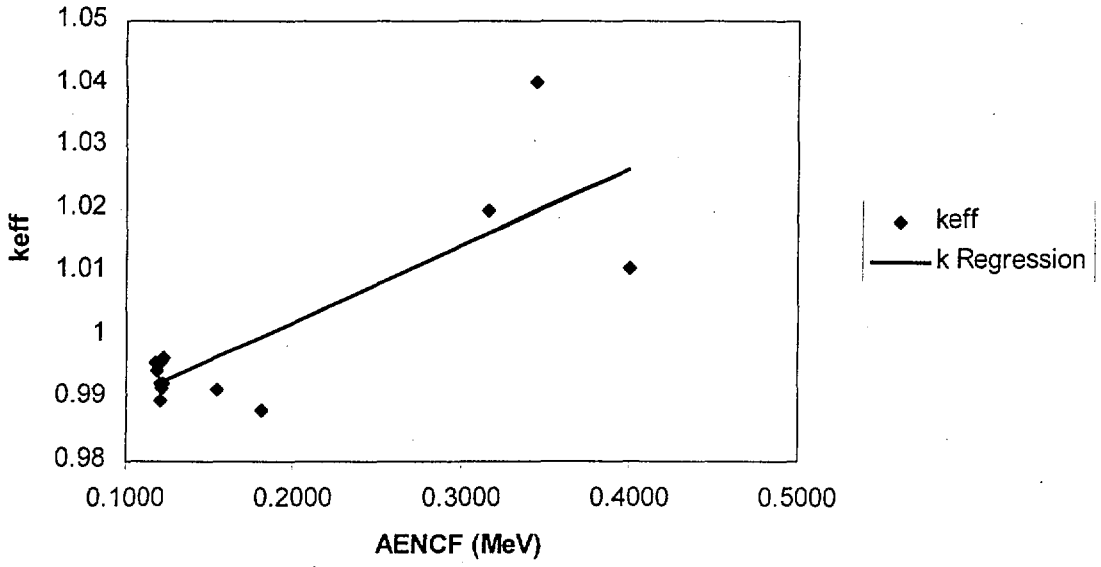

Figure VII-28. Plot of keff and the Regression of keff for LEU Systems Using ENDF/B-VI Cross Section Libraries

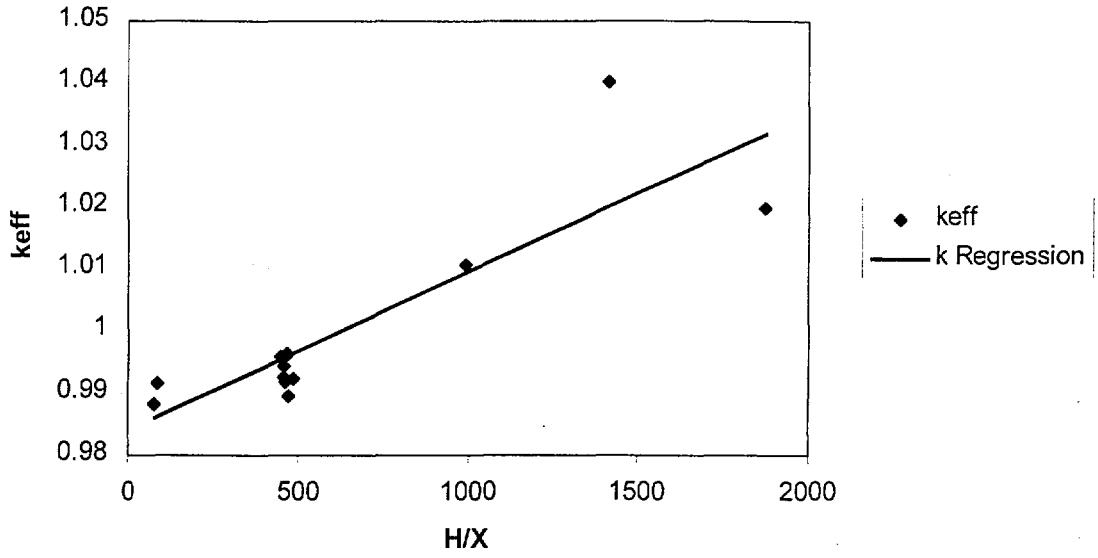

Figure VII-29. Plot of keff and the Regression of keff for LEU Systems Using WPO Selected Cross Section Libraries

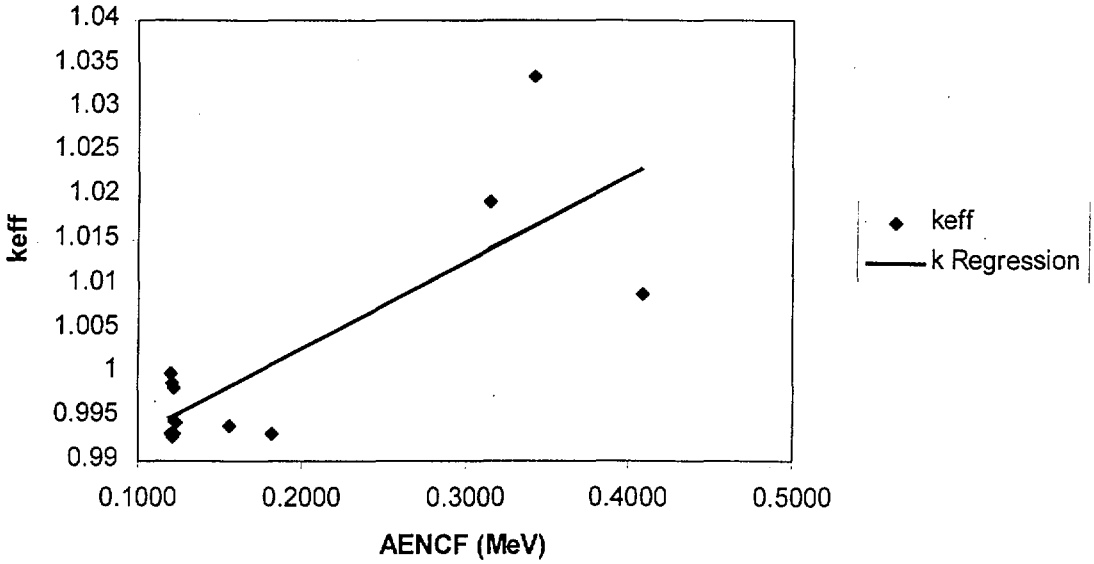

Figure VII-30. Plot of keff and the Regression of keff for LEU Systems Using WPO Selected Cross Section Libraries

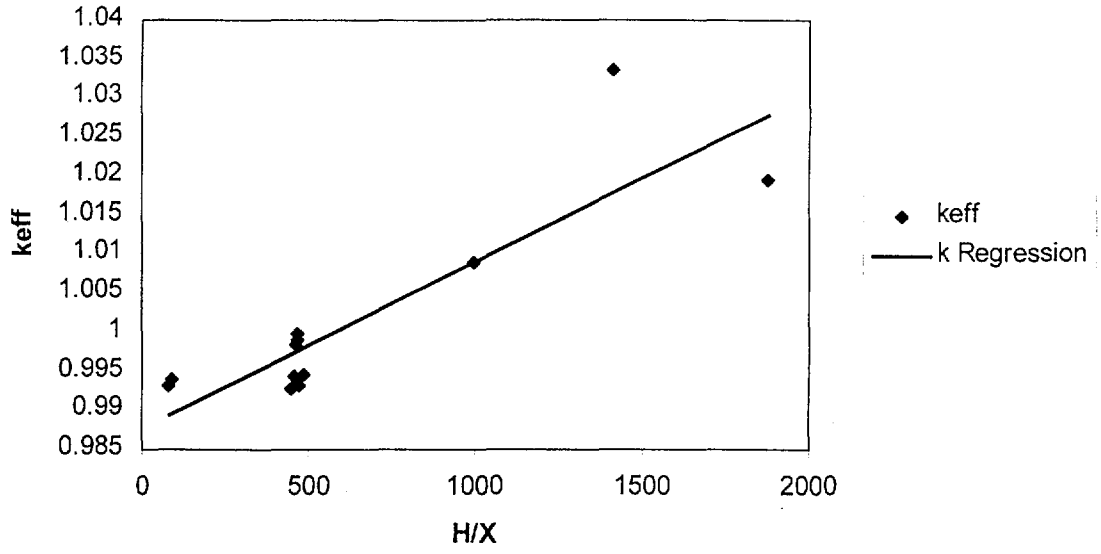

Figure VII-31. Plot of keff and the Regression of keff for Pu Fueled Thermal Systems Using ENDF/B-V Cross Section Libraries

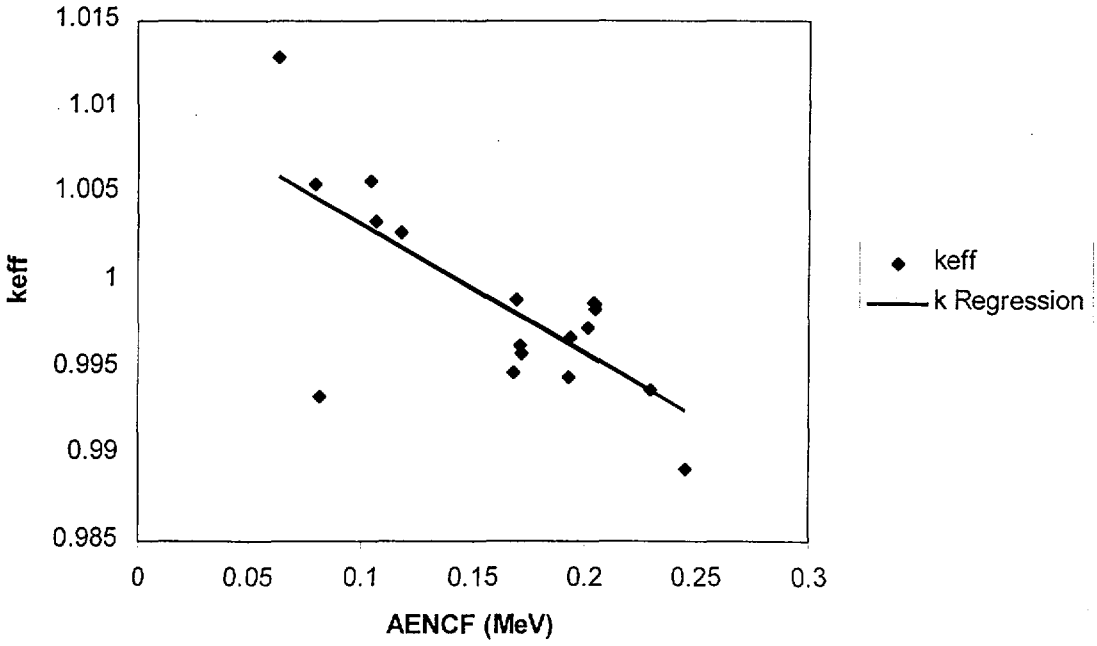

Figure VII-32. Plot of keff and the Regression of keff for Pu Fueled Thermal Systems Using ENDF/B-V Cross Section Libraries

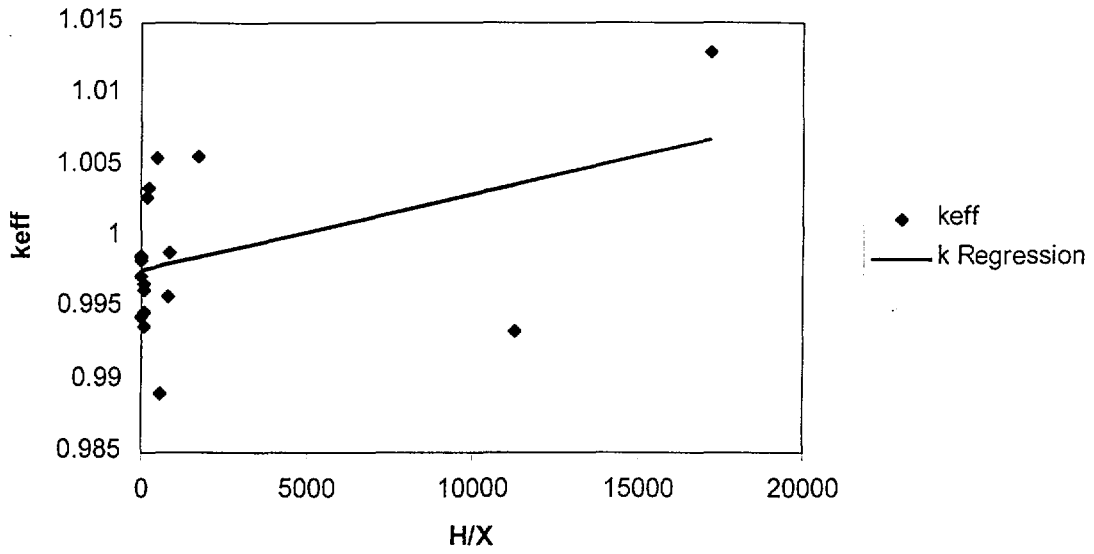

Figure VII-33. Plot of keff and the Regression of keff for Pu Fueled Thermal Systems Using ENDF/B-VI Cross section Libraries

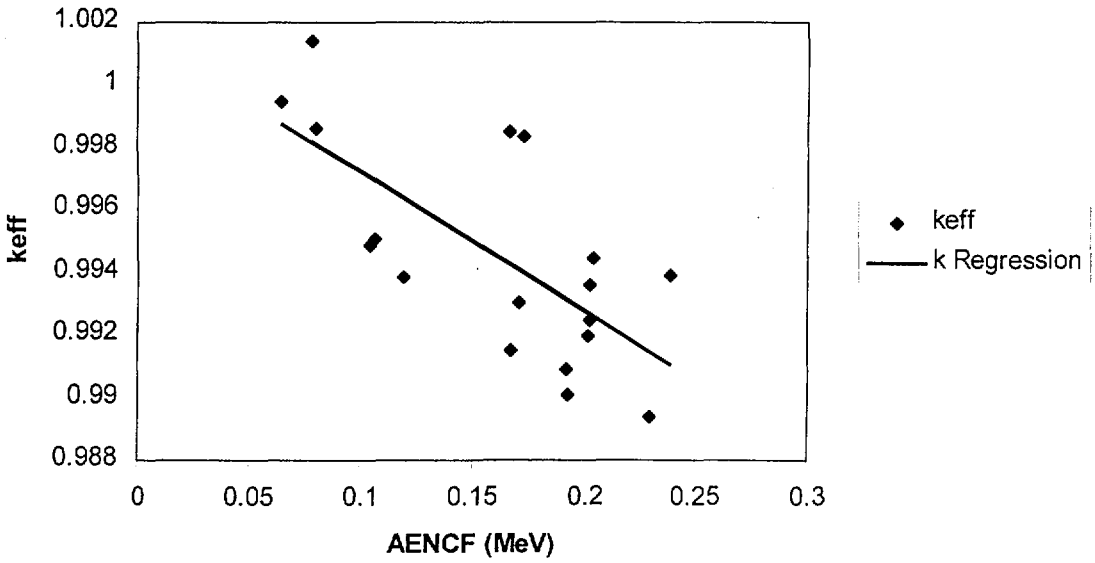

Figure VII-34. Plot of keff and the Regression of keff for Pu Fueled Thermal Systems Using ENDF/B-VI Cross Section Libraries

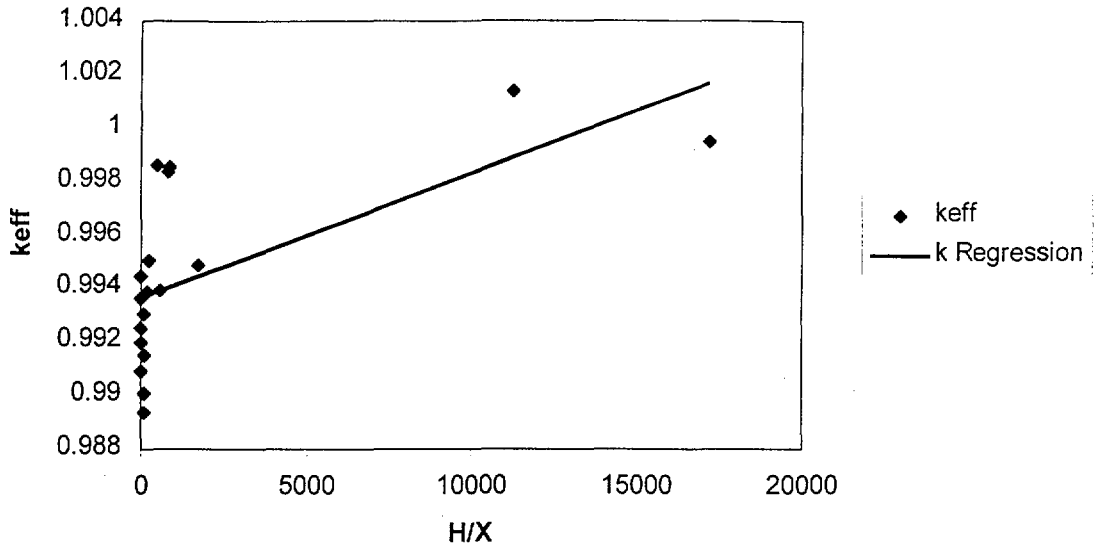

Figure VII-35. Plot of keff and the Regression of keff for Pu Fueled Thermal Systems Using WPO Selected Cross section Libraries

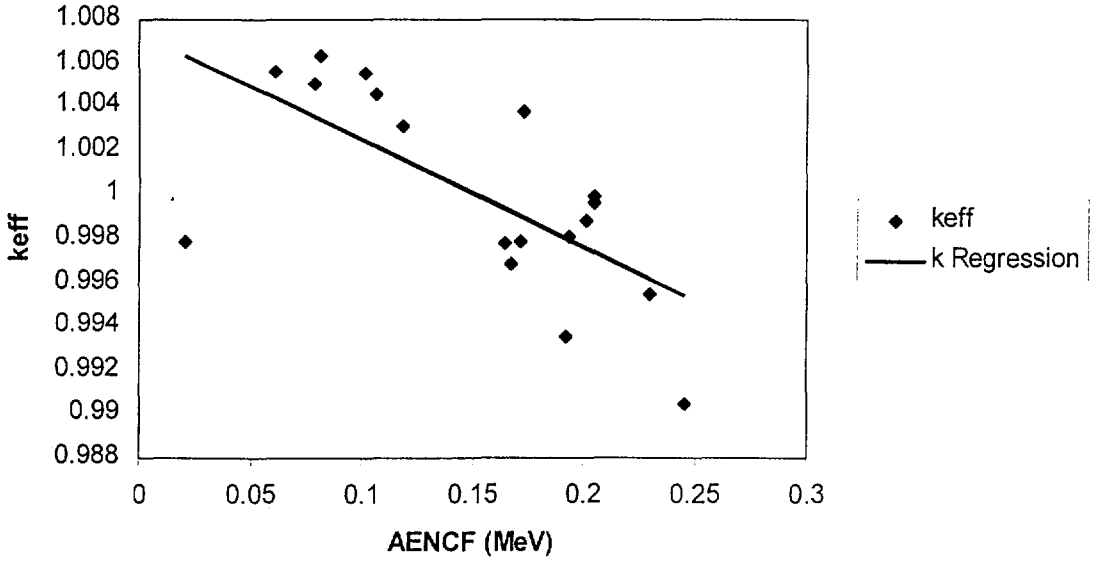

Figure VII-36. Plot of keff and the Regression of keff for Pu Fueled Thermal Systems Using WPO Selected Cross Section Libraries

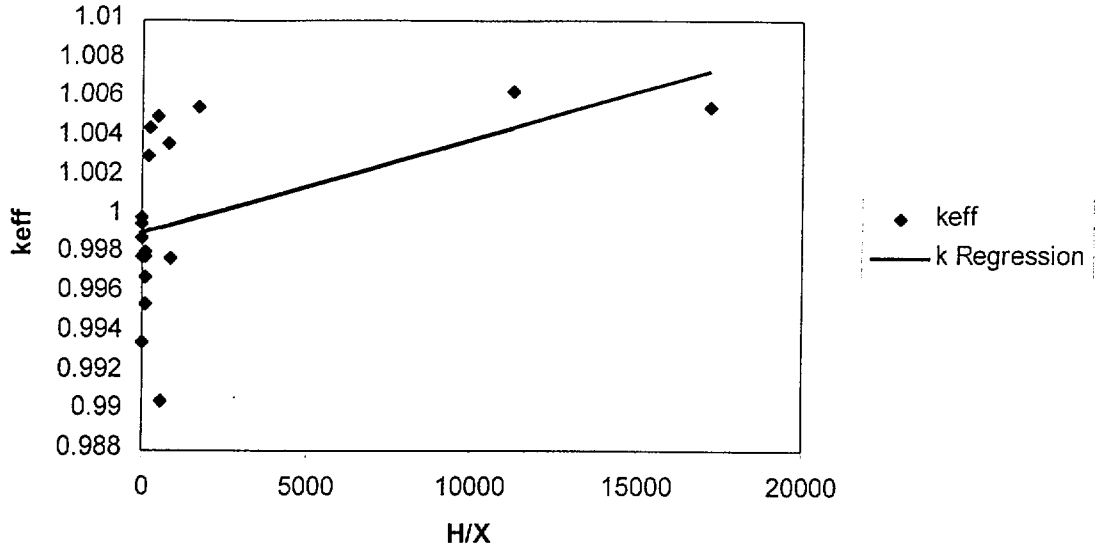

Figure VII-37. Plot of keff and the Regression of keff for Homogenous Critical Solutions Using ENDF/B-V Cross Section Libraries

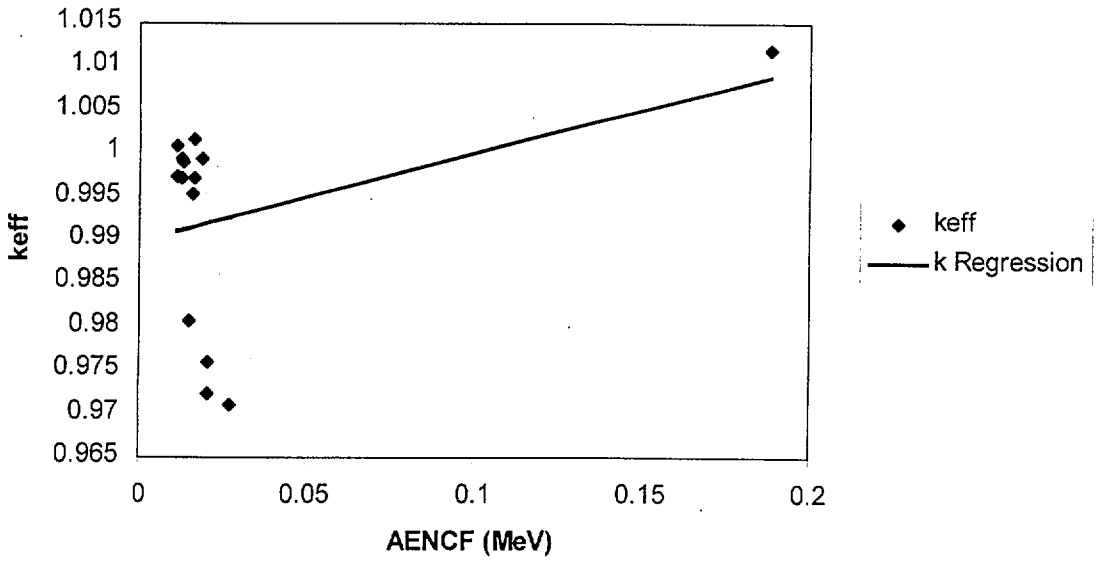

Figure VII-38. Plot of keff and the Regression of keff for Homogenous Critical Solutions Using ENDF/B-V Cross Section Libraries

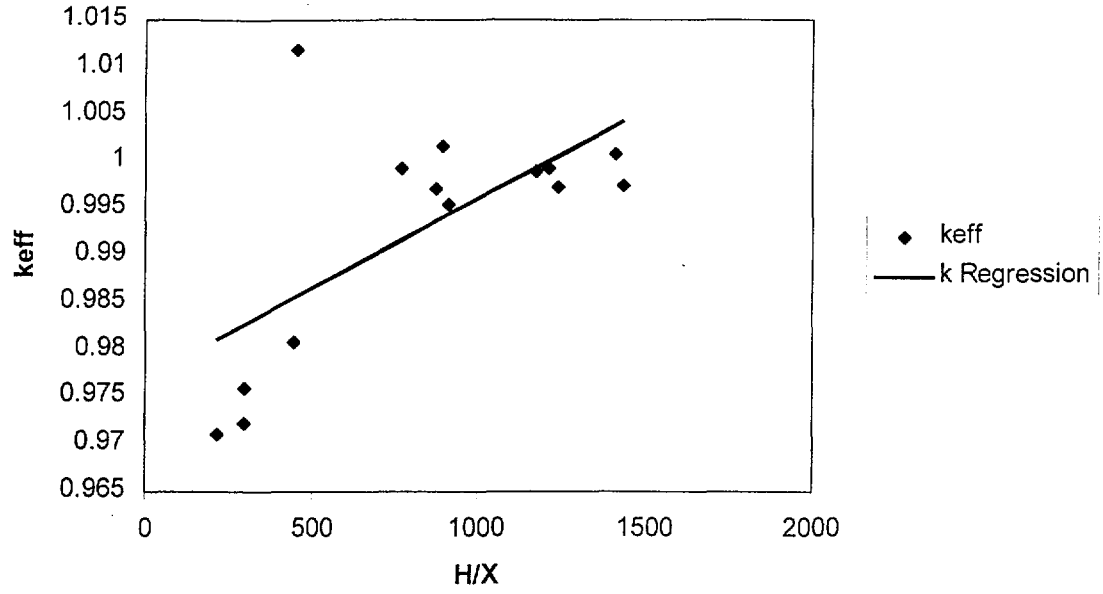

Figure VII-39. Plot of keff and the Regression of keff for Homogenous Critical Solutions Using ENDF/B-VI Cross Section Libraries

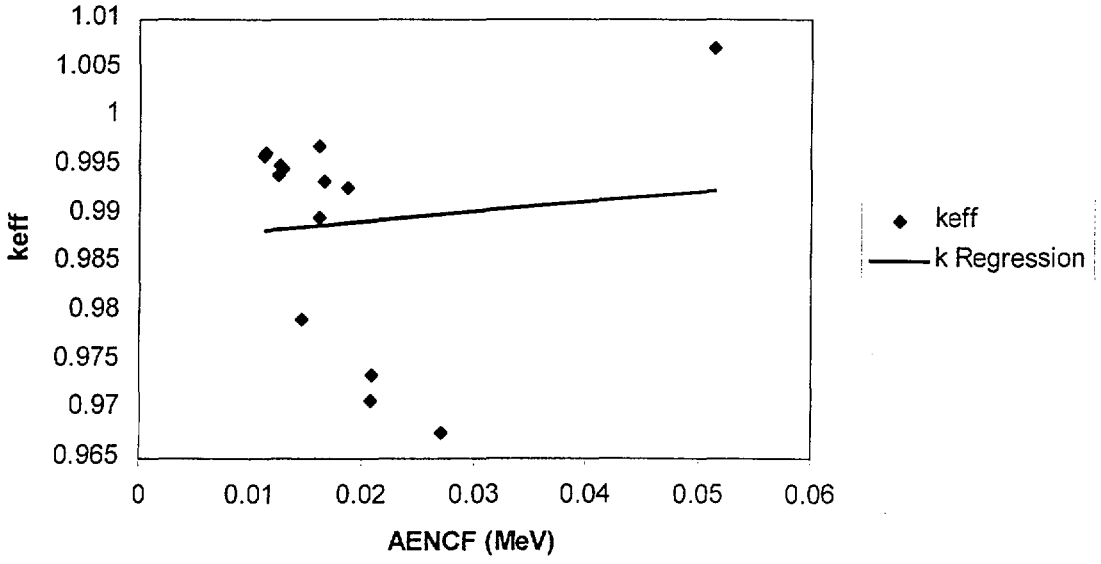

Figure VII-40. Plot of keff and the Regression of keff for Homogenous Critical Solutions Using ENDF/B-VI Cross Section Libraries

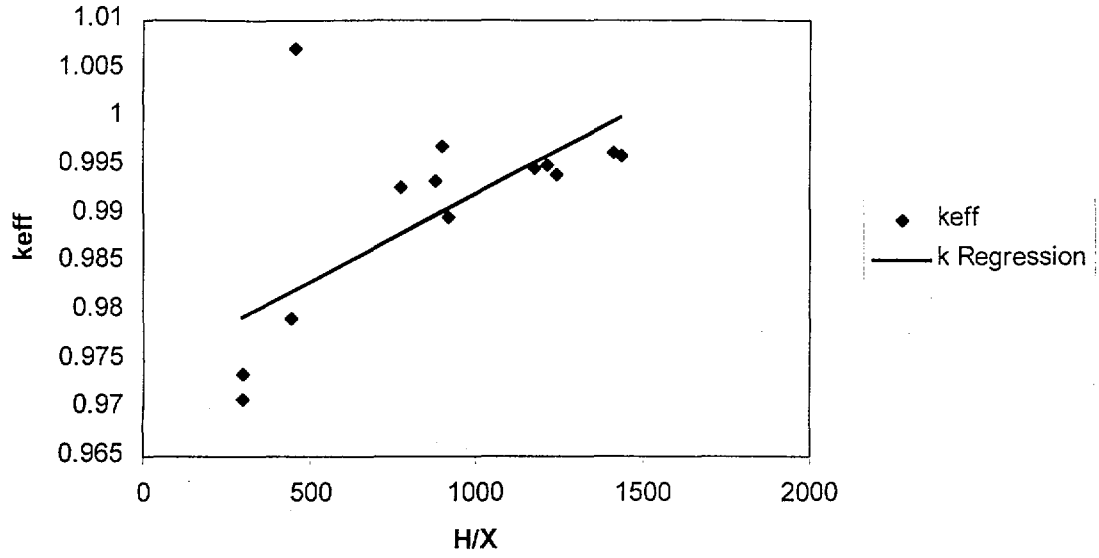

Figure VII-41. Plot of keff and the Regression of keff for Homogenous Critical Solutions Using WPO Selected Cross Section Libraries

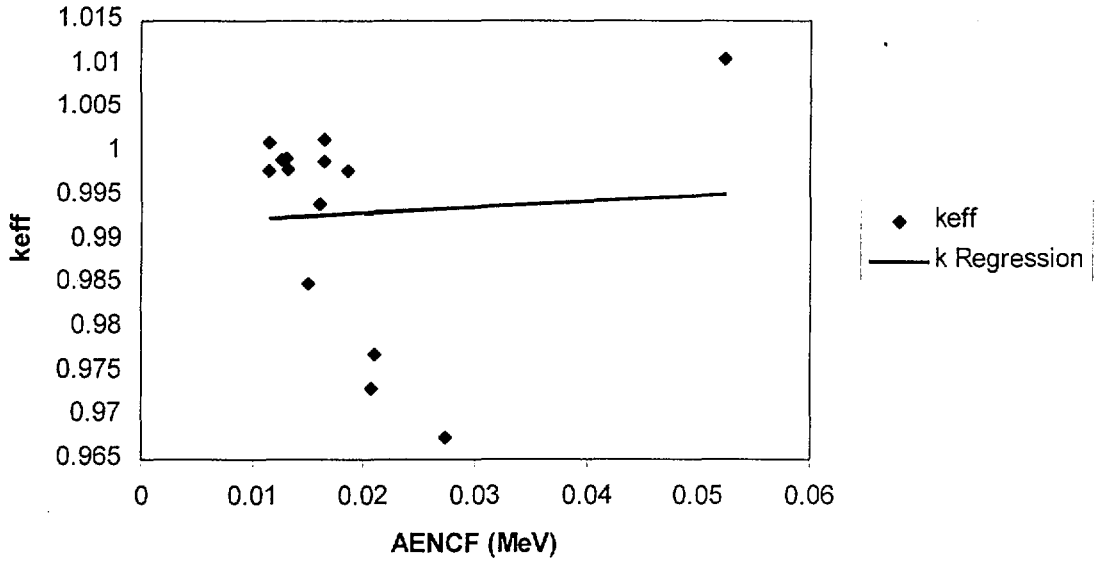

Figure VII-42. Plot of keff and the Regression of keff for Homogenous Critical Solutions Using WPO Selected Cross Section Libraries

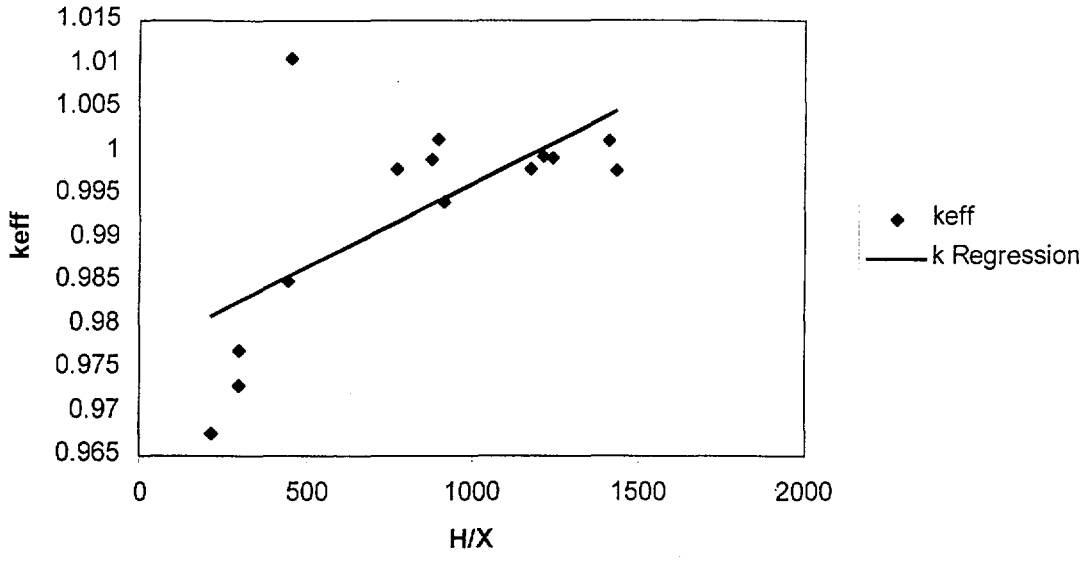

This Attachment contains the tests for normality in the 95% confidence interval for the LCE benchmark calculations. The plots contained in Attachment VIII were generated with NCSS 97 software routine. The information documented in Section 6 is sufficient to provide an independent repetition of the software routine to duplicate the plots contained in Attachment VIII.

Figure VIII-1

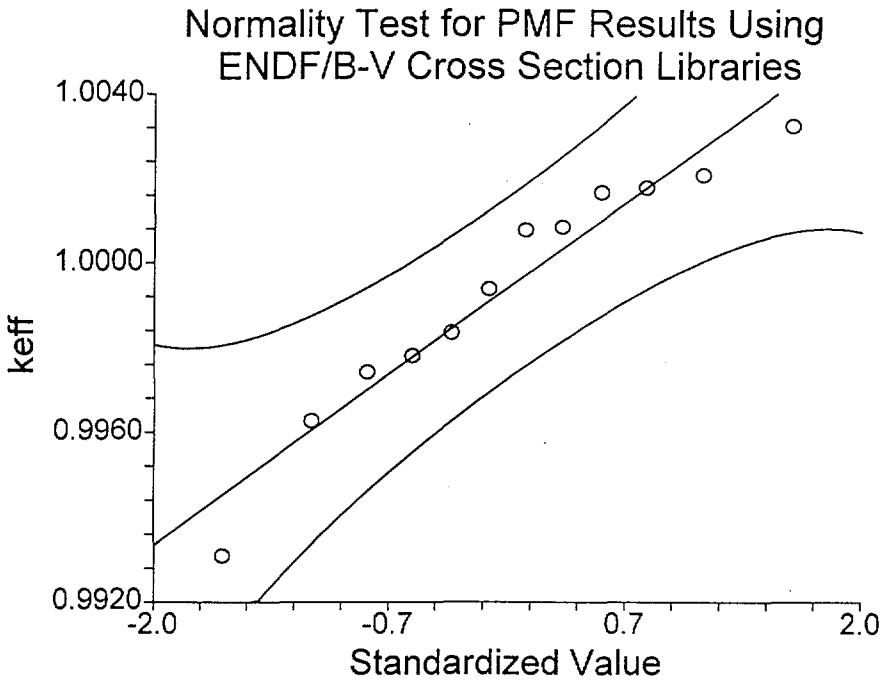

Figure VIII-2

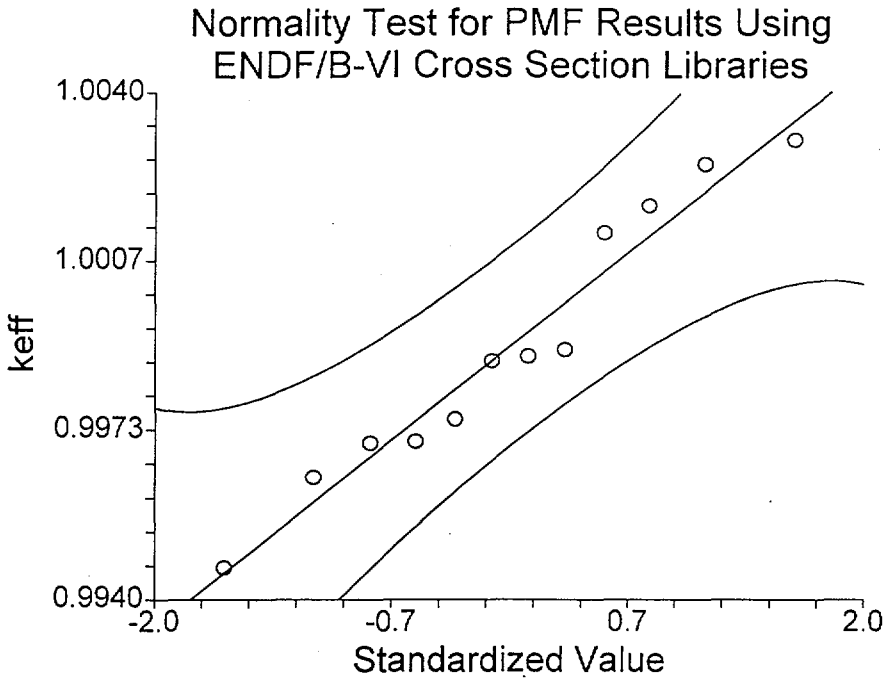

Figure VIII-3

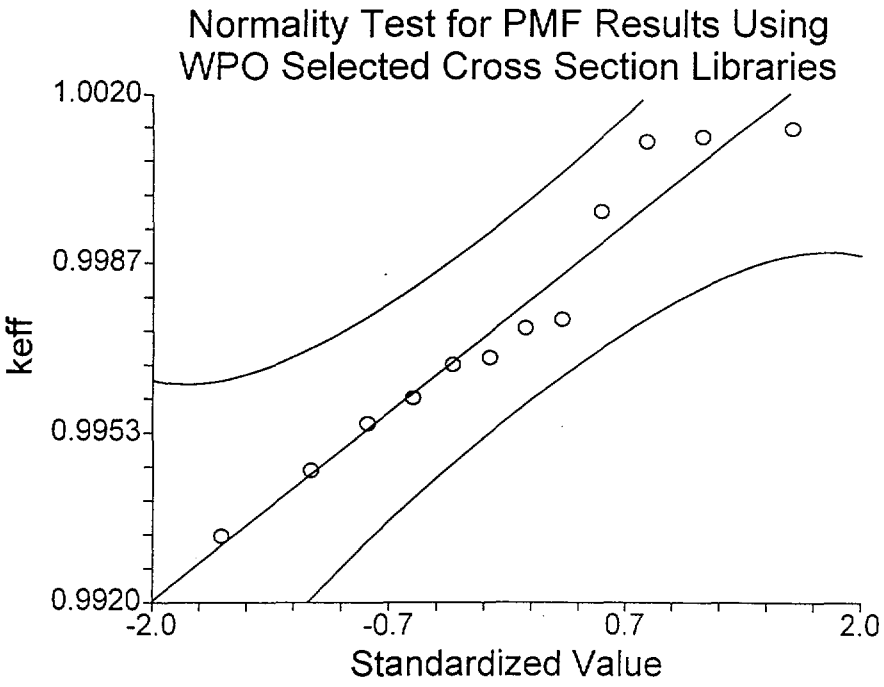

Figure VIII-4

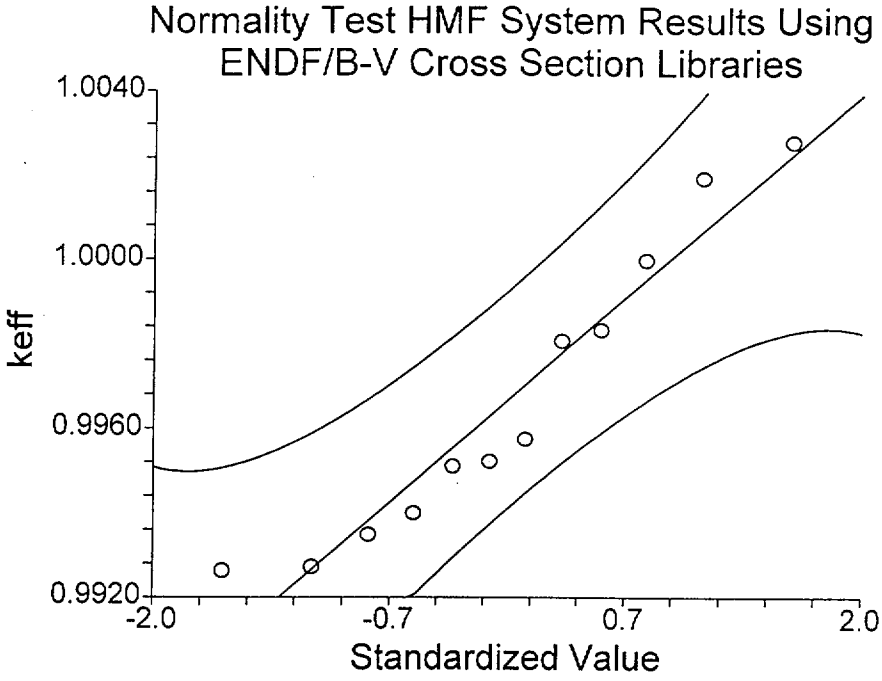

Figure VIII-5

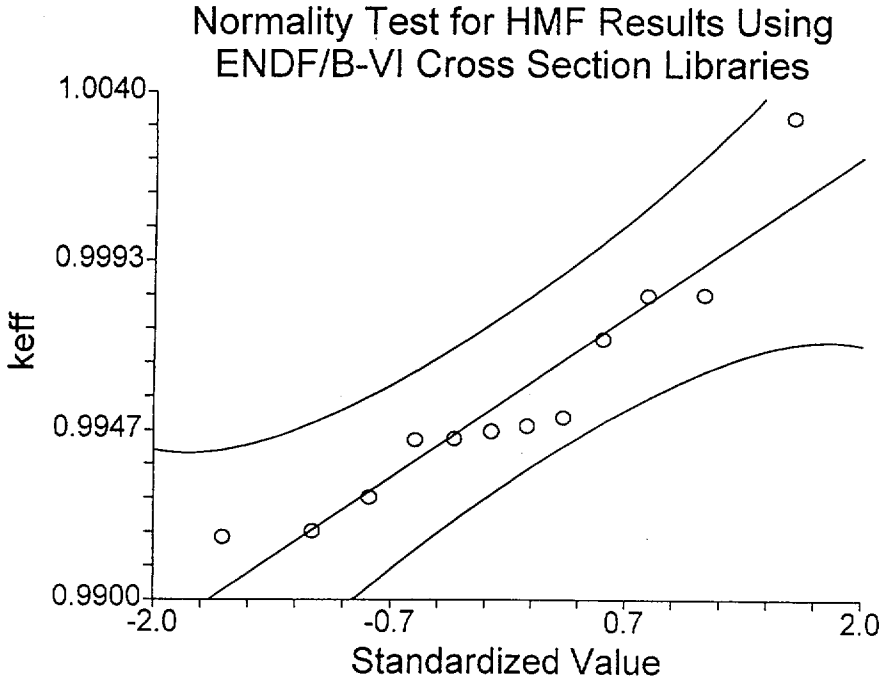

Figure VIII-6

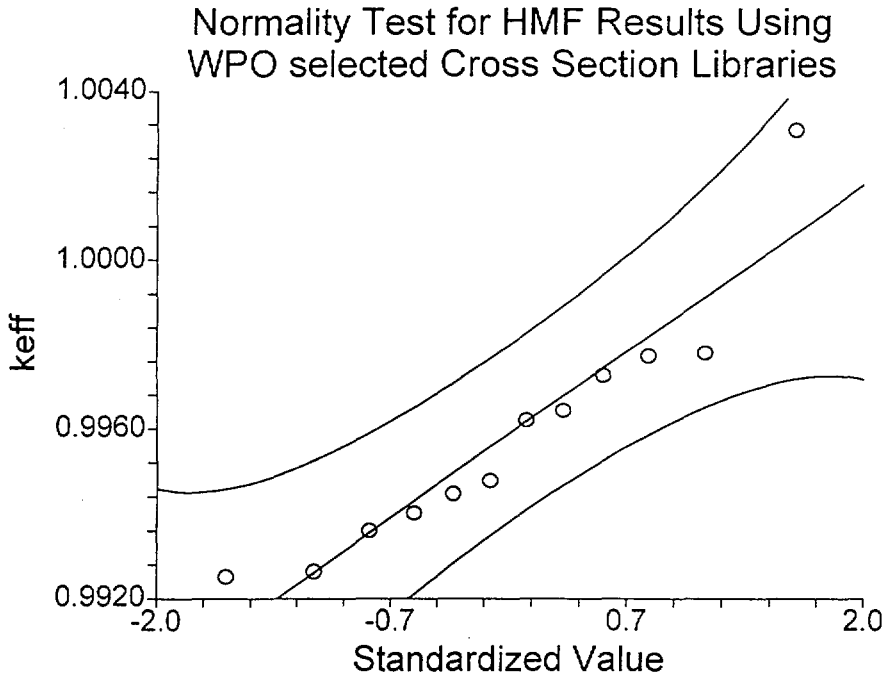

Figure VIII-7

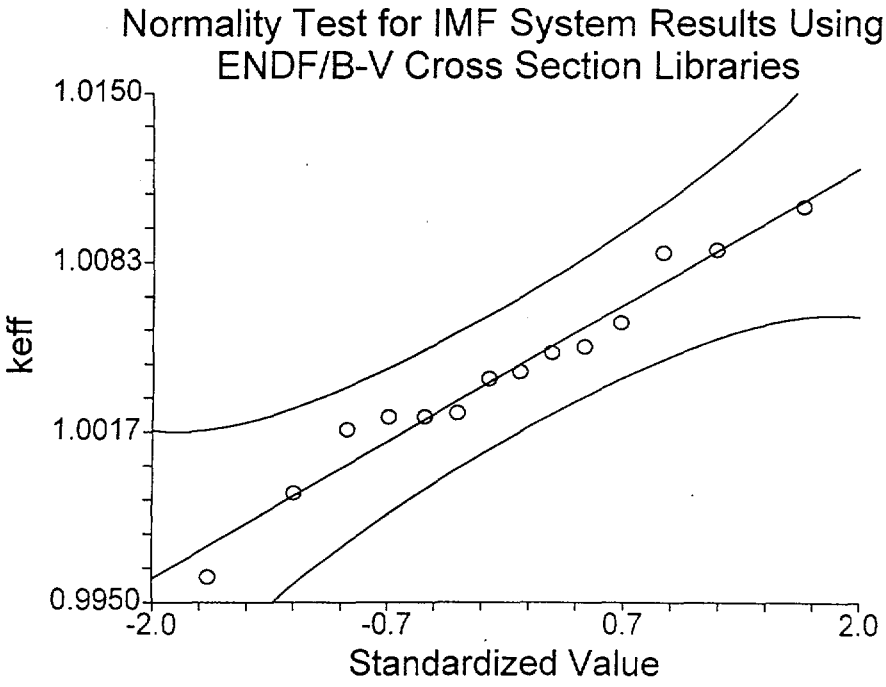

Figure VIII-8

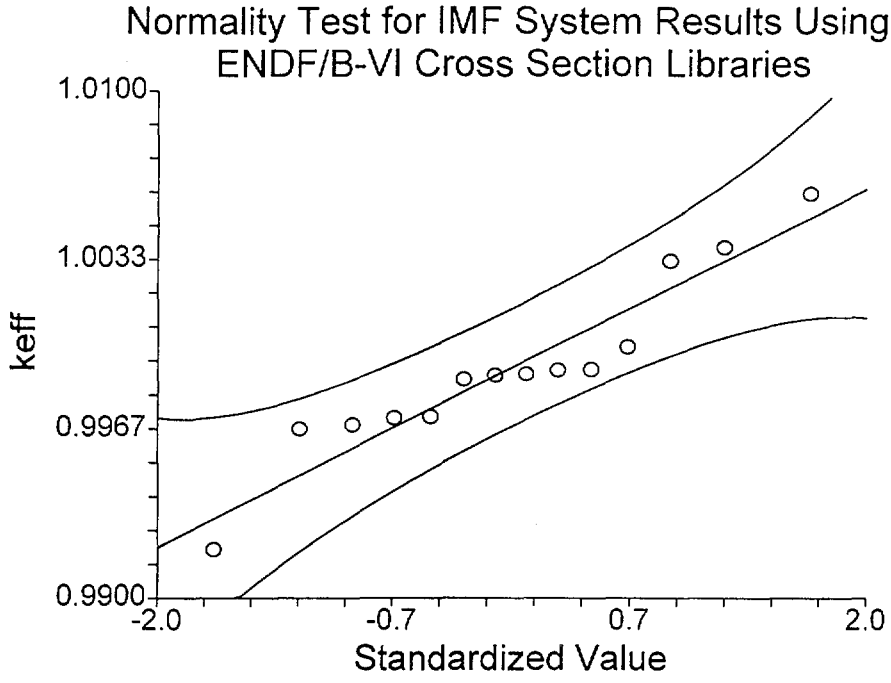

Figure VIII-9

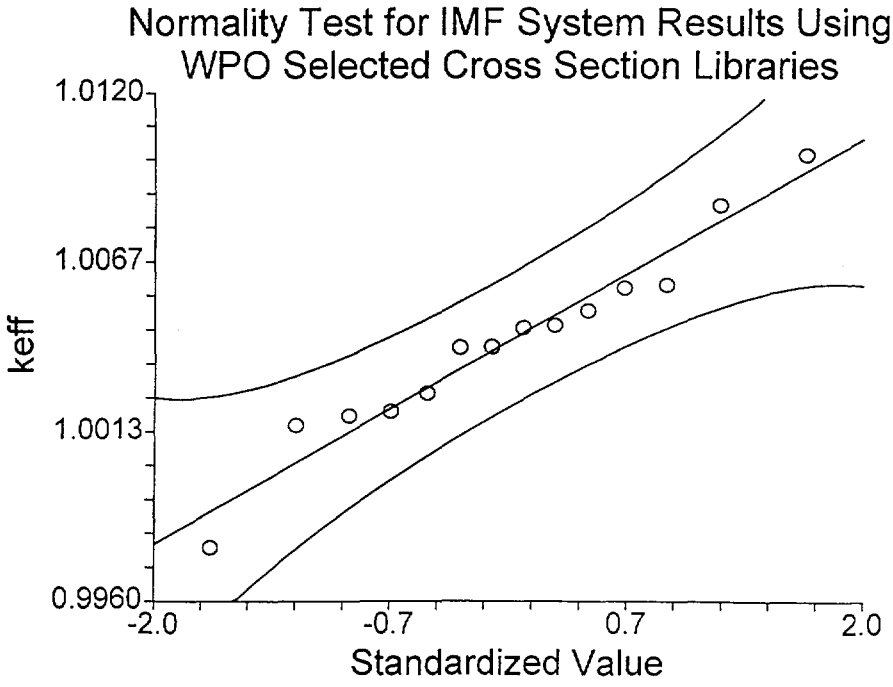

Figure VIII-10

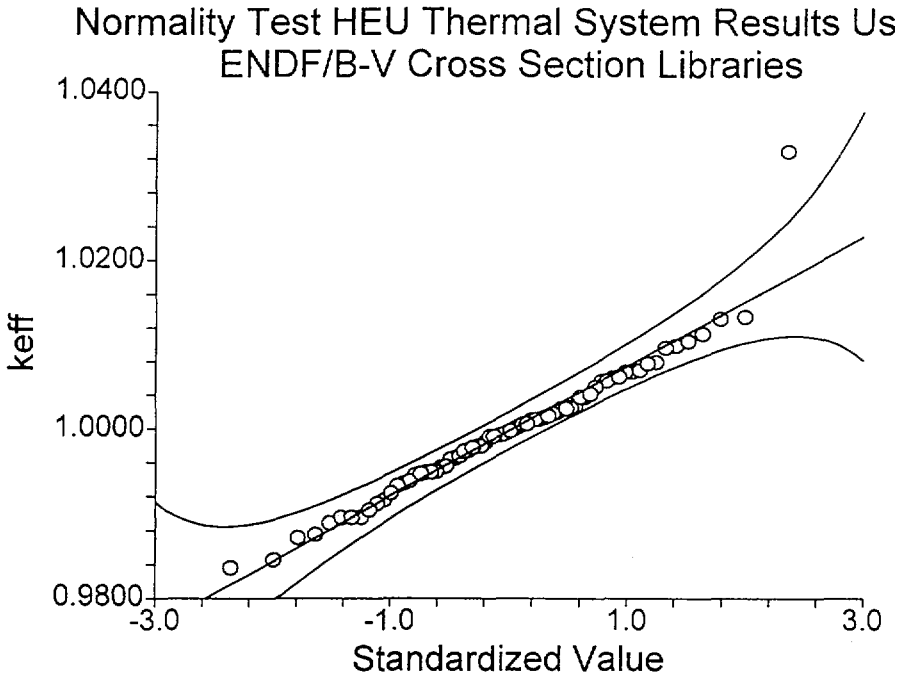

Figure VIII-11

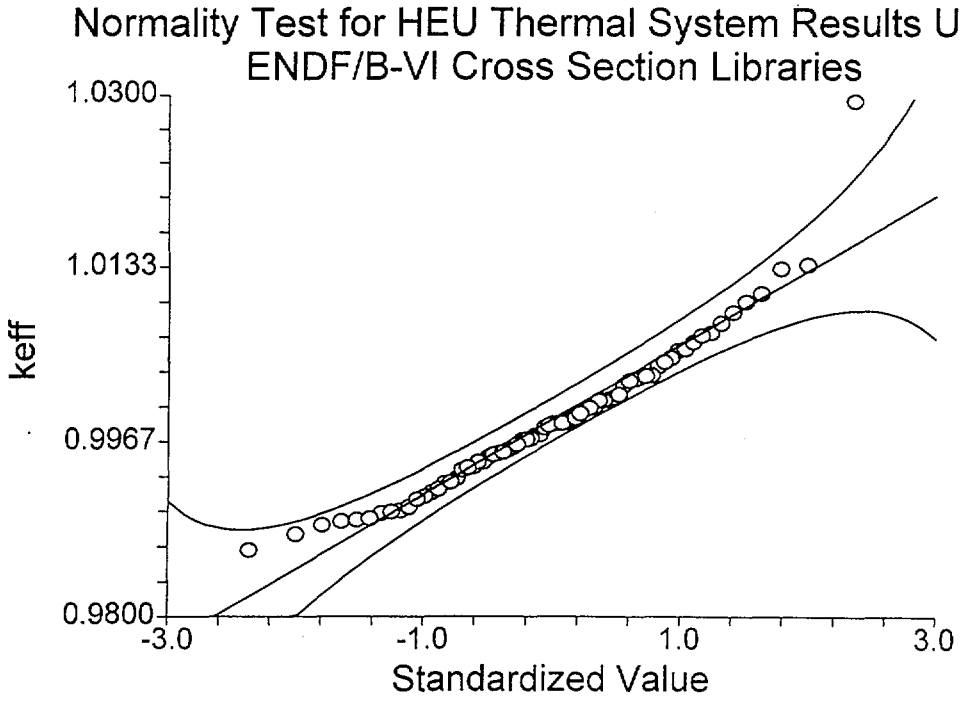

Figure VIII-12

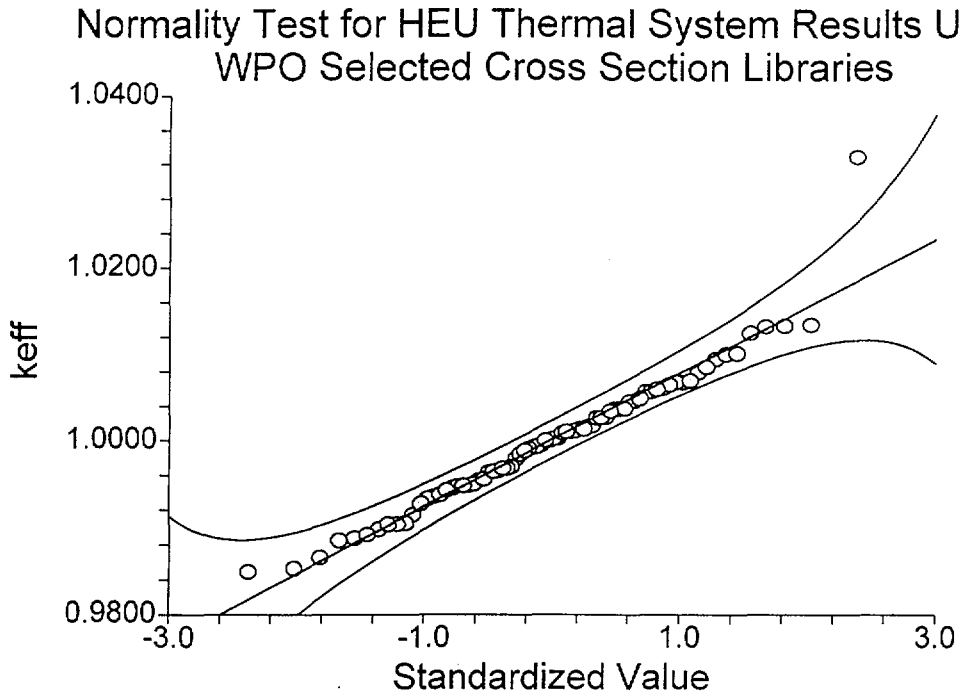

Figure VIII-13

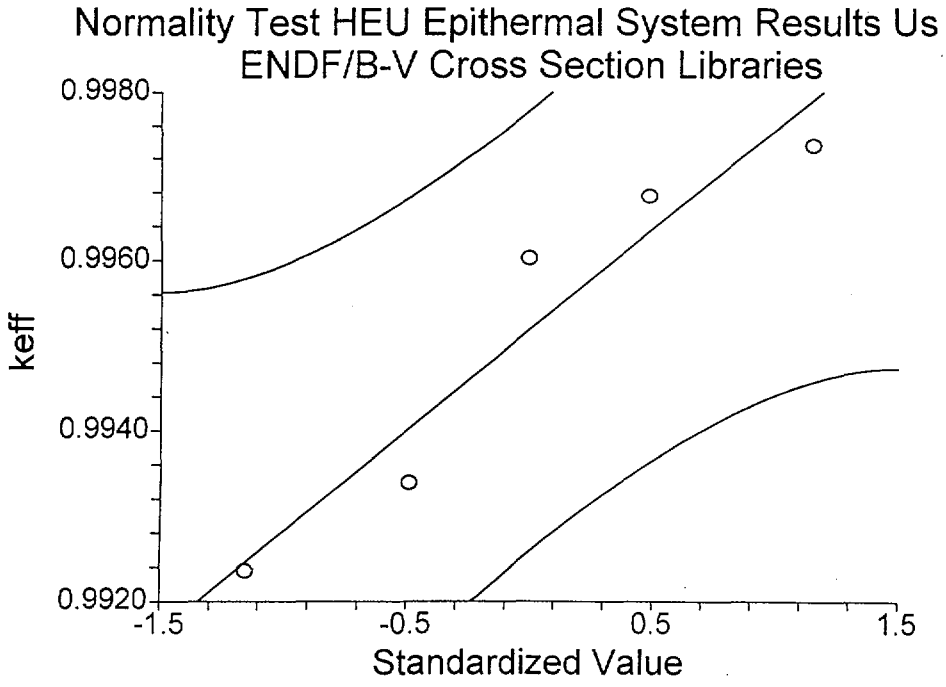

Figure VIII-14

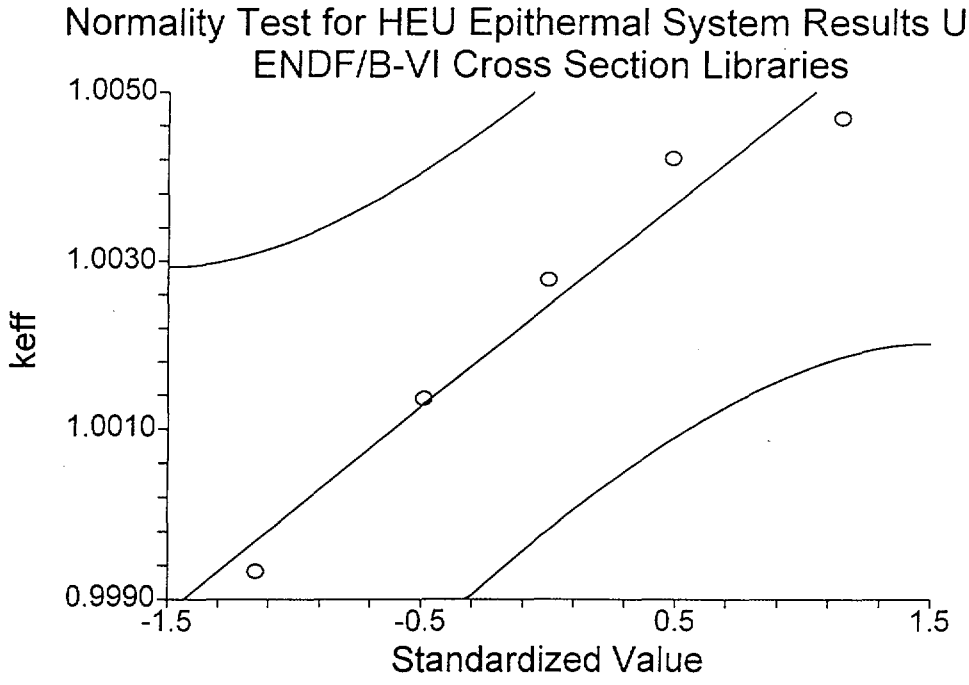

Figure VIII-15

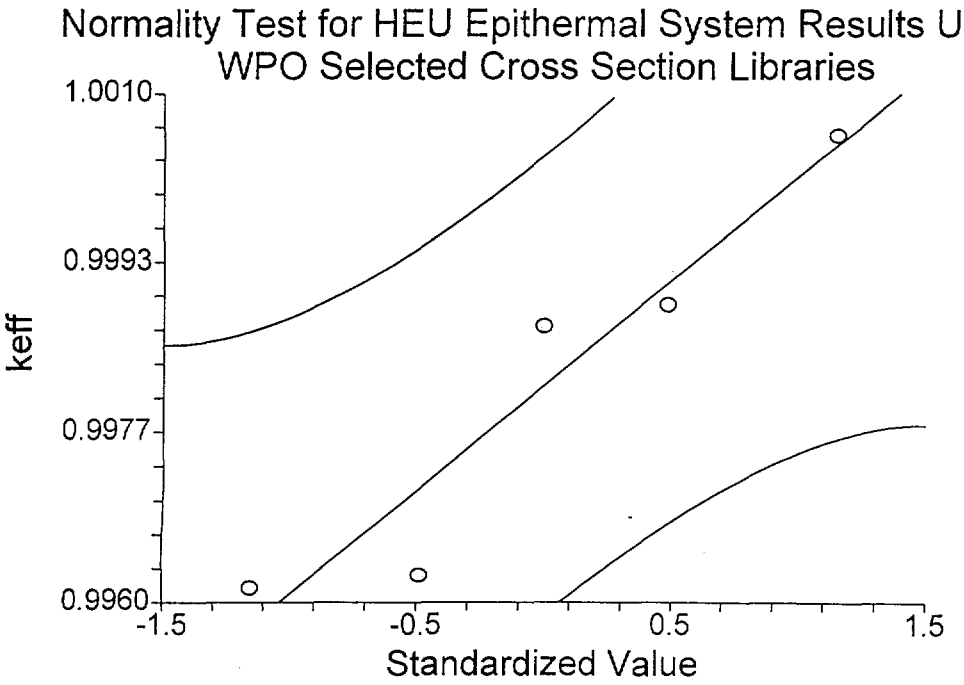

Figure VIII-16

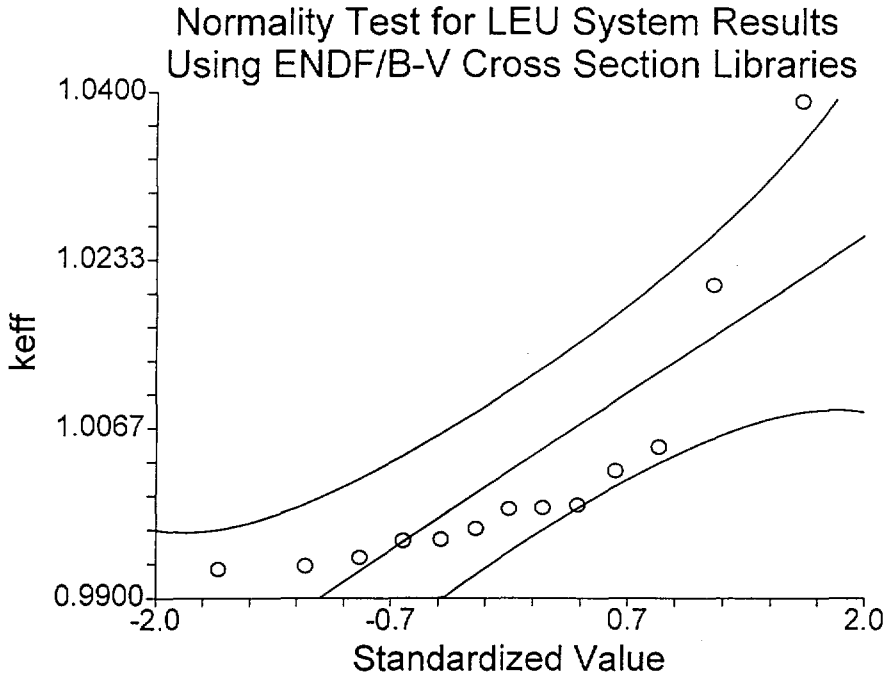

Figure VIII-17

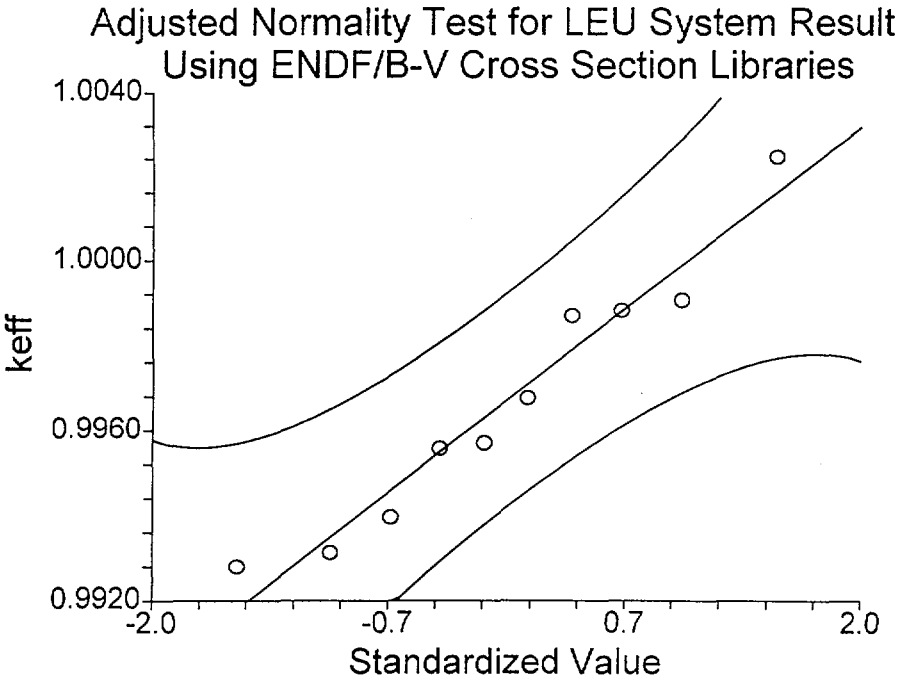

Figure VIII-18

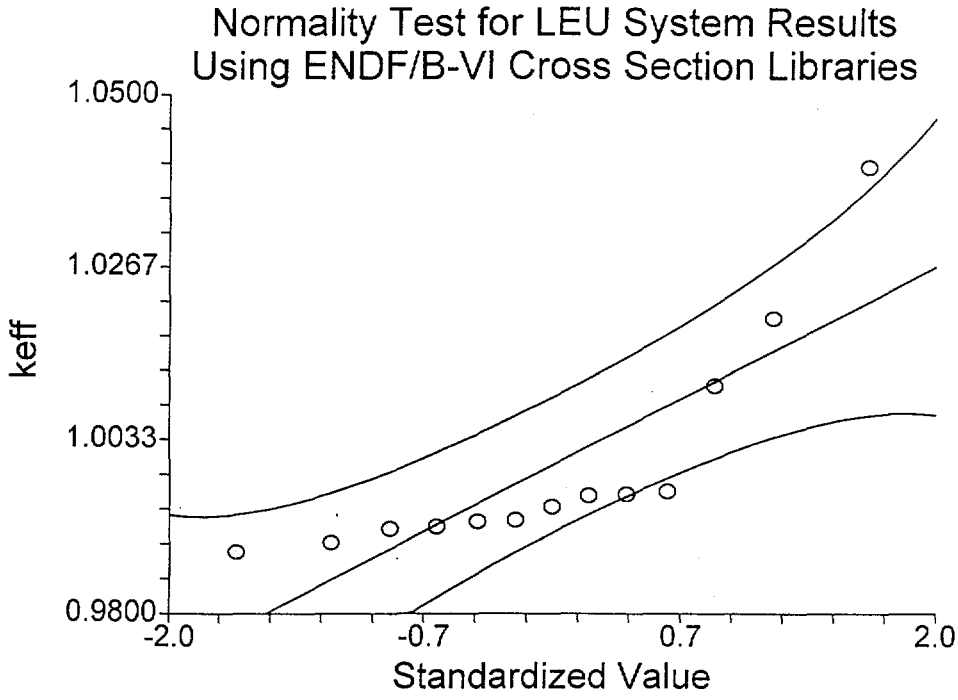

Figure VIII-19

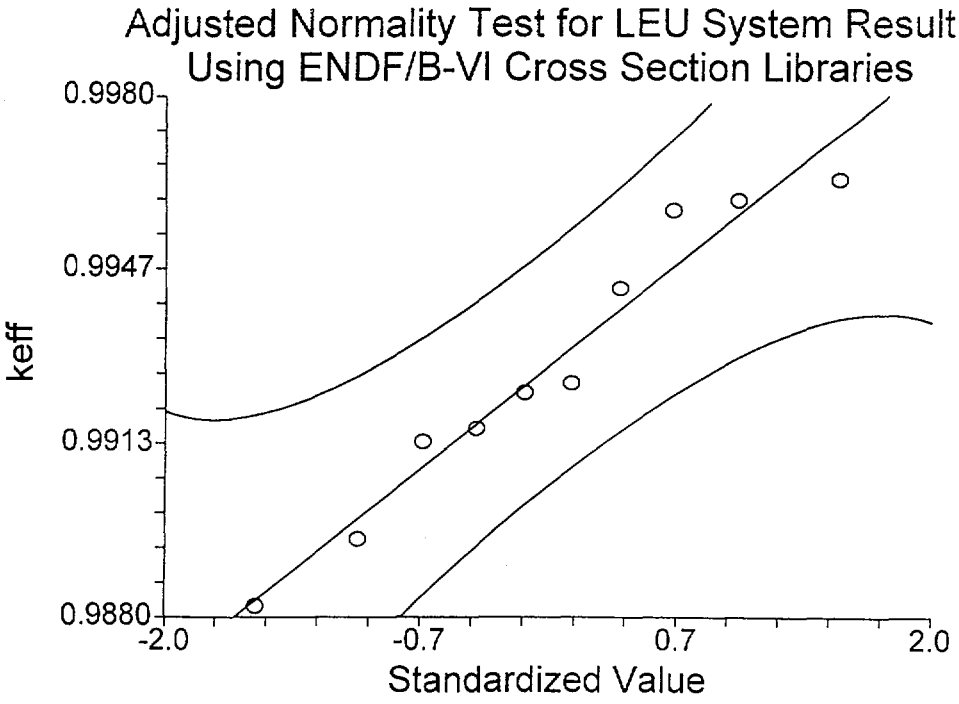

Figure VIII-20

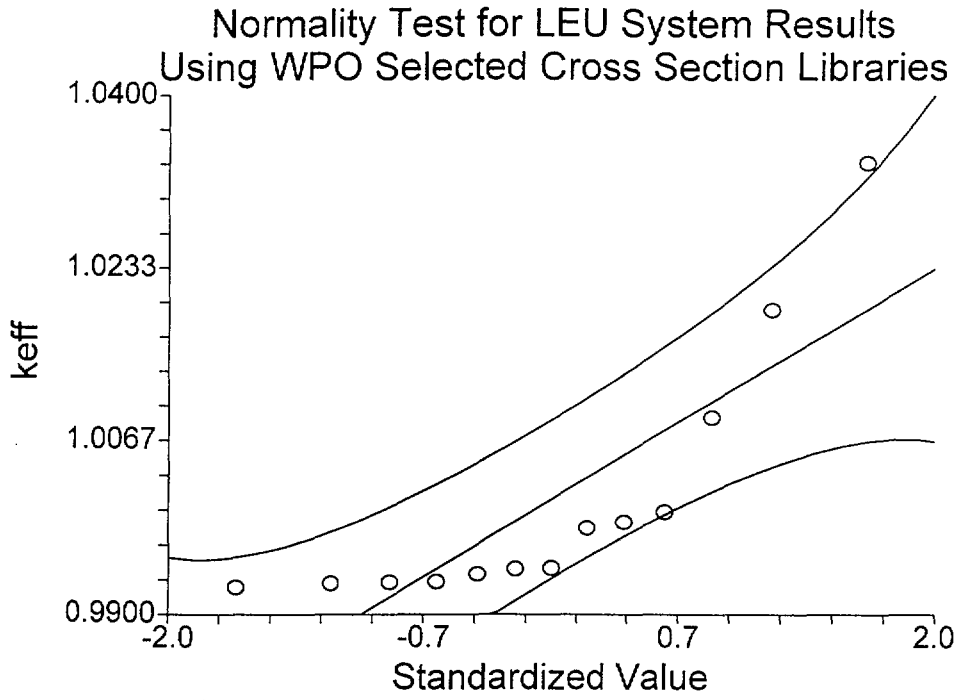

Figure VIII-21

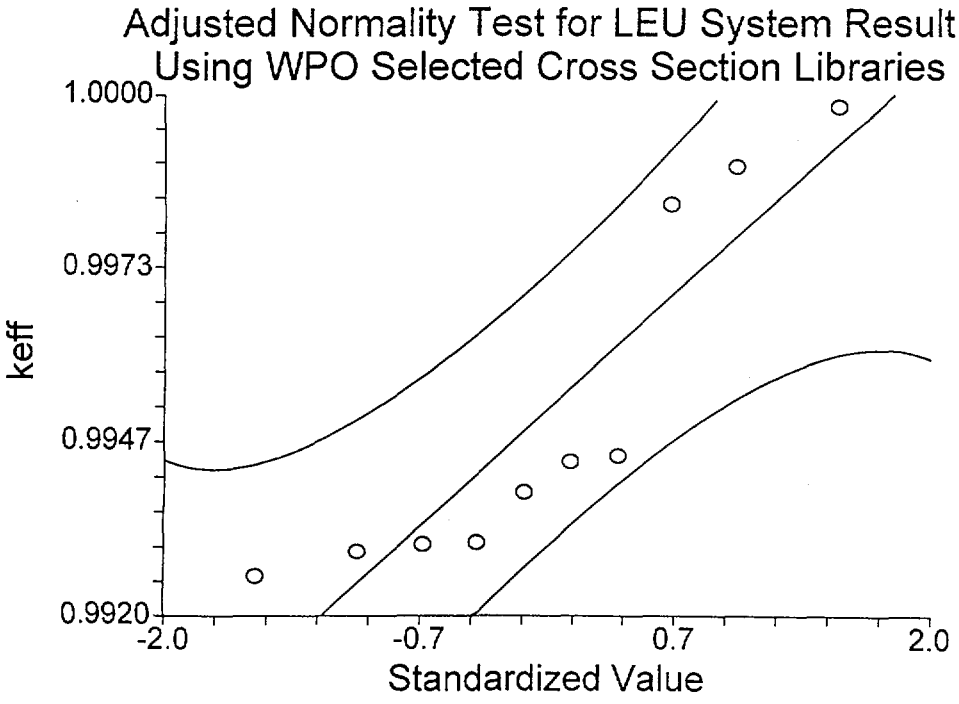

Figure VIII-22

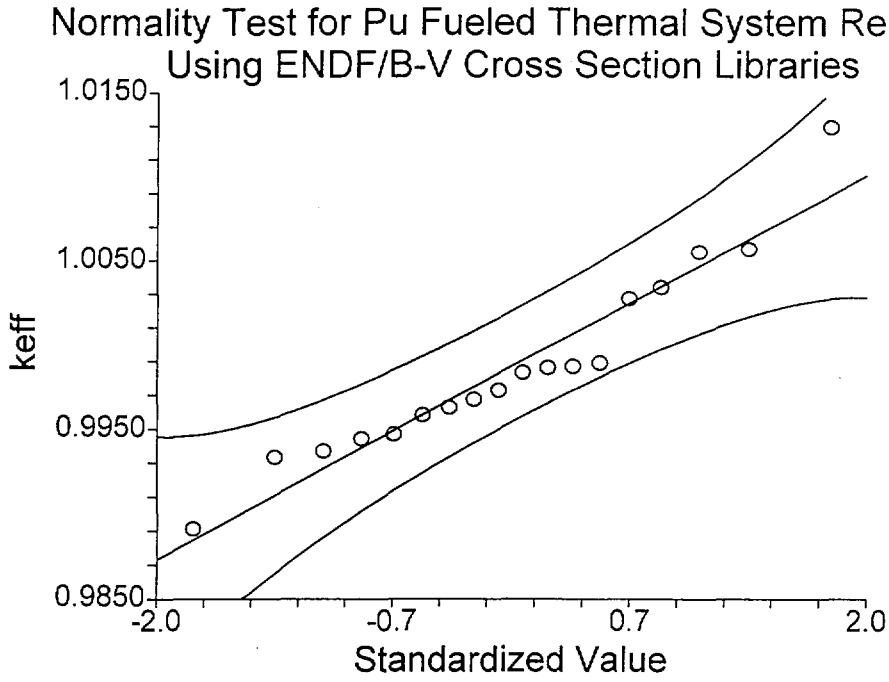

Figure VIII-23

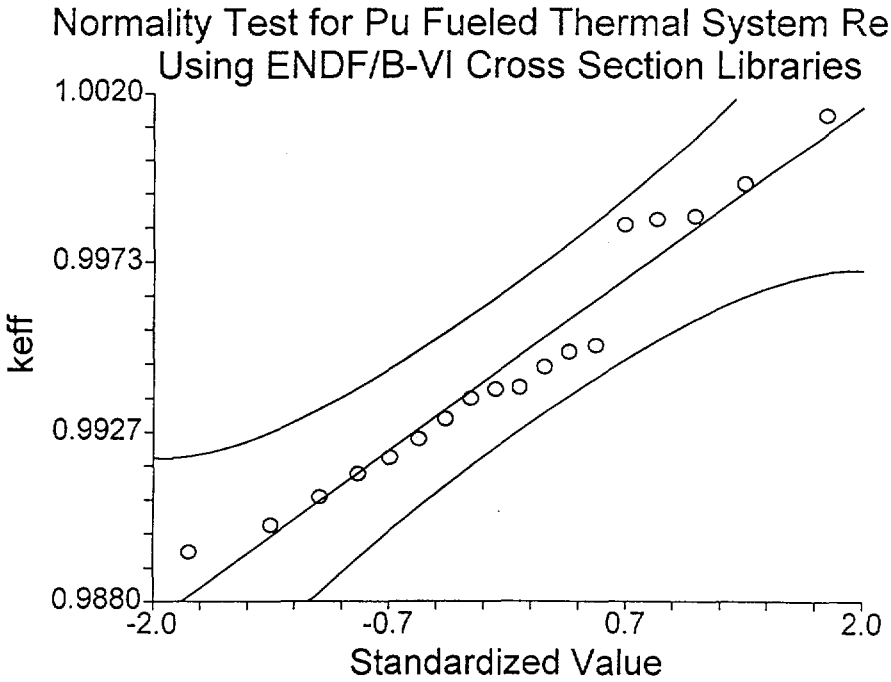

Figure VIII-24

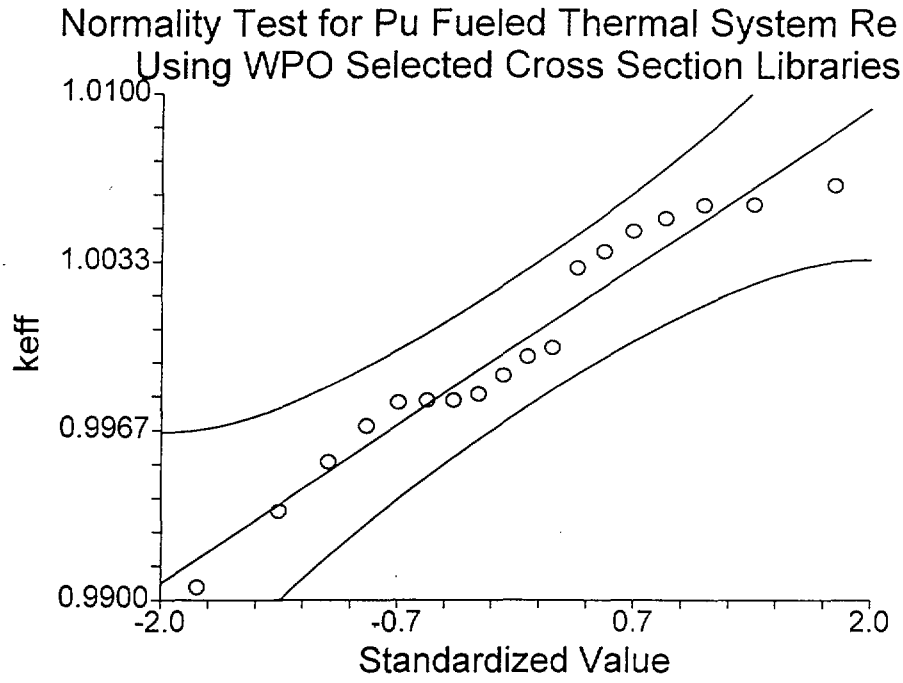

Figure VIII-25

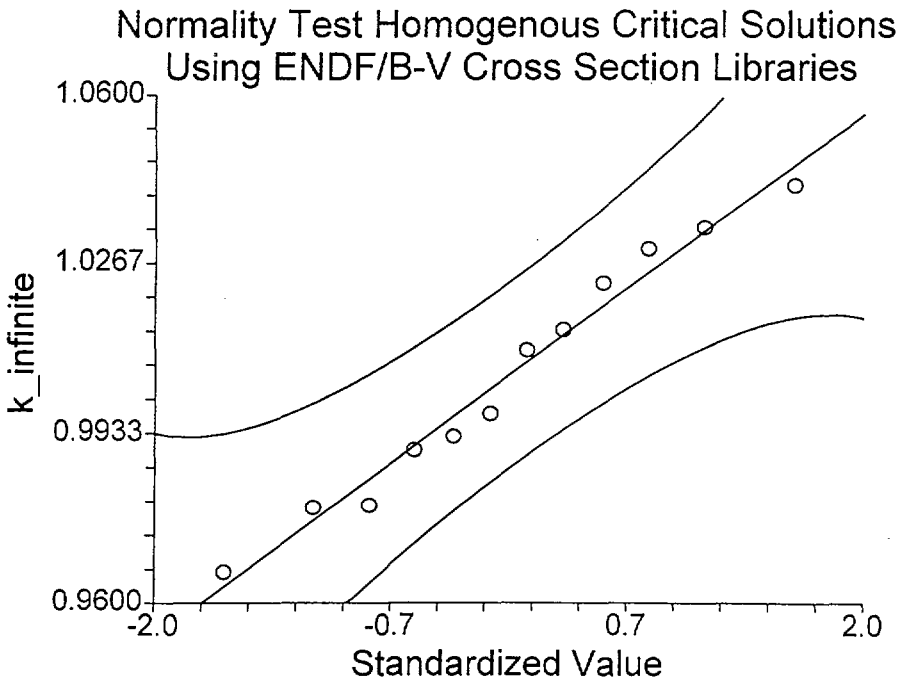

Figure VIII-26

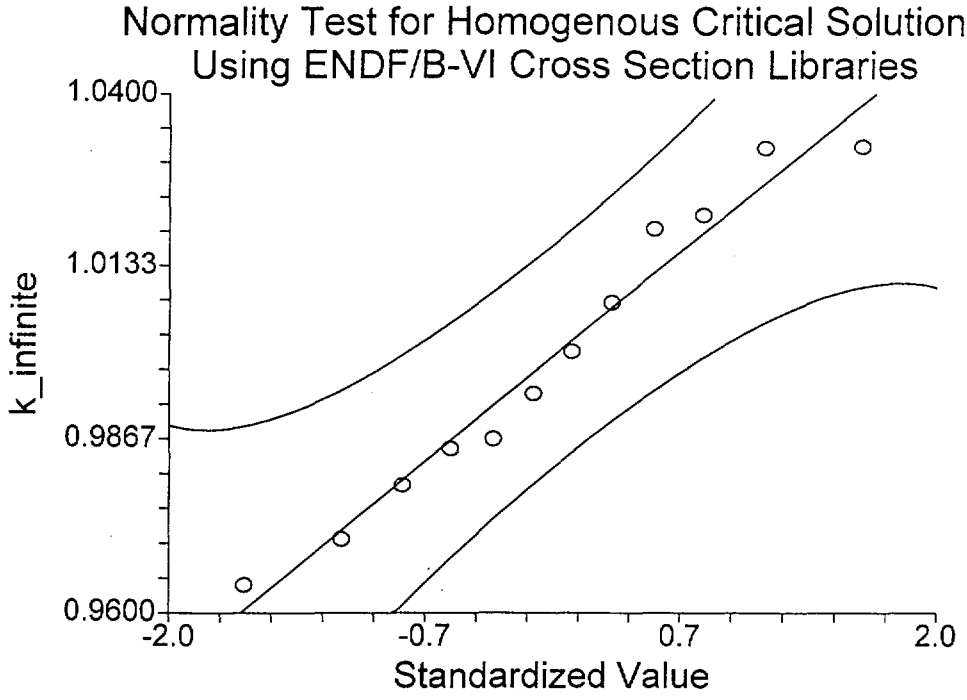

Figure VIII-27

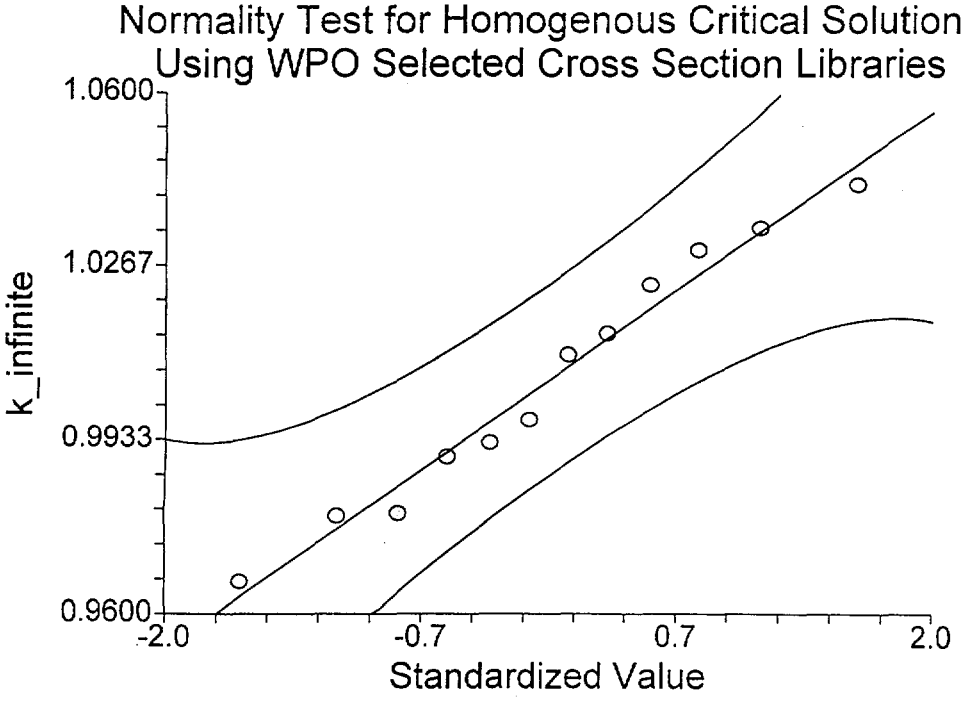

Figure VIII-28

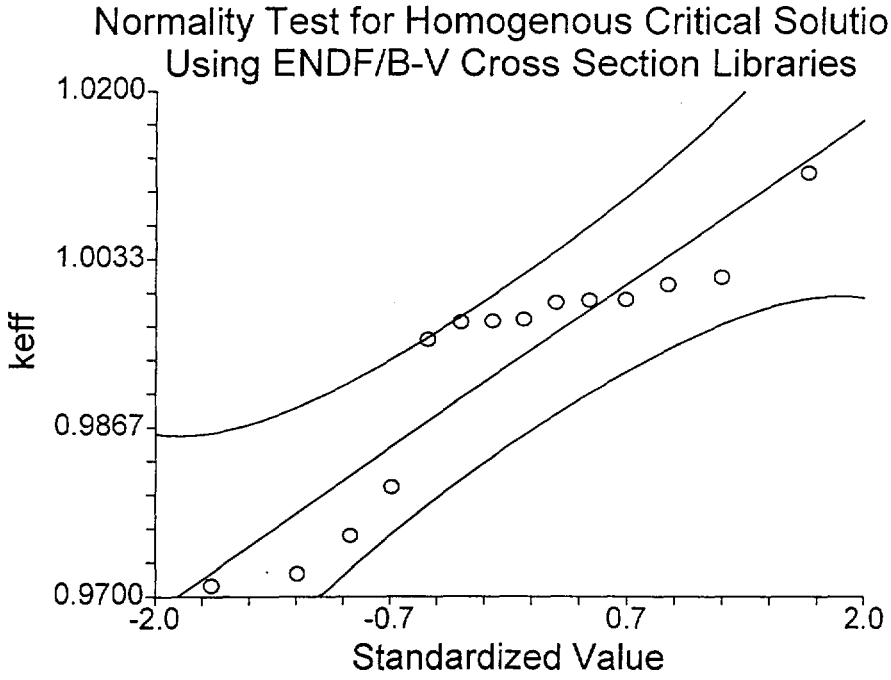

Figure VIII-29

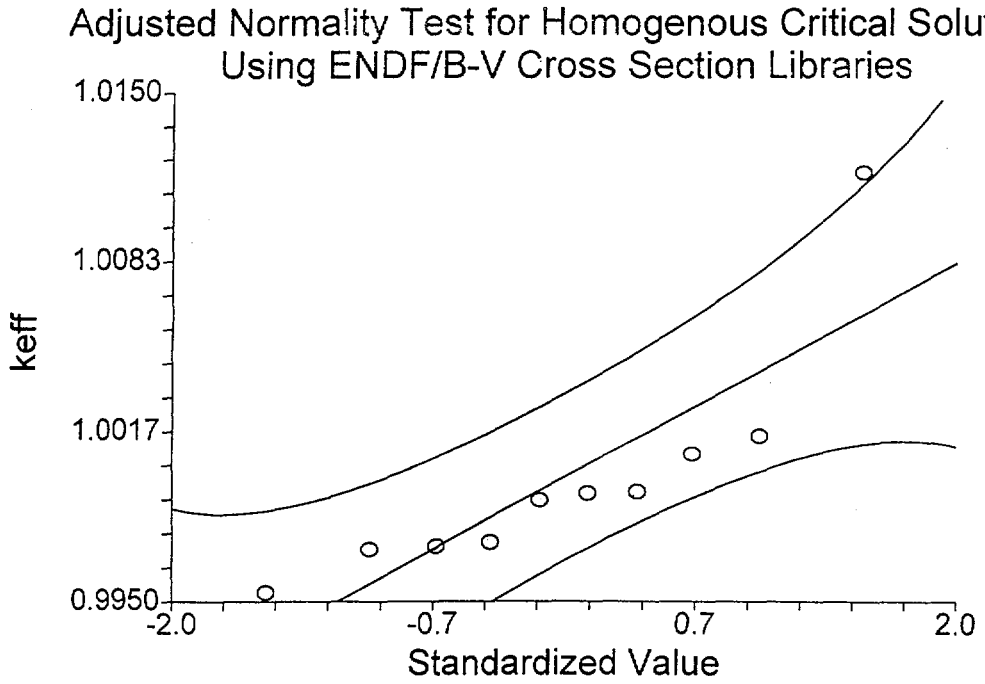

Figure VIII-30

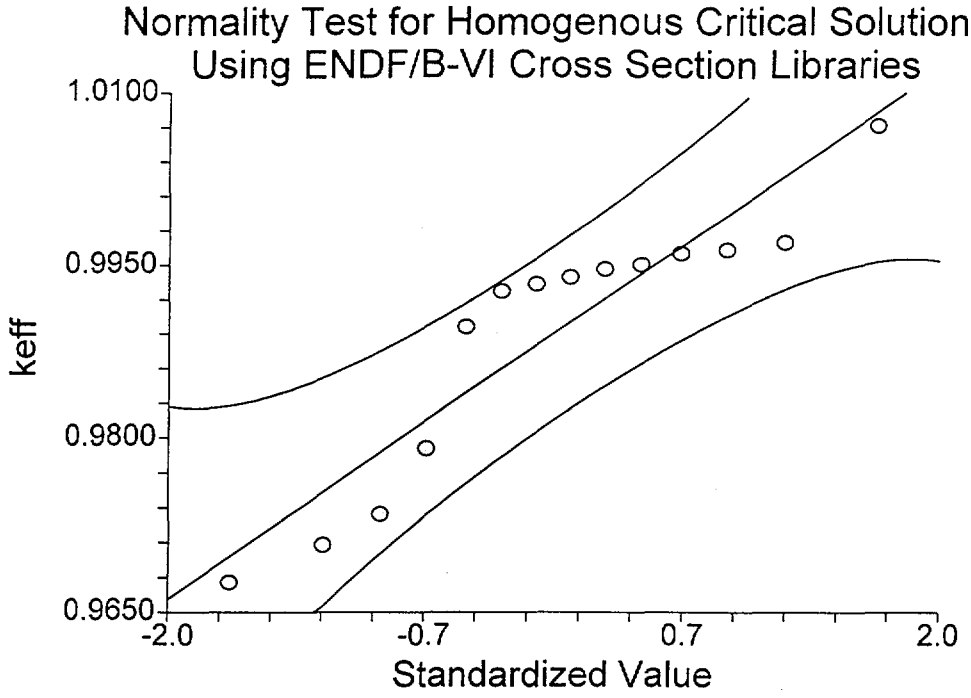

Figure VIII-31

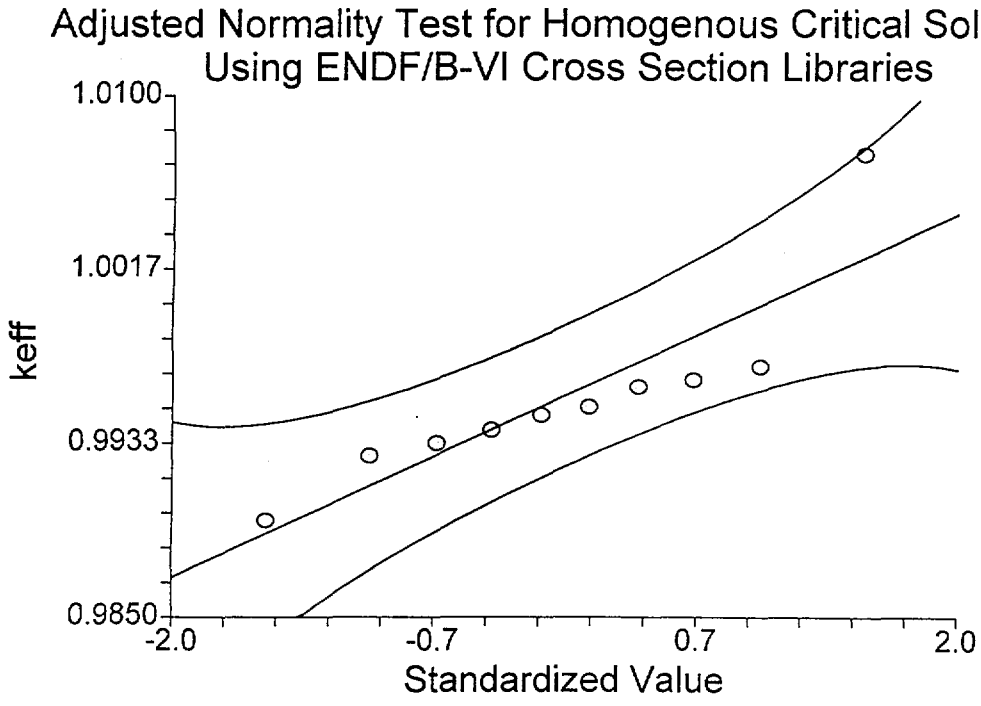

Figure VIII-32

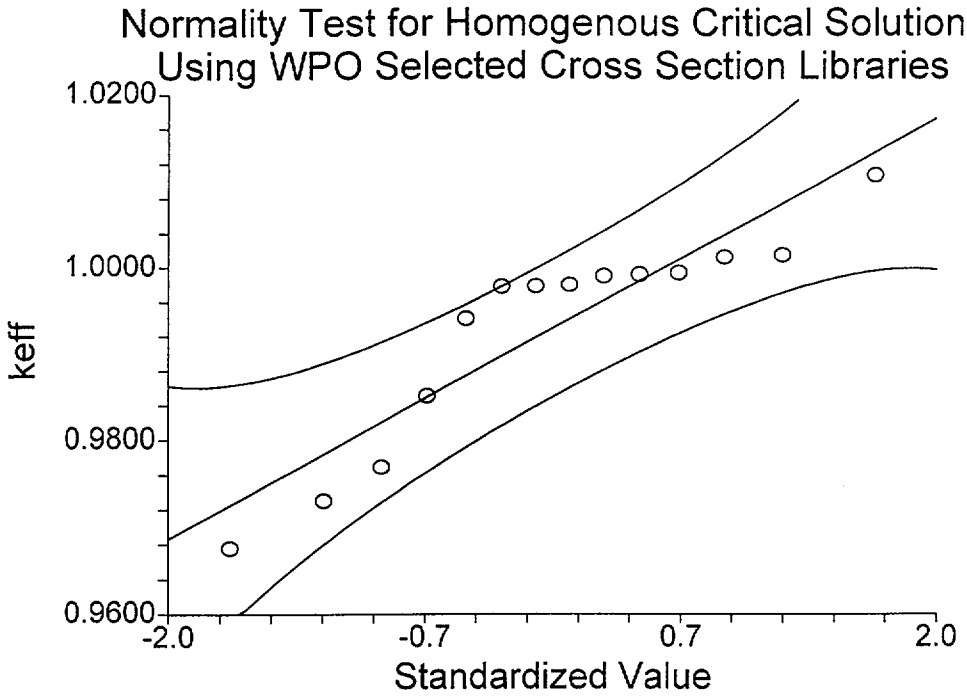

Figure VIII-33